Durham University

Durham E-Theses

Synthetic macrocyclic Ionophores

Patrick Edmund Nicholson

How to cite:

Nicholson, Patrick Edmund (1989) Synthetic macrocyclic Ionophores. Doctoral thesis, Durham University.

Use policy

The full-text may be used and/or reproduced, and given to third parties in any format or medium, without prior permission or charge, for personal research or study, educational, or not-for-profit purposes provided that:

- a full bibliographic reference is made to the original source
- a https://etheses.durham.ac.uk/id/eprint/6321/ is made to the metadata record in Durham E-Theses
- the full-text is not changed in any way

The full-text must not be sold in any format or medium without the formal permission of the copyright holders.

Please consult the full Durham E-Theses policy for further details.

Academic Support Office, The Palatine Centre, Durham University, Stockton Road, Durham, DH1 3LE
e-mail: e-theses.admin@durham.ac.uk Tel: +44 0191 334 6107
https://etheses.durham.ac.uk

SYNTHETIC MACROCYCLIC IONOPHORES

by

Patrick Edmund Nicholson, B.Sc.(Dunelm)

Durham University

The copyright of this thesis rests with the author. No quotation from it should be published without his prior written consent and information derived from it should be acknowledged.

A Thesis submitted for the degree of
Doctor of Philosophy at the University of Durham.

July 1989

- 9 MAR 1990

STATEMENT OF COPYRIGHT.

The Copyright of this thesis rests with the author. No quotation from it should be published without his prior written consent and information derived from it should be acknowledged.

DECLARATION

The work described in this thesis was carried out in the Department of Chemistry at the University of Durham between October 1985 and December 1988. All the work is my own, unless stated to the contrary, and it has not been submitted previously for a degree at this or any other University.

Dedicated to my Parents, Sister and Kate for their love, support and encouragement without which none of this would have been possible.

'Car ce n'est pas assez d'avoir l'esprit bon,

mais le principal est de l'appliquer bien'.

ABSTRACT

SYNTHETIC MACROCYCLIC IONOPHORES

14-Crown-4 derivatives bearing either one or two oxymethyl, benzyloxymethyl, methoxycarbonylmethyl or carbamoylmethyl substituents have been prepared in an attempt to obtain selective ionophores for lithium ions. Complexation has been monitored by IR, ^{13}C NMR, Fast Atom Bombardment Mass Spectrometry, and solvent polymeric membranes have been fabricated and evaluated using the fixed interference method.

Improved lithium selectivities of the disubstituted 14-crown-4 ligands compared to the monosubstituted analogues in the potentiometric experiments, bears out the premise that there is a need to suppress competitive 2:1 complex formation with sodium. The most encouraging lithium selectivity was observed with an electrode based on *trans*-(2S,3S)(-)-2,3-bis(N,N'-dibutylcarbamoylmethyl)-1,4,8,11-tetraoxacyclotetradecane which vindicates the choice of axial amide donors to enhance the Li/Na selectivity of the 14-crown-4 skeleton.

Triazacyclononane, triazacyclododecane and tetraazacyclododecane amide functionalised ligands were prepared in order to investigate the effect of donor number, macrocyclic ring size and chelate ring size on stability and selectivity of complexation with alkali and alkaline earth metal cations. Complexation has been monitored by IR, ^{13}C NMR, Fast Atom Bombardment Mass Spectrometry and pH-metric titration experiments. The most stable complex was formed between calcium and N,N'-dimethyl-1,4,7,10-tetraacetamido-1,4,7,10-tetraazacyclododecane, for which log K(CaL) = 6.81 (H_2O). Once again, measurable log K values $\geq$ 3.9 in aqueous media for lithium, sodium and calcium complexation vindicate the choice of amide donors to ensure strong coordination with small cations of high charge density ratio.

Patrick Edmund Nicholson (July 1989)

ACKNOWLEDGEMENTS

I would like to thank my supervisor, Dr. David Parker, for his support, endless enthusiasm and encouragement throughout the course of my research.

I am indebted to Dr. Ray Matthews for running N.M.R spectra, Vince McNeilly and Dr. Mike Jones for their patience and guidance during the FAB studies and Mrs. Molly Cox for combustion analyses.

My special thanks go Dr. Ritu Kataky who performed the potentiometric studies and analysed the pH-metric data. Without her knowledge, patience and expertise, the most informative section of this thesis would be missing.

Thanks go to my colleagues in Lab. 27 whose friendship, good humour and support will be greatly missed. Thanks also, to my close friend and confidante Dr. Simon Wait for his lateral wit and optimism.

I am indebted to Dr. Nigel Smith for his typing of this manuscript with considerable speed and accuracy.

Finally, I would like to thank the S.E.R.C. for support of this project.

CONTENTS PAGE

CHAPTER ONE

THERMODYNAMIC AND KINETIC ASPECTS OF CATION AND LIGAND INTERACTIONS

1.1 THERMODYNAMICS AND KINETICS OF COMPLEXATION

1.1.1 Valinomycin - A Naturally Occurring Ionophore

In the late 1960's[1], it was established that there was a class of neutral, naturally occurring antibiotics which show marked effects on alkali metal cation transport in respiring cell fragments of various kinds, and on the cation permeability of natural and artificial membranes.

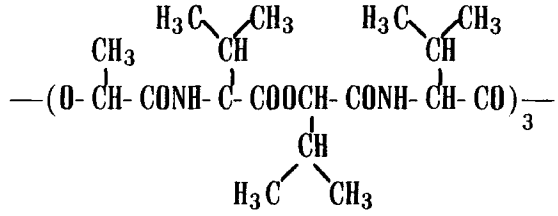

(1)

Figure 1.1 *Structure of Valinomycin (1).*

The most widely studied member of this family is valinomycin (1) (Figure 1.1) which has an extremely high preference for potassium over sodium ions.

In the potassium complex, the potassium ion is located in the centre of the 36-membered ring. The latter is folded into six β-turns, which are stabilised by four intramolecular NH···O=C hydrogen bonds that are of the common (4 → 1) type (Figure 1.2).

All carbonyl oxygens involved in hydrogen bonding belong to the amide groups and it is the six ester carbonyls that coordinate to the potassium ion with an almost perfect octahedral geometry.

In its uncomplexed form, valinomycin adopts an ellipsoid shape as determined by x-ray diffraction studies[2]. It is stabilised by the same (4 → 1) amide hydrogen bonds as found in its complexed form, but also by two hydrogen bonds of the rare (5 → 1) type (Figure 1.2) which involve

ester carbonyls.

(a)

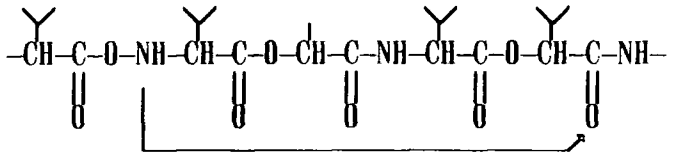

(b)

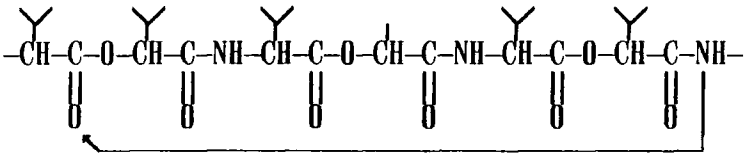

Figure 1.2 *(a) (4 → 1) Hydrogen Bond in Valinomycin, NH···O=C (Amide); (b) (5 → 1) Hydrogen Bond in Valinomycin, NH···O=C (Ester).*

The (5 → 1) hydrogen bonds are largely responsible for the oval shape of uncomplexed valinomycin. Moreover, they direct two of the ester carbonyls toward the surface of the molecule. These are thought to initiate complex formation prior to the placement of the potassium ion in the ligand cavity. It has been proposed that the formation of an initial loose complex with the potassium ion is followed by cleavage of both (5 → 1) hydrogen bonds, in order to enable all ester carbonyls to interact with the central cation.

The high selectivity that valinomycin displays for potassium over sodium is thought to be largely based on differences in their respective cationic radii. Whereas the potassium ion is of optimum size to fill the ligand cavity, the sodium ion is too small to fully interact with all ester carbonyls and cannot be complexed without an energetically unfavourable breaking of the intramolecular (1 → 4) hydrogen bonds.

In parallel to the realisation of the outstanding properties of neutral antibiotics as selective cation carriers, Charles Pederson[3] reported, in 1967, the synthesis of over thirty cyclic polyethers, noticing their unusual affinity for alkali metals and their cation selectivity characteristics. This has subsequently prompted the

synthesis of numerous acyclic and cyclic ligands in an attempt to mimic, and improve, selectivity and carrier properties displayed by natural ionophores, and develop a deeper understanding of the thermodynamics and kinetics of complexation.

1.1.2 Thermodynamics and Kinetics of Complexation

If the complexation of ligand L, with different cations (M_1^+, M_2^+, M_3^+) is characterised by similar or identical thermodynamic and kinetic parameters, L just distinguishes one M_x^+ ion from another one (DISTINCTION). However, if the association shows selectivity for a given cation, M_1^+, leading to the preferred formation of LM_1^+, a specific complex is formed (SELECTION).

The corresponding selectivity may be <u>static</u> (thermodynamic, related to the free energies of the free and associated states and hence to the stability constant), or <u>dynamic</u> (kinetic, related to the energy barrier leading to the formation of the transition state, to the rates of complex formation and of the complex dissociation), or both.

Clearly, design of a synthetic ligand that will form a stable, selective complex with cation M_1^+, is based on a thorough understanding of the thermodynamics and kinetics of complexation as gleaned from theoretical and, as much as possible, from experimental data. Hence it is thought appropriate to discuss the many factors that contribute to the stability and dynamics of complexation for neutral ligands with alkali and alkaline earth metal cations.

1.1.3 The Thermodynamics of Complexation

Alkali and alkaline earth metal cations exhibit high charge density ratios and low polarisability, and can be classified as 'hard' cations. Interactions between these cations and ligand donor atoms can be thought of as mainly electrostatic in nature (ion dipole, ion-induced dipole), in contrast to bonds with varying covalent character formed with 'soft' cations such as certain transition metals.

A pure electrostatic model has some advantages in the discussion of the complexation process, since it allows separate evaluation of the various effects influencing the thermodynamics of the cation ligand interaction. The complexation process may be represented:

$$M^+_{(s)} + L_{(s)} \rightleftharpoons ML_{(s)} \qquad (1.1)$$

where: M^+ = metal cation
L = ligand
s = solvent

The equilibrium (stability) constant (K_s) can then be written:

$$K_s = \frac{[ML]}{[M^+][L]} \qquad (1.2)$$

where [ML] = complex concentration at equilibrium
[M⁺] = free cation concentration at equilibrium and
[L] = free ligand concentration at equilibrium

The free energy change (ΔG) for complexation is related to the stability constant (Equation 1.3) and the free energy change (ΔG) may be divided into enthalpy (ΔH) and entropy (ΔS) changes that occur (Equation 1.4).

$$\Delta G = -RT \ln K_s \qquad (1.3)$$

$$\Delta G = \Delta H - T\Delta S \qquad (1.4)$$

Examination of Equations 1.1 and 1.2 shows that a negative ΔG value delineates a favourable free energy change for complexation in that the

equilibrium for Equation 1.1 will be to the right.

On examination of Equation 1.4 it is seen that for complexation to be favoured there are four possibilities:

(a) $\Delta H < 0$ (Dominant), $T\Delta S > 0$

(b) $\Delta H < 0$ (Dominant), $T\Delta S < 0$

(c) $\Delta H < 0$, $T\Delta S > 0$ (Dominant)

(d) $\Delta H > 0$, $T\Delta S > 0$ (Dominant)

1.1.4 Contributions to Complexation Enthalpy

1.1.4.1 Variations in the Nature and Energy of Cation-Solvent and Cation-Ligand Interactions.

In the complexation process, some or all of the solvent molecules comprising the cations first solvation sphere are replaced by basic ligand donor sites. Thus, there is a balance between the unfavourable endothermic desolvation of the cation, and the favourable exothermic solvation of that cation by the ligand.

LIGAND	SOLVENT	ΔH KJ mol^{-1}	REF
18-C-6 K^+	MeOH	-53.14	4
18-C-6 K^+	H_2O	-26.00	5
18-C-6 Na^+	MeOH	-31.38	4
18-C-6 Na^+	H_2O	- 9.41	5

Table 1.1 *Enthalpy Changes for Complexation of 18-crown-6 with Sodium and Potassium Ions measured Calorimetrically in Methanol and Water at 25°C.*

Obviously the nature of the solvent greatly influences the resultant enthalpy change. In solvents of high dielectric constant and/or high donor number, more energy will be required for desolvation

than in solvents of low dielectric constant and/or low donor number. For example, in Table 1.1 the enthalpies of complexation for potassium and sodium ions with 18-crown-6, as measured calorimetrically at 25°C in methanol[4] and water[5] are listed.

It can be clearly seen that the higher dielectric constant of water confers a lower favourable enthalpy for complexation than with a solvent of lower dielectric constant, in this case, methanol. Cations of high charge density ratio (Li^+, Na^+, Mg^{2+}, Ca^{2+}) exhibit higher solvation energies than those of lower charge density ratio, and so, changes in solvent will have more effect on the enthalpy of complexation of these small highly charged cations.

Clearly, the nature and number of donor sites on the ligand will determine the degree of stabilisation conferred by that ligand in solvating the cation.

1.1.4.2 Nature of Donors

The alkali and alkaline earth metal cations can be classified as hard according to the 'hard and soft acid-base principle'[6] and should interact most favourably with 'hard' donors. Donors can be represented in a scale of hardness (O > N > P,S) and thus the strongest electrostatic interactions are expected to arise from functional groups containing oxygen. Frensdorff[7], studied the effect of substituting ether donors with amine and thioether donors in 18-crown-6 on the stability of resultant complexes with potassium in methanol (Table 1.2). It can be seen that substitution by either nitrogen or sulphur, lowers the stability constant of resultant potassium complexes. Assignment of at least a proportion of this effect to enthalpic changes has been possible through further experiments (Table 1.3)[8-10].

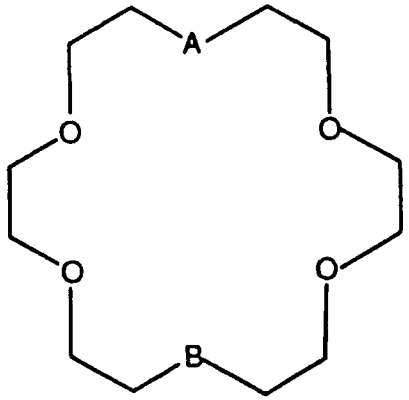

POLYETHER A	POLYETHER B	log K_S
O	O	6.10
NH	O	3.90
NH	NH	2.04
S	S	1.15

Table 1.2 *Effect of Substituting Ether Donors with Amine and Thioether Donors in 18-crown-6 on Stability of K^+ Complex in Methanol at 25°C; Reference 7.*

A glance at the data in Table 1.3 shows that, substitution of ether donors by amine or thioether donors, causes a less favourable enthalpic change for complexation, implying that the latter two donors interact less strongly with the potassium cation than the former.

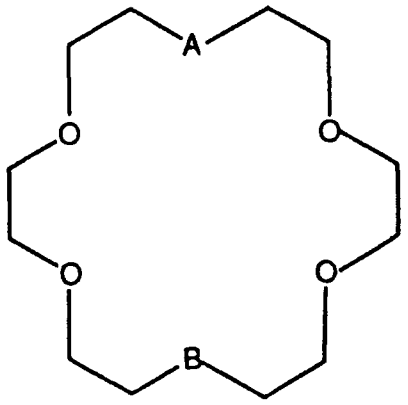

POLYETHER A	POLYETHER B	ΔH KJ mol^{-1}
O	O	-54.9
NH	NH	- 4.7
O	S	-37.7
S	S	----

Table 1.3 *Effect of Substituting Amine and Thioether Donors for Oxygen Donors on the Enthalpy of Complexation of Potassium with 18-crown-6 measured calorimetrically in Methanol at 25°C (References 8-10).*

For small highly charged cations, high polarisability of the donor will be important, in addition to high electron density, since charge induced dipole interactions vary as $1/r^4$ while charge dipole interactions vary as $1/r^2$ (where r represents the cation-donor distance).

Thus, for nitrogen and sulphur, the higher polarisability of these donors may serve to strengthen their interactions with small highly charged cations.

The electron density on the donor atom will be largely governed by the dipole moment between donor and substituents in the the free ligand *ie.* the higher the dipole moment, the more electron density will lie on that donor and hence the more favourable the interaction with alkali and alkaline earth metals will be. Some gas phase dipole moments are listed in Table 1.4.

LIGAND	DIPOLE
$HCONMe_2$	3.82
$HCONH_2$	3.73
HCO_2Me	1.77
HOMe	1.71
HCO_2H	1.40

Table 1.4 *Some Gas Phase Dipole Moments for Oxygen Based Functional Groups.*

It can be seen that amide groups should, by virtue of their high dipole moment, serve as efficient donor sites. Indeed, these donors feature prominently in natural ionophores for alkali and alkaline earth metal cations.

1.1.4.3 Number of Donors

The number of donor sites on the ligand should at least equal the coordination number of the cation. Reference points for the optimum coordination numbers for alkali and alkaline earth metal cations are provided by their coordination numbers with water molecules (Table 1.5).

Buschmann[8,10,11] has measured enthalpy changes for the complexation of potassium and sodium ions with a series of simple crown ethers and

these are represented graphically in Figure 1.3.

CATION	COORDINATION NUMBER	CATION	COORDINATION NUMBER
Li^+	4-6	Mg^{2+}	6
Na^+	6	Ca^{2+}	8
K^+	6	Sr^{2+}	8
Rb^+	6	Ba^{2+}	8
Cs^+	6		

Table 1.5 *Hydration Numbers for Alkali and Alkaline Earth Metal Cations.*

It can be seen that in the case of sodium, potassium, rubidium and caesium ions, where the coordination number of the ligand is lower than the optimal hexa-coordination for these cations, the enthalpy change is less favourable than for 18-crown-6 which is hexa-coordinate.

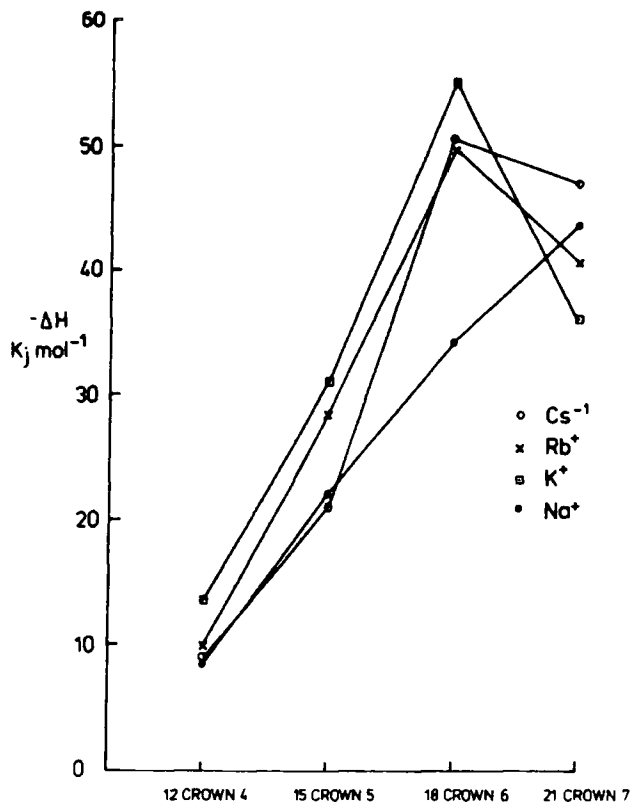

Figure 1.3 *Enthalpy of Complexation for Alkali Metal Ions with Simple Monocyclic Crown Ethers of Varying Ring Size.*

Because of their closed shell and inert gas structure, alkali and alkaline earth metal cations are not expected to show strong stereochemical requirements. They may be considered spherical, even in the complexed state. Maximal stability can therefore be achieved by providing donors that are arranged to form a basic sphere around the complexed cation. This has been demonstrated by measurements of cryptand and spherand enthalpy changes on complexation with alkali and alkaline earth metal cations. These types of ligands provide a three dimensional recognition for the cation and can, with appropriate design, exhibit highly favourable enthalpies of complexation (see discussion in Section 1.2).

Increasing the number of donors above and beyond the optimal coordination number of a cation, can potentially lead to a greater overall donor/cation interaction. However, the number of donors imposes a minimum cavity size owing to intra donor-donor repulsions. Hence the extra potential cation-donor attractive force generated by adding more donors to the ligand, may be nullified or even outweighed by the unfavourable free energy change (ΔG) associated with the deformation of the ligand from its unbound form in order to realise a conformation suitable for complexation. Clearly as donor number, and hence, minimum cavity size, increases, the destabilisation for smaller cations will be more extreme. If Figure 1.3 is inspected, it can be seen that the hepta-coordinate 21-crown-7 complexes the sodium ion with a more favourable enthalpy change than the hexa-coordinate 18-crown-6. It can be inferred that the difference is mainly due to the increased cation/donor interaction in the 21-crown-7 complex. However, the stability constant (K_S) for the 21-crown-7 Na^+ complex is lower than that of the 18-crown-6 complex, indicating that deformations of the 21-crown-7 ligand, in order to attain a binding conformation, result in

a markedly more unfavourable entropy change than that seen for the 18-crown-6 Na^+ complex.

Clearly, the type and number of binding sites and the topology of the ligand will greatly influence the enthalpy of complexation and hence stability of the resultant complex. Ligand design may therefore be used to realise a selectivity for cations on the basis of coordination number, size and charge/density ratio.

1.1.4.4 Repulsion Between Neighbouring Donor Atoms

Repulsions between solvent molecules forming the solvation shell around a metal cation destabilise the solvated state. This destabilisation increases as each additional solvent molecule is brought into the solvent shell. This can easily be seen in terms of the free enthalpy changes involved for consecutive solvation of alkali cations in the gas phase (Table 1.6)[12].

n	1	2	3	4	5	6
Li^+	142	108	87	68	58	52
Na^+	100	83	66	58	51	45
K^+	75	67	55	49	45	42
Rb^+	67	57	51	47	44	
Cs^+	57	52	47	44		

Table 1.6 *Enthalpy Changes for Consecutive Solvation in the Gas Phase (ΔH in KJ mol^{-1}).*

Linkage of all binding sites in a single polydentate ligand suppresses this destabilisation effect, since the binding sites are held in place and cannot be pushed out of the shell by repulsions, as is the case for monodentate ligands (solvent molecules). Furthermore, it allows the introduction of more binding sites than the balance between

cation donor attraction and donor/donor repulsion permits in the solvated state. Clearly, once again the magnitude of this stabilisation will depend on the solvent in which complexation takes place.

1.1.4.5 Changes in the Interaction of the Cation with Solvent Molecules Outside the first Solvation Shell

In complexation, if a ligand has completely replaced a cation's first solvation sphere, then the radius of that cation effectively increases. This results in a weakening or breaking of interactions with molecules outside the first solvation sphere which is accompanied by an unfavourable enthalpy change, destabilising the resultant complex. The magnitude of this destabilisation will depend on the solvent, the charge/density ratio of the cation and the ligand thickness, increasing with (i) increasing charge density ratio of the cation, (ii) increasing solvent dielectric constant and (iii) increasing ligand shielding of the cation from the surrounding solvent.

1.1.4.6 Changes in Ligand Solvation

The degree to which the ligand is solvated in its free (relative to complexed) state, will contribute to the overall enthalpy change during complexation. If, in order to undergo complexation, the free ligand must be desolvated, then an unfavourable enthalpy change will result. Therefore, it may be inferred that the lower the solvation of donor sites in the free ligand, the lower the destabilisation will be upon complexation. This effect is most evident in solvents that are either protic (can potentially form hydrogen bonds with O, N, P or S donors) or of high dielectric constant.

1.1.4.7 Steric Deformations of the Ligand Due to Cation Complexation

If the cation proves to be too large, or too small, for the lowest free energy cavity defined by the ligand, then steric deformations of the ligand are necessary in order to ensure maximum interaction with that cation. Any deformation will result in an unfavourable enthalpy change. The more rigid the free ligand, the more unfavourable the enthalpy change will be and the magnitude of destabilisation will be proportional to the degree of ligand deformation as dictated by cationic radii in comparison to ligand cavity radius.

1.1.5 Contributions to Complexation Entropy

1.1.5.1 Desolvation of Cation and Ligand

On complexation, translational entropy increases as solvent molecules are released from both cation and ligand. The magnitude of this favourable entropic change increases as, (i) the charge density ratio of the cation increases, (ii) the solvent dielectric constant increases, (iii) the solvent changes from aprotic to protic and (iv) the basicity of the ligand donor atoms increases.

1.1.5.2 Changes in Internal Entropy of the Ligand Due to Orientation, Rigidification and Conformational Changes

In its free state, a ligand may exist in a number of conformations. The number of conformations displayed in solution will depend both on the flexibility of the free ligand, and on the nature of the solvent. Complexation generally confers a more rigid structure on a ligand,

invariably resulting in:

Rigidification: A loss of internal entropy will be experienced resulting in a negative, unfavourable entropy change. The magnitude of this destabilisation will increase as the ligand becomes less and less preorganised for complexation, *ie.* as ligand flexibility increases compared to its relatively rigid complexed state.

Conformational/Orientational Change: Complexation may involve adopting one of the ligands lowest free energy conformers, or adoption of a higher free energy conformation specific to complexation. Any deformation of the ligand from its lowest free energy conformation(s) to a conformation suitable for complexation, will result in an unfavourable entropy change. The magnitude of this destabilisation will increase as the rigidity of the ligand increases, and as the degree of ligand deformation increases.

It can thus be surmised that in order to enjoy maximum complex stability a ligand should be extremely rigid in its free state, and be in a conformation/orientation that best matches that needed for complexation.

1.1.5.3 Changes in the Number of Species During the Reaction

When complexation takes place in a solvent of low dielectric constant, a negative, unfavourable contribution is expected to the overall entropy. Two species come together to form one and a loss in translational energy results.

1.1.6 The Anion Effect

The complexation process can be represented more fully than in Equation 1.1.

$$M^+A^-_{(s)} + L_{(s)} \rightleftharpoons M^+L\,A^-_{(s)} \quad \text{where } A^- = \text{Anion.}$$

The nature of the counteranion of the metal salt has marked effects on the complexation process. In water and other highly solvating media, the charged complex and the anion are separately solvated and little anion effect on complex stability is expected. However, in poorly solvating media, varying degrees of ion pairing and/or aggregation may occur. Most often complexed ion pairs or ligand separated ion pairs are formed. Two types of anion dependent effects are expected:

(1) The electrostatic cation-anion interactions will depend on the properties of the anion: its charge, size, shape and its polarisability, large anions tend to weaker interactions because of larger cation-anion distances.

(2) The anion-cation interactions will also be affected by the dielectric constant of the surrounding solvent, a decrease of which will increase the strength of these interactions, making complexation less favourable.

Any situation in which cation-anion association is weakened, or broken, will destabilise the resultant complex. The effect will be greater the higher the attractive force that exists between the cation and anion in the uncomplexed salt in the solvent concerned.

The solubility properties of the anion (its lipophilicity) are also extremely important for dissolution of the complex in solvents of low polarity, large and soft inorganic and, much more so, organic anions, strongly increase complex solubility. These effects are particularly

pertinent in anion activation, extraction and cation transport processes.

The Synthetic Chemist

Armed with a thorough knowledge of cationic properties and the parameters that govern thermodynamic stability, the synthetic chemist is potentially in a position to design ligands of a desired stability and selectivity for a particular metal cation. However, as we shall see, thermodynamic stability and selectivity is not the only concern. Complexation kinetics are equally important, and functions for which ligands are designed (extraction, transport, lipophilisation, detection) may each demand defined reaction kinetics in conjunction with thermodynamic stability and selectivity.

1.1.7 Kinetics of Complexation

Molecular kinetics, *ie.* the dynamic behaviour of a system composed of ligand, cation and solvent, gives information about the lifetime of a complex. The complexation may be represented as follows:

$$M^+_{(s)} + \text{Ligand}_{(s)} \underset{k_d}{\overset{k_f}{\rightleftharpoons}} [M^+ \text{ Ligand}]_{(s)}$$

where k_f/k_d is directly related to the thermodynamic stability constant, K_s as follows:

$$K_s = \frac{k_f}{k_d}$$

Metal complexation in solution is generally a very quick reaction. However, Nuclear Magnetic Resonance studies[12] and relaxation curves[13]

have shown that complex formation does not occur instantaneously.

Two main schemes for complexation have been proposed. The Chock mechanism[14], envisages first a fast conformational change of the ligand into a conformation suitable for complexation, followed by complexation to the metal cation. This can be represented by the following sequence, where CR_1 and CR_2 are different free ligand conformations, and CR_2 represents the appropriate conformation for complexation.

$$CR_{1(s)} \rightleftharpoons CR_{2(s)} + M^+ \overset{\text{Step 1}}{\rightleftharpoons} CR_{2(s)}\cdots M^+_{(s)} \overset{\text{Step 2}}{\rightleftharpoons} CR_2M^+_{(s)}$$

The ligand is thought to form an encounter complex (Step 1) in which the metal lies outside of the ligand cavity, followed by cation encapsulation by the ligand in the rate determining step (Step 2).

The second mechanism is the so-called Eigen Valinomycin mechanism[15] wherein the formation of the M^+-ligand encounter complex is the first step, while desolvation and ligand rearrangement constitutes the second step and leads to the final complex. In this scheme it is envisaged that the second step is the rate limiting process. It is, however, being realised that both schemes represent an oversimplification of the actual mechanism.

We can write a general scheme as follows, in which $L'_{(s)}$ may or may not be in an appropriate conformation for complexation:

$$M^+_{(s)} + L'_{(s)} \underset{k_{21}}{\overset{k_{12}}{\rightleftharpoons}} M^+_{(s)}\cdots L_{(s)} \underset{k_{32}}{\overset{k_{23}}{\rightleftharpoons}} [M^+L]_{(s)}$$

If the reverse diffusion rate (k_{21}) is quicker than the encapsulation step (k_{23}), more encounters are required before complexation may occur. In this situation, the overall rate constant for the process may be written:

$$k_f = k_{23} \left(\frac{k_{12}}{k_{21}} \right)$$

This situation, in which k_{23} is the rate limiting process, is thought to occur for the vast majority of acyclic, cyclic and bicyclic ligands.

If the encapsulation rate (k_{23}) is rapid relative to the reverse diffusion (k_{21}), every encounter between the partners leads to the desired product and the whole process can be considered to be diffusion controlled, where the forward rate constant for the whole process, $k_f = k_{12} \approx 10^9 - 10^{10}$ (l mol s^{-1}).

Studies of the kinetics of complexation with cryptands (211), (221) and (222) in methanol have been performed[16] (Table 1.7). In all three cases, it can be seen that selectivity of the cryptands is reflected almost entirely in the dissociation rates. The formation rates show a monotonic increase with increasing cation size. The results strongly suggest that the transition state for the formation reaction lies very close to the reactants. The relatively high formation rates suggest that the required desolvation of metal ions is largely compensated for by interaction with the ligand in the transition state; the energy required decreasing as the solvation energy of the ions decreases. It is clear, however, that at this stage there is no specific interaction between the cryptands and the cations that strongly differentiates between the various cations. The subsequent steps in which the metal ion enters the cavity of the ligand, where the more specific size dependent interactions occur, must then proceed rapidly from this stage.

As the cryptands become larger, their flexibility increases and the formation rates show a concurrent increase. This can be rationalised by the fact that the more flexible a ligand, the more able it is to affect stepwise removal of solvent molecules, which ensures that ligand binding

energy may compensate more effectively for loss of solvation energy.

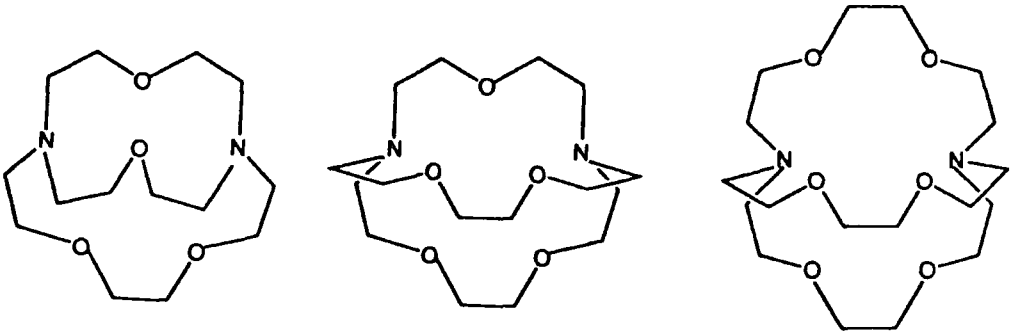

(2) (3) (4)

CRYPTAND	CATION	k_f (m^{-1} s^{-1})	k_d (s^{-1})
Cryptand 211 (2)	Li^+ (*)	4.8×10^5	4.4×10^{-3}
	Na^+	3.1×10^6	2.5×10^0
Cryptand 221 (3)	Li^+	1.8×10^7	7.5×10^1
	Na^+ (*)	1.7×10^8	2.35×10^{-2}
	K^+	3.8×10^8	1.09×10^0
	Rb^+	4.1×10^8	7.5×10^1
	Cs^+	5.0×10^8	2.3×10^4
Cryptand 222 (4)	Na^+	2.7×10^8	2.87×10^0
	K^+ (*)	4.7×10^8	1.8×10^{-2}
	Rb^+	7.6×10^8	8.0×10^{-1}
	Cs^+	9.0×10^8	$\approx 4 \times 10^4$

Table 1.7 *Complexation and Decomplexation Rates for Alkali Metal Cations With Cryptands (211), (221) and (222) Measured in Methanol at 25°C; *Cation which is most Selectively bound.*

This is a general trend, as the flexibility of the ligand decreases, traversing the series from left to right (Figure 1.4), so does the rate of complex formation.

ACYCLIC LIGAND	MONOCYCLIC LIGAND	BICYCLIC LIGAND	SPHERAND
10^7-10^9	10^6-10^8	10^4-10^8	10^2-10^5

Figure 1.4 *Rates of Complex Formation k_f (m^{-1} s^{-1}) for Common Ionophores for Alkali and Alkaline Earth Metal Cations.*

Studies by Cram[17] on spherands, and by Eyring and coworkers[18] on monocyclic systems, seem to suggest that, as for the cryptands, selectivity of these ligands for cations is also primarily governed by relative dissociation rates (Figure 1.5).

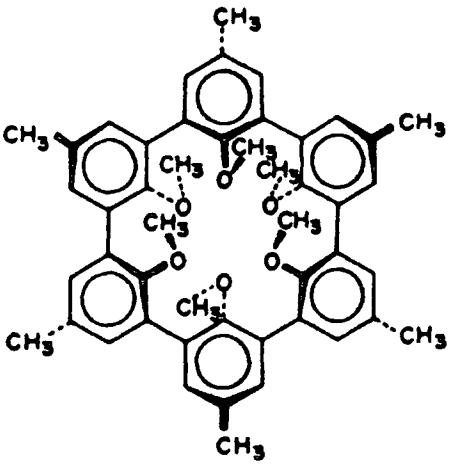

(5)

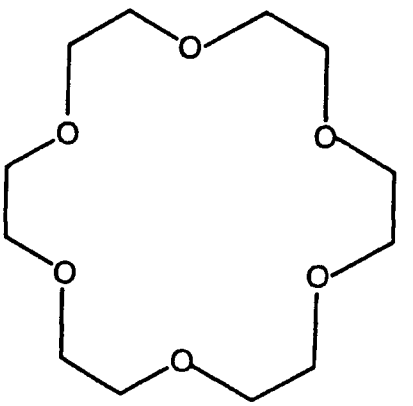

(6)

STRUCTURE	CATION	k_f (m^{-1} s^{-1})	k_d (s^{-1})
Spherand (5)	Li^+	7.5×10^4	$< 10^{-12}$
	Na^+	4.1×10^5	3.4×10^{-9}
Structure (6)	Na^+	2.2×10^8	3.4×10^7
	K^+	4.3×10^8	3.7×10^6
	Rb^+	4.4×10^8	1.2×10^7
	Cs^+	4.3×10^8	4.4×10^7

Figure 1.5 *Complexation and Decomplexation Rates for Alkali Metal Cations With Spherand (5) (Reference 18) and 18-crown-6 (6) (Reference 19) Measured in Water at 25°C.*

The factors affecting the kinetics of complexation are thus related to the flexibility of the free ligand, and the complex stability as governed by the thermodynamic parameters outlined in the first section. In the next section, various uses for ligands that form complexes with alkali and alkaline earth metals are outlined, along with the design features pertinent to to ligand applicability.

1.1.8 Uses of Synthetic Ligands that Complex Alkali and Alkaline Earth Cations

1.1.8.1 Lipophilisation

Solubilisation of salts in organic solvents of low polarity, and ion pair dissociation by complexation of the cation with a lipophilic ligand, may bring about interesting and useful changes in the properties of the associated anion.

Comparing different ligands, activation of associated anions should be highest for those ligands that impose a high cation-anion distance (*ie.* ligands with thick organic layers). However, the larger the separation of these ions, the less soluble the system is expected to be in organic media. Therefore, a compromise between cation-anion separation, and solubility of the complex, has to be found. Suitable ligands for this purpose should thus: (i) display high K_S values for complexation with the countercation (fast association, slow dissociation) and (ii) be of sufficient lipophilicity and thickness to allow both the solubility of ligand-cation complex, and reasonable cation-anion separation to occur.

Selectivity is not generally a consideration, though if the ligand is to be used in a system where two salts are present ($M_1^+X_1^-$ and $M_2^+X_2^-$), and lack of discrimination between M_1^+ and M_2^+ leads to naked anions X_1^- and X_2^- that compete to react with substrate(s), then selectivity may be important.

1.1.8.2 Substrate Detection

If a ligand is to act as a non-destructive analytical reagent for a particular cation, then:

(1) A functional grouping must be present in order to give a quantitative complexation signal. Chromogenic ligands have been popular, as they are subject to electronic influences, either from ligand, cation or both.

(2) If the detection is to reflect the concentration of a cation (M_1^+), then the stability of the complex need not be very high in the solvent chosen. The concentration of the complex as detected by a scaled spectral or other change, will be a function of the metal ion (M_1^+) concentration irrespective of the equilibrium constant. High association rate for complexation is the important criterion.

(3) If the ligand is designed to sense one particular cation, either it must show an extremely high selectivity for that cation, or be of such a design that only the binding of that cation will activate the complexation signal.

(4) The lipophilicity of the ligand must be sufficient so as to confer both its own solubility and solubility of the resultant complex in the solvent chosen.

1.1.8.3 Extraction

The extraction process can be represented diagrammatically (Figure 1.6).

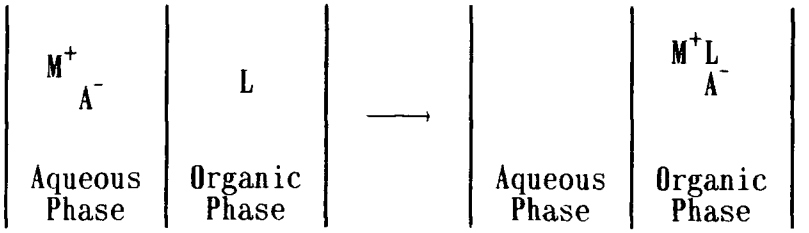

Figure 1.6 *Diagrammatic Representation of the Extraction Process; L = Ligand.*

This represents a situation in which all of the metal cation-anion salt has been extracted from the aqueous phase into the organic phase. In practice this is an unlikely occurrence.

An equation for the extraction process may be written (Equation 1.5) where the extraction constant is k_e.

$$M^+_{(aq)} + A^-_{(aq)} + L_{(org)} \overset{k_e}{\rightleftharpoons} M^+L\ A^-_{(org)} \qquad (1.5)$$

The individual equilibria as follows:

$$M^+_{(aq)} + A^-_{(aq)} + L_{(aq)} \overset{K_s}{\rightleftharpoons} M^+L\ A^-_{(aq)} \qquad (1.6)$$

$$\text{where } K_s = \frac{[M^+L\ A^-]_{aq}}{[M^+]_{aq}[A^-]_{aq}[L]_{aq}}$$

$$L_{(aq)} \overset{P_e}{\rightleftharpoons} L_{(org)} \qquad \text{where: } P_e = \frac{[L]_{org}}{[L]_{aq}} \qquad (1.7)$$

$$M^+L\ A^-_{(aq)} \overset{P_c}{\rightleftharpoons} M^+L\ A^-_{(org)} \qquad \text{where: } P_c = \frac{[M^+L\ A^-]_{org}}{[M^+L\ A^-]_{aq}} \qquad (1.8)$$

Therefore, it can be seen that the extraction constant, $k_e = K_s P_e P_c$. The extraction constant (k_e) is thus strongly influenced by the aqueous stability constant (K_s) and the partition coefficient of the ligand and its complex between the aqueous and organic phases.

If a ligand is to act as a selective extractant for a particular

metal ion (M_1^+) then: (i) the thermodynamic stability of the resultant complex must be high, (ii) the kinetics of complexation should display high association and slow dissociation rates, (iii) the ligand should show a high selectivity for the cation (M_1^+) and finally, (iv) the lipophilicity of the ligand should be sufficient so as to confer high values for P_e and P_c. Added to this, the nature of the counteranion will have a large effect on the efficiency of extraction: large, soft inorganic or organic anions will aid the extraction process, whereas small, hard anions will be detrimental.

1.1.8.4 Carrier Facilitated Transport

Diffusion controlled carrier facilitated passive transport amounts to extraction at one interface and release at another (Figure 1.7).

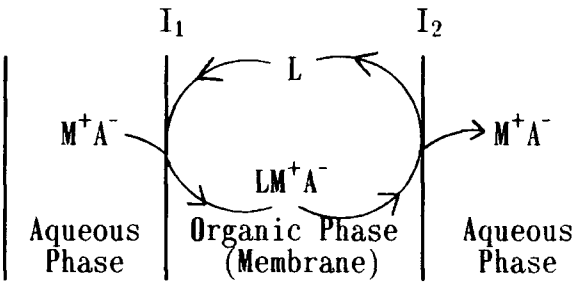

Figure 1.7 *Diagrammatic Representation of Carrier Mediated Transport Through a Membrane; I_1, I_2 = Interfaces; M^+ = Metal Cation; L = Ligand; A^- = Anion.*

Many of the considerations pertinent to extraction, lipophilicities of carrier and counteranion, solvent, and the binding of the ligand, are also pertinent to transport.

The early work on carrier facilitated diffusion of salts through liquid membranes involved acyclic ligands, monocyclic ligands and bicyclic ligands (Cryptands). It has been demonstrated that simple modifications applied to basic (2) cryptands can dramatically alter the transport rates and selectivities for alkali and alkaline earth metal

cations[19] (Figure 1.8).

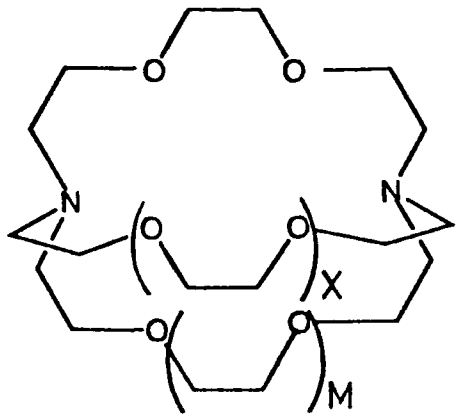

	M	X
(1a)	1	O
(1b)	1	CH_2
(1c)	2	O
(1d)	2	CH_2
(1e)	2	OCH_2CH_2O
(1f)	2	$(CH_2)_4$

CATION	TRANSPORT RATE (μmol/hr).		COMMENTS
	(1a)	(1b)	
Li^+	0.05	1.00	(1a) binds Li^+ best but
Na^+	0.60	3.00	transports Na^+ best; (1b) binds
Ca^{2+}	0.10	2.00	and carries Na^+ best.
	(1c)	(1d)	
Li^+	3.50	0.03	(1c) binds Na^+ best but
Na^+	0.25	3.50	transports Li^+ best; (1d) binds
Ca^{2+}	0.40	0.08	and carries Na^+ best.
	(1e)	(1f)	
Li^+	0.60	1.60	(1e) binds K^+ best but carries
Na^+	0.03	3.60	Ca^{2+} best; (1f) binds and
Ca^{2+}	2.90	0.07	carries K^+ best.

Figure 1.8 *Structural Modifications of Receptors into Carriers of Picrate Salts.*

Cryptands (1a), (1c) and (1e) selectively bind lithium, sodium and potassium ions respectively, yet they do not selectively transport these ions. However, in the case of ligands (1b), (1d) and (1f), the cation selectively bound is also the cation that is selectively transported. It has been shown[20,21] that carrier facilitated transport is neither proportional to stability constants, nor to extraction constants, but

rather shows a bell-shaped dependence on extraction constants. Transport proceeds most efficiently at one half carrier saturation and stops when the concentration gradient becomes vanishingly small [the value of $\log k_e \simeq 5$ at this point and the value of k_e is termed $k_e(max)$]. It is apparent that if the extraction constant is too high ($\log k_e > 5$), then there will be a tendency for carrier saturation to occur. Extraction into the organic phase will begin at a high rate in proportion to the high extraction constant, but slow dissociation of the complex into the receiving phase, will mean the number of free ligands at interface 1 (Figure 1.7) will quickly fall, resulting in a concurrent drop in transport rate.

The goal of most transport experiments through either bulk liquid or emulsion based membranes, is to achieve selective removal of a given cation (M_1^+) among others. The selectivity for one cation over another is not directly related to transport ratios measured in separate experiments, nor to the ratio of extraction constants, but rather, the selectivity of transport in a competition experiment depends on where the cations individual extraction constants lie with respect to $k_e(max)$. The following situations may occur:

1. $k_e(B) << k_e(A) << k_e(max)$ $\qquad V_B < V_A$
2. $k_e(B) << k_e(max) << k_e(A)$ $\qquad V_B \leq V_A$ or $V_B \geq V_A$
3. $k_e(max) << k_e(B) << k_e(A)$ $\qquad V_B > V_A$

where: $k_e(A)$ = extraction constant for cation A
$k_e(B)$ = extraction constant for cation B
V_A = transport rate for cation A
V_B = transport rate for cation B

Therefore, it may be surmised that maximum selectivity for a ligand for cation (A) in a membrane transport competition experiment will be experienced when k_e for the (Ligand, Cation A) extraction is as near as

possible to $k_e(max)$ and the ratio of $k_e(A)$ to $k_e(B)$ or $k_e(C)$ is as high as possible.

A short appraisal of the thermodynamics and kinetics of complexation between alkali and alkaline earth metal cations and neutral ligands has been given. The synthetic chemist, as experimental data increases, is more and more able to design ligands for a particular function.

1.1.9 Measurement of Selectivity and Stability of Complexation

There are many methods by which people have sought to measure the stability and selectivity of complexation between ligand and cation. It is thought best to list these methods in a tabular form outlining the limitations and disadvantages of each technique. Table 1.8 includes references to these experimental methods and the theory behind the methodology.

True comparisons for selectivity and stability of complexation cannot be made if different techniques have provided data for that comparison. It is vital to report the conditions in which measurements have been made, for, as has been pointed out, the nature of solvent and counteranion can markedly affect both the stability and selectivity of complexation. A worthwhile comparison may thus only be made when: (i) the same technique is used for measurement, (ii) a constant counteranion is used, (iii) the temperature remains constant and (iv) solvent remains unchanged for all measurements.

TECHNIQUE	ΔG	ΔS	ΔH	LOG‡	COMMENTS	SELECTIVITY DATA	COMMENTS
1. CALORIMETRY (Ref.22-25)	√	√	√	√	1) Accurate for the range log k(s) = 1-5. 2) Relies on ΔH being non-zero.	Thermodynamic selectivity by comparing separate LOG‡ values.	Not directly proportional to competitive selectivity.
2. CONDUCTANCE (Ref.26-29)	√	√	√	√	For large complexes mobility of the cation is low & k(s) values are unreliable.	Thermodynamic selectivity by comparing separate LOG‡ values.	Not directly proportional to competitive selectivity.
3. POTENTIOMETRIC							
a) Ion selective electrodes (Ref.30-32)	√	x	x	√	1) Accurate for the range log k(s) = 1-5. 2) Assumes constant anion activity. 3) Assumes complete dissociation. 4) Limited to certain cations and solvents.	1) SINGLE SOLUTION METHOD - Selectivity by comparing separately measured LOG‡ values. 2) MIXED SOLUTION METHOD - Selectivity by competition experiment.	1) Not directly proportional to competitive selectivity. 2) Is directly proportional to competitive selectivity.
b) pH metric (Ref.33-36)	√	x	x	√	1) Demands solubility in water or alcoholic solvents. 2) Requires pH sensitive ligands. 3) Protonation and deprotonation must be fast.	Thermodynamic selectivity by comparing separate LOG‡ values.	Not directly proportional to competitive selectivity.

Table 1.8 *Methods Used to Measure Stability and Selectivity of Complexation; ‡LOG = Log* k_s.

TECHNIQUE	ΔG	ΔS	ΔH	LOG‡	COMMENTS	SELECTIVITY DATA	COMMENTS
4. $^{13}C/^{1}H$ NMR (Ref.37-40)	√	x	x	√	1) LOG‡ limits 1-4. 2) Must determine the stoichiometry of complexation before accurate k(s) can be calculated.	^{7}Li, ^{23}Na, ^{137}Cs NMR competition experiments are possible.	Can gain information on energetics of cation exchange from free ligand → bound, hence gain ΔG values (exchange) which are related to relative dissociation rates.
5. FAST ATOM BOMBARDMENT MASS SPECTROMETRY (Ref.41-44)	?	x	x	?	1) LOG‡ values claimed for fast exchanging systems. Qualification is dangerous.	Competition experiments give selectivity ratios where cations are competing for a deficiency of ligands	TRUE competitive selectivity, though questionable whether it represents selectivity at equilibrium. The technique is quick and easy to perform.
6. EXTRACTION	x	x	x	*	Log k(e) values seem to parallel trends in log k(s) values.	1) SINGLE EXTRACTION - Can compare separate extraction constants. 2) MIXED EXTRACTION - Competitive extraction experiment.	1) Not proportional to competitive selectivity. 2) Proportional to competitive selectivi though questionable whether selectivity a equilibrium is being measured. Must use constant counteranion for measurement of accurate selectivity.

Table 1.8 *Methods Used to Measure Stability and Selectivity of Complexation;* **(cont'd)** ‡*LOG = Log* k_s; * = *Log* k_e.

1.2 EVOLUTION OF CATION RECOGNITION

The discovery by Pederson in 1962[45], only reported in 1967[3,46] of the remarkable properties of the polyether macrocycles led to the synthesis and study of numerous macrocyclic ligands. Since that time, a great many varieties of cation receptor architectures have been explored. In this section, a short review of the evolution in cation recognition is given. Figure 1.9 depicts an evolution in topological complexity of cation complexes.

1.2.1 Acyclic Ligands

Acyclic ligands represent collections of binding sites held together by appropriate spacer units. These ligands are generally flexible, and will exist in a number of low energy conformations in solution, and therefore cannot be described as preorganised for binding of alkali and alkaline earth metal cations. Complexation necessitates:

(1) Desolvation of ligand binding sites - In their lowest free energy conformations in solution, acyclic ligands will tend to be rather open structures and hence binding sites will tend to be solvated. In order for favourable interactions to occur between binding site and metal cation, desolvation of these sites must occur. This results in a greater enthalpy loss than for the generally less solvated monocyclic and bicyclic structures.

(2) Adoption of a wrapped complexed state - The guest cation must organise the acyclic ligand into a relatively fixed binding conformation. For these flexible ligands, considerable unfavourable entropy loss is experienced as well as an increase in ground state conformational enthalpy.

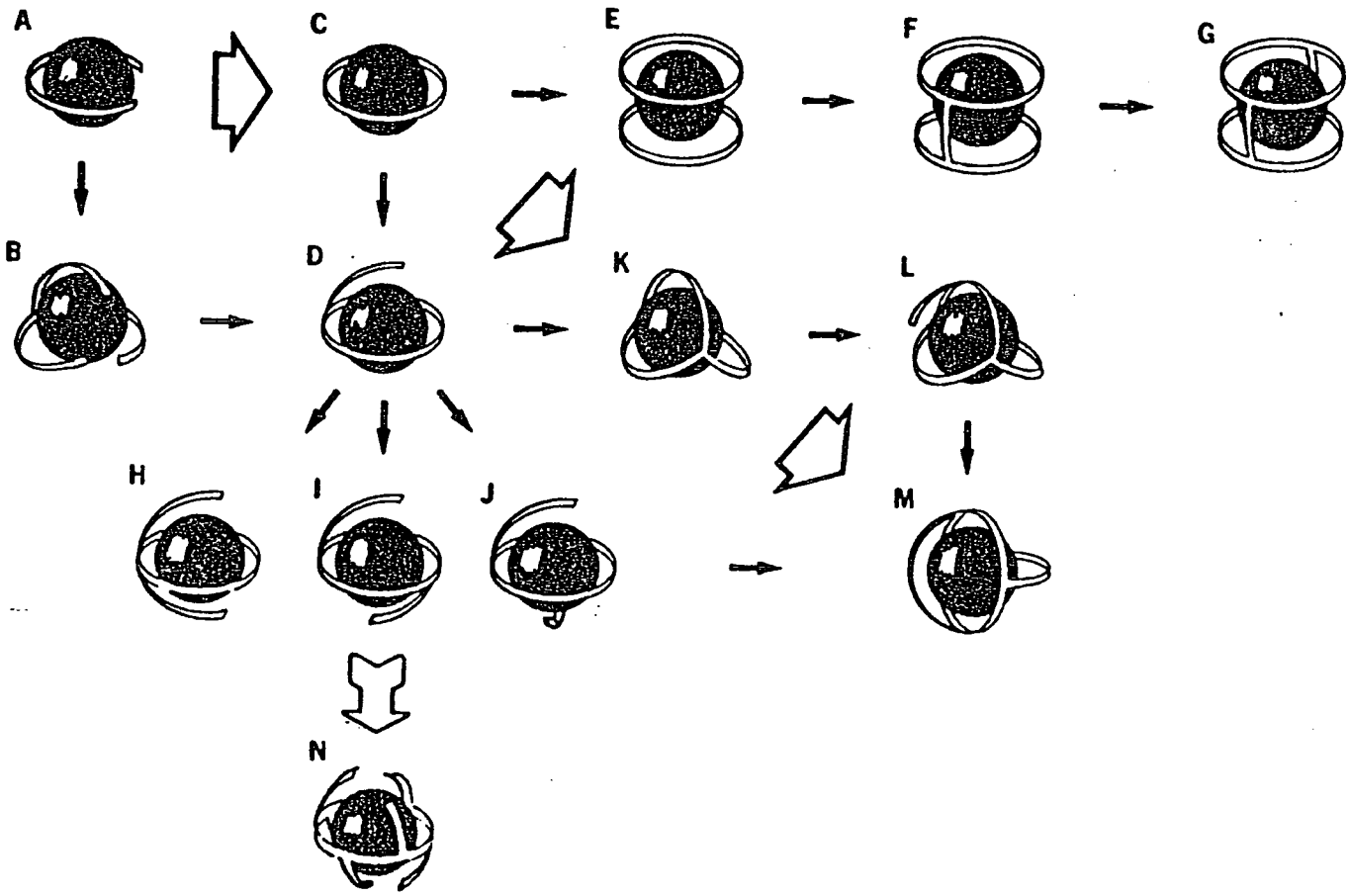

Figure 1.9 *Evolution in Topological Complexity of Cation Complexes.*

For these reasons, acyclic ligands will generally form less stable complexes than the more preorganised, less flexible, monocyclic and bicyclic structures. However, this doesn't imply that high selectivities for particular cations will be impossible. The selectivities and stabilities of complexes with these ligands will depend on the factors outlined in Section 1.1. Through appropriate design, acyclic ligands may show high selectivity for a particular cation.

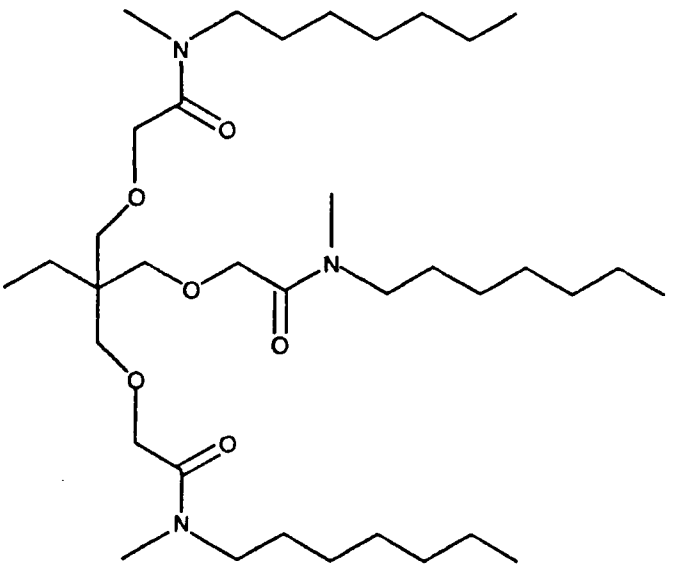

(7)
(Sodium Selective Ionophore)

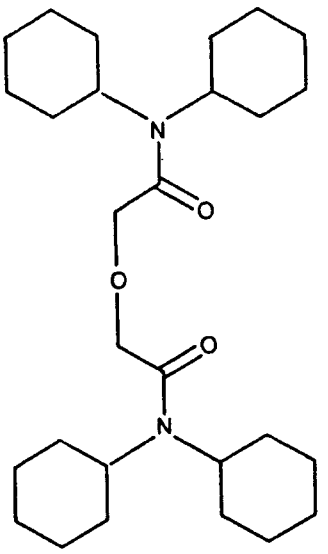

(8)
(Calcium Selective Ionophore)

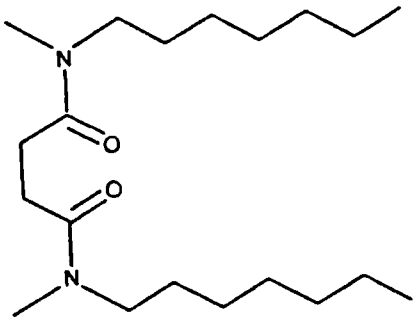

(9)
(Magnesium Selective Ionophore)

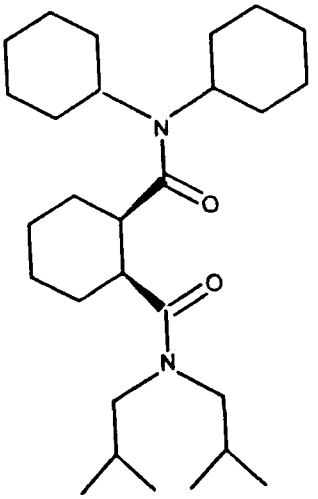

(10)
(Lithium Selective Ionophore)

Figure 1.10

The flexibility of acyclic ligands renders the rates of complex formation and dissociation reasonably fast. They are thus viable candidates as neutral ion selective carriers for membranes. Indeed, ion selective electrodes for sodium[47], potassium[48], magnesium[49] and lithium[50] have been developed (Figure 1.10).

1.2.2 Cyclic Ionophores

1.2.2.1 Two Dimensional Recognition: Crown Ethers

When the ends of a polyethylene chain are connected to form a ring as in crown ethers, the number of possible low energy conformations for the free ligand in solution is greatly diminished. Accordingly, crown ethers form complexes that are more stable than their open chain counterparts. If the stability constants for ligands (11) and (12) with potassium in 99% methanol/water are compared (Figure 1.11) it can be seen that stabilisation on going from the acyclic ligand (11) to 18-crown-6 (12) amounts to nearly 10^4.

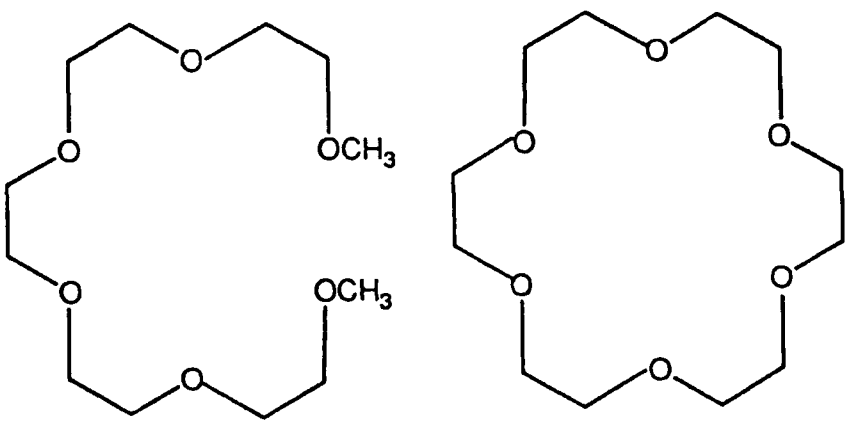

	(11)	(12)
log k_S (K^+)	2.27	6.05

Figure 1.11 *Log K(s) measured at 25°C in 99% MeOH/H_2O.*

This behaviour had been dubbed the *macrocyclic effect* and it can be quantified as the ratio of complex stabilities for a macrocyclic receptor over an analogous acyclic one bearing the same set of binding sites, with a given cation, in a give solvent, at a given temperature. The thermodynamic origins of this effect are still matters of debate[7,51-57].

The backbone of crown ethers is inherently less flexible than open chain polyethers and these ligands can be thought of as more highly preorganised for complexation than their acyclic counterparts. However, Dunitz' crystal structures[58-61] of 18-crown-6 (13) and those of its K^+SCN^- complex (14) show that the free ligand and the ligand in its potassium complex have different conformations (Figure 1.12).

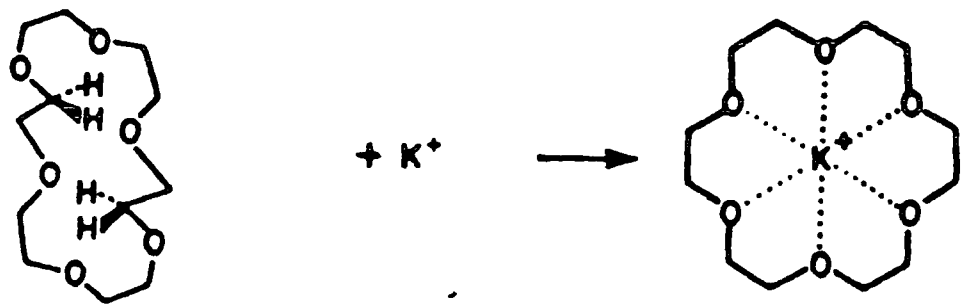

(13) (14)

Figure 1.12 *Representation of the Crystal Structures of 18-Crown-6 (13) and its Potassium Thiocyanate Complex (14).*

The potential crown cavity of the free ligand is filled with two inwardly turned methylene groups, and the electron pairs of two of the oxygen donors face outward and away from the best centre of the roughly rectangular structure. Therefore, the free ligand does not have a crown shape nor a cavity. Only when the oxygen donors become engaged with a cation such as potassium, does a filled cavity develop. In other words, potassium conformationally organises 18-crown-6 on complexation. This shows that unsubstituted crown ethers cannot be thought of as wholly

rigid molecules, but rather, relatively flexible ligands that can be organised by the incoming cation so as to enjoy maximum interaction.

The cyclic structure, however, does restrict ligand adaptation, and so monocyclic ligands can be expected to show a peak selectivity for size. Table 1.9 lists the cationic radii for alkali and alkaline earth metal cations along with the cavity diameters of simple crown ethers[9,62-64].

COMPOUND	DIAMETER (Å)	RADIUS (Å)
12-CROWN-4	1.2	Li^+ 0.73
15-CROWN-5	1.8	Na^+ 1.02
18-CROWN-6	2.8	K^+ 1.38
21-CROWN-7	3.8	Rb^+ 1.49
		Cs^+ 1.70

Table 1.9 *Radii of Alkali Metal Cations and Cavity Diameters of Some Simple Crown Ethers.*

Indeed we see that for potassium and caesium ions, the crown ethers that exhibit the most complementary cavity radius (18-crown-6 and 21-crown-7 respectively), form the most stable complexes (Figure 1.13)[10,24]. However, various studies have shown[2,10,24,65] that the relative size of ligand cavity and cationic radii are not the only factors that determine the stability and selectivity of complexes formed (Figure 1.14). The anomaly in this graph is sodium. Instead of showing the highest log K_S value for the best fit 15-crown-5, its most stable complex is found with 18-crown-6. Furthermore, 15-crown-5, rather than showing a distinct preference for sodium over other cations, appears to bind indiscriminately. The reason for this is that sodium prefers a coordination number of six , and is able to organise the flexible 18-crown-6 skeleton into a conformation such that interaction with all six donors is possible. The flexibility of the 18-crown-6 ligand

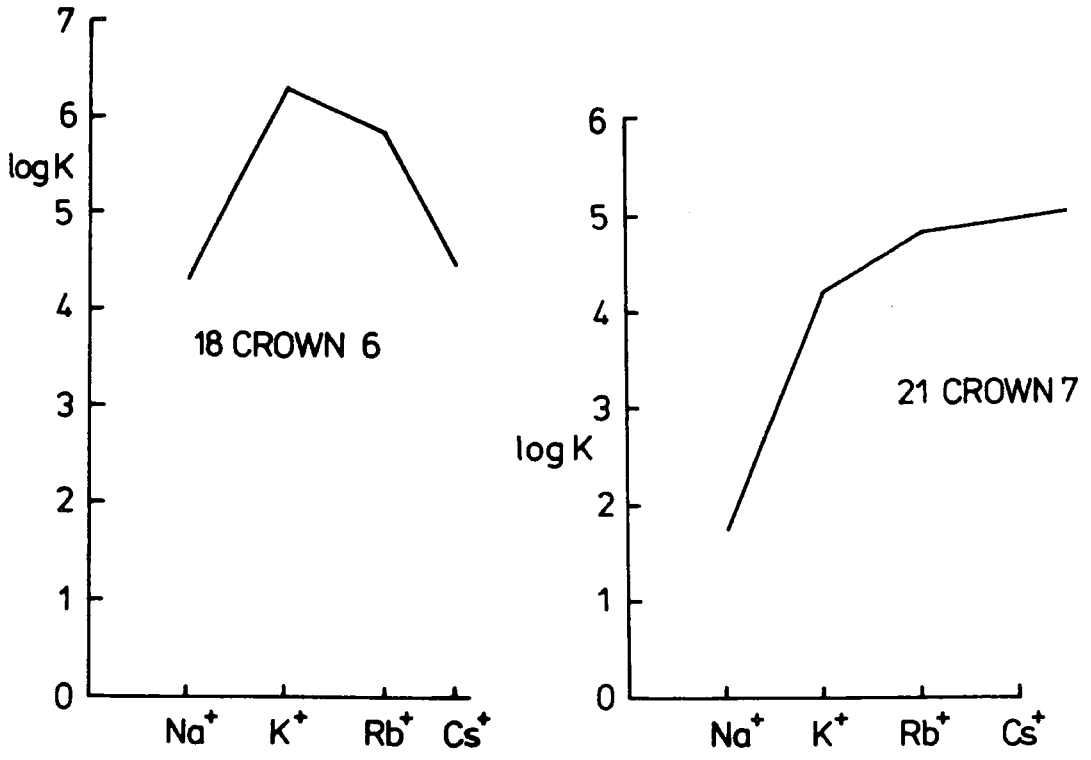

Figure 1.13 *Stability of Crown Ether Complexes With Various Alkali Metal Ions in Methanol at 25°C.*

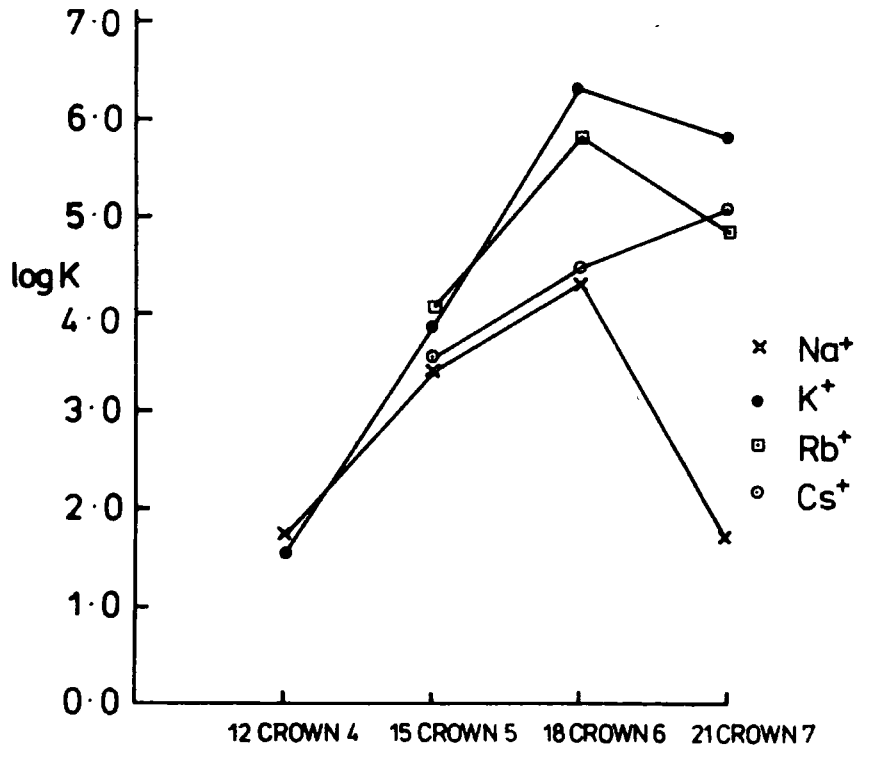

Figure 1.14 *Stability and Selectivity of Crown Ether Complexes in Methanol at 25°C.*

ensures that conformational changes are not highly energetically unfavourable. For these relatively flexible simple crown ethers, there are effects other than spatial fit operative in determining selectivity and stability patterns.

Crown ethers mentioned to date, effect a circular recognition. The optimal 1:1 complexes are bidimensional and desolvation of the cation is incomplete. The crowning of 18-crown-6 by K^+SCN^- as revealed by X-ray crystallography (Figure 1.12), still leaves two accessible surfaces of the ion.

As mentioned in Section 1.1.4, the complexing ability of a ligand will tend to increase as the number of donor sites increases, provided the advantage associated with the number of donor sites is not over-compensated by steric crowding. Clearly, as the alkali and alkaline earth metal cations can be considered spherical in shape, a three-dimensional recognition might lead to higher complex stabilities and selectivities than those displayed through two-dimensional recognition by crown ethers. The crystal structure of the potassium complex of dibenzo-30-crown-10[66] is shown in Figure 1.15.

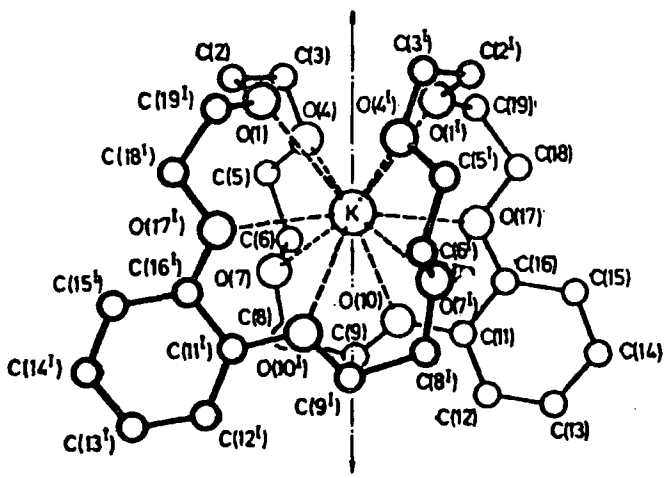

Figure 1.15 *Crystal Structure of the Potassium Complex of Dibenzo-30-Crown-10.*

This exhibits a three-dimensional recognition of the potassium ion. However, if the stability constant for this potassium complex (K_S = 4.6 in methanol at 25°C) is compared to that of the potassium 18-crown-6 complex (K_S = 6.29 in methanol at 25°C), it is seen that the former is less stable. This reflects the fact that in order to complex the potassium ion, the dibenzo-30-crown-10 ligand undergoes large deformation from its lowest free energy equilibrium conformation(s). The unfavourable free energy change that results from this deformation over-compensates for the spherical array of ten donor sites that coordinate to the potassium ion constituting a higher interaction energy than the six donor sites available in the 18-crown-6 ligand.

1.2.3 Three Dimensional Recognition

1.2.3.1 Bis Crown Ethers

Three dimensional recognition of an alkali or alkaline earth metal cation is possible through further interaction by a crown ether complex with another crown ether moiety, such that the cation is sandwiched between the two crown ether rings (Figure 1.16).

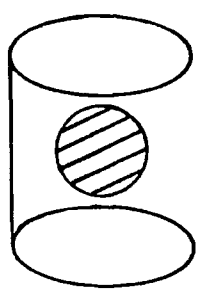

Figure 1.16 *Diagrammatic Representation of a 2:1 Crown Ether: Cation Complex.*

The 2:1 complexes may form when the cation is too large to fit into

one crown ether cavity and the counteranion does not strongly coordinate. However, complexes formed in this manner tend to be less stable than their respective 1:1 complexes (Table 1.10)[67].

COMPLEX	A	B
1:1 log K_S (1)	3.6	4.2
2:1 log K_S (2)	2.9	1.9

Table 1.10 *Log K(s) values for 1:1 and 2:1 Complexes of Caesium Measured in Methanol at 25°C; A = Cs^+ Dibenzo-18-crown-6; B = Cs^+ Dibenzo-21-crown-7.*

Outright covalent linkage of two crown ether moieties would be expected to eliminate some of the intercrown repulsions and some of the unfavourable loss of entropy associated with the formation of 2:1 sandwich complexes. However, this linkage must neither be so short as to limit the size of the tridimensional cavity, nor so long as to require energetically demanding conformational changes of the bridge in order to bring the rings close enough for cooperative interaction with the metal cation.

Demonstration of the importance of an appropriate geometry of the linking moiety between crown ether units can be seen by examining the complexation of bis-crown ethers (15) and (16)[68,69] (Figure 1.17).

The bis-crown derived from maleic acid (15), forms 2:1 sandwich complexes with potassium, rubidium and caesium ions, whereas the bis-crown derived from fumaric acid (16) does not form a sandwich complex with any such cation. This is because the unfavourable geometry of the linking chain in ligand (16) prevents the cooperation of the two crown ether moieties. Thus, it is seen that the extraction of potassium by bis-crown-(15) is fourteen times more efficient than for bis-crown-(16).

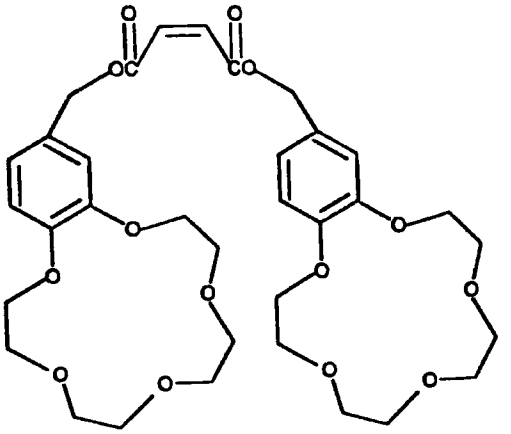

(15)

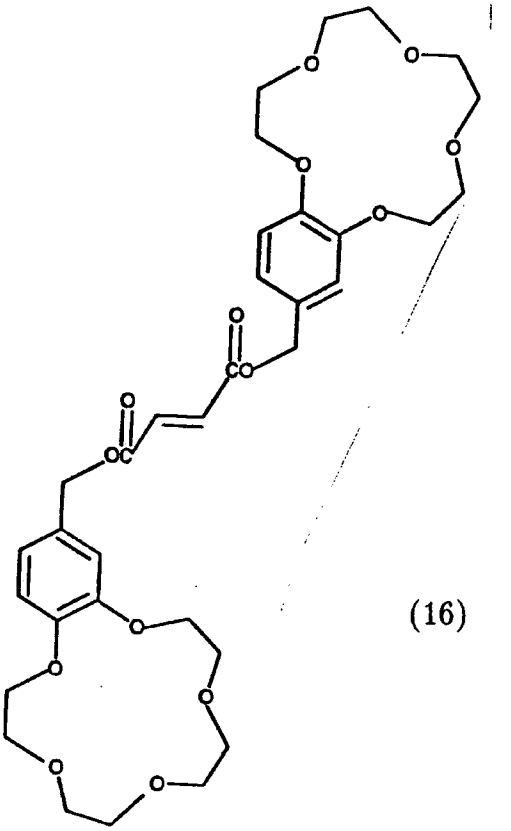

(16)

Figure 1.17

The length of the linking chain is also important. Kimura[70] synthesised the ligands (17)-(19) and the selectivities of these ligands for sodium and potassium were measured (Figure 1.18).

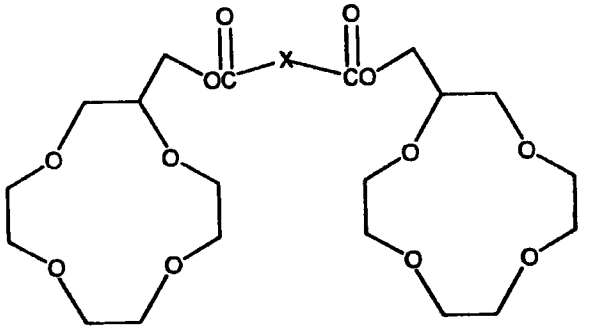

(17) X = $>C(C_2H_5)_2$
(18) X = $>C(CH_3)(C_{12}H_{25})$
(19) X = C_2H_4

LIGAND	$\frac{K_S(Na^+)}{K_S(K^+)}$	log $K_S(Na^+)^{\ddagger}$
(17)	27	3.25
(18)	34	3.26
(19)	9.5	2.88

Figure 1.18 *The Effect of the Linking Moiety in Complexation of Sodium and Potassium for Bis-Crowns (17), (18) and (19); ‡Values were measured in methanol at 25°C using sodium and potassium selective electrodes.*

On increasing the malonate linking chains of ligands (17) and (18) to the succinate chain of ligand (19), a decrease in sodium selectivity

relative to potassium is seen. Furthermore, it can be seen that the stability (log K_S) for the ligand (19) sodium complex, is significantly lowered relative to the log K_S values for sodium complexes of ligands (17) and (18).

The size of the crown rings are important. As has been mentioned, it is only possible for strong cooperative interactions to occur between two crown ether moieties if the cation size exceeds that of the crown ether cavity. If there is a good size fit between cation and crown ether, then the cation will only interact effectively with one ring.

Therefore, through appropriate choice of ring size and linking moiety, high selectivities can be achieved. Indeed, research into bis-crowns has generated viable candidates for use in ion selective electrodes for sodium[71], potassium[72] and caesium[72] (Figure 1.19).

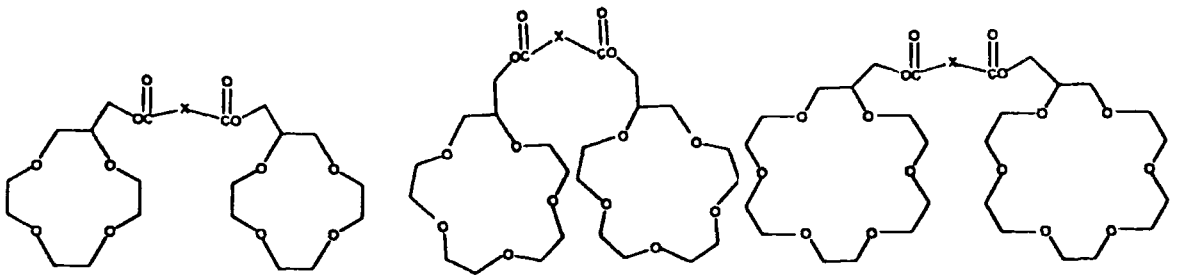

(18) *(Na^+ Selective) Ionophore*

(20) *(K^+ Selective) Ionophore*

(21) *(Cs^+ Selective) Ionophore*

Figure 1.19

The bis-crowns (18), (20) and (21) are composed of flexible crown ether moieties and a flexible linking chain. This ensures that complexation and decomplexation rates are fast, which coupled with high selectivities and lipophilicity, renders them as viable candidates for neutral carrier mediated transport across membranes.

A recent development in the chemistry of bis-crowns is the use of photo responsive bis-crowns, such that extraction and transport of cations may be photo-regulated[73-76] (Figure 1.20).

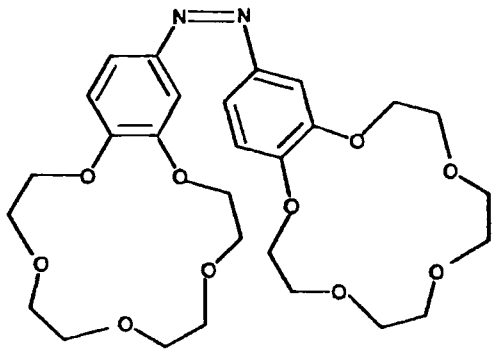

(*cis*)-(22)

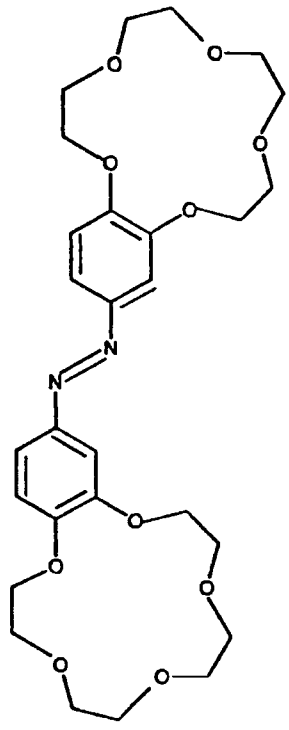

(*trans*)-(23)

Figure 1.20

Irradiation converts the *trans* form into the *cis* form. The process is reversible in that once the irradiation ceases the *cis* form relaxes back into the *trans* configuration.

Extraction experiments were performed with alkali metal salts of methyl orange in a water/dichloromethane system[76]. It was found that the *trans* form extracted sodium 5.6 times more efficiently than the *cis* form, and that the *cis* form extracted potassium 42.5 times more efficiently than the *trans*. Therefore it can be seen that the photo-regulated *trans* ⇌ *cis* isomerism results in a potential 238-fold selectivity for sodium with respect to potassium.

Kimura[77], has shown that through the use of monoaza bis-crown ethers, cation transport may be regulated by pH. The ligand (24) was synthesised and dissolved in nitrophenyl-octylether and impregnated into microporous polypropylene films. Competitive transport of alkali metal cations was carried out at 25^{o}C using a glass cell which was divided into two compartments by the impregnated membrane. The pH of the

aqueous source phase was varied and the selectivity patterns were measured (Figure 1.21).

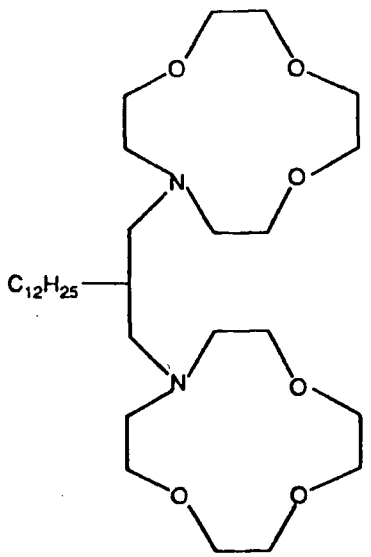

(24)

pH	Li^+	Na^+	K^+	Rb^+	Cs^+
10	0.01	1	0.05	0.03	0.01
9	0.09	1	0.18	0.11	0.02
8	0.34	1	0.71	0.79	0.60
7	0.41	1	0.94	1.05	0.68
5	0.79	1	1.78	1.90	1.90

Figure 1.21 *Variation in the Selectivity Ratios for Alkali Metal Cations for Ligand (24), Changing pH as Measured Potentiometrically at 25°C.*

As the pH of the aqueous source phase is lowered, ligand (24) gradually becomes protonated. This leads to a suppression of alkali metal complexing ability due to electrostatic repulsion between the proton and the incoming metal ion. Therefore the selectivity for sodium is lowered until eventually (pH 5) the membrane exhibits a selectivity pattern identical to that of a nitrophenyl-octylether membrane containing no ionophore. This ionophore system is of academic interest only and has no practical value.

1.2.3.2 C-Pivot Lariat Ethers

Gokel[78] surmised that there is a possibility of augmenting the binding of a simple monocyclic crown ether by incorporating a side arm which contains a donor atom. To examine this he synthesised a family of

C-pivot lariat ethers (25a)-(25f) where the side arm is joined directly to a carbon atom on the crown ether ring. Extraction studies were performed in a dichloromethane/water system at 25°C using picrate salts of sodium and potassium and a number of C-pivot lariat ethers (Figure 1.22).

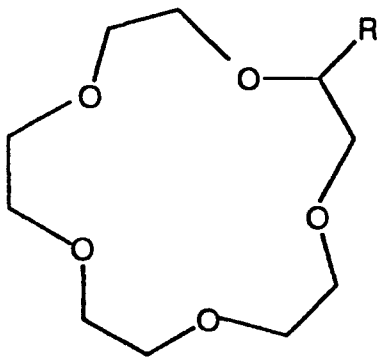

(25)

LIGAND	Na^+	K^+
(25a) R=H	7.6	5.7
(25b) R=CH_2OMe	5.1	3.3
(25c) R=$CH_2O(CH_2)_2OMe$	18.0	13.7
(25d) R=$CH_2(OCH_2CH_2)_2OMe$	15.7	24.4
(25e) R=$CH_2OC_6H_4OMe$ (para)	6.4	
(25f) R=$CH_2OC_6H_4OMe$ (ortho)	15.7	

Figure 1.22 *Extraction Constants for C-Pivot Lariat Ethers with Sodium and Potassium Ions in a Dichloromethane-Water System (25°C).*

It was inferred that for ligand (25b) the donating group is inappropriate for axial ligation and hence merely functions so as to sterically inhibit 1:1 complexation of both sodium and potassium rendering extraction lower than that of the unsubstituted cycle (25a).

Extraction increases markedly for ligands (25c) and (25d) over that of the unsubstituted ligand (25a). Clearly, donor groups are now in a favourable orientation to interact with the metal cations. Equally, the more efficient extraction by ligand (25e) over (25f) re-emphasises the point that enhanced extraction over an unsubstituted crown ether will only be seen if the donor group of the sidearm is in an appropriate orientation to augment interaction of the crown ether ring with the metal cation.

In a later study, Gokel[79] measured the stability constants of ligands (25a)-(25c), (25e) and (25f) with sodium in a 90% methanol-water

system using sodium ion selective electrodes at 25°C (Figure 1.23).

LIGAND	log $K_S(Na^+)$
(25a)	2.97
(25b)	2.74
(25c)	2.83
(25e)	2.97
(25f)	2.56

Figure 1.23 *Stability Constants for Complexation of some C-Pivot Lariat Ethers with Sodium Ions, Measured Using a Sodium Selective Electrode in 90% Methanol/Water at 25°C.*

This data conflicts with the extraction studies, in that no augmentation in stability for sodium complexation by C-pivot crown ethers is seen, over the unsubstituted derivative (25a). Indeed, data would suggest that any substitution on the crown ring is detrimental to sodium complexation in homogeneous media.

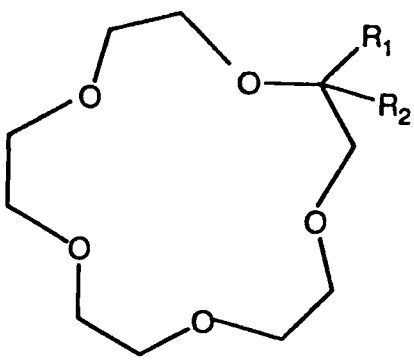

LIGAND	log K_S (Na^+)
(25a) R^1=H; R^2=H	2.97
(25b) R^1=H; R^2=CH_2OMe	2.74
(25c) R^1=H; R^2=$CH_2O(CH_2)_2OMe$	2.83
(25d) R^1=H; R^2=$CH_2(OCH_2CH_2)_2OMe$	3.13
(26a) R^1=CH_3; R^2=$CH_2O(CH_2)_2OMe$	3.87
(26b) R^1=CH_3; R^2=$CH_2(OCH_2CH_2)_2OMe$	3.89
(27a) R^1=CH_3; R^2=$CH_2OC_6H_{13}$	3.57
(27b) R^1=CH_3; R^2=$CH_2SC_6H_{13}$	3.08
(27c) R^1=CH_3; R^2=$CH_2NHC_6H_{13}$	3.08

Figure 1.24 *Stability Constants for Complexation of Some C-Pivot Lariat Ethers with Sodium, Measured Using a Sodium Selective Electrode in Methanol at 25°C.*

When the hydrogen atom of the C-pivot ring carbon is replaced by a methyl group, enhancement of stability is seen, where sidearms contain appropriately orientated donor atoms (Figure 1.24). Perusal of this data shows that the presence of the methyl group significantly enhances the sodium binding of crowns (26a), (26b) and (27a), that have donor atoms that are suitably placed to afford axial solvation.

The presence of the methyl group exerts a gem-dimethyl effect on complexation. The origin of the effect is probably complex, and may in part be due to changes in population of the rotational conformers of the free ligand, such that binding conformations are favoured in the methylated ligands over those of their non-methylated counterparts.

Evidence for axial ligation can be deduced by comparing ligands (27a), (27b) and (27c). It has been stressed that hard cations such as sodium, will interact favourably with hard donors such as oxygen. The drop in complex stability for ligands (27b) and (27c), containing the softer donors sulphur and nitrogen respectively, is indicative of axial ligation by the oxygen donor of ligand (27a).

Further evidence for axial ligation in carbon pivot systems has been shown by Lehn[80], who synthesised a number of C-functionalised 18-crown-6 derivatives of R,R(+)-tartaric acid (Figure 1.25).

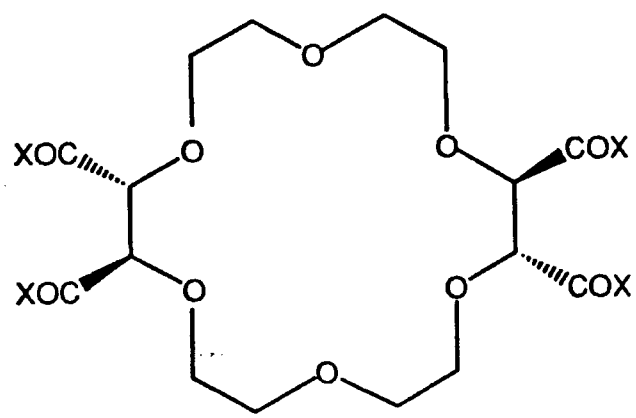

(28)

Figure 1.25

In the crystal structure of the K^+SCN^- with 18-crown-6[58-61] the orientations of the hydrogen atoms that occupy the positions of (X) in the general structure (28) for compounds synthesised in this study, are (e,e) for one (R)CHX-(R)CHX fragment and (a,a) for the other (Figure 1.26).

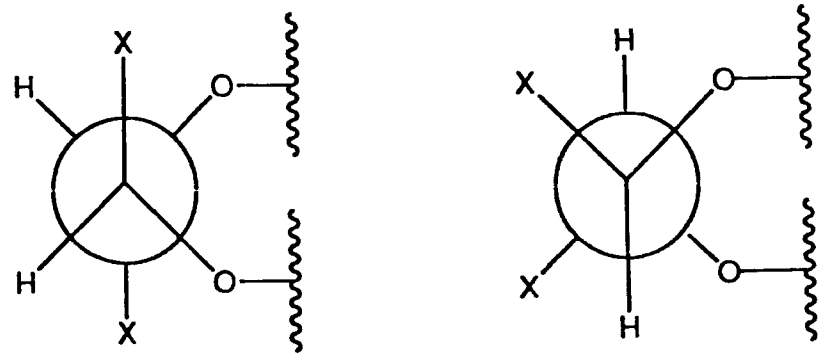

(a,a) orientation *(e,e) orientation*

Figure 1.26

In the orientation (a,a), the (X) groups are approximately vertical and may interact with bound substrates, whereas in the (e,e) conformation, they are inclined and directed outwards such that the chains which they bear interact less well with the substrates.

Information about the orientation of (X) groups in compounds in solution, was obtained from the vicinal coupling constants of the CHX-CHX fragment. From the usual angular dependence of vicinal coupling constants[81] J_{HH} is expected to be small for (a,a) ≈ 2-3 Hz, and larger for (e,e) ≈ 8-10 Hz. The J_{HH} values were calculated from the ^{13}C satellite resonances of these protons.

As the free ligand [X = $C(O)NMe_2$], J_{HH} is approximately 8 Hz which indicates that the (X) groups are primarily in the (e,e) conformation. However, when one equivalent of potassium is added, J_{HH} decreases to approximately 2-3 Hz, indicating that the potassium ion has 'axialised' the (X) groups. This provides clear evidence (as do other examples in

this study) for axial ligation by a carbon pivot side arm to the centrally bound metal cation in solution.

The nature of the (X) group affects the orientation in the free ligand. For example, studies showed that where X = C(O)NHMe, the conformation of the free ligand is primarily (a,a). This is thought to be due to a hydrogen bond between the NH of the (X) group and an ether ring oxygen. Complexation by potassium in solution made very little difference to the J_{HH} value indicating that the (a,a) conformation of the free ligand is suitable for potassium complexation.

This study shows clearly that augmentation of complex stability and selectivity over that of a simple, unsubstituted monocyclic crown ether is possible, in solution, through carbon pivot axial ligation. Carbon pivot axial ligation has also been demonstrated in the solid state in the x-ray structure depicted in Figure 1.27[82].

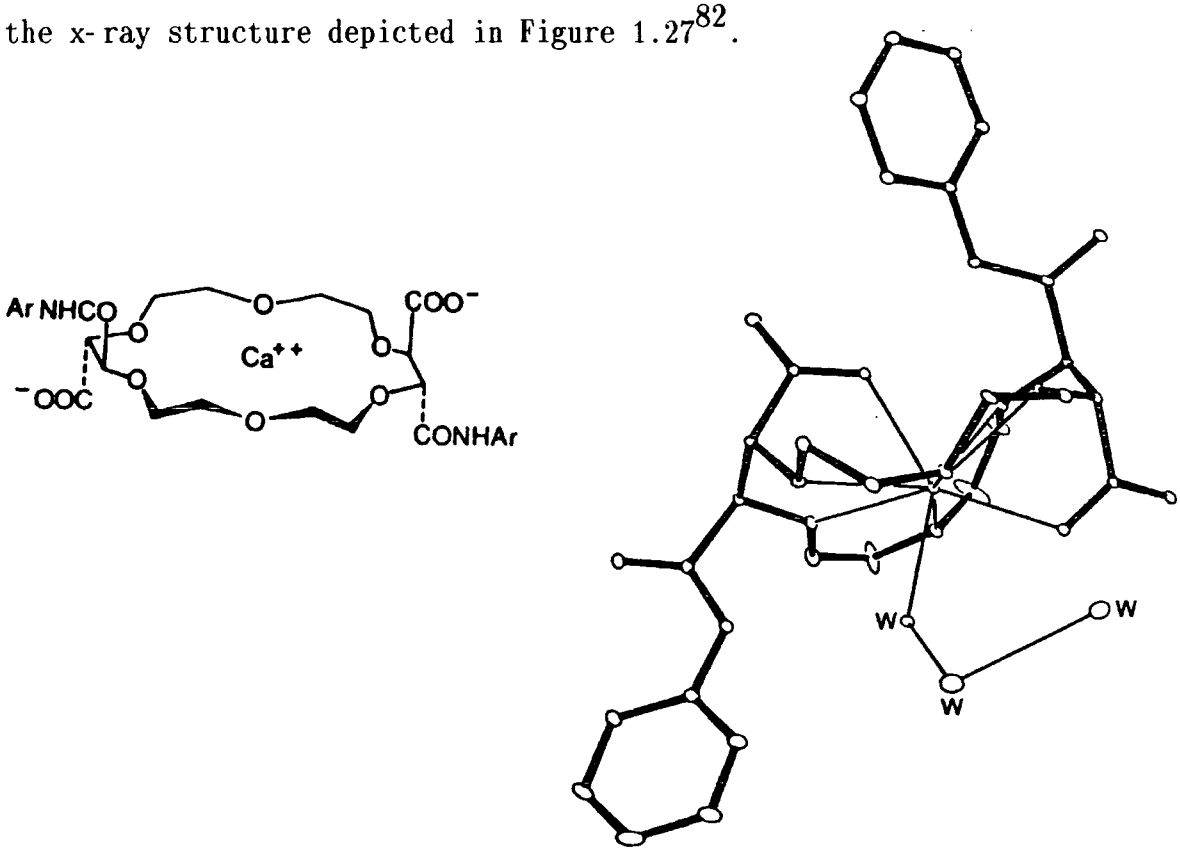

Figure 1.27 *'C'-Pivot Axial Ligation in the Solid State.*

1.2.3.3 N-Pivot Lariat Ethers

Gokel reasoned that attaching the side arm at a flexible molecular pivot atom such as nitrogen should, by virtue of its facile inversion, lead to a more dynamic complexing agent than the carbon pivot lariat ethers.

In order to test this hypothesis, he studied relaxation processes for ligands (29) and (30) using a ^{23}Na NMR technique at variable temperatures (Figure 1.28)[83].

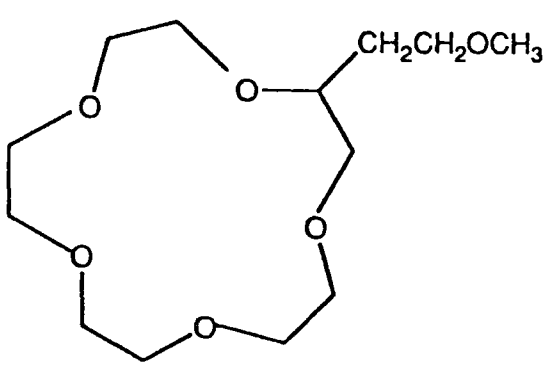

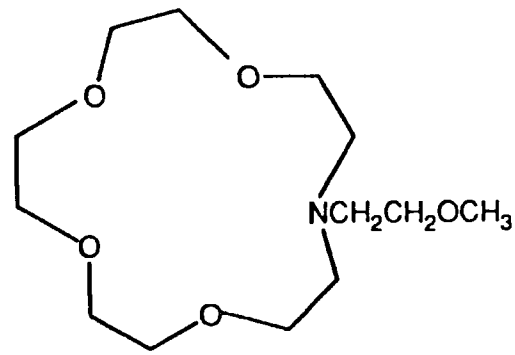

(29) (30)

TEMPERATURE (°C)	LINE WIDTHS ($\Delta V_{\frac{1}{2}}$ /Hz)	
	(29)‡	(30)‡
25	96	58
0	202	87
-25	587	190
-50	~2500	490
-75	>2500	~1300

Figure 1.28 *^{23}Na Relaxation Studies of C-Pivot (29) and N-Pivot (30) Lariat Ethers Measured in Methanol-D_2O (9:1); ‡These experiments were conducted with a ratio of 1:2 (ether:Na^+).*

These results confirm that faster exchange rates are seen for the nitrogen pivot ligand (30) than for the carbon pivot ligand (29). Indeed, ultrasonic relaxation studies[84] have shown that complexation

with N-pivot lariat ethers can probably be represented as in Equation 1.9, where the intermediate (X) represents a complex in which sodium ion is residing outside the crown ether ring.

$$RN15C5 + Na^+ \underset{k_{-1}}{\overset{k_1}{\rightleftharpoons}} \underset{(X)}{RN15C5\ Na^+} \underset{k_{-2}}{\overset{k_2}{\rightleftharpoons}} (RN15C5\ Na^+)$$

The nitrogen inversion was reasoned to be the rate limiting process for the forward rate constant (k_1) which was measured as almost a diffusion controlled process. It was thus concluded that nitrogen inversion is a very fast process.

Studies by Gokel[85] strongly suggest that axial coordination is operative in solution for N-pivot lariat ethers, and that a stronger enhancement of complex stabilities is seen than for C-pivot systems. The ligands (31)-(34) were synthesised and their stability constants for complexation with sodium, potassium and calcium ions were measured in methanol at 25°C using sodium and potassium selective electrodes (Figure 1.29).

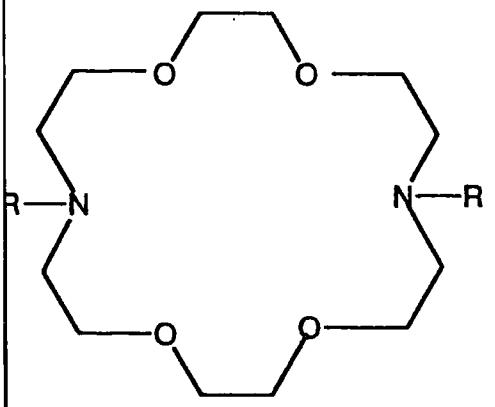

LIGAND	Na^+‡	K^+‡	Ca^{2+}‡
(31) R=H	~1.5	~1.8	----
(32) R=CH_2CH_2OMe	4.75	5.46	4.48
(33) R=CH_2CH_2OH	4.87	5.08	6.02
(34) R=CH_2COOEt	5.51	5.78	6.78

Figure 1.29 *Log K(s) Values for Some N-Pivot Lariat Ethers with Sodium, Potassium and Calcium Ions, Measured Potentiometrically Using Sodium and Potassium Selective Electrodes; ‡Log K(s) Values Measured in Methanol at 25°C. (Source: Reference 85).*

The first point to notice is the substantial stability increase conferred by N-pivot sidearms over that of the unsubstituted ligand (31). The second point is that the nature of the donor group is seen to

be important in determining complex stability with a particular cation. For the high charge density cation (Ca^{2+}) the stability increases by two orders of magnitude on going from ligand (32)-(34), whereas for cations of lower charge density (Na^+, K^+) the increase is less than one order of magnitude. This is undoubtedly due to the higher dipole moment of the axial donor in ligand (34) as compared to ligand (32) which, as has been made clear previously, will favour cations of high charge density. Thus, whereas ligand (32) is indiscriminate between sodium and calcium, ligand (34) is calcium selective. This demonstrates that in N-pivot lariat ethers, the nature of the donating group on the side arm, can strongly affect both the stability and selectivity of the resultant complexes.

Enthalpy and entropy changes for complexation of N-pivot lariat ethers with sodium and potassium ions have been measured, and provide further support for axial ligation in solution by N-pivot lariat ethers[86] (Figure 1.30).

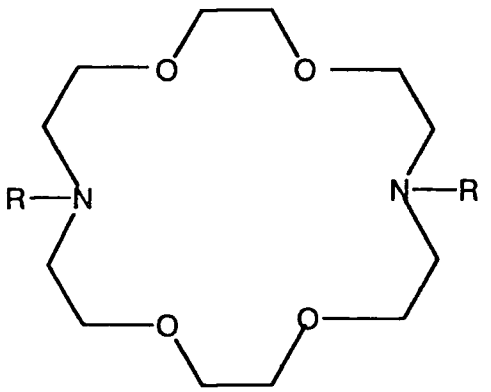

LIGAND	Log K_s‡	ΔH‡	TΔS‡
(35) R=$(CH_2)_3$ (Na^+)	2.86	-2.82	1.08
(33) R=CH_2CH_2OH (Na^+)	4.83	-5.82	0.76
(32) R=CH_2CH_2OMe (Na^+)	4.77	-7.24	-0.73
(35) R=$(CH_2)_3$ (K^+)	3.77	-6.28	-1.14
(33) R=CH_2CH_2OH (K^+)	5.07	-8.80	-1.89
(32) R=CH_2CH_2OMe (K^+)	5.52	-8.81	-1.28

Figure 1.30 *Enthalpy and Entropy Changes for Complexation of Some N-Pivot Lariat Ethers with Sodium and Potassium Ions; ‡As measured using sodium and potassium selective electrodes, 15-41°C in methanol. (Source: Reference 86).*

As can be seen from this data, the origin of the higher complex stabilities for N-pivot lariat ethers (32) and (33) which possess donor

groups on the side arms, over that of ligand (35) which has a non-donating side arm, is largely enthalpic. An increase in interaction with the metal cation by axial ligation is expected to lead to a more favourable enthalpy change on complexation, and so this data strongly supports side arm participation during complexation in these N-pivot systems.

The stability of complexation for a variety of monoaza-crown ethers of differing ring size, with sodium was measured[87] (Figure 1.31).

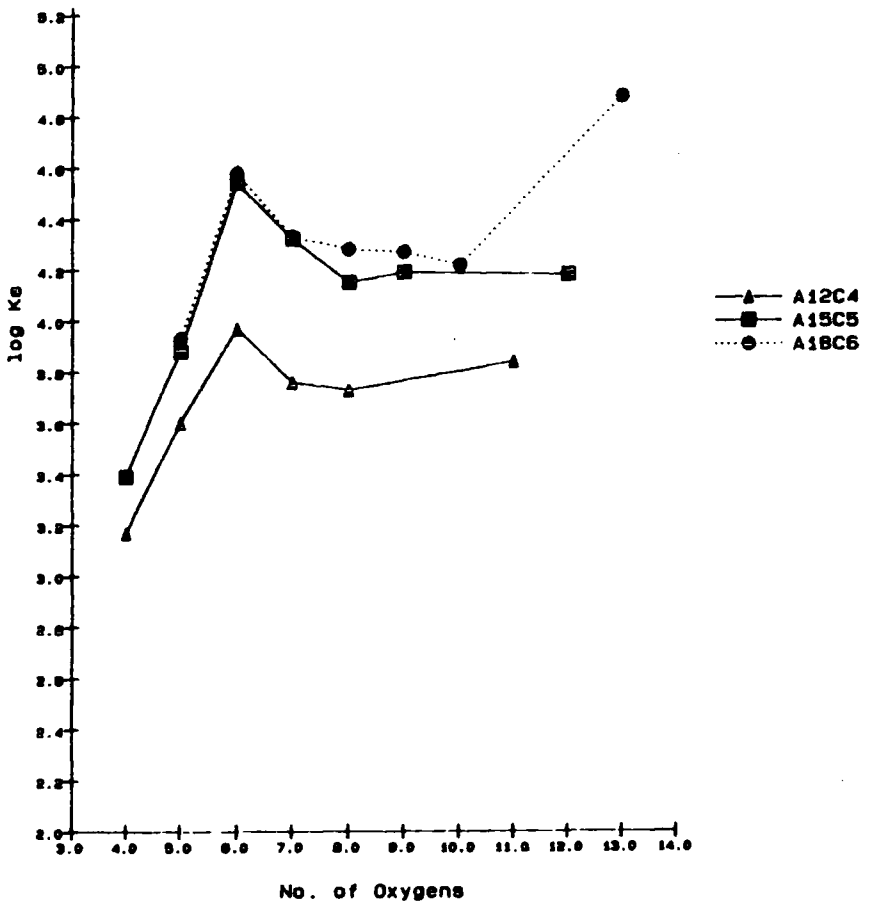

Figure 1.31 *Stability of Complexation for a Variety of Monoaza Crown Ethers of Differing Ring Size Measured Using Sodium Selective Electrodes in Methanol at 25°C.*

The first inference from this data is that the presence of nitrogen seems to have little effect on binding. The curves for monoaza-15-crown-5 and monoaza-18-crown-6 closely parallel one other, and this

tends to suggest that it is the number of oxygens in the ligand that is important and that nitrogen is redundant as an effective donor.

The second point to note is that there is a peak for all three ligand systems when the total number of ligand oxygens is six. This indicates that these ligands are flexible enough to allow sodium to organise binding sites around itself without a large unfavourable free energy change as a result of ligand deformation.

The ability of potassium to organise N-pivot lariat ethers such that it can enjoy hexa-coordination has been demonstrated in the solid state[88] (Figure 1.32).

In flexible monocyclic N-pivot lariat ethers, the carbon framework primarily maintains connectivity relationships between donors rather than imposing rigid conformational or steric bias to the system. Thus for the five ligands in Figure 1.32, potassium is able to organise six oxygen donors around itself.

It can thus be seen that bis-crown ethers, N-pivot and C-pivot lariat ethers effect three-dimensional discrimination and, with appropriate design, high selectivities for particular cations may be realised. Furthermore, their inherent flexibility ensures that kinetics of complexation and decomplexation remain fast and thus, highly selective ligands of these types are viable candidates for incorporation into ion selective electrodes and as carriers for membrane transport.

1.2.3.4 Cryptands

Lehn and Sauvage synthesised a series of bicyclic ligands[36,89-92] (cryptands) designed to offer the incoming cation a three dimensional array of binding sites (Figure 1.33).

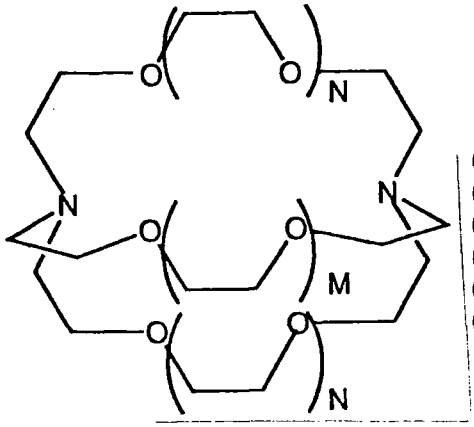

CRYPTAND	(211)	m=0	n=1
CRYPTAND	(221)	m=1	n=0
CRYPTAND	(222)	m=1	n=1
CRYPTAND	(322)	m=1	n=2
CRYPTAND	(332)	m=2	n=1
CRYPTAND	(333)	m=2	n=2

Figure 1.33 *Structure of Some Bicyclic Cryptands.*

These bicyclic ligands are inherently less flexible than acyclic or monocyclic derivatives, they are thus less able to adapt to a range of cation sizes, and exhibit a peak selectivity for the cation whose radius best matches that of the three-dimensional cavity (Figure 1.34)[93].

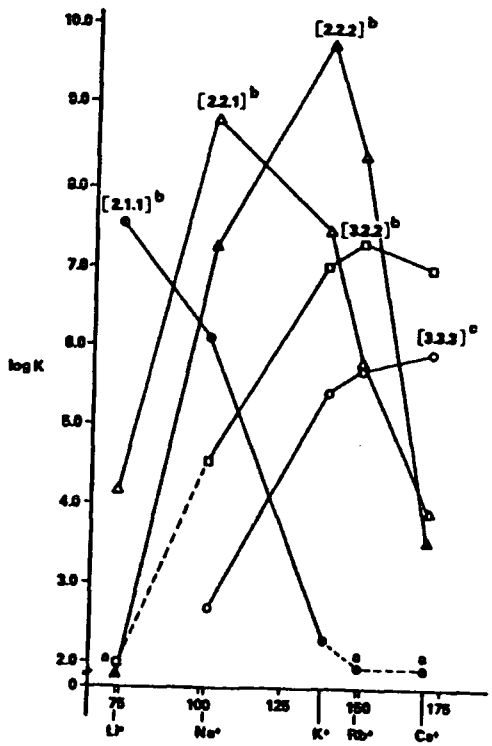

Figure 1.34 *Variation in Complex Stability of Cryptands with Alkali Metal Cations.*

As can be seen from Figure 1.34, as the cryptand becomes larger and more flexible, peak selectivity is less pronounced, reflecting the increased ability of the larger cryptands to adapt to a range of cation

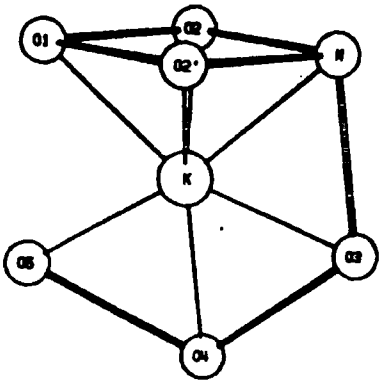

K^+SCN^- +
$12NO_3$-$(CH_2CH_2O)_2CH_2CH_2OCH_3$

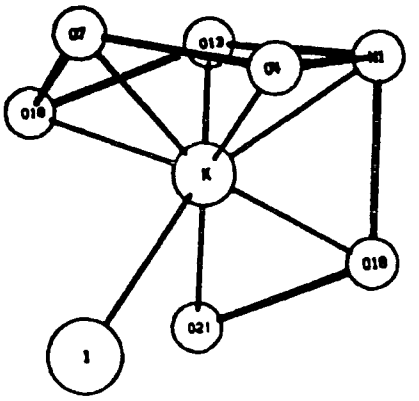

K^+I^- +
$15NO_4$-$CH_2CH_2O_2CH_2CH_2OCH_3$

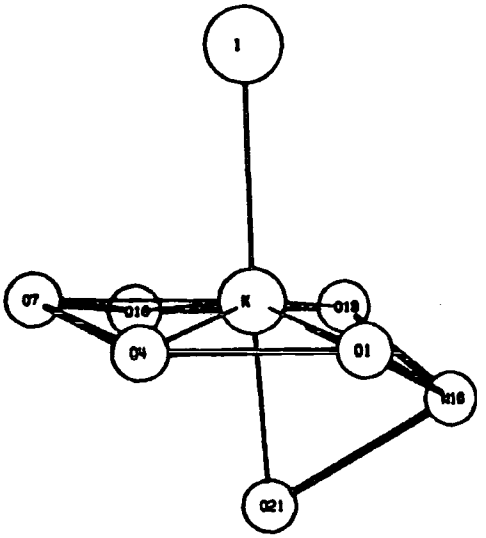

K^+I^- + $18NO_3$-$CH_2CH_2OCH_3$

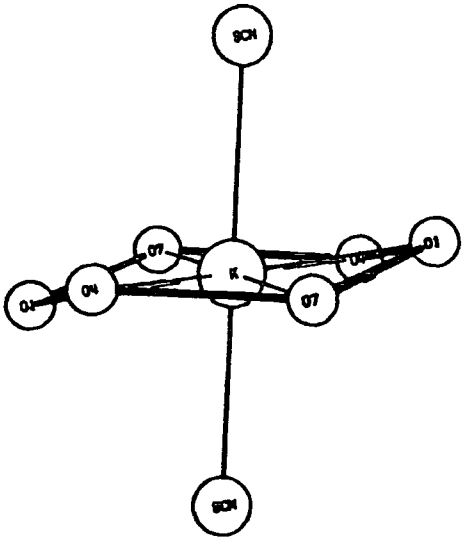

K^+SCN^- + 18C6

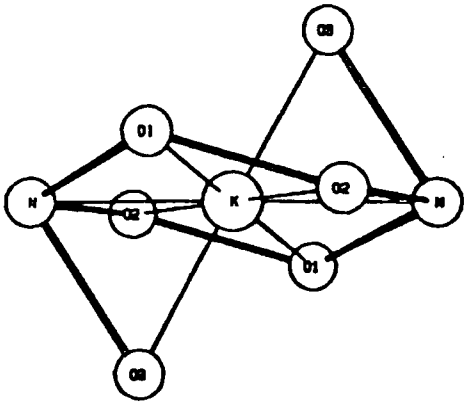

K^+SCN^- + $18N_2O_4(CH_2CH_2OH)_2$

Figure 1.32 *Organisation of N-Pivot Lariat Ethers by Potassium.*

sizes. The smaller cryptands, however, show a prominent peak selectivity on the basis of size.

Though cryptands can be considered more rigid than their acyclic or monocyclic counterparts, they are by no means wholly preorganised to accommodate an appropriately sized metal cation. The x-ray structure of the free (222) cryptand[94] (Figure 1.35) shows that two methylene groups occupy the middle of the bicyclic structure, and that the lone pairs of the two oxygen atoms face outward.

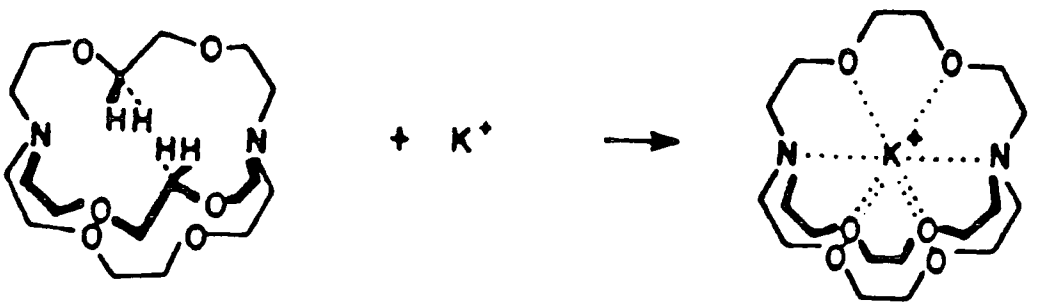

Figure 1.35 *Complexation of Potassium Iodide with Cryptand (222).*

Upon formation of a potassium capsular complex, the ligand reorganises so that a potassium occupied cavity develops. Also it has been shown that, in solution, the free cryptands may exist as one of three isomers, depending on the orientation of the nitrogen lone pairs (in-in, in-out, out-out). However, inversion of the nitrogen is very fast, and in order to acquire the (in-in) conformation suitable for cation complexation, little energy is required[84].

The fact that cryptands are more preorganised for binding than their acyclic or monocyclic counterparts, translates into higher complex stabilities for these bicyclic structures (Figure 1.36).

The example shows that the potassium complex of cryptand (222) is nearly 10^5 times more stable than the potassium complex of the monocyclic ligand (36). The increased stabilisation on going from a monocyclic structure (36) to a cryptand with an identical number of

binding sites, at a given temperature, in a given solvent, is termed the *cryptate effect*. The thermodynamic origins of this effect are still matters of debate[95,96], though the increased stability of these bicyclic structures is in no doubt.

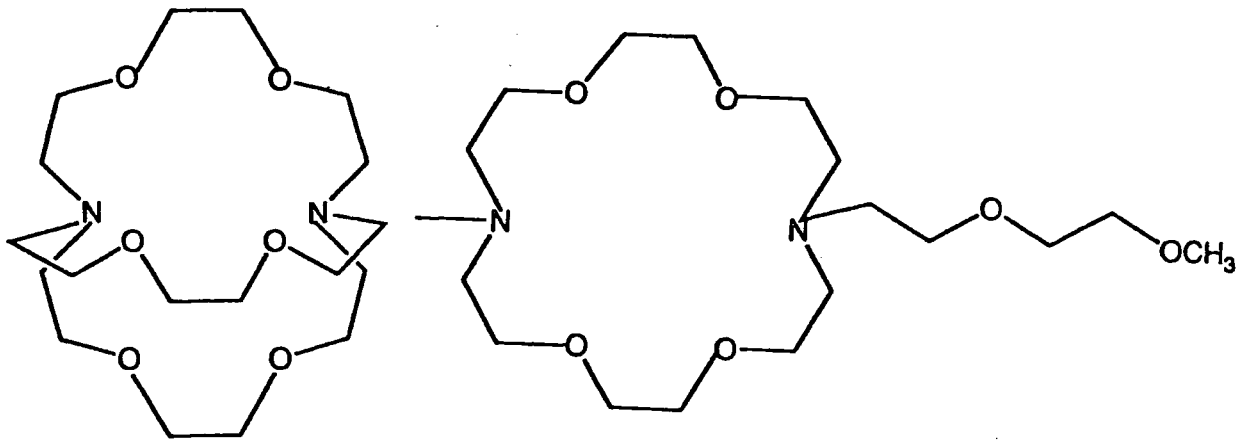

Figure 1.36 *"The Cryptate Effect"; log K(s) values measured in 95:5 Methanol:Water at 25°C.*

The increased rigidity of these ligands however, means that though they exhibit high selectivity and stability, complexation rates (especially those of dissociation) are markedly slower than for acyclic and monocyclic derivatives. As has been shown in Section 1.1.6, cryptands are thus generally unsuitable as candidates for use in ion selective electrodes or as membrane carriers. The high selectivities and stabilities of their complexes do, however, render them as useful receptors.

1.2.3.5 Spherands

Unlike any other ligands mentioned to date, the spherands are almost fully organised for complexation during their synthesis. No significant further organisation need, or can, occur during complexation (Figure 1.37)[97].

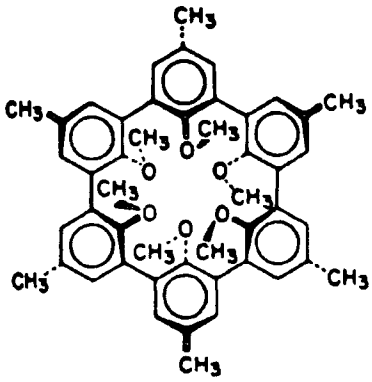

(37)

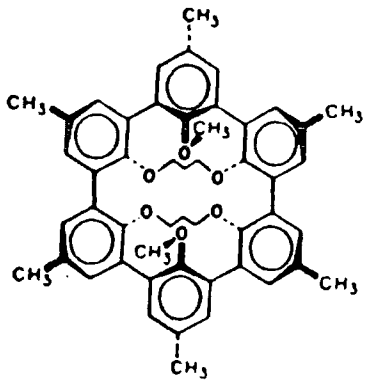

(38)

Figure 1.37 *Structure of Spherands (37) and (38).*

The extremely high rigidity of the aryl backbone ensures that a fixed three-dimensional binding site is delineated. For cations whose diameter matches that of the cavity, complexes of very high stability will be formed (Figure 1.38)[97].

	CRYPTAND 221	SPHERAND (37)	SPHERAND (38)
$-\Delta G$	+16.3	+ 10.0	+ 22.0

Figure 1.38 *Free Energy Changes for Complexation of Sodium Picrate with Cryptand (221) and Spherands (37) and (38), Measured in $CDCl_3$ Saturated with D_2O.*

It can be seen that spherands (37) and (38) form complexes that are appreciably more stable with sodium ions, than even the best fit cryptand (221) for this cation.

The rigidity of these ligands also means that very high selectivities can be achieved in that ligand adaptability to cations of different size is extremely energetically demanding. However, high stabilities and selectivities of spherands are accompanied by slow complexation kinetics, especially decomplexation rates. This means that they behave as highly efficient receptors, yet are redundant as candidates for ion selective electrodes or as neutral membrane carriers.

Cram has synthesised[98-101] hemi-spherands and cryptahemi-spherands (Figure 1.39).

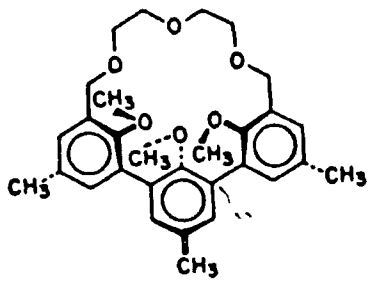

(39)
HEMI-SPHERAND

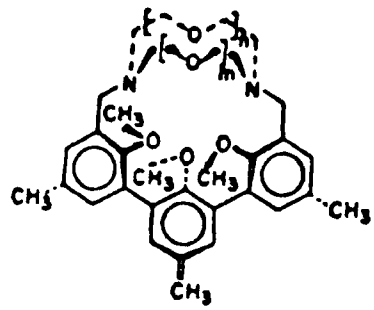

(40)
CRYPTAHEMI-SPHERAND

Figure 1.39 *Structure of the Hemispherand (39) and Cryptahemispherand (40).*

The anisyl groups in both structures (39) and (40) are self-organising whereas the bridging ethyleneoxy groups can turn their unshared electron pairs and methylene groups either inward or outward, depending on the demands of solvent or guests[98]. Because of this blend of rigidity and flexibility, the hemi-spherands and cryptahemi-spherands provide complexes of high stability and selectivity which are also complemented by reasonable rates of complexation and decomplexation. They are thus viable potential candidates as receptors in ion selective electrodes and as carriers in membrane transport.

In this short review of the evolution of cation recognition, selectivity amongst alkali metals has been stressed. Clearly, as we have seen, size discrimination plays an important role in determining ligand selectivities. In considering selectivity for alkali metals over alkaline earth metals, a glance at Table 1.11 reveals that lithium has the same hexa-coordinate ionic radius as magnesium, and that sodium is of a very similar size to calcium.

CATIONIC RADII (Å)	
Mg^{2+}	0.78
Ca^{2+}	1.02
Li^{+}	0.78
Na^{+}	0.98

Table 1.11 *Cationic Radii (for Hexa-coordination) of Some Alkali and Alkaline Earth Metal Cations (Ref.63,64).*

Clearly, ligands that select either lithium over magnesium, or sodium over calcium, cannot be discriminating on the basis of size. In comparison to alkali metals, alkaline earth metals exhibit: (i) higher solvation energies, (ii) higher charge densities, (iii) lower polarisability and (iv) higher coordination numbers. Therefore, in order to affect monovalent/divalent selectivity, these differences must be considered for appropriate ligand design. Variations in the nature and number of ligand donors,ligand thickness and ligand flexibility will be of paramount importance in this respect.

1.3 LITHIUM SELECTIVE IONOPHORES

1.3.1 Uses of a Lithium Selective Ionophore

1.3.1.1 Lithium Selective Electrodes

There is a clear need to develop a neutral lithium selective electrode for measurement of lithium ion activity in both physiological and environmental systems[51,102-107].

At present, lithium carbonate is used in the treatment of manic depression and other neurological disorders. It is the slow penetration of lithium through the blood-brain barrier and across other membranes

which delays the onset of drug action. This necessitates large doses, with accompanying undesirable side effects[102,107]. Clearly, a method of measuring lithium ion activity in whole blood taken from a treated patient is needed.

In whole blood, there are ions present that may interfere with the measurement of lithium ion activity (Na^+, K^+, Ca^{2+}, H^+). The activities of these ions generally lie between narrow limits and these have been ascertained (Figure 1.40).

	CONCENTRATION RANGE (mmol dm^{-3})
Na^+	135-150
K^+	3.4-5.2
Ca^{2+}	1.04-1.45
Li^+	0.5-1.0

Figure 1.40 *Concentration Range of Interferent Ions in Whole Blood.*

This means that it is possible to estimate reasonably accurately, the selectivity of a neutral carrier in a lithium selective electrode, that is required in order to accurately measure the lithium concentrations in whole blood (at which less than 1% interference is experienced from other cations) (Figure 1.41).

M	Log K^{Pot}_{LiM} ‡
Na^+	-4.5
K^+	-3.0
Ca^{2+}	-2.3
H^+	1.06

Figure 1.41 *Selectivities Required at which $[Li^+]$ in Whole Blood may be Accurately Measured (With $\leq$ 1% Interference); ‡Equals log $[1/(Li^+/M^+)]$ where (Li^+/M^+) = Selectivity of the Ligand for Lithium over the Metal Cation, M^+.*

The lithium selective electrode typically consists of the selective ionophore embedded in a matrix consisting of polyvinylchloride (PVC), n-nitrophenyl-octylether (NPOE) and potassium tetrakis(p-chlorophenyl-borate) (KTpClB). The membrane is then incorporated into a cell (Figure 1.42) so as to measure lithium ion activity potentiometrically.

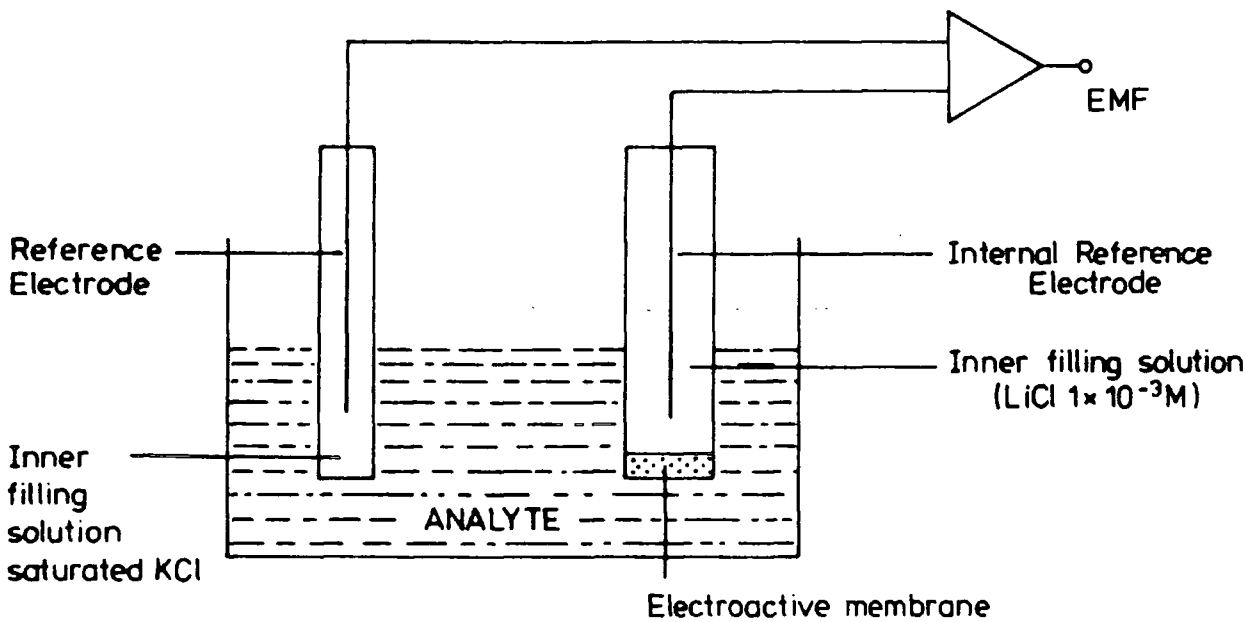

Hg | $HgCl_2$ | Saturated KCl | ANALYTE | Electroactive PVC Membrane | Inner Filling Solutions | AgCl | Ag

Figure 1.42 *Electrochemical Cell Used to Measure Selectivity of an Ionophore Potentiometrically.*

By using a fixed background of interfering ions (at concentrations found in whole blood) whilst variations in lithium ion concentrations are made, and EMF potentials measured, the selectivity of a particular ionophore for lithium can be ascertained (FIXED INTERFERENCE METHOD)[108]. The applicability of such an ionophore for measurement of lithium ion activity in whole blood can then be assessed by comparing selectivities

achieved for lithium to those that are required (Figure 1.41).

Though adequate selectivities for lithium over potassium, calcium and hydrogen have been realised, the lithium to sodium selectivity ratio has so far not been reached.

1.3.1.2 Extraction

The natural abundance of lithium ores is low, and with increasing demand for lithium in the next century, the extraction of lithium from sea water is under consideration. This predicted rise in demand is due to the probable use of lithium as a blanket material for breeding tritium in thermonuclear reactors and its incorporation into high performance low density batteries[109].

1.3.1.3 Pharmacological Applications

There is a medical application in the design of a lithium selective ionophore able to transport lithium through the blood-brain barrier membrane as well as through other membranes, in the treatment of manic depression and other psychiatric disorders. The use of such an ionophore would: (i) increase the rate of lithium uptake into the brain and so shorten the delay between drug administration and therapeutic effect, and (ii) reduce the necessary lithium dosage required to attain a therapeutic effect.

1.3.2 Lithium Selective Ionophores for use in Ion Selective Electrodes and as Membrane Carriers

A suitable ionophore for use in a neutral lithium selective

electrode to be used to measure lithium ion activity in whole blood or aqueous systems must exhibit the following characteristics:

(1) It must display an extremely high selectivity for lithium over other alkali metal and alkaline earth metal cations. Furthermore, the selectivity of the neutral ionophore, by definition, must display complexation characteristics that are largely independent of the pH of the sample solution.

(2) It must display sufficient lipophilicity to ensure: (i) it remains within the membrane, (ii) it transports the lithium ion effectively across that membrane.

(3) It must form stable complexes with the lithium cation, but also exhibit reasonably fast dissociation rates so as to maintain a constant, reasonable level of free carrier available at the source phase to which the lithium may bind.

CATION	6-COORDINATE IONIC RADIUS[110] (Å)	σ SOFTNESS[111]	SURFACE CHARGE DENSITY[112] (zÅ^{-2}) z=1,2	POLARISABILITY[113]
Li^+	0.78	0.247	0.130	0.03
Na^+	0.98	0.211	0.085	0.30
K^+	1.33	0.232	0.045	1.10
Rb^+	1.49	0.229	0.035	1.90
Cs^+	1.65	0.218	0.030	2.90
Be^{2+}	0.34	0.172	1.370	0.01
Mg^{2+}	0.78	0.167	0.260	0.20
Ca^{2+}	1.06	0.180	0.140	0.90
Sr^{2+}	1.27	0.172	0.100	1.28
Ba^{2+}	1.43	0.184	0.080	2.50

Figure 1.43 *Ionic Radii, Hydration Numbers, Softness Parameters, Surface Charge Densities and Polarisabilities for Alkali and Alkaline Earth Metal Cations.*

From the data in Figure 1.43 it is seen that lithium: (i) is the smallest element of the alkali metals and, aside from beryllium, the alkaline earth metals, (ii) again, aside from beryllium, it is the least polarisable of the alkali and alkaline earth metals and (iii) exhibits the highest charge density ratio among the alkali metals. Design of a lithium selective ionophore must concentrate on these features.

1.3.2.1 Size of the Macrocycle Ring

The small size of the lithium ion dictates that ligands exhibiting a cavity size complementary to the effective ionic radius of lithium will be inherently less flexible than those ligands complementary in size to other larger cations. As has been mentioned previously, the 'size fit' concept assumes increasing importance in determining complex stability as the free ligand becomes more rigid. Therefore, size fit complementarity has received much attention in lithium ionophore design.

The two most lithium selective ligands synthesised to date are spherand (37)[97] and cryptand-211 (41)[114], and crystal structures of their lithium complexes are shown in Figure 1.44.

The aryl backbone of spherand (37) provides high rigidity for the free ligand. The diameter of the cavity is 1.62Å and the oxygen lone pairs point inwards and line an almost perfect octahedron. In the lithium complex, the lithium cation (octahedral diameter 1.52Å) resides in the centre of the cavity, being equidistant from all six oxygen atoms (Li-O distance = 2.14Å) and exhibits near perfect octahedral geometry.

The high rigidity of the ligand backbone dictates that slight perturbations in the lowest free energy free ligand conformation will lead to a marked decrease in resultant complex stability. This confers a high selectivity for lithium over the slightly larger sodium cation

whose octahedral diameter (1.98Å) is too large to fit the spherand cavity in its lowest free energy conformation.

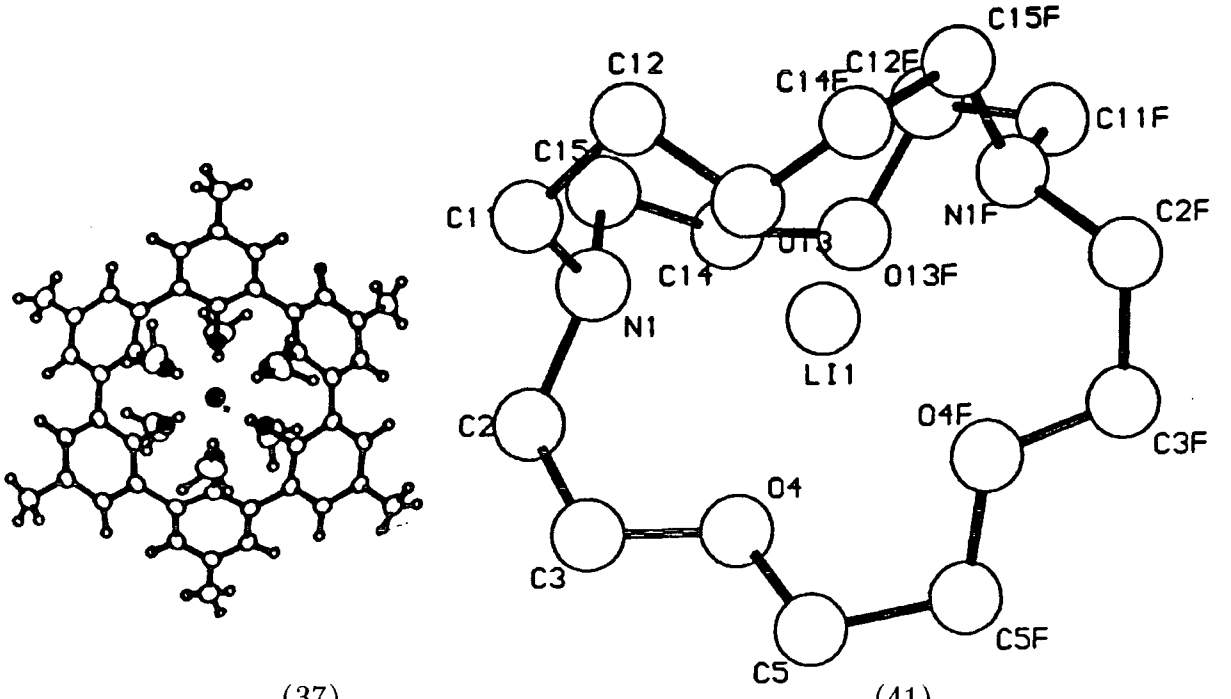

(37)
SPHERAND[97]

(41)
CRYPTAND (211)[114]

Figure 1.44 *Crystal Structures of Lithium with Spherand (37) and Cryptand (211).*

In the 211-cryptand the lithium ion resides within the three-dimensional cavity and coordinates to all four oxygens (average Li-O distance = 2.14Å) and two nitrogens (Li-N distance = 2.28Å). The cavity diameter of cryptand-(211) is 1.6Å, which is clearly too small to accommodate the sodium cation. Indeed, sodium forms an exclusive complex (Figure 1.45)[115] not residing within the three-dimensional cavity of the ligand, but rather in the 15-membered ring that constitutes the 'cryptand face'. Thus the (211)-cryptand selects lithium over sodium primarily on the basis of size.

The complementary size of ligands (37) and (41) with respect to the effective octahedral ionic radius of the lithium cation, coupled with high ligand preorganisation for complexation, and rigidity, means that resultant lithium complexes are highly stable (Figure 1.46).

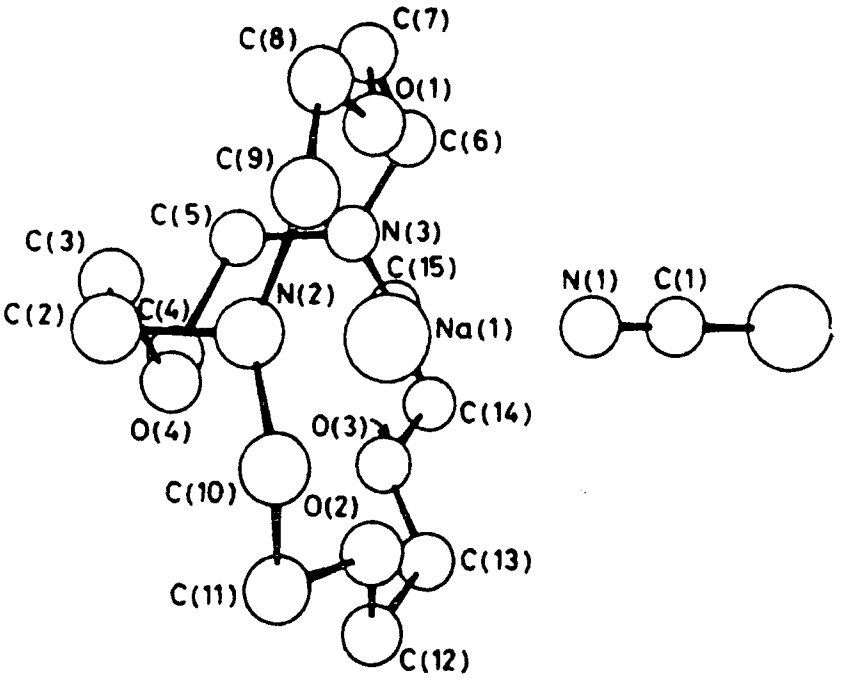

Figure 1.45 *Crystal Structure of the 211-Cryptand-Na^+ Exclusive Complex (Reference 115).*

COMPOUND	log K_S	k_A (m^{-1} s^{-1})	k_D (s^{-1})
(37)[97]	> 16.8	7.5×10^4	$< 10^{-12}$
(41)[116]	7.9	4.8×10^5	4.4×10^{-3}

Figure 1.46 *Complexation Rates, Decomplexation Rates and Stability of Complexes Formed by Lithium with Spherand (37) and Cryptand-(211) (41) Measured in Methanol at 25°C.*

The high log K_S values (primarily caused by slow dissociation rates) render these ligands unsuitable for passive carrier mediated transport across membranes.

The search for lithium selective ionophores, for use in ion selective electrodes and membrane transport, has thus centred around acyclic and monocyclic ligands. Being more flexible, these ligands should combine high lithium selectivity with appropriate, reasonably fast complexation kinetics.

1.3.2.2 Nature of Donors

Lithium is a 'hard' small cation of high charge density which interacts most favourably with 'hard' oxygen donors. As has already been pointed out, cations of high charge density interact most strongly with functional groups containing oxygen that exhibit a high dipole moment and high polarisability such as amide, ester and phosphonate groups.

These oxygen based functional groups must, however, in order to augment stability of lithium complexes, be in a suitable orientation so as to interact with the central metal cation. Ligands (42) and (6) are compared in Figure 1.47 [116,117].

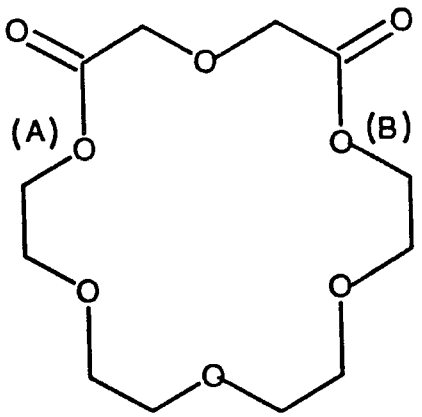

(42)

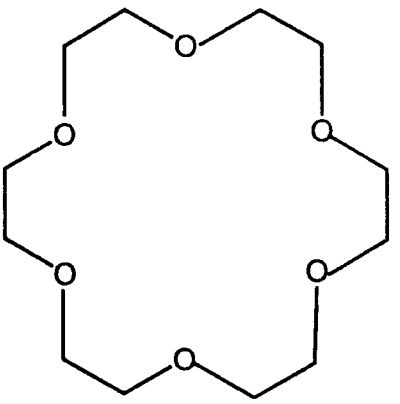

(6)

LIGAND		ΔH (Kcal mol^{-1})	TΔS (Kcal mol^{-1})	Log K_S (MeOH/25°C)
(6)	Na^+	-8.40	-2.4	6.05
	K^+	-13.80	-5.2	6.67
(42)	Na^+	-2.27	+1.1	4.36
	K^+	-5.87	-2.06	4.90

Figure 1.47 *Enthalpies and Entropies of Complexation for Sodium and Potassium Ions with Ligands (6) and (42); Data from reference 116, 117.*

The complexing properties of (42) are drastically reduced when ester functions are incorporated directly into the ring skeleton. This is because the orientation of carbonyl donors is inappropriate for interaction to the central metal cation. Added to this, the electron withdrawing effect of the carbonyl oxygen atoms reduces the basicity of ethereal groups (A) and (B), resulting in a less favourable enthalpy of complexation for sodium and potassium ions.

Therefore it can be seen that for smaller cyclic ligands, amide and ester functional groups can only really affect an interaction with the central metal cation if they are incorporated into sidearms (N-pivot, C-pivot) off the macrocycle ring skeleton.

In the case of acyclic ligands or large cyclic ligands, increased flexibility means that amide and ester groups may be incorporated within a ligand backbone, whose appropriate design can ensure their optimal interactions with the enveloped cation.

1.3.3 Ligands Designed as Lithium Selective Ionophores

1.3.3.1 Acyclic Ligands

Based on octahedral coordination of lithium inferred from the crystal structure of aluminium silicates and other minerals[118], Shanzer *et al.*[102] designed an acyclic hexa-functional lithium ionophore (43). This ligand, in a competitive extraction experiment in a dichloromethane-water system, showed a lithium:sodium selectivity of approximately forty. The ligand is thought to wrap around the lithium ion so that all six donors coordinate in an octahedral geometry.

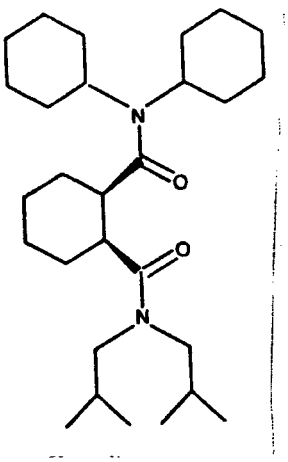

(10)

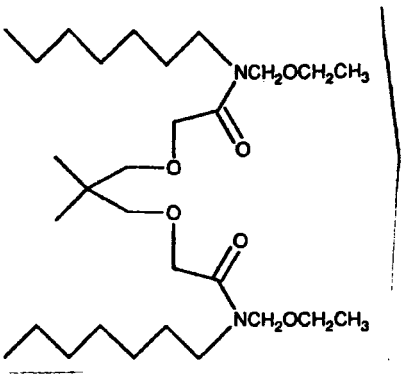

(43)

Simon *et al.*[50] synthesised ligand (10) in a membrane composed of (i) carrier (10) (1 - 1.4 wt%), (ii) NPOE (66 wt%), (iii) PVC (33 wt%) and (iv) KTpClB (0.4 wt%). A selectivity of log $K^{Pot}_{Li^+Na^+}$ = -2.5 was measured by the fixed interference method. X-ray and NMR studies have shown that, in the solid state, lithium is complexed by two molecules of the ligand. The four carbonyl oxygen atoms interact with the lithium ion in a tetrahedral coordination sphere. This ligand exhibits the highest selectivity for lithium over Group 1 and Group 2 metal ions of any acyclic ionophore made to date.

1.3.3.2 Monocyclic Ionophores: Ring Size

A table of unsubstituted crown ether cavity diameters is shown in Figure 1.48[119].

COMPOUND	CAVITY DIAMETER (Å)
12-CROWN-4	1.2
15-CROWN-5	1.8
18-CROWN-6	2.8
21-CROWN-7	3.8

Figure 1.48 *Cavity Diameters for Some Simple Crown Ethers.*

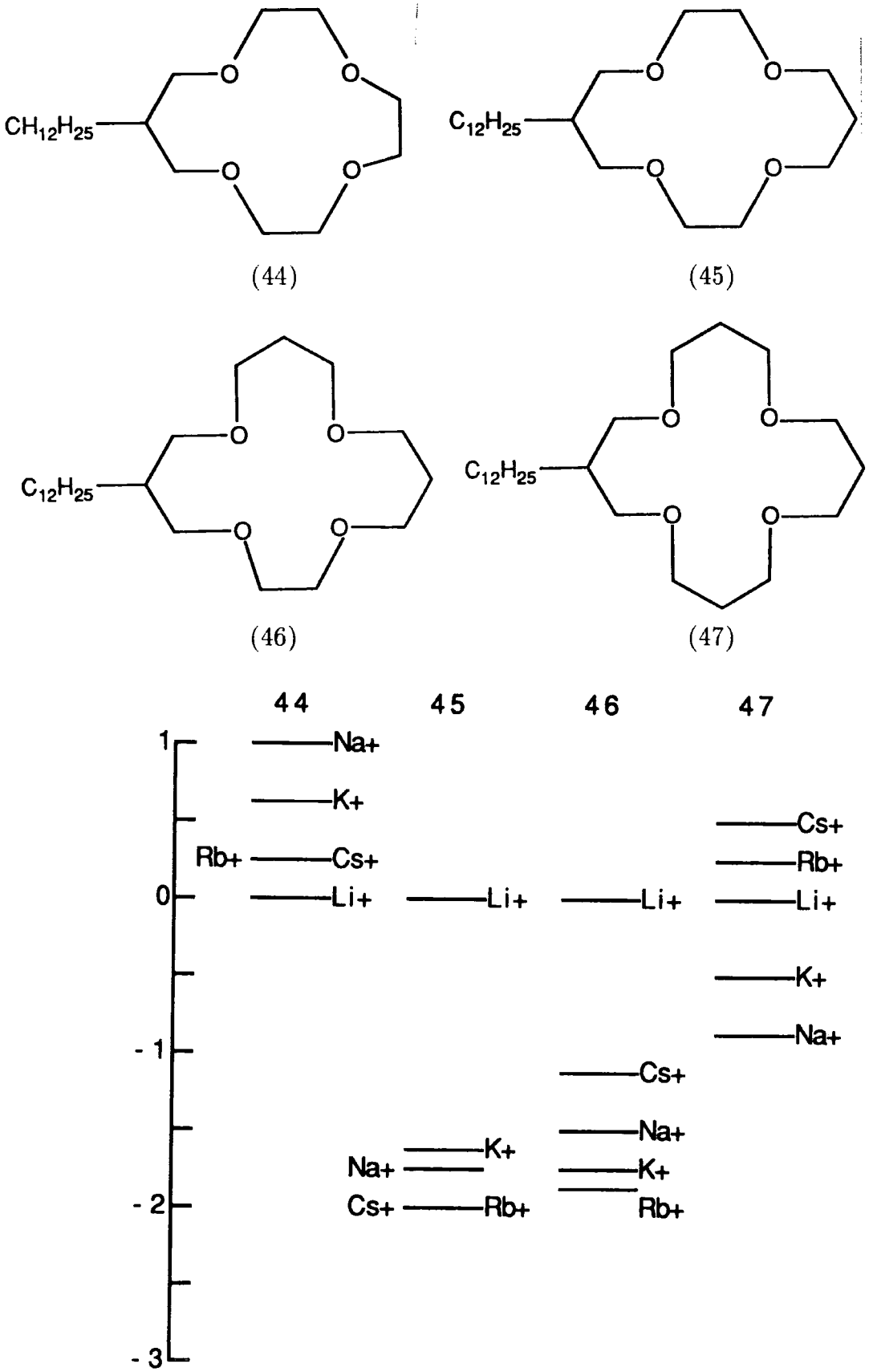

Figure 1.49 *Lithium Selectivities of Ligands (44)-(47) Measured Potentiometrically Using the Fixed Interference Method.*

The diameter of the lithium ion lies between 1.18Å and 1.52Å depending on its coordination number (4-6). From a glance at Figure 1.48, it is obvious that ring sizes 12-15 will be most suitable in terms of maximum size fit for the lithium ion.

Numerous studies have been undertaken to evaluate the effect of ring size on the selectivity of crown ethers for lithium[106,120-122] and all have come to the conclusion that the 14-crown-4 ring skeleton forms the basis for optimum selectivity. For example, Kitizawa *et al.*[106] synthesised a series of crown ethers from 13-membered to 16-membered (Figure 1.49). All four ligands were embedded in PVC-based membranes and their selectivities for lithium over other alkali metals and alkaline earth metal cations were measured potentiometrically by the fixed interference method. The results clearly point to the 14-crown-4 skeleton being optimum for lithium selectivity over other alkali and alkaline earth metal cations.

Hancock[123] has argued that ring size of monocyclic ligands may not be the only factor governing selectivity for metal cations. By using molecular mechanics, it was inferred that cavity sizes of tetraaza macrocycles increase monotonically with increasing number of atoms (Figure 1.50).

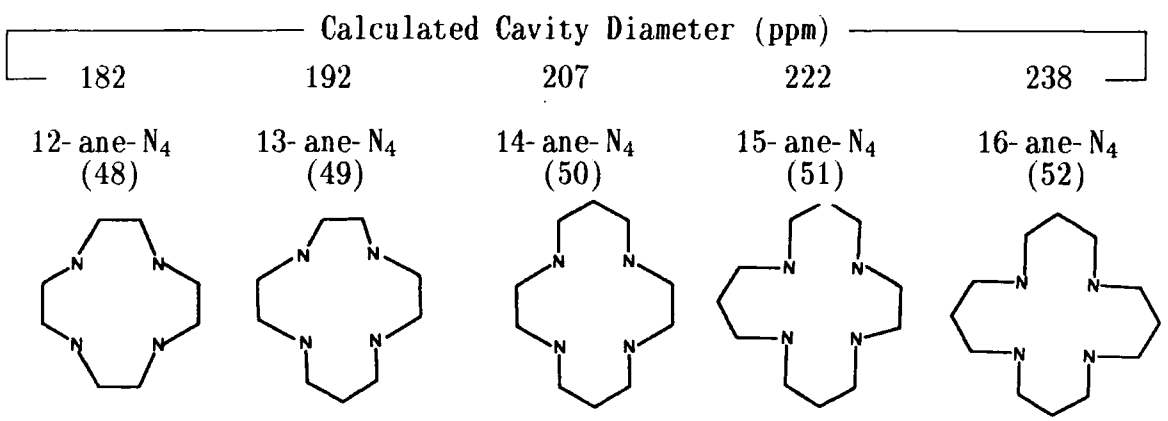

Figure 1.50 *Cavity Diameters of Some Tetraaza Macrocycles.*

If metal ions are constrained to lie in the plane of the macrocycle, large metal ions would be expected to complex more strongly with larger tetraaza macrocycles. However, it was proved by experiment that this was not the case. If ΔLog K_S is plotted as a function of ionic radius for compounds in the series 12-ane-4 to 13-ane-4 and from DOTA (53) to CYTA (54) then the graph shown in Figure 1.51 is observed.

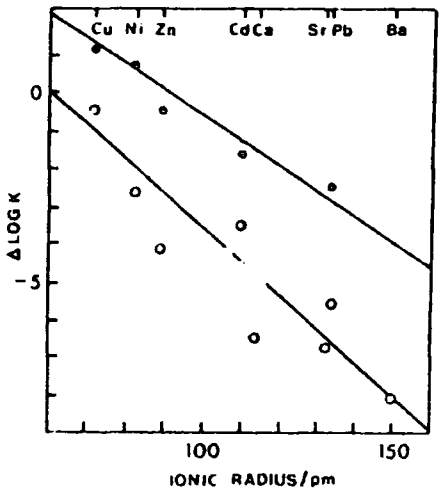

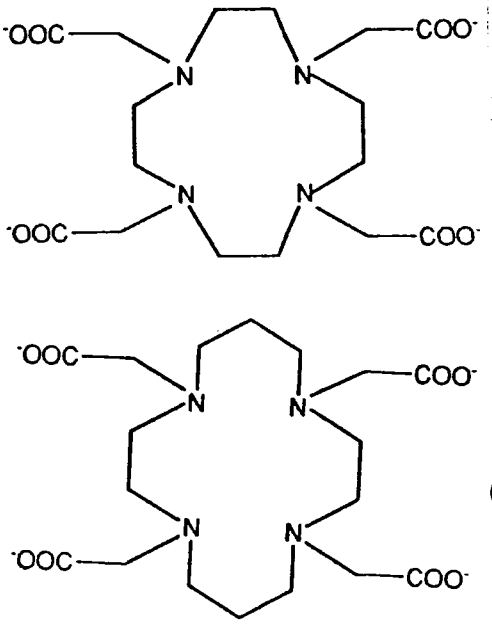

Figure 1.51 *A Graph of ΔLog K(s) <u>vs</u> Ionic Radius (ppm) for the series 12-ane-N_4 to 13-ane-N_4 (•) and for DOTA (53) and CYTA (54) (o).*

As the ring size increases from the series 12-ane-4 to 13-ane-4 and from DOTA (53) to CYTA (54), the stability of the complexes decrease with increasing cationic radius.

Molecular mechanics was used to rationalise the metal ion size selectivity for 12-ane-4 relative to 14-ane-4 complexes. The calculations suggest that the two six-membered chelate rings present in the 14-ane-4 system, are able, with very small metal ions, to have all hydrogen atoms in the energetically more favoured staggered orientation. However, as the size of the metal cation increases, the hydrogens are

increasingly forced into the less favourable eclipsed orientation. There is thus an increase in strain energy and a decrease in complex stability. For five-membered chelate rings, no such favourable arrangement with all hydrogens staggered is possible and the effect of an increase in metal ion size is much less marked.

This effect of increasing chelate ring size on metal ion selectivity appears to be present for all ligands containing nitrogen and/or oxygen donors so far studied by Hancock. He infers that the fact that the crown ether (54) extracts the small lithium ion from the aqueous phase to the organic phase with an unprecedentedly high selectivity over other alkali metals is to be expected on account of its two six-membered chelate rings, whereas crown ether (55) shows only a small selectivity for lithium on account of possessing only five-membered chelate rings.

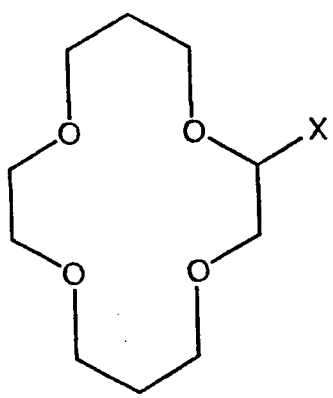

(54)

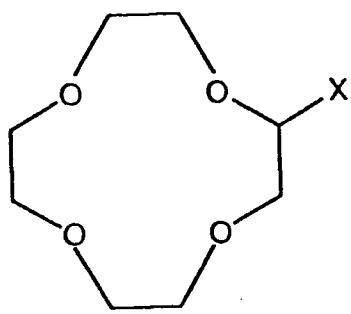

(55)

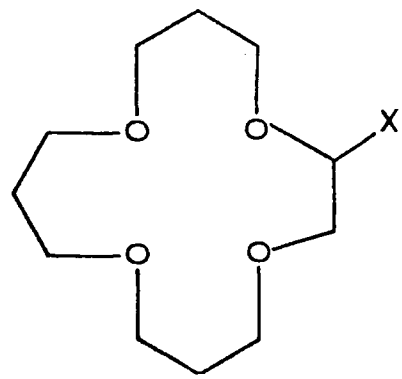

(56)

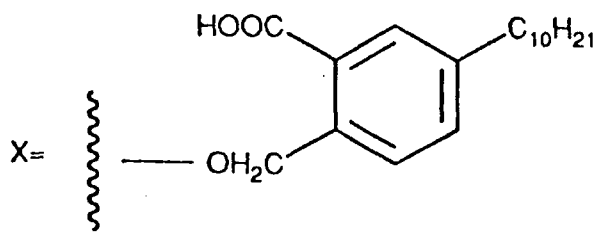

Likewise the lithium selectivity of crown ether (56) being far lower than for crown ether (55) can be rationalised by the extra steric crowding caused by the third six-membered chelate ring, which for small

metal ions (*ie.* lithium) overwhelms the effects caused by the favourable staggered orientation of hydrogen atoms.

1.3.3.3 Non-Donating Substituents on the 14-Crown-4 Skeleton

Kitizawa *et al.*[106] made a study in order to evaluate the effect of substitution on the 14-crown-4 ring in relation to lithium selectivity. Four ligands (57)-(60) were synthesised, each ligand was incorporated into a membrane composed of PVC (100 mg), nitrophenyl-octylether, NPOE (250 mg), crown ether (3.6 mg, 1 wt%) and potassium tetrakis-para-chlorophenyl borate (2.4 mg; 50 mol% : crown ether) and lithium selectivities were calculated by the fixed interference method.

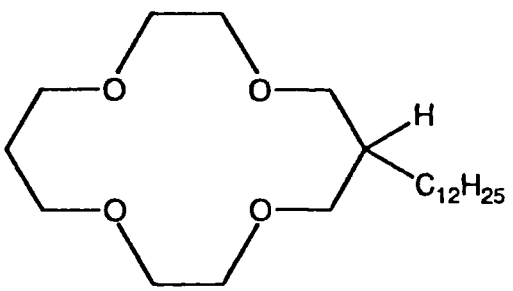

(57)

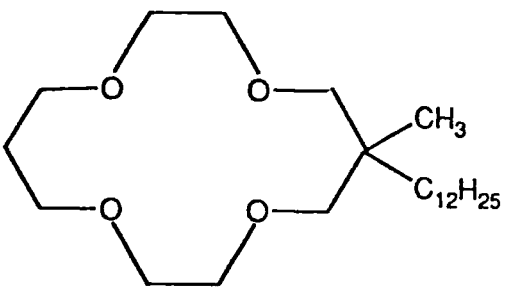

(58)

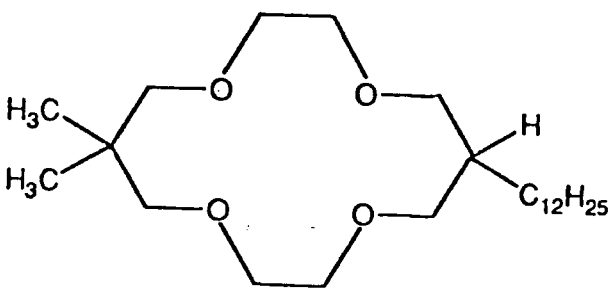

(59)

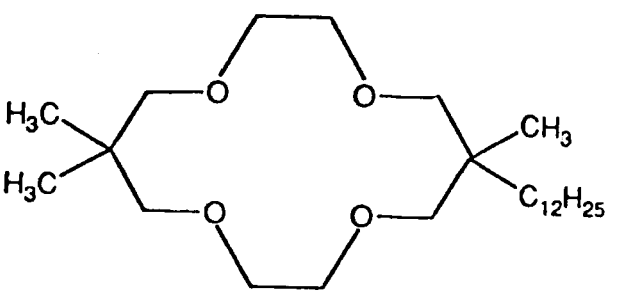

(60)

Comparison of ligands (57) and (58) indicated that the methyl derivative (58) showed an appreciably higher selectivity for lithium, particularly over sodium and potassium, than the non-methylated derivative (57). The obvious implication is that the methyl group of ligand (58) causes a steric effect on complexation such that

complexation of lithium is increasingly preferred over the sodium or potassium cations. Since sodium and potassium exceed the 14-crown-4 cavity size, there is a possibility of forming sandwich 2:1 complexes of crown ether:cation.

According to the bi-ionic potential theory of liquid membranes containing neutral carriers[124], the value of the selectivity coefficient K_{XY}^{Pot} ought to be independent of neutral carrier concentration in the membrane if both (X) and (Y) ions form only 1:1 complexes. Therefore an experiment was performed where membrane concentrations of ligands (57) and (58) were varied and K_{LiM}^{Pot} values were calculated. For ligand (57), increasing the crown ether concentration resulted in a drastic decrease in the selectivity for lithium, whereas for ligand (58) no change in selectivity patterns was observed. This indicates that for ligand (57), 2:1 and 1:1 complexation may occur for those ions (Na^+, K^+) that are larger than its cavity diameter, whereas for ligand (58), the presence of the methyl group geminal to the dodecyl group sterically inhibits 2:1 sandwich formation. Though not stressed in this study, the geminal dimethyl effect will operate for ligand (58), reducing the number of conformations available for the free ligand in solution relative to the non-methylated derivative (57). Furthermore, the methyl group may act so as to favour binding conformations in ligand (58) relative to ligand (57). All that may be said in this case is that the geminal dimethyl effect is operative for ligand (58), but whether or not this acts to enhance selective lithium complexation is unclear.

Ligand(59) exhibited a lithium selectivity that was very similar to that of ligand (58). However, ligand (60) exhibited a lower lithium selectivity than for ligands (58) and (59), yet was still slightly higher than the non-methylated derivative (57). There is no doubt that the substituents of ligand (60) will inhibit 2:1 complexation by sodium

or potassium. They may, however, act so as to inhibit 1:1 complexation by lithium where the geminal dimethyl effect in this case may hamper lithium complexation relative to larger sodium and potassium cations.

In a further study, Kitizawa[127] synthesised the bis-crown ether (61) and assessed the lithium selectivity of this ligand under identical experimental conditions to the previous study.

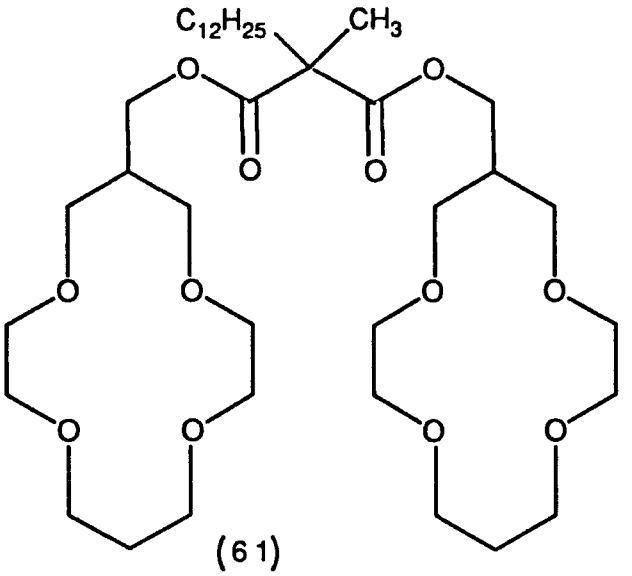

(61)

Ligand (61) was found to exhibit a much lower lithium selectivity than ligand (57) of the previous study. The linking moiety in ligand (61) confers greater stability on 2:1 complexes formed with larger cations (Na^+, K^+) than those formed by the two unlinked crown rings as for ligand (57), and hence the lower lithium selectivity of ligand (61) may be rationalised.

There is no doubt that the selectivity of the unsubstituted 14-crown-4 skeleton for lithium can be drastically changed and, in many cases augmented, by appropriate choice of non-donating substituent(s).

1.3.3.4 Donating Substituents on the 14-Crown-4 Skeleton

It has been shown that high selectivity for lithium over alkali and

alkaline earth metal cations can be attained using four-coordinate ligands. However, crystal structures (62)[126] and (63)[127] (amongst others)[128,129] indicate a coordination number of five for lithium (Figure 1.52).

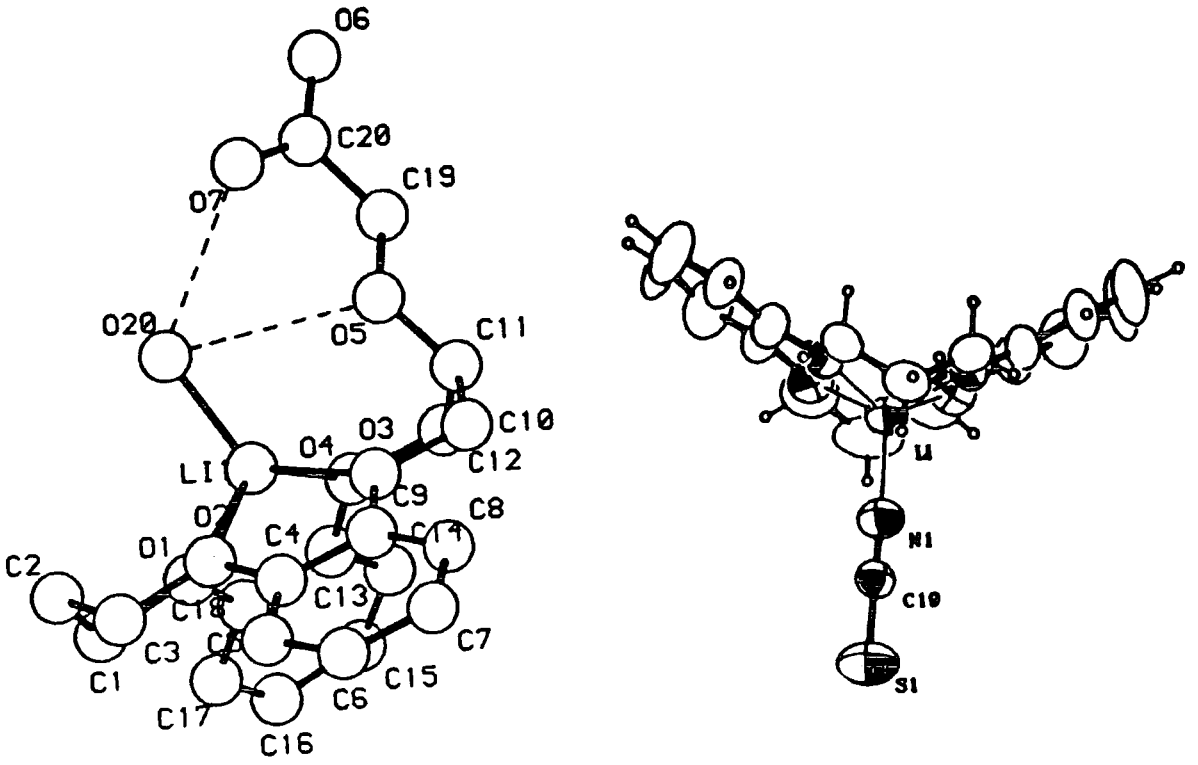

(62) (63)

Figure 1.52 *Crystal Structures of LiSCN with (62) and Dibenzo-14-Crown-4-(63).*

In the case of the lithium complex of dibenzo-14-crown-4 (63), the lithium ion coordinates to all four oxygen atoms and its fifth coordination site is occupied by the thiocyanate counteranion. In the lithium complex of ligand (62), the lithium ion is coordinated to all four ring oxygen atoms but, in this case its fifth coordination site is occupied by a water molecule which is hydrogen bonded to ether and carbonyl oxygens in the side arm. No coordination to the thiocyanate counteranion is seen in this complex.

The crystal structure of ligand (62) aroused interest in the possibility of augmenting the stability and selectivity of 14-crown-4

lithium complexes by incorporating a side arm containing a donor atom capable of coordinating to the central lithium ion. In the case of ligand (62), the side arm was of inappropriate design to afford direct axial coordination. With this in mind, Kitizawa *et al.*[125] made a detailed study to ascertain the effect of additional binding sites on the lithium selectivity of 14-crown-4 derivatives, and ligands (64)-(70) were synthesised. Selectivities were measured by embedding the ligands in a PVC/NPOE membrane and using the fixed interference method. The selectivities of ligands (64)-(70) measured for lithium over sodium and lithium over potassium are shown in Figure 1.53.

There is obviously a distinct effect of additional binding sites on selectivity for lithium. However, a significant enhancement in selectivity relative to ligand (70) (containing only four binding sites) is only realised in the case of ligand (67), containing an amide group, and ligand (69) containing a phosphonate group. This can be rationalised by the fact that amide and phosphonate groups, exhibiting high dipole moments and being relatively polarisable, will interact most strongly with cations of high charge density such as lithium.

Ligands (64), (66) and (68) exhibit a lower selectivity for lithium than ligand (70). This could be because of: (i) a more pronounced lariat ether effect being exerted on larger cations (Na^+, K^+) than on the smaller lithium cation and (ii) the fact that the ester groups of ligands (66) and (68) and ether group of ligand (64) function as less effective inhibitors of 2:1 complexation of larger cations than the dodecyl group of ligand (70). The likelihood is that a combination of these factors results in the measured selectivities for these ligands.

The clear message from this study is that through appropriate choice of side arm donor (amide and phosphonate), augmentation of the lithium selectivity displayed by the 14-crown-4 skeleton is possible

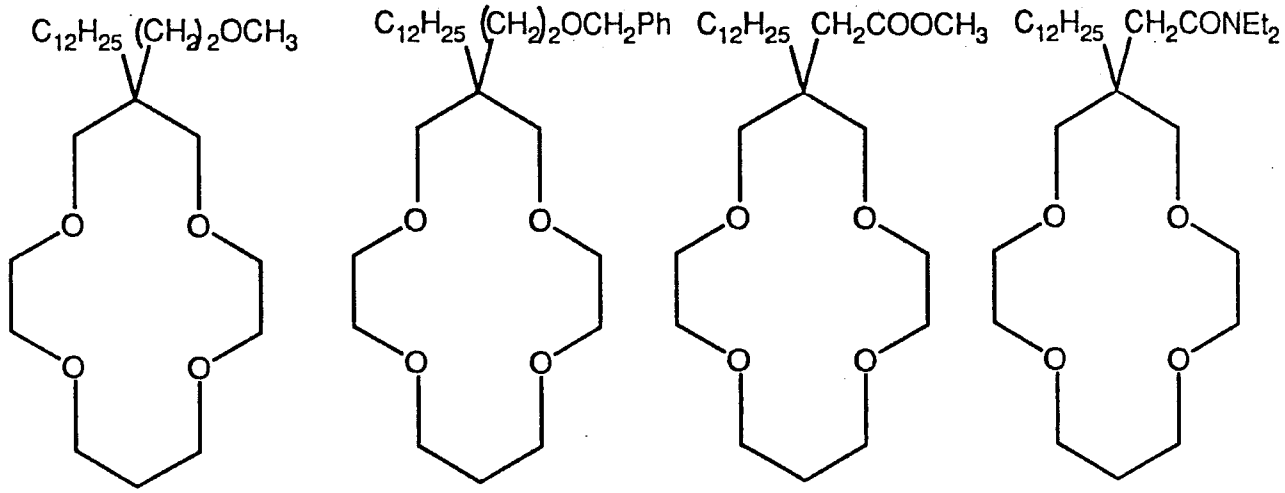

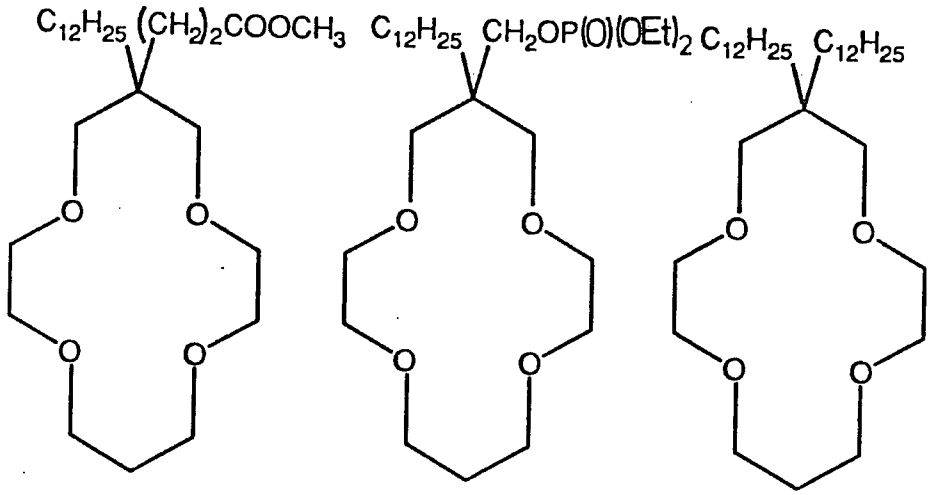

(68) (69) (70)

LIGAND	$1/K^{Pot}_{LiM}$ (Na^+)	$1/K^{Pot}_{LiM}$ (K^+)
(64) $R^2=CH_2CH_2OCH_3$	91	54
(65) $R^2=CH_2CH_2OCH_2Ph$	129	162
(66) $R^2=CH_2C(O)OCH_3$	105	93
(67) $R^2=CH_2C(O)NEt_2$	229	316
(68) $R^2=CH_2CH_2C(O)OCH_3$	72	38
(69) $R^2=CH_2CH_2OP(O)OEt_2$	182	288
(70) $R^2=C_{12}H_{25}$	145	91

Figure 1.53 *Lithium Selectivity of Some 14-Crown-4 Derivatives Bearing Additional Axial Donor Sites, as Measured Potentiometrically by the Fixed Interference Method.*

through axial coordination.

Synthetic work on cyclic and acyclic systems has, to date, not arrived at a lithium ionophore capable of accurately monitoring lithium levels (0.5 mM - 1.0 mM) in the blood of a patient being treated with lithium carbonate. Three of the most promising ionophores to date are shown in Figure 1.54, along with log K^{Pot}_{LiM} values for differing interfering ions. A table of log K^{Pot}_{LiM} required in order to attain less than 1% interference from other ions during clinical lithium ion measurement is also shown as a comparison.

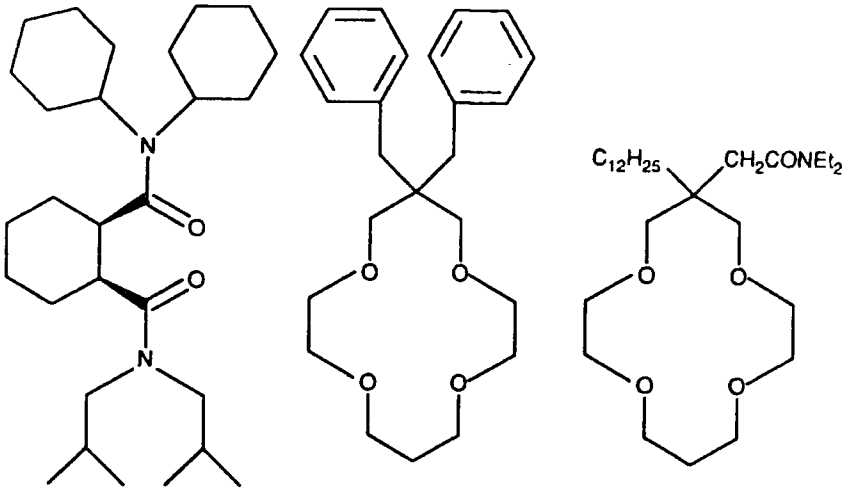

(10) (71) (72)

ION	Log K^{Pot}_{LiM} (10)	Log K^{Pot}_{LiM} (71)‡	Log K^{Pot}_{LiM} (72)‡	Log K^{Pot}_{LiM} *
Na^+	-2.3 (140 mM)	-2.3 (50 mM)	-2.2 (50 mM)	-4.5 (140 mM)
K^+	-2.4 (4.3 mM)	-2.2 (50 mM)	-2.3 (50 mM)	-3.0 (4.3 mM)
Mg^{2+}	-4.0 (0.8 mM)	-4.3 (500 mM)	-4.5 (500 mM)	-3.8 (0.8 mM)
Ca^{2+}	-2.7 (1.5 mM)	-4.7 (500 mM)	-3.5 (500 mM)	-2.3 (1.5 mM)

Figure 1.54 *Lithium Selectivities of the Most Promising Lithium Ionophores as Measured Potentiometrically by the Fixed Interference Method; Values in parentheses indicate fixed background concentrations; ‡Reference 130; *Required Values for ≤ 1% Interference.*

In all three cases, measurements were performed using the fixed interference method in membranes that were, aside from carriers, of

identical composition. Ligand (10) values were measured with interferent ions at concentrations comparable to those found in whole blood. However, values for ligands (71) and (72) were measured against a background concentration of 50 mM sodium chloride, which probably means that log K^{Pot}_{LiNa} values for these ligands are somewhat higher than would be expected under physiological conditions (140 mM NaCl).

1.3.4 Ionophores Designed for Lithium Extraction

Many of the same considerations pertinent to transport ability (lipophilicity of ligand and counterion, binding ability and selectivity of ligand) are also pertinent to extraction. However, the lithium selective ligands described so far in Section 1.3 have primarily been designed for use in ion selective electrodes and in membrane transport. Therefore studies have reflected the functions for which these ligands are intended and extraction studies are relatively sparse.

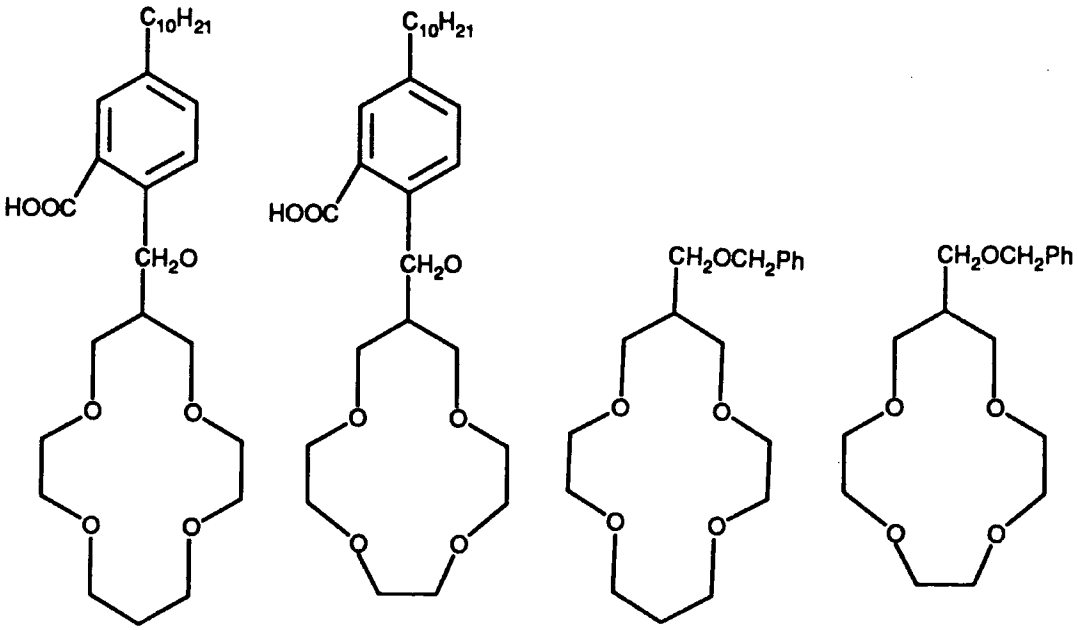

(73) (74) (75) (76)

Figure 1.55

Studies by Bartsch[120-122] however, indicate that the 14-crown-4 skeleton provides the most efficient and selective extraction for lithium over alkali and alkaline earth metal cations. Furthermore, when lithium extraction efficiencies and selectivities were compared[120] to corresponding values for lithium transport in PVC-based membranes for ligands (73)-(76) a good correlation was seen (Figure 1.55).

It thus seems likely that highly selective ligands for lithium transport already outlined, will also function as efficient, highly selective ligands for lithium extraction.

1.3.5 Anionic Ligands for Lithium Extraction

The nature of the counteranion has marked effects on the efficiency and, in some cases, the selectivity of extraction. Small, hard anions will extract less easily than large, lipophilic ones. Bartsch[122] reasoned that incorporation of the highly lithium selective 14-crown-4 skeleton into a lipophilic crown ether carboxylic acid might provide novel reagents for the solvent extraction of the lithium cation from aqueous solutions. Such ionisable crown ethers would thus have the advantage that concomitant transfer of an aqueous counteranion is not required. To this end, he synthesised ligands (75) and (77) and performed competitive solvent extractions of aqueous solutions of lithium, sodium, potassium, rubidium and caesium chlorides (Figure 1.56).

It was shown that both ligands (75) and (77) selectively extracted lithium over sodium with a ratio of 19:1 and 20:1 respectively. Furthermore, no extraction of K^+, Rb^+ or Cs^+ was seen for either ligand. The extraction efficiency was highly dependent on the pH of the aqueous source phase. Under acidic or neutral conditions, little or no

extraction was observed, whereas maximum extraction efficiency (85% or greater loading) was observed at pH 10-11. The fact that extraction was possible with the small, hard chloride counteranion, added to the pH dependence of extraction, both suggest that extraction is effected by the ionised form of the ligand.

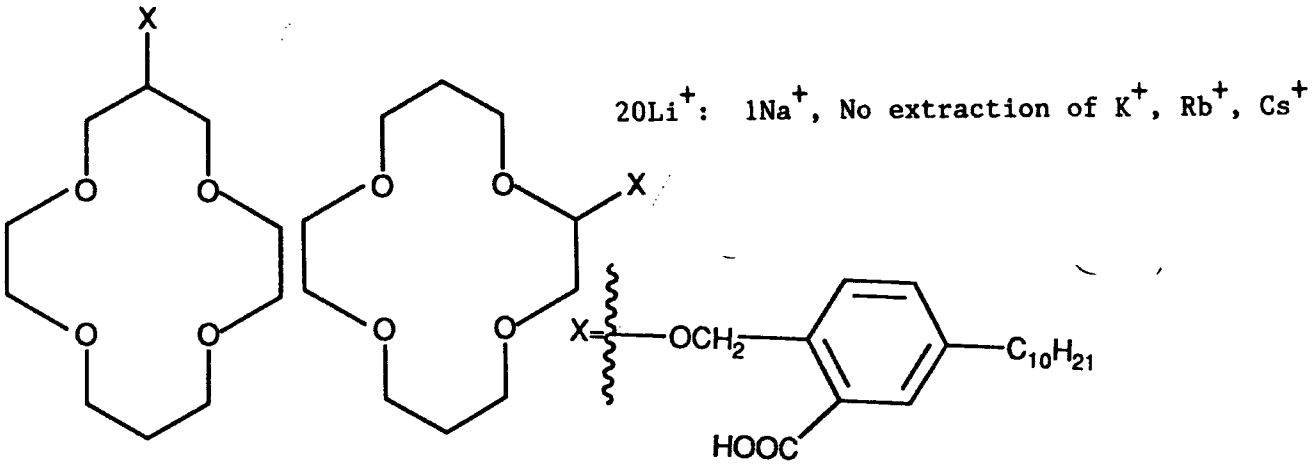

Figure 1.56 *Results of Competitive Solvent Extractions of Aqueous Solutions of Lithium, Sodium, Potassium, Rubidium and Caesium Chlorides with Ligands (75) and (77).*

The outstanding lithium selectivity obtained with lipophilic ligands (75) and (77) encourages application of these, and closely related, complexing agents for the recovery of lithium from natural sources and waste streams. Subsequent studies by Bartsch[131] on 16-crown-5 carboxylic acid and phosphonic acid derivatives as sodium selective extractants, indicate a strong influence of the nature of the anionic group and the length of side arm incorporating the anionic group, on extraction behaviour. Clearly optimal lithium extraction might be achieved when: (i) the anionic donor is in an optimum orientation for coordination to the cavity bound lithium cation and (ii) a phosphonic acid group is used, both to complement the small, highly charged lithium cation and, as it is more acidic, to increase the pH range over which effective lithium extraction might take place.

1.3.6 Scope of This Work

The work reported in this thesis can be divided into two distinct areas. The first involves the synthesis of a series of mono- and di-functionalised 14-crown-4 derivatives. All functional groups contain oxygen donors, but differ in two respects: (i) in the nature of the donor sites (alcohol, ether, ester, amide) and (ii) in the chelate ring size (five or six) formed by coordination of side arm donors to the metal cation.

The purpose of this study was two-fold: (i) to synthesise a neutral lithium selective ionophore and (ii) to gain a more thorough understanding of the effect of chelate ring size and nature of donor groups on resultant lithium selectivity.

Complexation studies between these ligands and a number of alkali and alkaline earth metal cations by Fast Atom Bombardment, NMR and Potentiometric methods have been undertaken (Chapter 2).

The second area involves the synthesis of a series of amide N-functionalised macrocycles. The effect of ring size, chelate ring size and ligand coordination number, on selectivity for alkali and alkaline earth metal cations was investigated using Fast Atom Bombardment, NMR and pH metric techniques (Chapter 3).

Finally (Chapter 4) contains the experimental procedures for the preparation of compounds, and also briefly describes the methods used to determine the stabilities and selectivities of complexation.

CHAPTER TWO

SYNTHESIS AND COMPLEXING STUDIES OF SOME 14-CROWN-4 DERIVATIVES.

2.1 INTRODUCTION

The aim of this work was to synthesise a neutral lithium selective ionophore for incorporation into a lithium selective electrode to monitor lithium ion concentrations in physiological and aqueous media. As has been mentioned in Chapter 1, the C-functionalised, tetra coordinate 14-crown-4 (1,4,8,11-tetraoxacyclotetradecane) skeleton has formed the basis of many existing neutral lithium selective ionophores. X-ray crystal structures of dibenzo-14-crown-4 (63)[127] and benzo-13-crown-4 (78)[132] with LiSCN (Figure 2.0) have shown that the lithium cation coordinates to all four ring oxygens, but that there is a fifth axial coordinate site, that is in both cases, occupied by the thiocyanate counteranion. Further, the crystal structure of spherand (37) with LiSCN[97], has shown the lithium ion to exhibit an almost perfect octahedral coordination with the six methoxy groups (Figure 2.0). This suggests the possibility of augmenting the lithium stabilities and selectivities exhibited by the 14-crown-4 skeleton through incorporating additional axial donor sites attached directly to the ring, to effect three-dimensional discrimination. Further, for reasons previously outlined (Chapter 1), axial amide donors would seem the most promising candidates. With this in mind the first target ionophore at the outset of this study was ligand (79). In this ligand, the axial amide donors above and below the plane of the crown ether ring might be expected to complete an octahedral coordination sphere around the cavity bound lithium ion.

2.2 SYNTHESIS OF LIGANDS

In the first attempted synthesis of ligand (79), a procedure

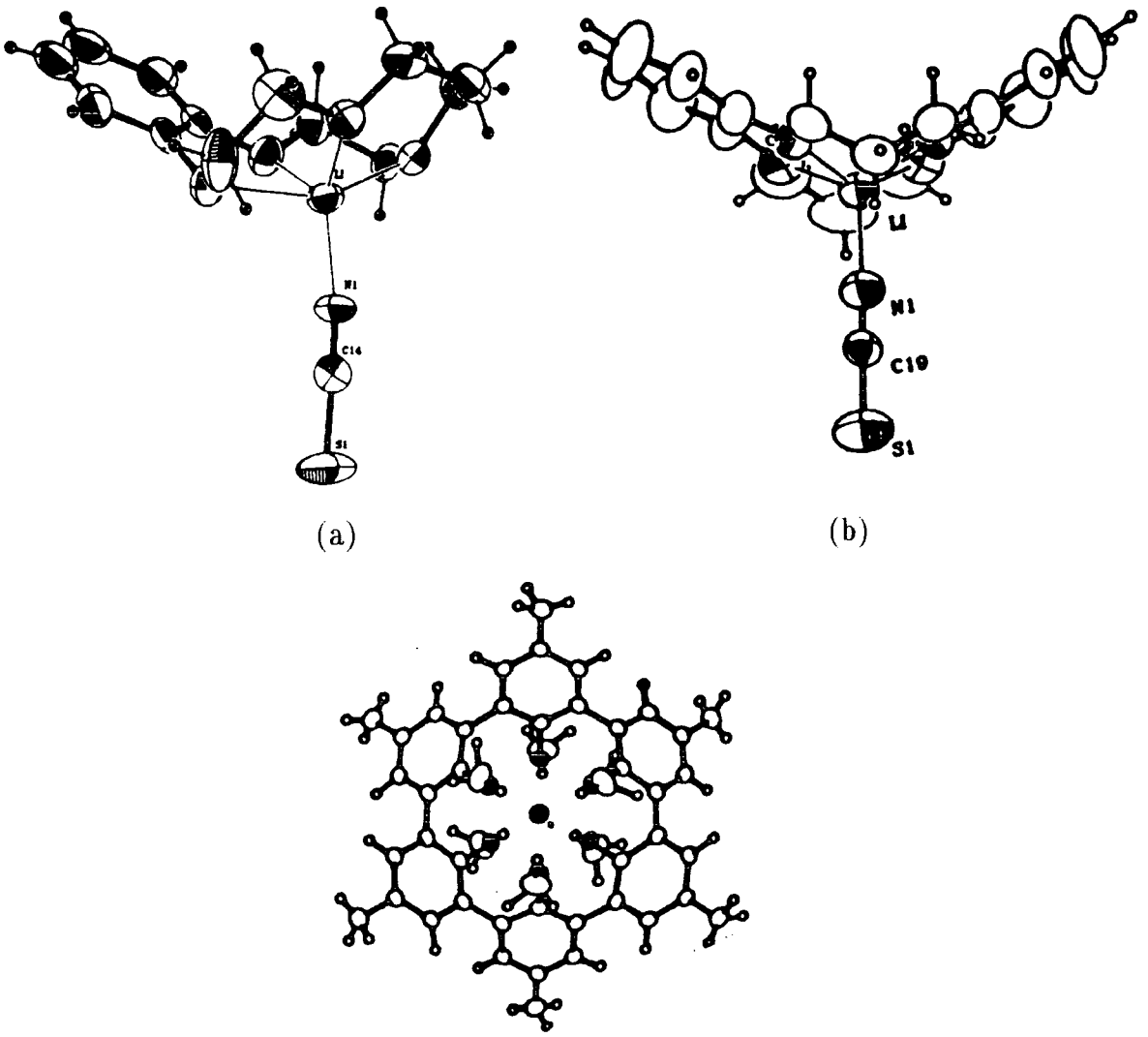

(a) (b)

(c)

Figure 2.0 *Crystal Structures of (a) (78)·LiSCN (Ref 134); (b) (63)·LiSCN (Ref 129) and (c) (37)·LiSCN (Ref 99).*

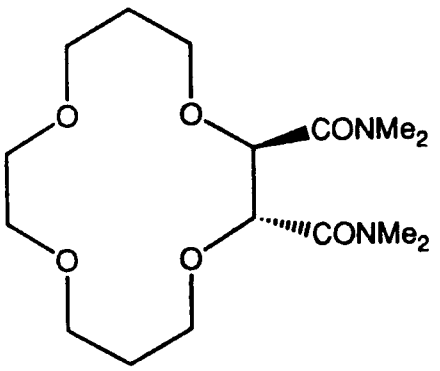

Structure (79)

developed by Lehn[80] was followed. This involved reacting the dithallium alkoxide of RR(+)-N,N,N',N'-tetramethyl tartramide (80) with 4,7-dioxa-diiododecane (81) in anhydrous dimethyl formamide at 70°C (Scheme 2.1).

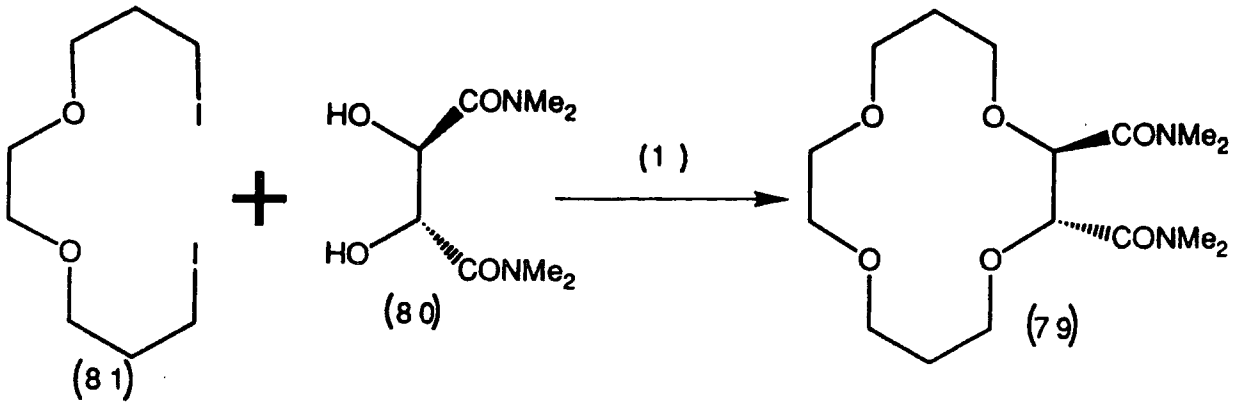

Scheme 2.1 *(1) DMF (dry), TlOEt, N_2, 70°C.*

RR(+)-N,N,N',N',-tetramethyl tartramide was prepared from RR(+)-diethyl tartrate (82) by adding anhydrous dimethylamine to a solution of (82) in anhydrous ethanol (Scheme 2.2).

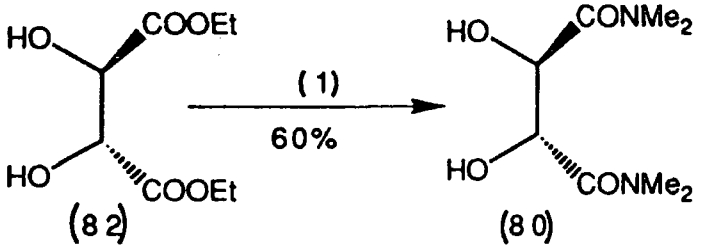

Scheme 2.2 *(1) NMe_2H (dry), EtOH (Dry), N_2.*

4,7 Dioxa-1,10-diiododecane (81) was prepared from 4,7 dioxa-1,10-dichlorodecane (83) by refluxing in a solution of analar acetone with powdered sodium iodide. The dichloride (83) was in turn prepared by dropwise addition of thionyl chloride to a refluxing mixture of 4,7 dioxadecane-1,10-diol (84) and pyridine in toluene, and refluxing the resulting system for 24 hours (Scheme 2.3).

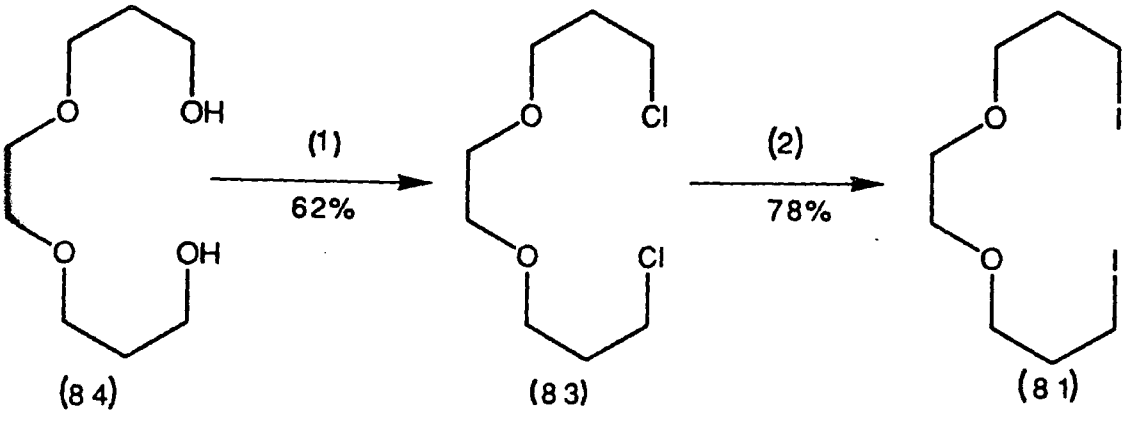

Scheme 2.3 *(1) $SOCl_2$, pyridine, toluene, N_2, Reflux*
(2) NaI, acetone, N_2.

The synthesis of the diol (84) was attempted by three different routes:

The first route (Scheme 2.4) involved tosylation of the readily available triethylene glycol (85) using p-toluenesulphonyl chloride and pyridine at $0^{o}C$.

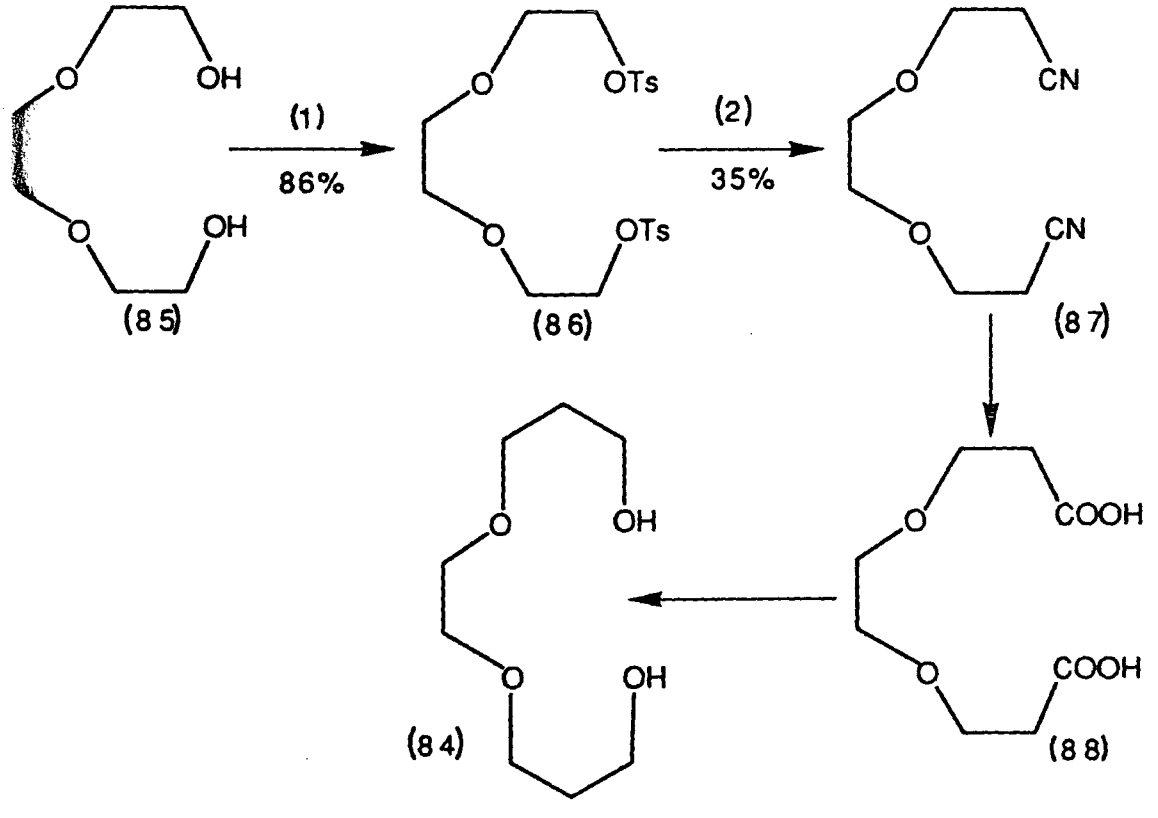

Scheme 2.4 *(1) TsCl, pyridine, $0^{o}C$, N_2;*
(2) DMSO, KCN, RT.

The white crystalline ditosylate (86) was then reacted with potassium cyanide in anhydrous dimethyl sulphoxide at room temperature for five days, to yield the dinitrile (87). However, attempts to hydrolyse the dinitrile, both under acidic and basic conditions, yielded very low amounts of impure product and this route was abandoned.

The second route (Scheme 2.5), involved reacting two equivalents of the monosodium salt of 1,3-propanediol with one equivalent of ethane-1,2-di-p-toluene sulphonate (89) under anhydrous conditions, at 60°C, using excess 1,3-propanediol as a solvent. Though this route gave the desired product, the yield (9%) was very low and purification proved difficult.

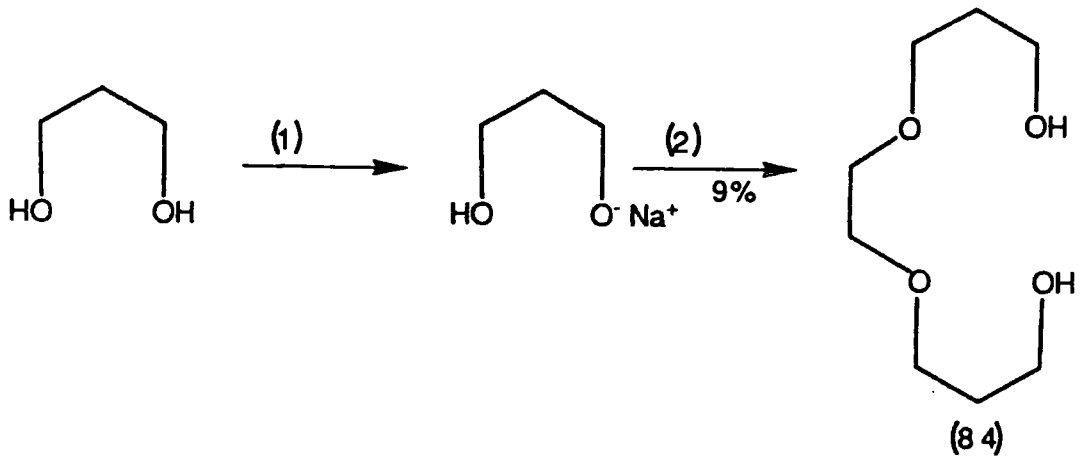

Scheme 2.5 *(1) Na(s), excess 1,3-propanediol, N_2; (2) Ethane-1,2-di-p-toluene sulphonate, N_2, 60°C.*

The third route (Scheme 2.6) involved firstly, the dropwise addition of two equivalents of acrylonitrile (90) to a stirred two phase system composed of one equivalent of ethane-1,2-diol (91) and a 2% aqueous sodium hydroxide solution at 0°C. This yielded the dinitrile (87), which was converted into the corresponding diester (92) by refluxing in an ethanol/sulphuric acid mixture. Finally the diester (92) was reduced using lithium aluminium hydride to yield the desired diol product (84). The overall yield of this process was 37% and

purification at each stage proved straightforward. Therefore, it was this route that was used in order to prepare bulk quantities of 4,7-dioxadecane-1,10-diol (84).

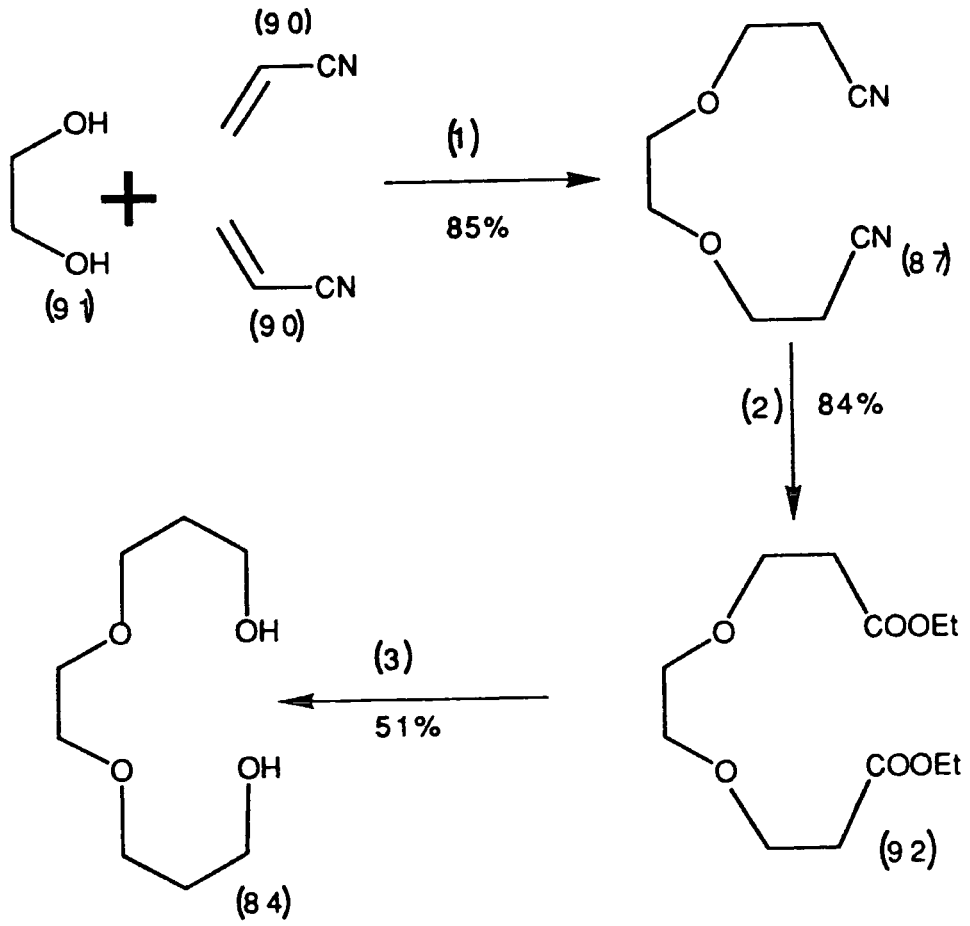

Scheme 2.6 *(1) 2% NaOH(aq), RT; (2) EtOH, H_2SO_4(conc), Reflux; Et_2O, $LiAlH_4$, N_2.*

The cyclisation (Scheme 2.1) however, was largely unsuccessful. Some evidence for ligand (79) was seen but this proved to be a very minor product, and furthermore, separation of the desired cycle (79) from other products by both chromatography and crystallisation was not entirely successful. ^{1}H NMR, ^{13}C NMR, IR and mass spectral data showed that the major product was 4,7-dioxadeca-1,9-diene (93). The preference for elimination in this system is surprising since a primary alkyl iodide is used in dimethylformamide, both of which should promote nucleophilic substitution by the S_N2 mechanism. However, the reaction

was repeated and once again 4,7-dioxadeca-1,9-diene was found to be the major product.

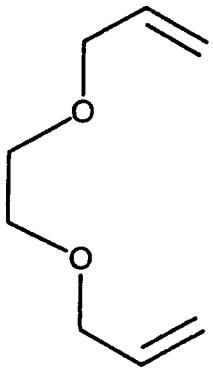

Structure (93)

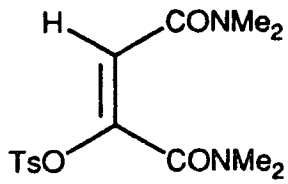

Structure (95)

In order to alleviate the problem of elimination, two possible alternatives were considered:

The first alternative is depicted in Scheme 2.7. In this reaction, the disodium alkoxide of 4,7-dioxadecan-1,10-diol was formed in DMF under anhydrous conditions and to this was added 1,2-di-p-toluene sulphonyl N,N,N',N'-tetramethylsuccinamide (94).

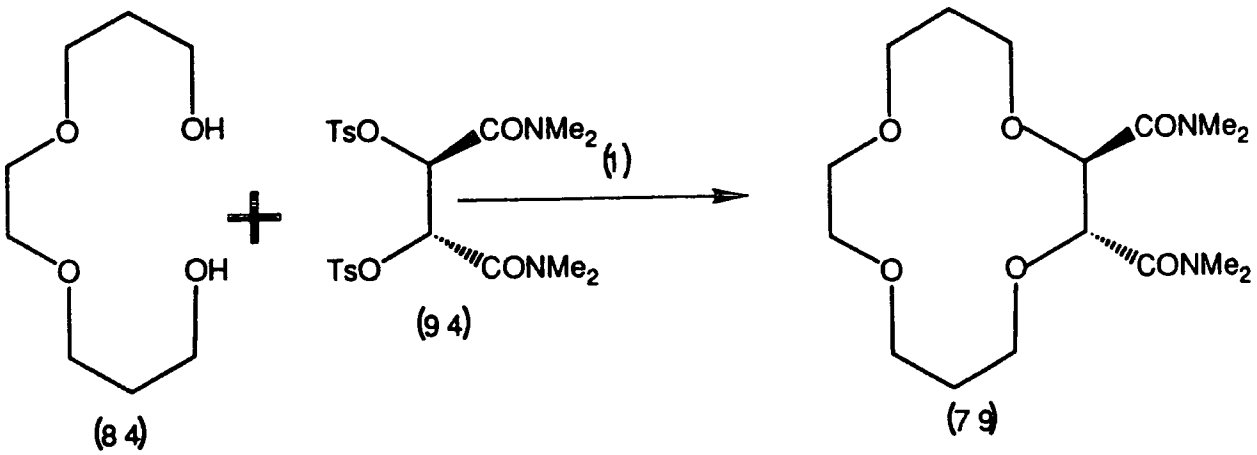

Scheme 2.7 *(1) DMF, Na(s), 60°C, N_2.*

The reaction mixture was then heated to 60°C and maintained at this temperature overnight. Unfortunately, rather than yielding the desired cycle (79), the disodium alkoxide acted as a base to yield eliminated product (95) (above). In retrospect, this seemed a reaction unlikely to

succeed owing to the high acidity of the hydrogen atoms attached to the secondary carbon atoms in 1,2-di-p-toluene sulphonyl N,N,N',N-tetramethylsuccinamide (94) that promote base catalysed elimination.

The second alternative was to synthesise 2,2,9,9-bis-dimethyl-4,7-dioxa-1,10-diiododecane (96), in which hydrogen atoms (β) to the primary iodide groups are replaced by methyl groups, therefore rendering elimination during the cyclisation impossible (Scheme 2.8).

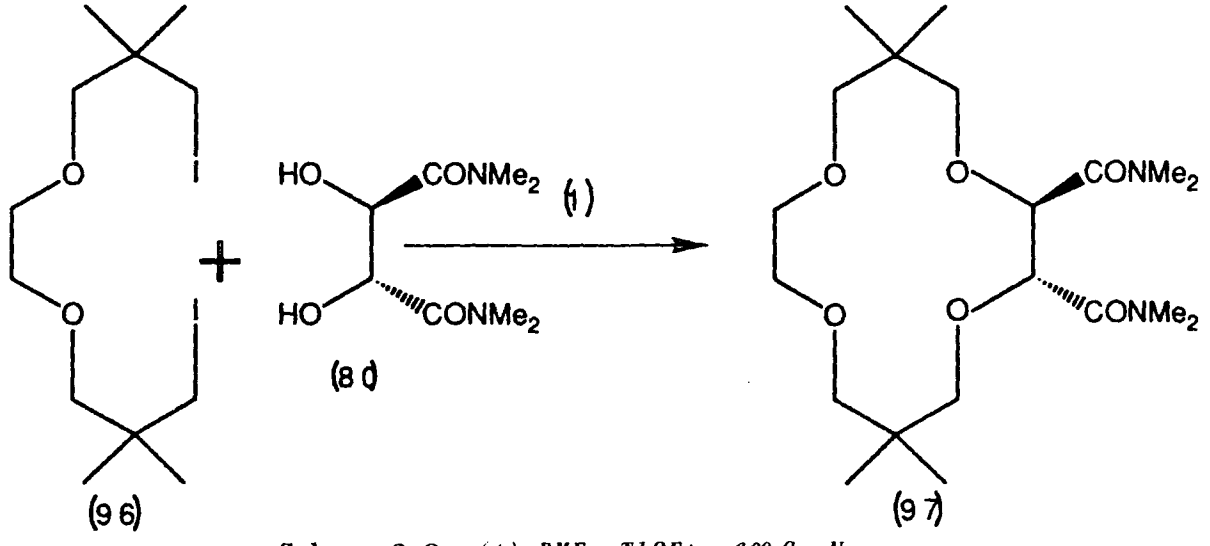

Scheme 2.8 *(1) DMF, TlOEt, 60°C, N_2.*

In order to synthesise the diiodide (96), it was first necessary to form 2,2,9,9-bisdimethyl-4,7-dioxa-decane-1,10-diol (98). This was attempted by two routes:

In the first route, sodium metal was added to an excess of 2,2-dimethyl-1,3-propanediol (99) stirred at 50°C in anhydrous dimethylformamide, so as to form the monosodium salt. To this was added ethane-1,2-di-p-toluene sulphonate (89) and the mixture stirred at 50°C under nitrogen for 12 hours (Scheme 2.9). The yield of crude desired product (98) was low (15%) and complete separation from excess diol (99) by crystallisation, distillation and chromatography was not successful. Furthermore, attempts to separate (99) and (98) by tosylation, mesylation or chlorination followed by chromatography, distillation or

crystallisation of respective tosylates, mesylates or chlorides, also proved unsuccessful.

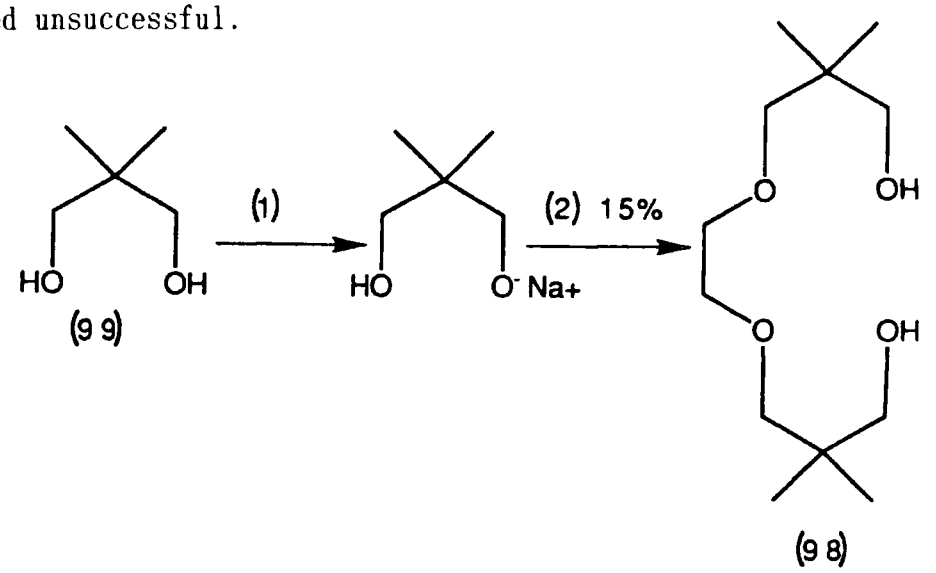

Scheme 2.9 *(1) Na(s), DMF (dry), N_2, 50°C; (2) Ethane-1,2-di-p-toluene sulphonate, N_2, 150°C.*

The second route is depicted in Scheme 2.10.

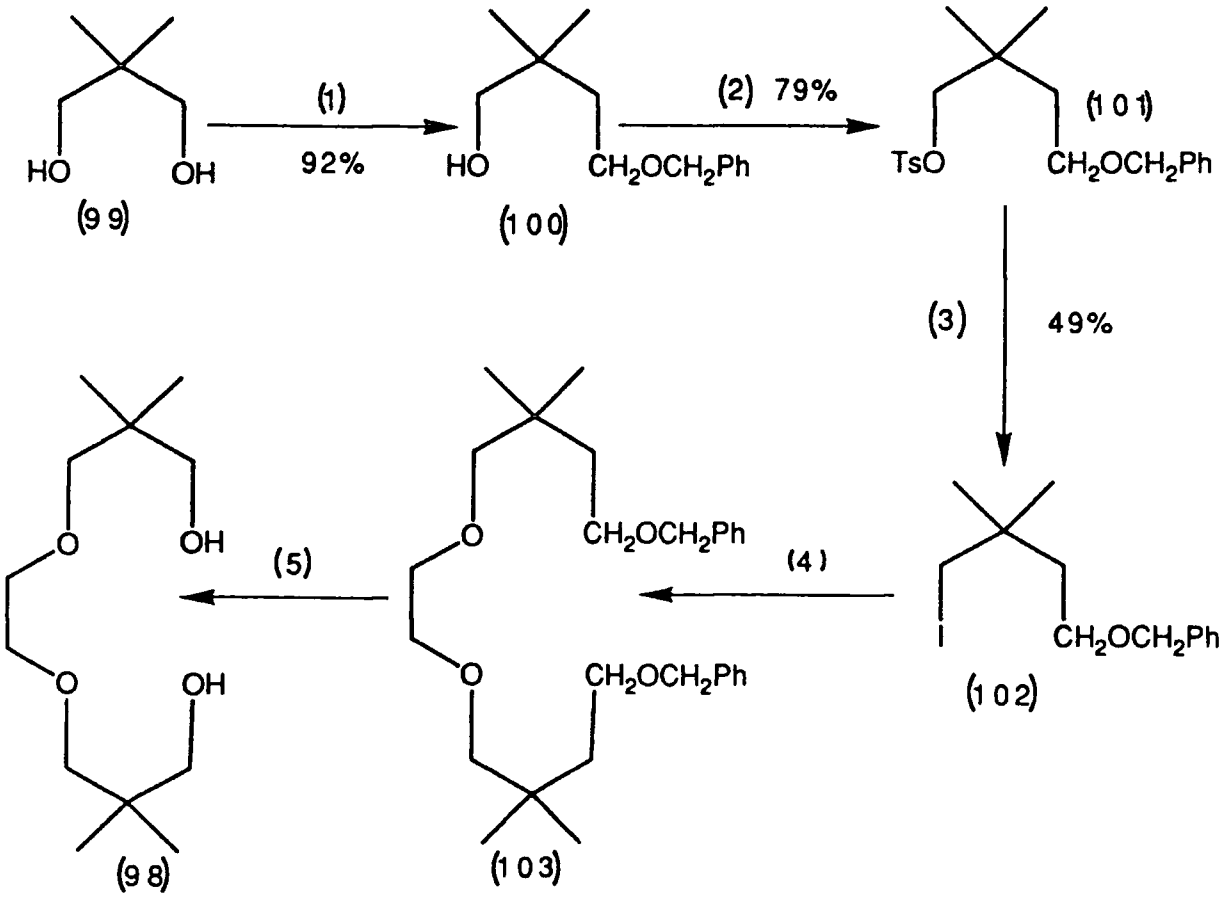

Scheme 2.10 *(1) $PhCH_2Cl$, $Pr_4N^+Br^-$, THF, NaOH(s), Reflux(N_2); (2) TsCl, pyridine, 0°C; (3) KI, DMF, 90°C; (4) Ethane-1,2-diol, NaH, DMF(N_2); (5) Pd/C hydrogenation).*

Formation of the monobenzylether (100) proved successful. This was then tosylated using p-toluenesulphonyl chloride and pyridine at $0^{o}C$ to yield the tosylate (101) as a white solid. Attempts to form the iodide (102) in analar acetone using potassium iodide failed, but when the solvent was changed to dimethylformamide the reaction proved successful. Dimethylformamide is more able than acetone, to solvate the potassium cation so as to leave a 'naked' iodide ion. It may therefore be inferred that S_N2 substitution on the tosylate (101) is appreciably more difficult than for 4,7-dioxa-1,10-dichlorodecane (Scheme 2.3). Attempts to form the dibenzylether (103) by reacting the iodide (102) with the disodium alkoxide of ethane-1,2-diol in dimethylformamide proved unsuccessful, re-emphasising the hindrance imposed on S_N2 substitution by the bulky electron donating dimethyl moiety.

A second attempt to synthesise the target cycle (79) followed a procedure by Okahara[133] (Scheme 2.11).

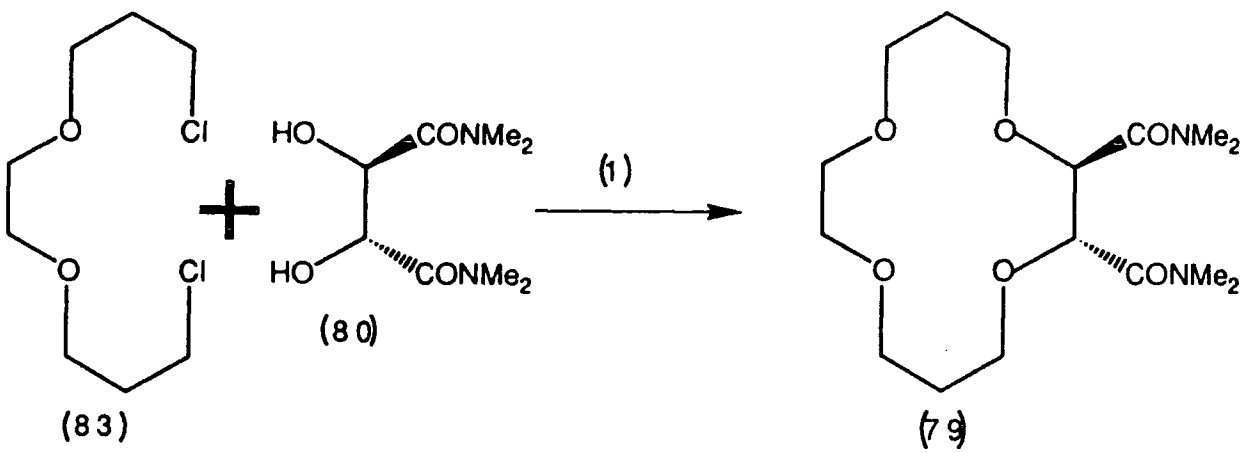

Scheme 2.11 *(1) t-BuOH, LiBr, H_2O, Li(s), Reflux(N_2).*

This process involved the formation of the dilithium alkoxide of RR(-)-N,N,N',N'-tetramethyl tartramide (80) in ^{t}butanol under nitrogen, followed by the addition of 4,7-dioxa-1,10-dichlorodecane and lithium bromide. The mixture was refluxed for 2 weeks. The use of lithium bromide was essential to ensure cyclisation in the original procedure by

Okahara[133] (Scheme 2.12), and it was inferred that its function was to promote a halogen exchange to form the bromide/dibromide derivative of (83).

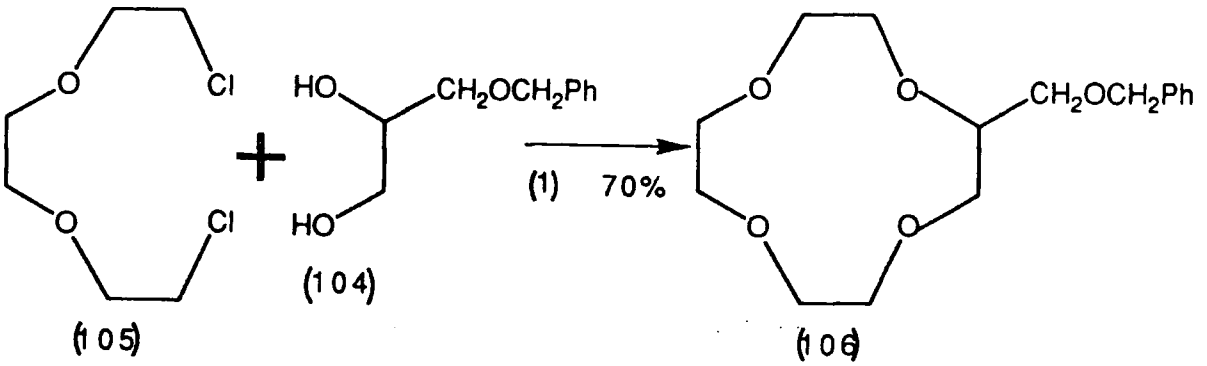

Scheme 2.12 *(1) Li(s), t-BuOH, LiBr, H_2O, Reflux(N_2).*

The successful cyclisation depicted in Scheme 2.12 was attributed to the heterogeneous reaction of the dispersed lithium salt of the diol (104), in which the coupling by the attack of the primary alkoxide of the diol (104), and the subsequent intramolecular attack of the secondary alkoxide, must occur advantageously under the influence of a lithium template effect. By way of example, in the cyclisation attempt by Okahara (Scheme 2.13), the dilithium alkoxide of ethane-1,2-diol was soluble in the ^{t}butanol solvent - this resulted in a homogeneous reaction and no product could be detected after 10 days.

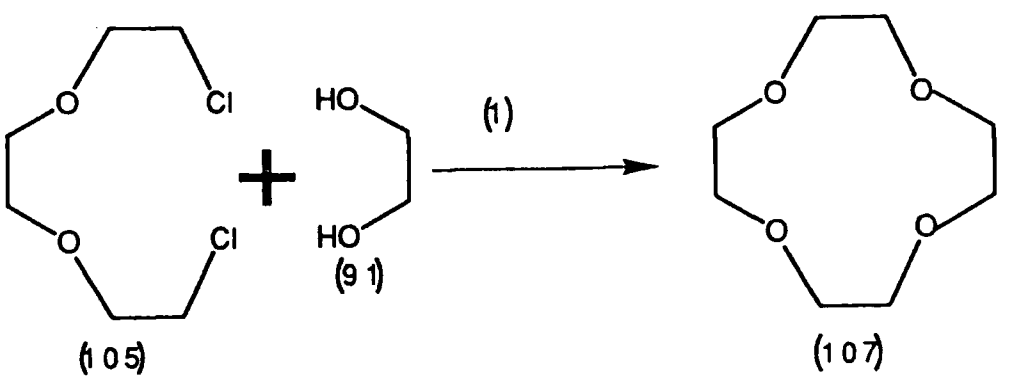

Scheme 2.13 *(1) Li(s), t-BuOH, LiBr, H_2O, Reflux(N_2).*

The formation of the cycle (79) by this procedure yielded desired product at the first attempt, but the yield (~ 2%) was very low and the

reaction proved irreproducible: two further cyclisation attempts yielded no further cycle (79). The dilithium alkoxide of the diol (80) was soluble in the reaction solvent and a homogeneous system resulted. The importance of a heterogeneous system in order to achieve a reasonable yield of desired product by this method, was thus re-emphasised.

Stimulated by the successful cyclisation by Bartsch[121] of 2-benzyloxy-1,4,8,11-tetraoxacyclotetradecane (108) (Scheme 2.14) by following the Okahara procedure[133], the possibility of synthesising monobenzyloxy- (108) and dibenzyloxy- (109) 14-crown-4 derivatives became apparent.

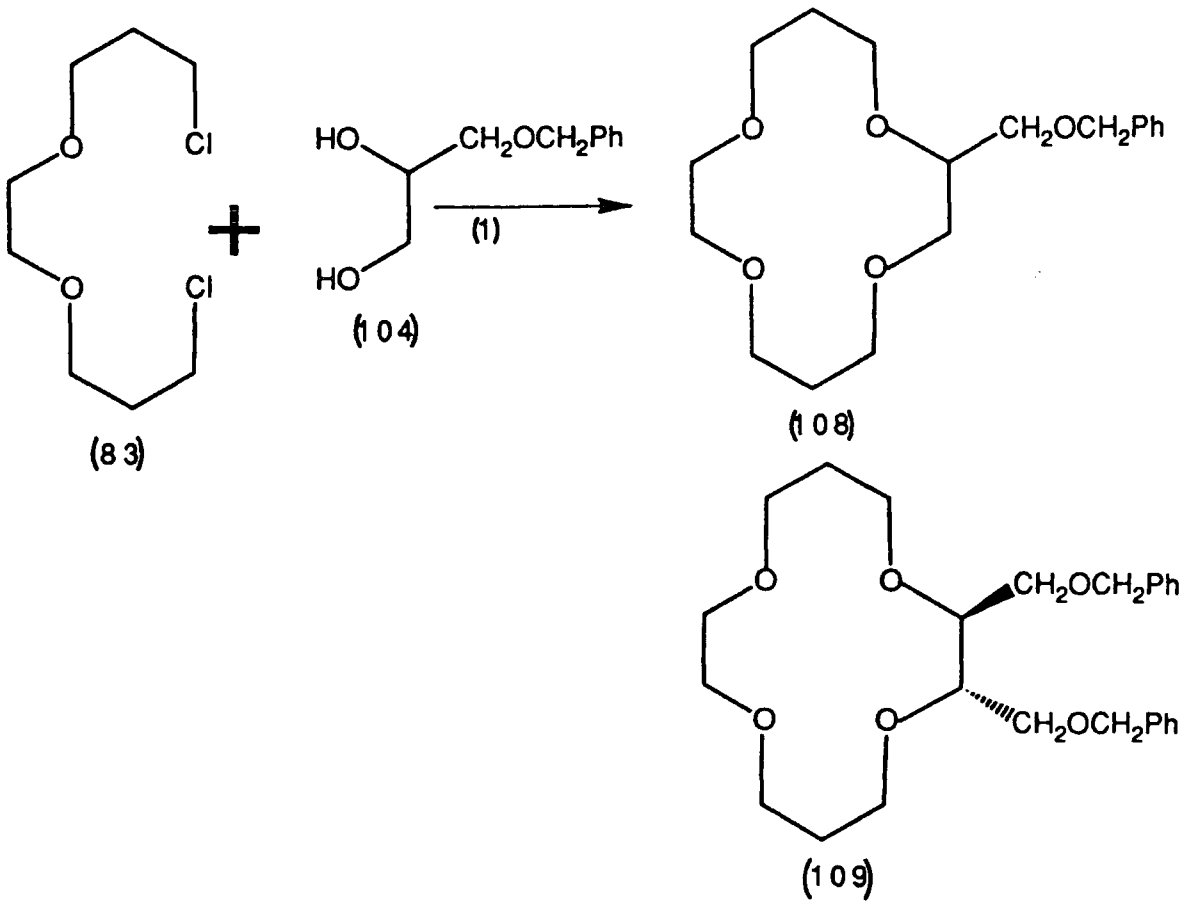

Scheme 2.14 *(1) Li(s), t-BuOH, LiBr, H_2O, Reflux(N_2).*

It was hoped that once the benzyloxy derivatives (108) and (109) had been made, the ring system might remain intact whilst reactions were performed to vary the length and nature of axial groups. Thus, 3-

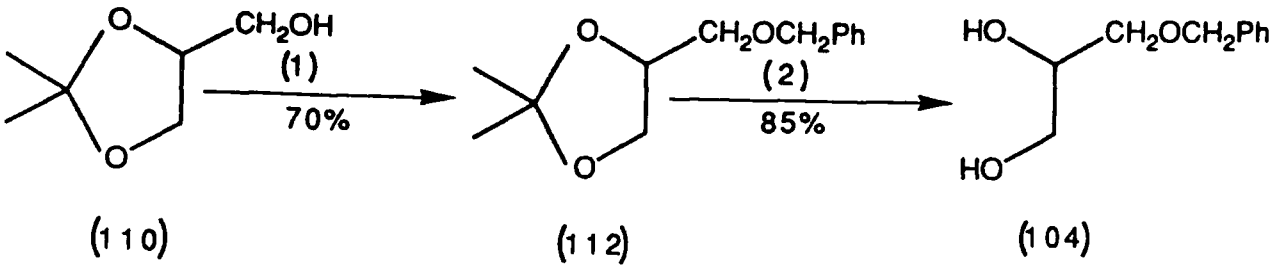

(110) (112) (104)

Scheme 2.15 *(1) NaOH(s), $PhCH_2Cl$, $Pr_4N^+Br^-$, THF, Reflux(N_2); (2) 1M acetic acid, 100°C, 1h.*

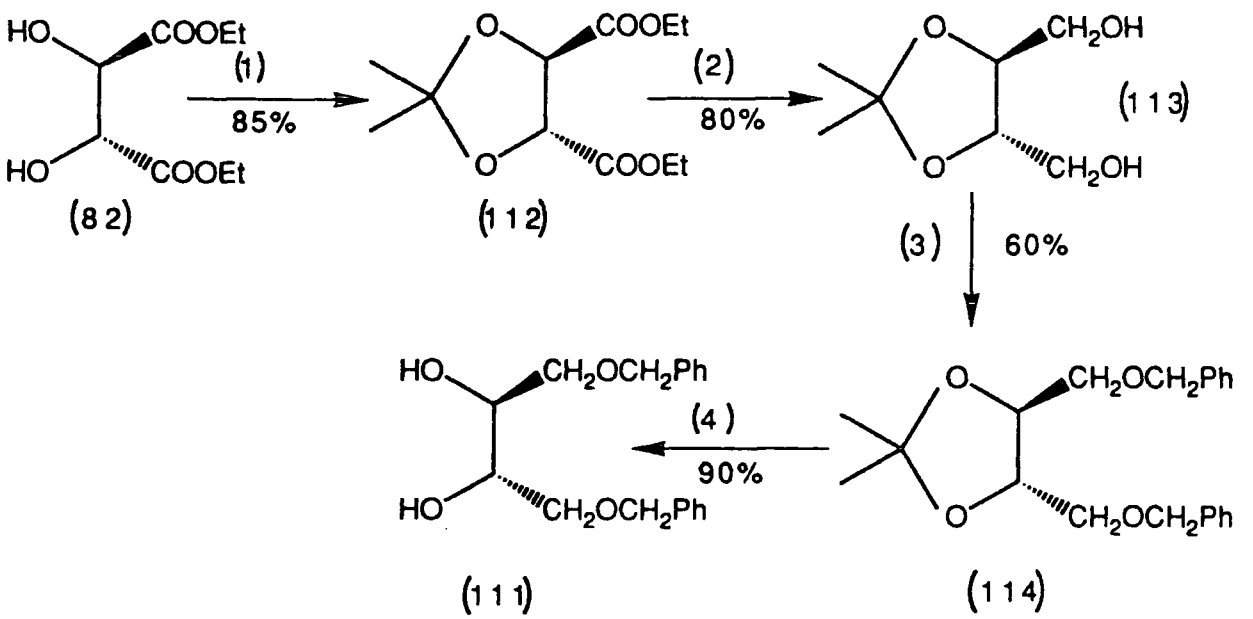

(82) (112) (111) (114)

Scheme 2.16 *(1) Dimethoxypropane, toluene, p-toluene sulphonic acid, 90°C, 3h, N_2; (2) $NaBH_4$, Et_2O; (3) NaOH(s), $PhCH_2Cl$, $Pr_4N^+Br^-$, THF, Reflux(N_2); (4) 1M acetic acid, 100°C, 1h.*

benzyloxy-propane-1,2-diol (104) was prepared from commercially available 2,2-dimethyl-4-hydroxymethyl-1,3-dioxalane (110), by benzylation followed by hydrolysis of the dioxalane ring according to the procedure by Howe and Malkin[134] (Scheme 2.15); and (2S,3S)(-)-1,4-dibenzyloxy-2,3-butanediol (111) was prepared from the commercially available RR(+)-diethyltartrate (82) according to Scheme 2.16.

Cyclisations to yield monobenzyloxy- (108) and dibenzyloxy- (109) 14-crown-4 derivatives were then performed according to the Okahara procedure (Scheme 2.17).

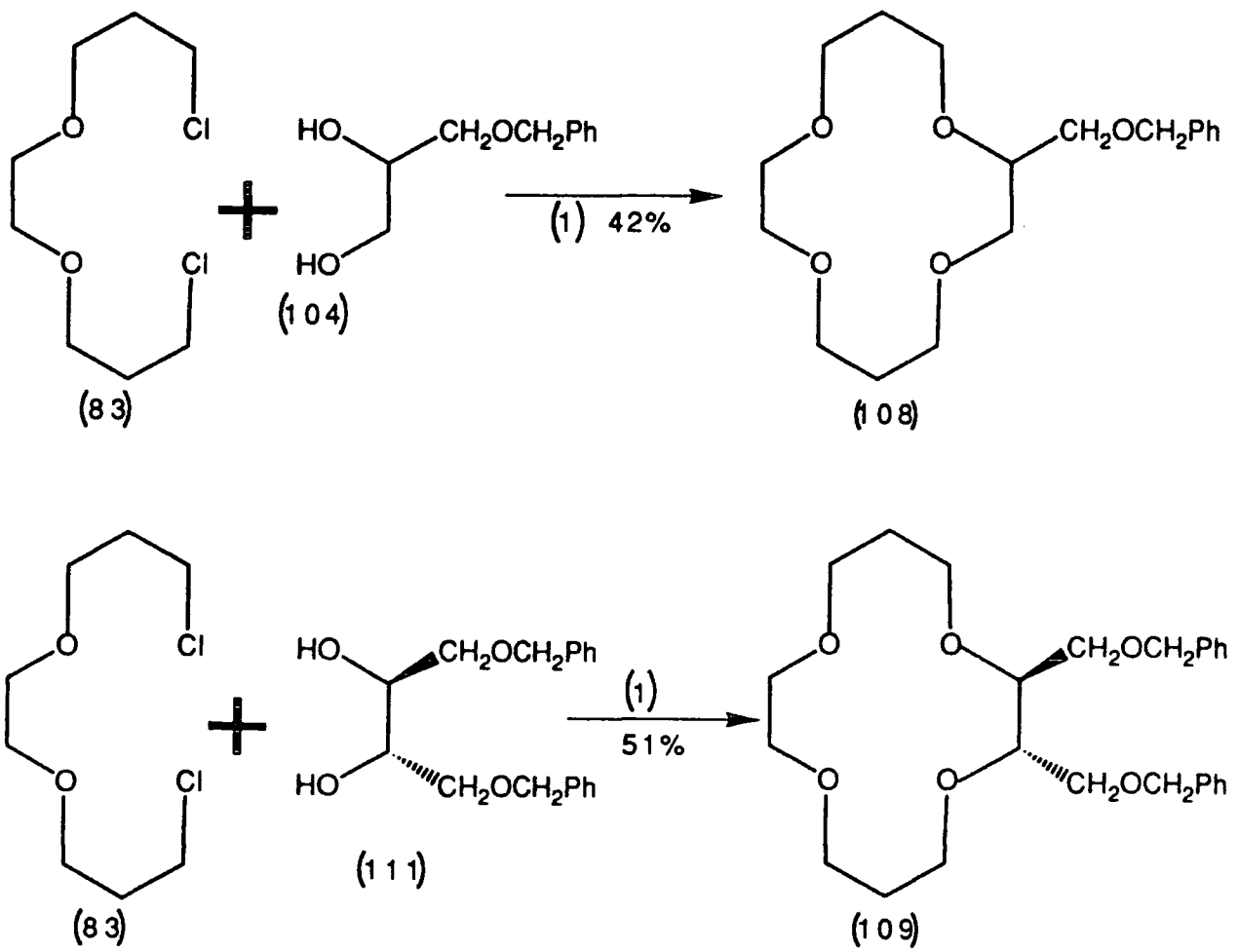

Scheme 2.17 *(1) Li(s), t-BuOH, LiBr·H2O, Reflux(N2).*

In both cases the dilithium salts were present as a fine white suspension in the reaction solvent. The systems were heterogeneous and successful isolation of desired products (108) and (109) resulted in

reasonable yield.

According to Bartsch[121], debenzylation of (108) was achieved by hydrogenation at room temperature at a pressure of just over one atmosphere of hydrogen, using palladium on carbon with a catalytic amount of p-toluenesulphonic acid in ethanol. Attempts to repeat this reaction for both ligand (108) and (109) failed. Even at higher pressures of three atmospheres hydrogen, no desired product was seen. Successful debenzylation was in fact achieved by use of Pearlman's catalyst [$Pd(OH)_2$ 30% v/v H_2O] with a catalytic amount of p-toluene-sulphonic acid in ethanol under a hydrogen pressure of three atmospheres at room temperature (Scheme 2.18).

It was hoped that 14-crown-4 derivatives (115) and (116) would be versatile, in that oxidation under mild conditions might afford the acid derivatives (117) and (118) from which the ester and amide derivatives might be made (Scheme 2.19). However, attempts to oxidise (115) and (116) through mild oxidation conditions using pyridinium chlorochromate, pyridinium dichromate, Jones' reagent and nitric acid, yielded at best, traces of aldehyde products.

Ligands (115) and (116) may also be used to synthesise amide and ester derivatives of 14-crown-4, in which the length of the axial substituent is extended by one carbon atom (Schemes 2.20 and 2.21).

These ligands were in fact successfully synthesised by the methods outlined in Schemes 2.20 and 2.21. The benzyloxy, alcohol, ester and amide derivatives provided the basis for a study of the effect of donor number, type of donor and chelate ring size on the stability and selectivity of lithium complexes by ^{13}C NMR, Fast Atom Bombardment (FAB) and potentiometric studies. Furthermore, [α_D], measurements indicated that there was no racemisation throughout the synthetic scheme (dibutyl-amide 128 [α_D] = -33.7^0, C = 1.00, CH_2Cl_2). Thus, for difunctionalised

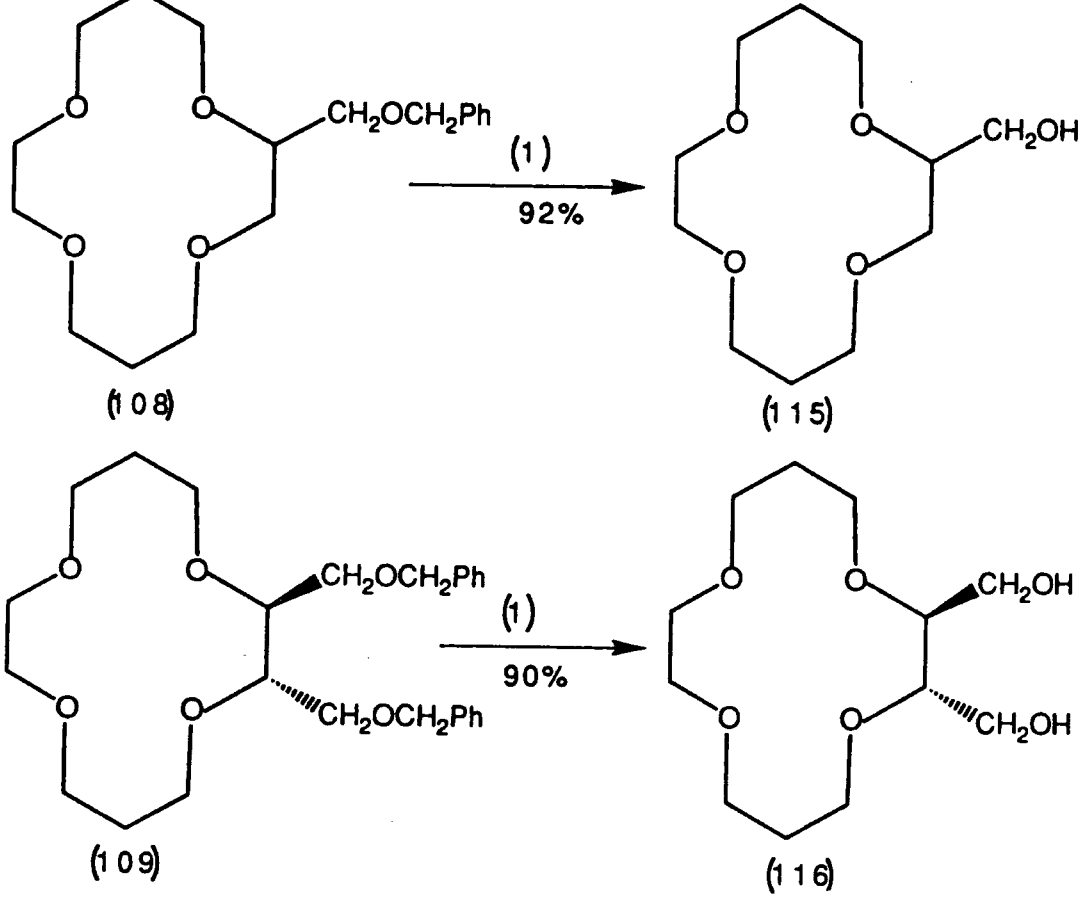

Scheme 2.18 *(1) Pearlmans catalyst, p-toluenesulphonic acid, ethanol, H_2 (3 atmospheres), RT.*

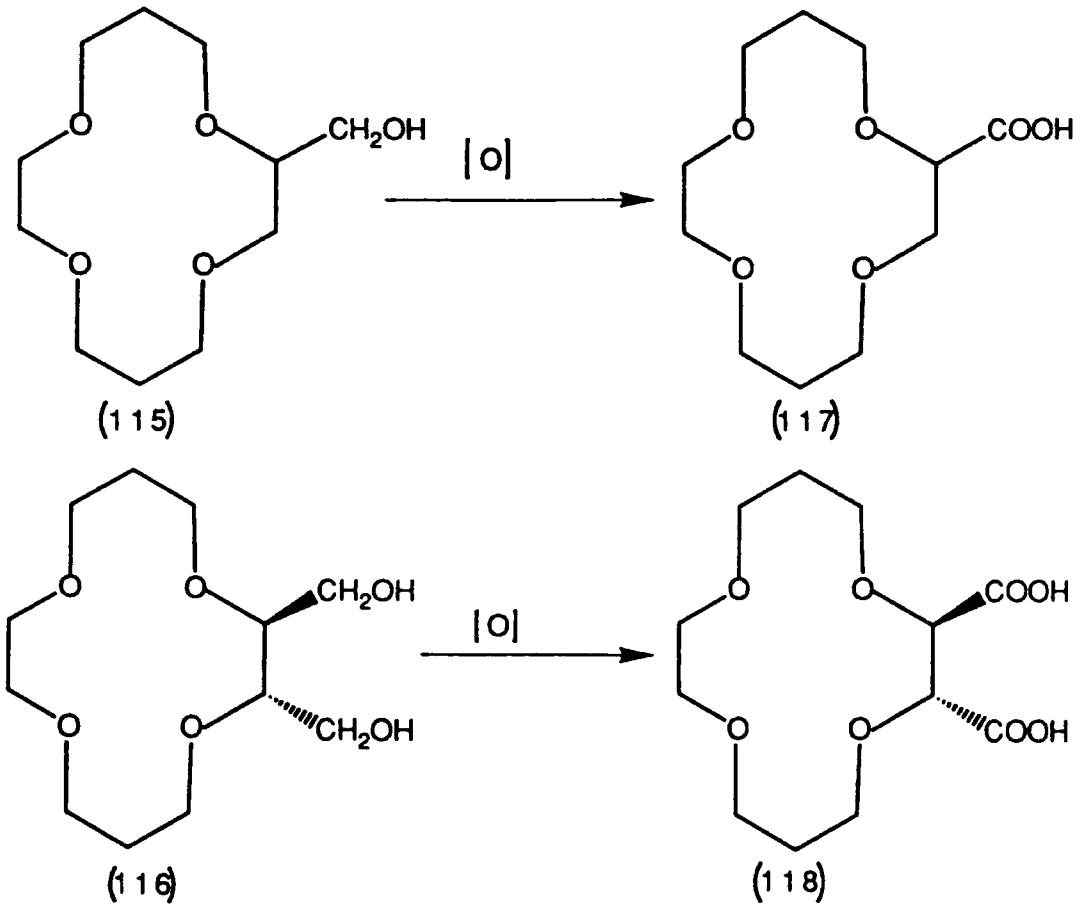

Scheme 2.19 *Attempted Oxidation of (115), (116) to give (117), (118)*

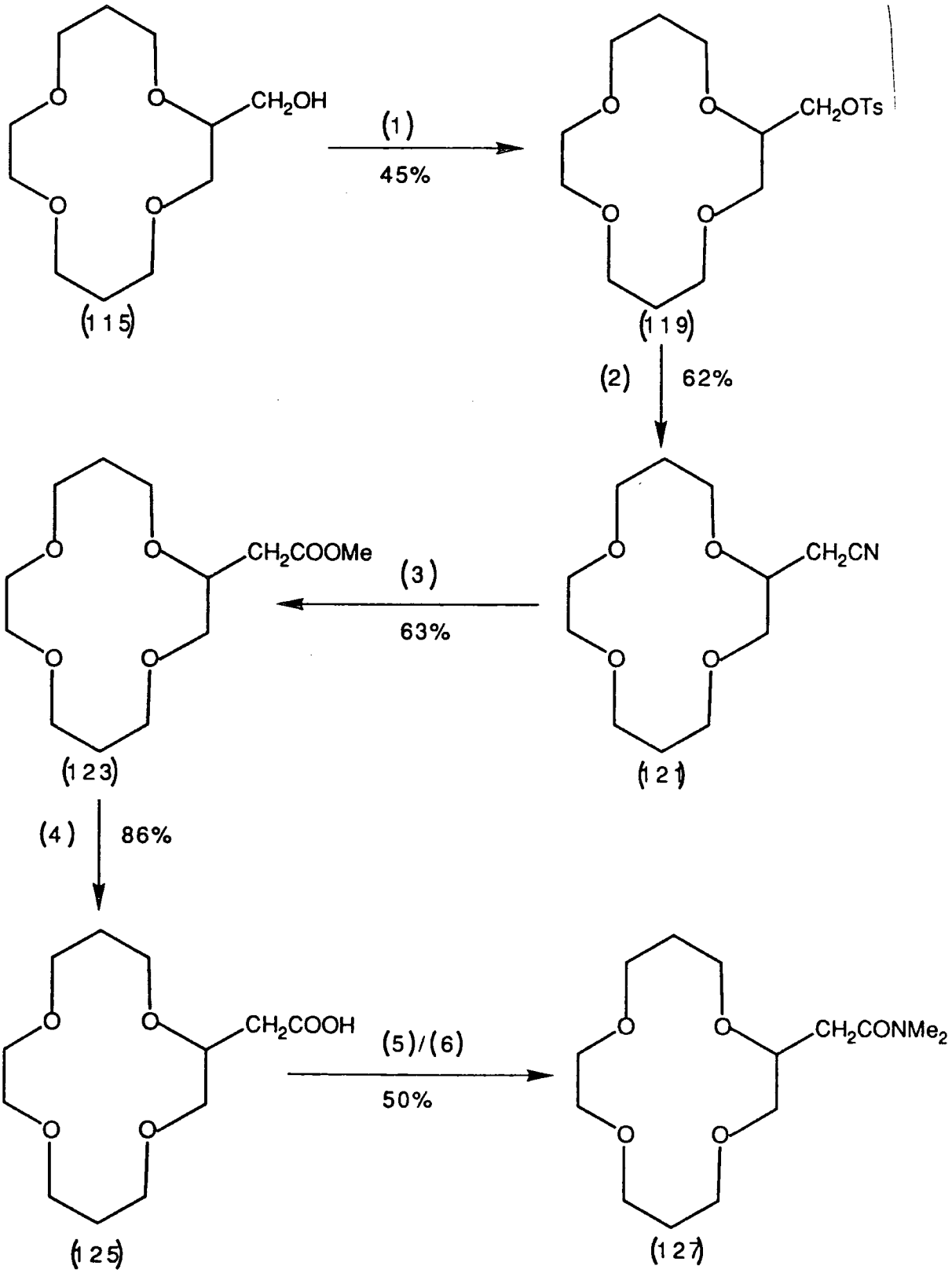

Scheme 2.20 *(1) TsCl, pyridine, 0°C; (2) KCN, DMSO(dry), N_2, 90°C; (3) MeOH, HCl, Reflux(N_2); (4) Me_4NOH, H_2O/MeOH, Reflux 2h; (5) PCl_5/CH_2Cl_2(dry), RT, N_2; (6) Me_2NH/H_2O (30% v/v), CH_2Cl_2, RT; (7) Et_3N, tBu_2 NH, CH_2Cl_2, N_2, 0°C.*

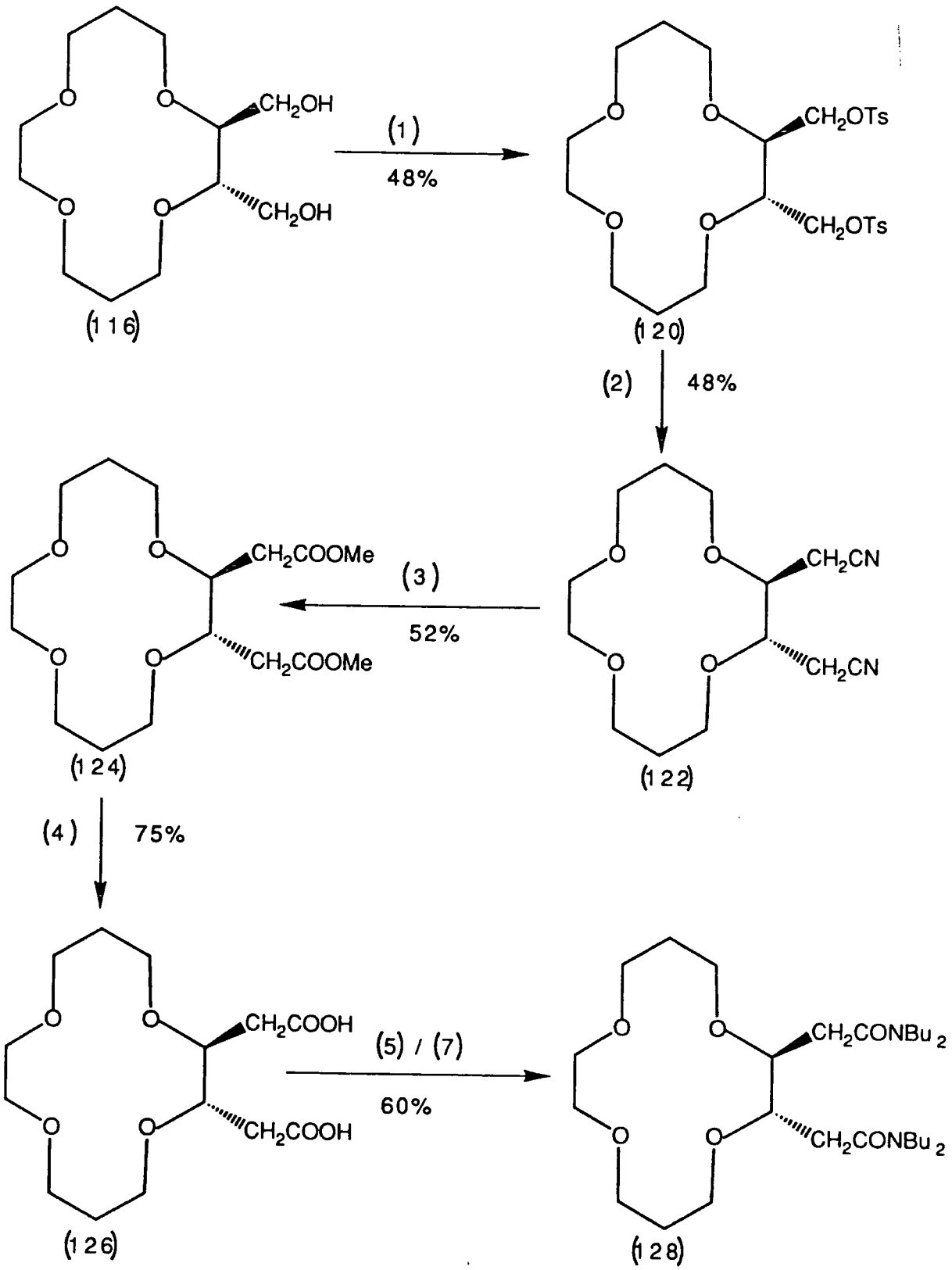
CH2OH
CH2OH
(116)
(1)
48%
CH2OTs
CH2OTs
(120)
(2)
48%
CH2CN
CH2CN
(122)
(3)
52%
CH2COOMe
CH2COOMe
(124)
(4)
75%
CH2COOH
CH2COOH
(126)
(5) / (7)
60%
CH2CONBu2
CH2CONBu2
(128)

Scheme 2.21

derivatives, one axial donor lies above, and one below, the 14-crown-4 ring plane, promoting the possibility of octahedral coordination for these ligands.

2.3 NMR EXPERIMENTS

NMR experiments permit the determination of the stoichiometry of a complex, give a qualitative indication of the strength of that complex and allow a measure of the dynamics of complexation.

In a typical experiment, a solution of ligand in a deuterated solvent is titrated with solid alkali metal salt. The spectra recorded after each titre may reveal the above mentioned information by monitoring the shift of ^{13}C NMR resonance signals. If no complexation between ligand and metal cation occurs, the spectra are identical. However, if complexation does occur, two possible situations arise. Firstly, if the rates of complexation and decomplexation are fast on the timescale of the NMR experiment at room temperature, an averaged signal for the carbon atoms in the free ligand and the corresponding carbon atoms in the ligand complex will be observed. If this is the case, a curve may be plotted representing the ^{13}C NMR shift displacement (Δd) for particular carbon atoms in the ligand against the alkali metal salt-ligand ratio. The stoichiometry of complexation may be derived from the position of the curve bend, and a qualitative idea of the strength of the complex may be gained from the deviation from a sharp bend. The theoretical curve in Figure 2.1 represents a relatively strong complex with 1:1 stoichiometry, whereas the theoretical curve in Figure 2.2 represents a relatively strong complex with 2:1 stoichiometry. When the stoichiometry of the complex is estimable, the stability constants of the complex formation may also be calculated[39,40]. For criteria and

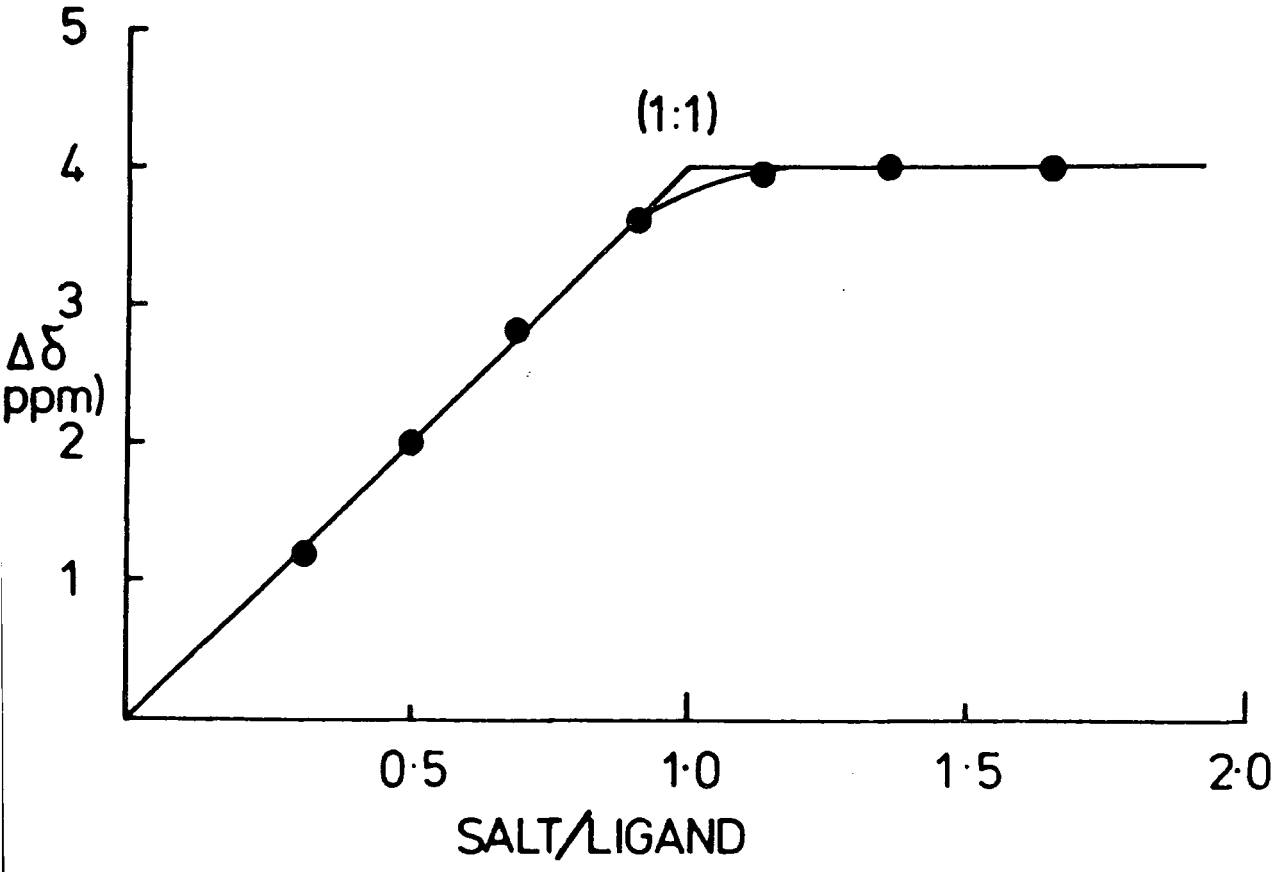

Figure 2.1 *Example of Curve Shape Exhibited for a Strong 1:1 Complex Measured by ^{13}C NMR.*

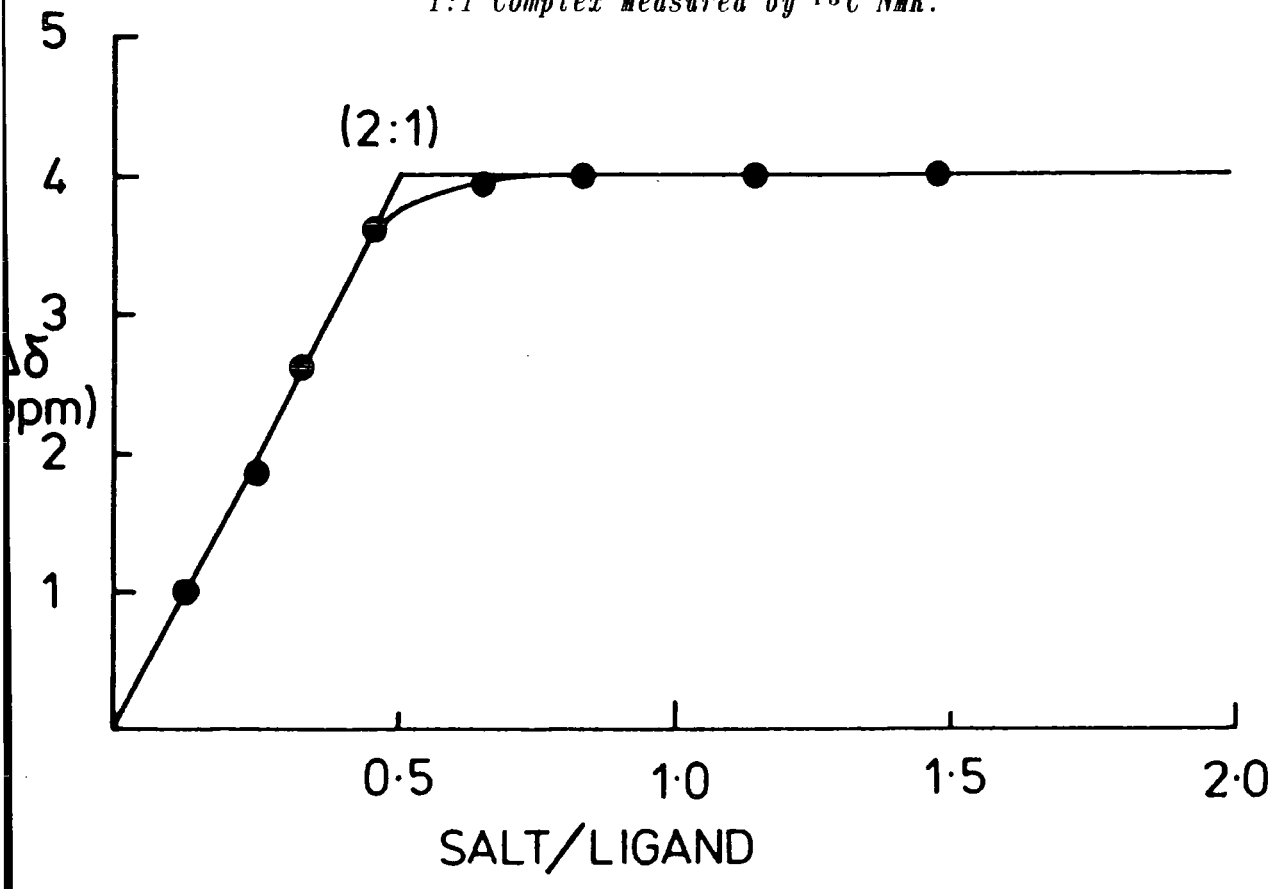

Figure 2.2 *Example of Curve Shape Exhibited for a Strong 2:1 Complex Measured by ^{13}C NMR.*

reliability, the discussion by Lenkinski may be considered[39]. Stability constants are reliable only for the weaker complexes with log K $\leq$ 3.

The second situation arises if the rate of complexations and decomplexations are slow on the timescale of the NMR experiment. Here, two discrete signals will be observed for each carbon atom of the ligand, one signal corresponding to free ligand and the other signal to complexed ligand. In this case the stoichiometry of complexation may be estimated by calculating the salt-ligand ratio at which resonance lines corresponding to the free ligand can no longer be seen.

When either averaged shifted signals corresponding to free and complexed ligand carbon atoms (fast exchange), or discrete lines (slow exchange), are observed, the difference (Δd) between observed resonance lines and those of the free ligand may give further information. If the relative Δd values for carbon atoms within the ligand are compared, the largest differences are often seen for those carbons that undergo the largest conformational change during complexation. It is, however, dangerous to assume that carbon atoms exhibiting the largest Δd values during complexation will necessarily surround those heteroatoms (*ie.* oxygen) that coordinate most strongly to the metal cation. Comparisons between Δd values for different carbon atoms within the ligand structure are only meaningful where Δd values show a distinct plateau, such that the limiting shift change may be assigned to a relatively strong complex of estimable stoichiometry.

The complexing properties of ligands (79), (109), (116) and (127) were measured using ^{13}C NMR methods.

2.3.1 Ligand (79)

Ligand (79) was dissolved in D_2O and titrated with lithium chloride. The resulting shift differences (Δd) are shown in Figure 2.3. It is impossible to estimate the stoichiometry of complexation in this case. The Δd values are small and certainly do not reach a limiting value corresponding to either 1:1 or 2:1 stoichiometry.

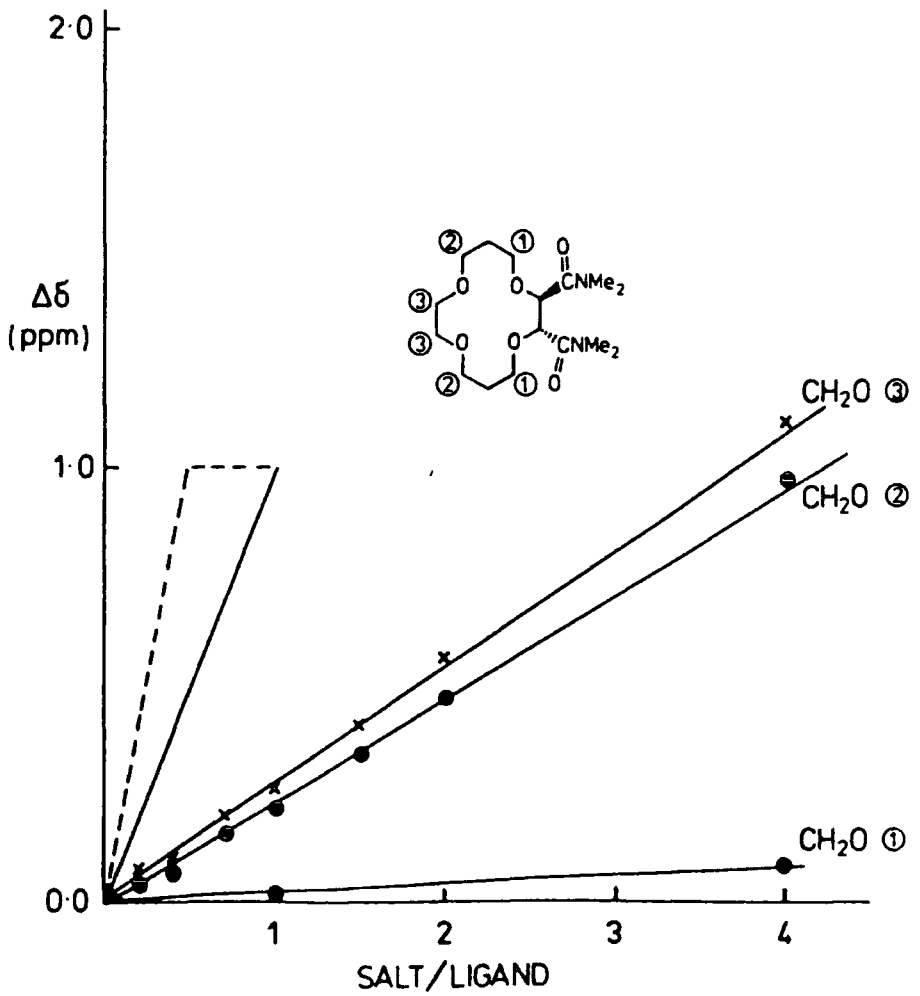

Figure 2.3 *^{13}C Chemical Shift Displacement (Δd) for the OCH_2 Ring Carbons of Ligand (79) in D_2O solution Relative to Salt(LiCl):Ligand Ratio.*

It can only be inferred that the complex stability is certainly low (log K < 3) in this solvent. The insolubility of ligand (79) in d^4-methanol precluded the use of that solvent, and it likely that the

higher solvation energy of the lithium cation in D_2O prevents strong complexation. Interestingly it appears that ring carbon atoms (2) and (3) exhibit far greater Δd values than ring carbon atom (1).

2.3.2 Ligand (116)

Ligand (116) was dissolved in a 2:1 mixture of d^4-methanol/$CDCl_3$ and titrated with lithium chloride. The relative shift changes (Δd) for carbon atoms are depicted in Figure 2.4. The first point to be noted is that for all carbon atoms a limiting shift difference is quickly reached after the addition of one equivalent of lithium chloride. This indicates the formation of a relatively strong complex of 1:1 stoichiometry. However, the fact that averaged shifted resonance signals are seen, as opposed to discrete signals, implies that exchange is fast on the NMR timescale at room temperature and that log $K \leq 4$. At low salt concentrations, there is evidence for a relatively strong 2:1 complex, yet the fact that the limiting shift values occur when one equivalent of lithium chloride has been added, tends to suggest that the 2:1 complex is somewhat less stable than the 1:1 complex. Interestingly, carbon atoms (1) and (2) show limiting Δd values that are appreciably greater than for those of other carbon atoms in this ligand. Since a 1:1 stoichiometry is estimable, it may be be inferred that it is carbon atoms (1) and (2) that probably experience greatest conformational change during formation of a 1:1 complex. However, as has already been pointed out, it is dangerous to assume that this is a result of oxygen atoms (A,B) coordinating most strongly to the lithium cation.

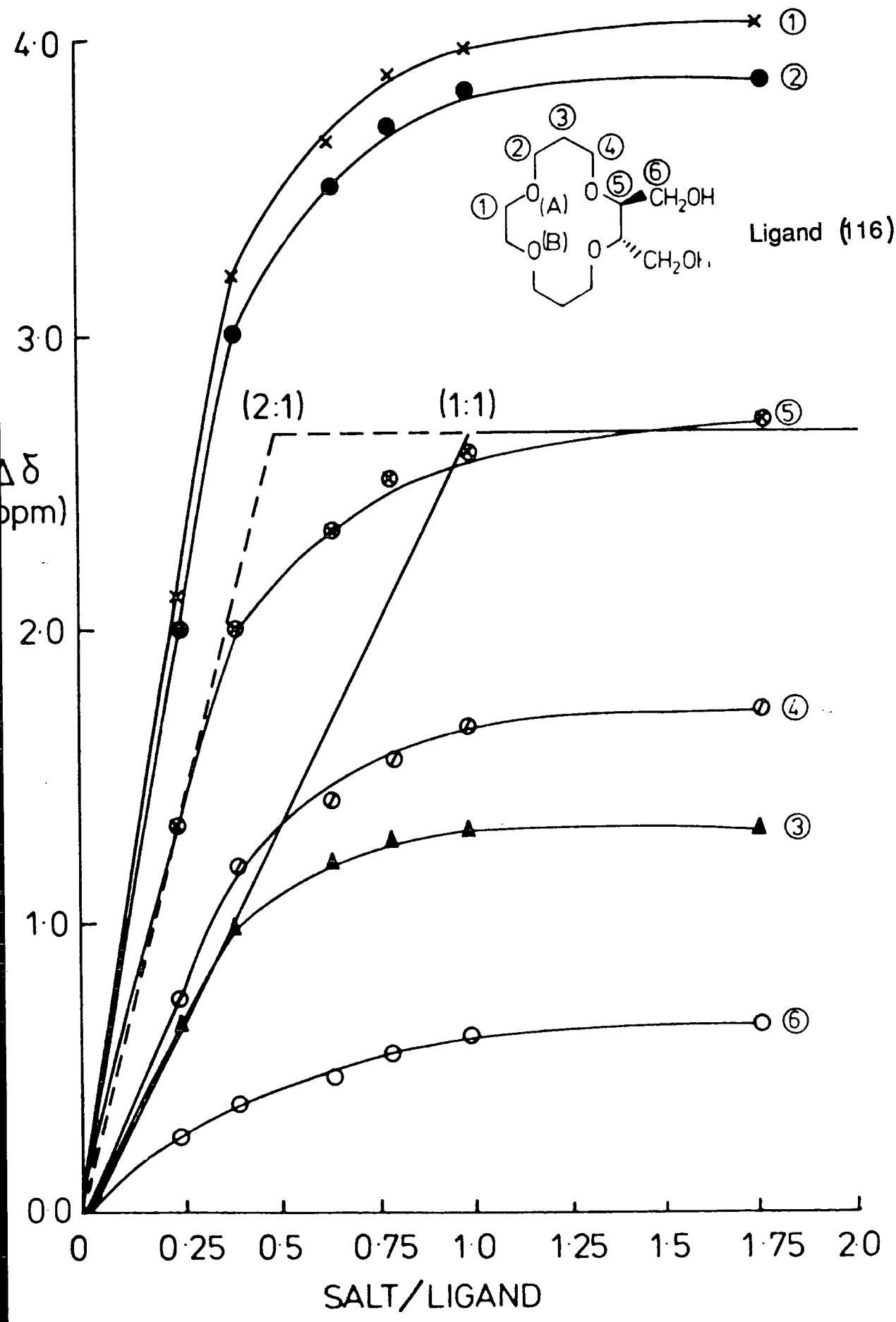

Figure 2.4 ^{13}C *Chemical Shift Displacement (Δd) for Carbon Atoms of Ligand (116) in a 2:1 d^4-methanol/$CDCl_3$ Mixture Relative to Salt(LiCl):Ligand (116) Ratio.*

2.3.3 Ligand (109)

Ligand (109) was dissolved in a 2:1 mixture of d^4-methanol/$CDCl_3$ and titrated with lithium chloride. The relative ^{13}C shift changes (Δd) are depicted in Figure 2.5. As with ligand (116), a limiting chemical shift is quickly reached when one equivalent of lithium chloride has been added, indicating the formation of a relatively strong complex of 1:1 stoichiometry. At low salt concentrations, there is some evidence for formation of a 2:1 complex though the strength of this complex appears to be much weaker than the 2:1 complex formed at low salt concentrations with ligand (116). Though the sharp curve bend indicates strong complexation for ligand (109), averaged signals corresponding to free and complexed carbon atoms, as opposed to discrete lines, are seen. It can be inferred that $\log K \leq 4$. Interestingly, in accord with relative shift values for ligand (116), it appears that the same carbon atoms [(9) and (10) in this case] show appreciably higher Δd values than any other carbon atoms of ligand (109). Further, Δd values of side arm carbons (1)-(4) were extremely low, and have been omitted from Figure 2.5, whilst carbon (5) shows only a moderate Δd value for 1:1 complexation. If these results are examined with a view that Δd values are proportional to conformational change experienced by carbon atoms on complexation, then it may be tentatively suggested that either:

(1) complexation involves first, coordination to side arm ether donors resulting in little conformational change of side arm carbons, and second, deformation of the crown ether ring (particularly for those carbons (9) and (10) furthest from the lithium cation) in order to complete the lithium solvation sphere, or

(2) complexation involves coordination to the crown ether ring with little or no coordination from the ether oxygens of the side arm.

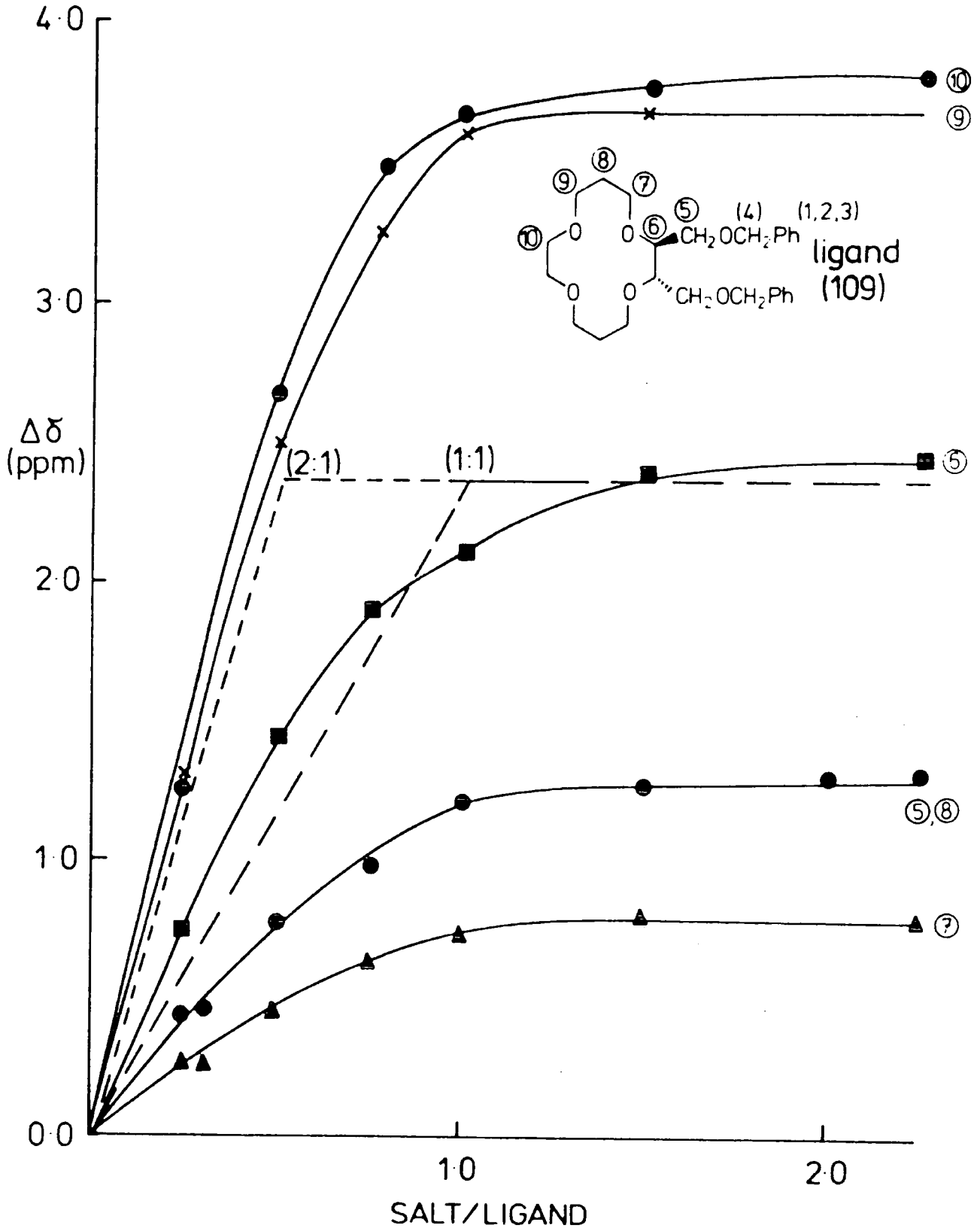

Figure 2.5 *^{13}C Chemical Shift Displacement (Δd) for Carbon Atoms of Ligand (109) in a 2:1 d^4-methanol/$CDCl_3$ Mixture Relative to Salt(LiCl):Ligand (109) Ratio.*

2.3.4 Ligand (127)

Ligand (127) was dissolved in a 2:1 mixture of d^4-methanol/$CDCl_3$ and titrated with lithium chloride. The ^{13}C shift changes (Δd) are depicted in Figure 2.6. As with ligands (116) and (109), a limiting chemical shift is quickly reached when one equivalent of lithium chloride has been added. The sharp curve bend indicates a relatively strong 1:1 complex, indeed, ligand (127) displays a sharper curve bend than ligands (116) and (109). This suggests that for the ligands studied in this series, ligand (127) forms the strongest 1:1 complex with lithium. Averaged signals are measured as opposed to discrete signals implying that log $K \leq 4$. Unlike ligands (116) and (109), there is little evidence for 2:1 complexation for ligand (127) even at very low salt concentrations. Examination of Δd values for 1:1 complexation, reveals the same relative pattern as for ligands (109) and (116); in that ring carbons (7)-(10) show appreciably higher Δd values than any other carbon atoms. The side arm carbon atoms (1) and (2) have been omitted from Figure 2.6 due to very low Δd values, whilst carbon atoms (3) and (14) show only moderate Δd values. Thus, as with ligands (116) and (109), it appears likely that the greatest conformational change occurs in the 14-crown-4 ring upon 1:1 lithium complexation.

2.3.5 Conclusions

Taken as a whole, the results of ^{13}C experiments point very definitely to the formation of relatively strong lithium complexes of 1:1 stoichiometry. There is little doubt, that had solubility problems not precluded the use of d^4-methanol as a solvent for ligand (79), the same pattern would have been extended. The relatively strong 2:1

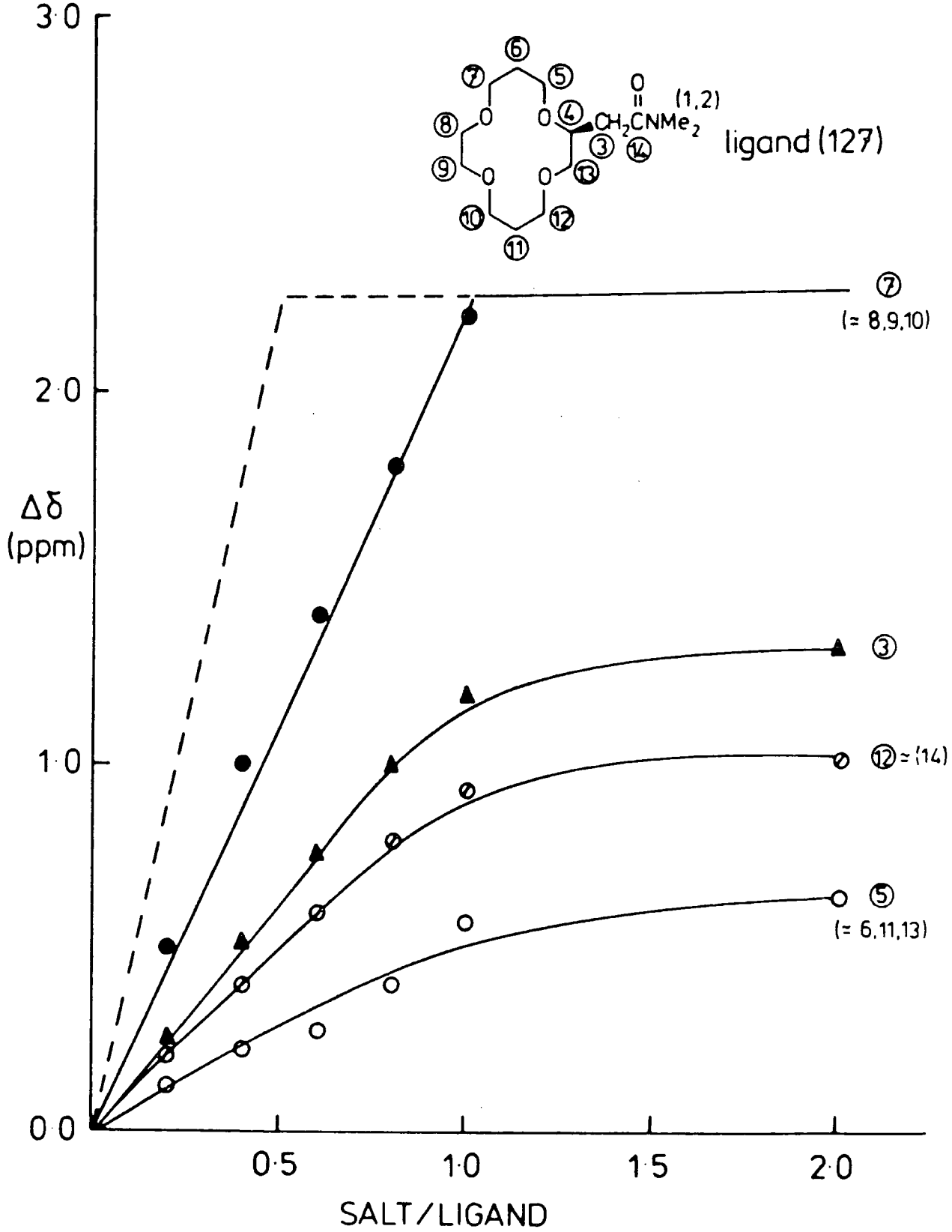

Figure 2.6 *^{13}C Chemical Shift Displacement (Δd) for Carbon Atoms of Ligand (127) in a 2:1 d^4-methanol/$CDCl_3$ Mixture Relative to Salt(LiCl):Ligand (127) Ratio.*

complex exhibited by ligand (116) at low salt concentration is at variance with the other ligands of this study, the only inference at this stage is that this must result from the nature of the hydroxy side arms.

Finally, though it is dangerous to infer too much from measured relative Δd values, it is interesting to note that ligands (109), (116) and (127) all show the same relative pattern. The four carbons furthest from the side arms exhibit substantially higher Δd values than any other carbon atoms for all three ligands. By comparison, carbon atoms adjacent to side arm donor oxygens for ligands (109), (116) and (127) show much lower Δd values, as do all side arm carbon atoms. These results would seem to suggest that complexation involves a much larger conformational change in the crown ether ring than in the side arm for these ligands. However, this does not necessarily imply that axial coordination is weak or absent, since small Δd changes for carbon atoms adjacent to axial donors cannot definitely be associated with correspondingly weak coordination by these axial donors. Whether or not axial coordination is operative for these ligands, results suggest that similar overall conformational changes in ligand structure are experienced in the formation of 1:1 complexes with lithium.

2.4 FAST ATOM BOMBARDMENT MASS SPECTROMETRY EXPERIMENTS

Fast atom bombardment (FAB) mass spectrometry has been used to determine the selectivity of ligands (108), (109), (115), (116), (123), (124) and (127) (Figure 2.8) for alkali metals lithium, sodium, potassium and caesium using a procedure adapted from that reported by Johnstone and Rose[44], and Meili and Seibl[135]. An aqueous solution of the chlorides of lithium, sodium, potassium and caesium was prepared,

with each cation being present at 1.25×10^{-2} M. Methanol solutions of ligands were also prepared at a concentration of 1.25×10^{-2} M. Analytical solutions were prepared by mixing an equal volume of the cation solution with each of the ligand solutions together with an equal volume of glycerol.

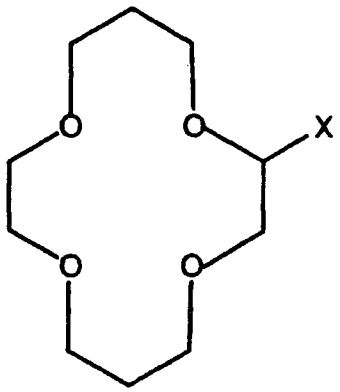

LIGAND	X =
(108)	CH_2OCH_2Ph
(115)	CH_2OH
(123)	$CH_2C(O)OMe$
(127)	$CH_2C(O)NMe_2$

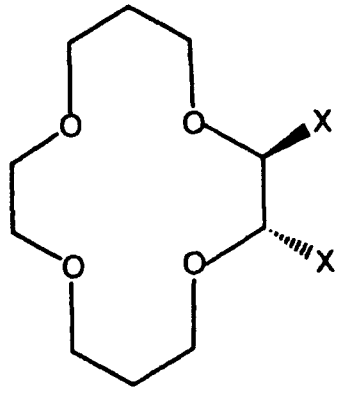

LIGAND	X =
(109)	CH_2OCH_2Ph
(116)	CH_2OH
(124)	$CH_2C(O)OMe$

Figure 2.8

Thus, all components were present in equal concentrations as a (1:1:1) methanol:water:glycerol solvent mixture which allowed the metal cations to compete for a limited amount of ligand. The stainless steel tip of the FAB probe was coated with a thin layer of the analytical solution and positive FAB mass spectrometry was performed (see experimental, Chapter 4).

Cation selectivity has been evaluated using the expression:

$$S = \log \left[\frac{I(L + Li)^+}{I(L + M)^+} \right]$$

where: S = Selectivity factor

$I(L+Li)^+$ = Signal Intensity of (Ligand + Lithium)$^+$

$I(L+M)^+$ = Signal Intensity of (Ligand + Metal cation)$^+$

The selectivity values are calculated with respect to the lithium cation; the lower the value(s), the poorer the selectivity for lithium over that cation. The selectivities are represented in Figure 2.9. There are several discernible trends:

(1) For all ligands studied, selectivity follows the order $Li^+ > Na^+ > K^+ > Cs^+$. This is to be expected on the basis of the size-fit concept.

(2) For the benzyl derivatives (108,109) and alcohol derivatives (115, 116) the difunctionalised ligands display higher lithium selectivities than their monofunctionalised counterparts. The difference in selectivities must therefore be due to the sixth donor site that is present for difunctionalised derivatives. Enhancement of lithium selectivity might occur for one of two reasons:

   (i) The sixth donor site coordinates to the lithium cation preferentially over larger alkali metal cations, as well as in conjunction with the other axial substituent, inhibiting 2:1 complexation by larger cations more effectively than when only one axial substituent is present.

   (ii) The sixth donor site is non-coordinating, but serves to render the difunctionalised ligand a more effective inhibitor of 2:1 complexation by larger cations than when only one axial substituent is present.

(3) The benzyl (108,109) and alcohol (115,116) derivatives exhibit higher lithium selectivities than the ester (123,124) and amide (127) derivatives. There are two major differences between these two sets of ligands.

   (i) In coordinating alkali metal cation, benzyl and alcohol axial donors form five membered chelate rings whereas the ester and

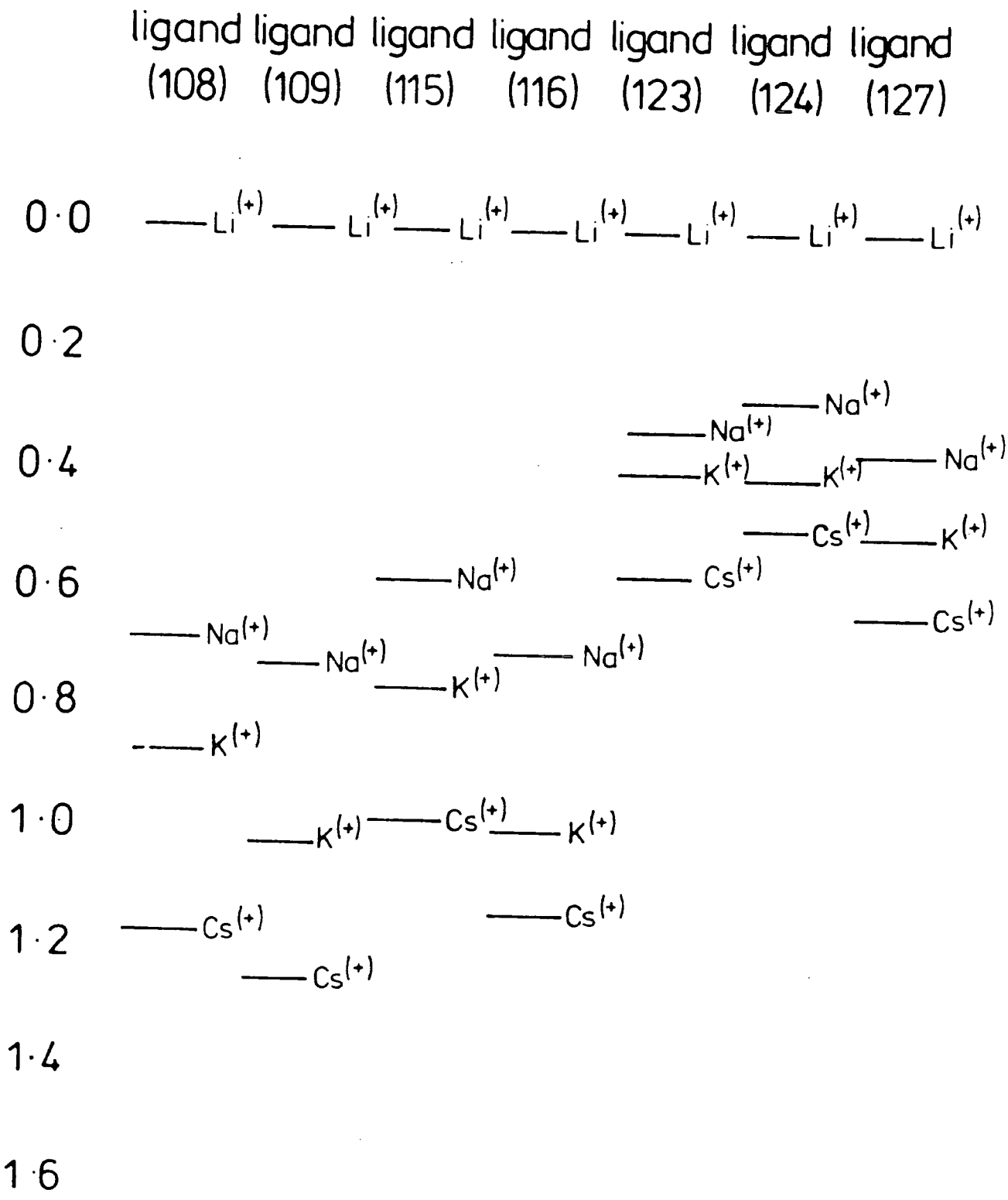

Figure 2.9 *Plot of Selectivity (S) for Lithium Over Other Group 1A Cations Measured by FAB Mass Spectrometry.*

amide axial donors form six membered chelate rings.

(ii) The distance of axial donors from the lithium cation in the ring plane will be greater for ester and amide derivatives than for benzyl and alcohol derivatives.

Either one, or other, or both of these factors may contribute to the observed selectivity differences. The very similar selectivity values displayed by amide (127) and ester (123,124) derivatives, do however, tend to suggest that coordination to lithium by axial donors is relatively weak for these ligands, since there is a large difference in σ-donating power of axial donors.

Thus, all ligands studied are lithium selective, though differences in relative lithium selectivities are apparent. It is difficult to fully understand these differences, X-ray data is needed and further experiments need to be performed to gain a clearer picture. The relative selectivity of these ligands for lithium parallels that found in the potentiometric experiments described in section 2.6. Reasons for differing selectivities are discussed in more detail in section 2.6 as well as suggested further experiments that might lead to a more thorough understanding of these differences.

2.5 IR EXPERIMENTS

The complexation of ester derivatives (123,124) and amide derivatives (127,128) with lithium was studied using IR spectroscopy.

Each ligand was dissolved in methanol and solid lithium thiocyanate was added to each solution, such that the ratio of ligand to lithium thiocyanate was 1:1. These solutions were left to stand for two days. IR spectra were recorded by taking a drop of methanol solution and allowing it to evaporate on a KBr plate to form a thin film. IR spectra

of the free ligands were recorded by first dissolving the ligand in methanol and then taking a drop of the methanol solution and allowing it to evaporate on a KBr plate to form a thin film. The results of these measurements are depicted in Table 2.1.

LIGAND	ν_{max} (C=O)	ν_{max} (C-O-C)	Δ(C=O)	Δ(C-O-C)
(123)	1742	1120		
(123)+LiSCN	1726	1082	16 ± 2	38 ± 5
(124)	1742	1115		
(124)+LiSCN	1729	1087	13 ± 2	28 ± 5
(127)	1637	1120		
(127)+LiSCN	1622	1080	15 ± 2	40 ± 5
(128)	1638	1115		
(128)+LiSCN	1622	1090	16 ± 2	25 ± 5

Table 2.1 *IR Data (cm^{-1}) for Free Ligands (123),(124),(127) and (128), and their Lithium Complexes, measured as a Thin Film in Methanol on a KBr Plate.*

There are discernible trends in this study:

(1) For all ligands in this study, complexation by lithium thiocyanate causes shifts for both (C-O-C) and (C=O) stretches. This tends to suggest cooperation between ring donors and axial donors in 1:1 complexation of the lithium ion in solution.

(2) The frequency of radiation in infrared measurements is 1×10^{-12} ν/s. Therefore in the case of the difunctionalised derivatives, if only one side arm axial donor was coordinating then two separate carbonyl stretches would be seen, one corresponding to the coordinating carbonyl donor and one to the free carbonyl donor. The fact that a single carbonyl stretch is seen for lithium complexes of both diester (124) and diamide (128) derivatives, would therefore strongly suggest coordination by both axial donors in forming a 1:1 complex with the lithium ion in solution.

2.6 POTENTIOMETRIC EXPERIMENTS

Selectivities of ligands (108), (109), (115), (116), (123), (124), (127) and (128) for lithium were measured potentiometrically by the fixed interference method.

Each ligand was incorporated into a PVC membrane of the following composition: 1.2% sensor (ligand); 65.6% plasticiser (o-nitrophenyl octyl ether, ONPOE); 32.8% high molecular weight PVC (FLUKA); 0.4% lipophilic anion (tetrakis-4-chlorophenyl borate, KTpClPB). The function of the ONPOE plasticiser was to provide a good, non-volatile solvent for the potential lithium ionophores and to improve the plasticity of the polymeric membrane.

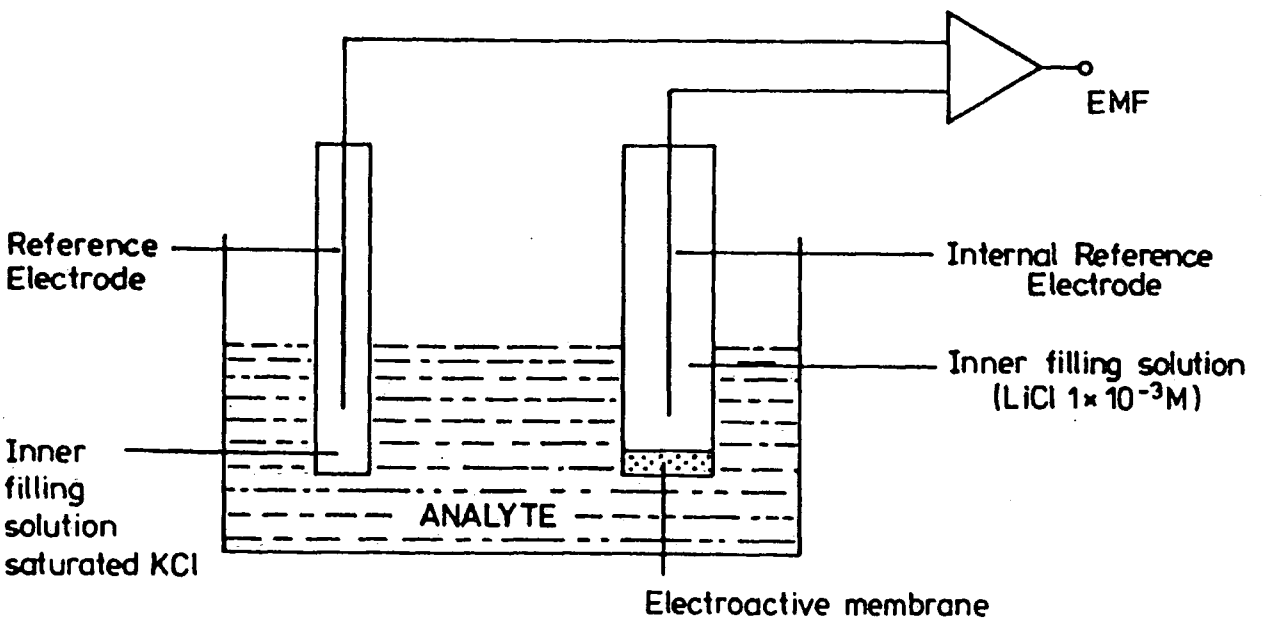

Hg | $HgCl_2$ | Saturated KCl | ANALYTE | Electroactive PVC Membrane | Inner Filling Solutions | AgCl | Ag

Figure 2.10 *Diagrammatic Representation of the Electrochemical Cell Used in Potentiometric Experiments.*

The lipophilic anion (KTpClPB) functions in two ways: firstly it reduces interference from sample anions, and secondly, it reduces membrane resistance. Details of the method used to prepare these membranes are given in the experimental section (Chapter 4). The Philips lithium ionophore (Li^+561) was measured as a comparison.

In order to conduct the potentiometric experiments the membrane was incorporated in an ion selective electrode which was incorporated into an electrochemical cell (Figure 2.10). The reference electrode used was an RE1 Peta court calomel electrode with saturated potassium chloride as the inner filling solution.

2.6.1 Electrode Calibration (Dip-Type Method)

If an electrode is behaving ideally then it should display a Nernstian response to variations in lithium ion concentration, such that the Nernst equation is followed:

$$E = E^{o} + \frac{2.303\ RT}{zF} \log\ [Li^+] \qquad \text{NERNST EQUATION}$$

where:
- E = Measured EMF Potential
- E^o = Standard Electrode Potential
- R = Gas Constant
- T = Absolute Temperature
- z = Charge on the Primary Ion (Li^+)
- F = Faraday Equivalent (96,487 C/eq)

Calibration measurements were performed at 37^{o}C (since these ligands were being assessed as candidates for measuring lithium ion activity in whole blood, it was thought sensible to perform experiments at natural body temperature). Under those conditions the Nernst Equation can be re-written:

$$E = E^{o} + \frac{61.54\ mV}{z} \log\ [Li^+]$$

Therefore, ideally ΔE should be 61.54 mV per decade change in lithium ion concentration. Deviation from this ideal Nernst behaviour and limits of detection of each electrode in pure solutions of the primary ion (Li^+) were calculated. Limits of detection were measured according to IUPAC recommendations which define the limit as "the concentration of primary ion at which E deviates by 18.5/z mV (at 37°C) from the extrapolation of the linear portion of the calibration graph". In order to perform calibration measurements, the following procedure was used:

(1) The ion selective electrode was conditioned for 24 hrs in 10^{-3} M lithium chloride solution at 25°C.

(2) The ion selective electrode and reference electrode were then immersed in solutions of varying lithium chloride concentration (1×10^{-1} M - 1×10^{-6} M) where each solution was maintained at 37°C and the electodes were thoroughly rinsed between measurements. ΔE values were thus calculated for decade changes in lithium ion concentration at 37°C. The results are summarised in Table 2.2 and there are several points to note:

(1) In no cases do the electrodes exhibit ideal Nernstian slopes of 61.54 mV/decade [LiCl] change.

(2) Of the electrodes measured, the alcohol derivatives (115) and (116) stand out as the poorest. Furthermore, owing to their low slope values, limits of detection should be treated with caution for these ligands, since departure from the ideal Nernstian behaviour is substantial.

(3) Ligands (108), (109), (123), (124) and (128) all exhibit a near Nernstian response, the most promising being the dibenzyl (109) and diamide (128) derivatives both in terms of slope and limits of detection.

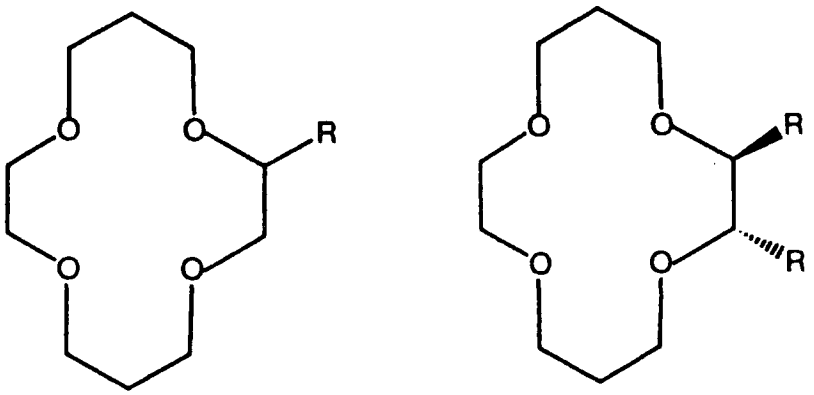

(A) (B)

LIGAND	R	ΔE/decade [LiCl]†	Detection Limit†
(108)	(A) CH_2OCH_2Ph	53.1	$10^{-4.80}$
(109)	(B) CH_2OCH_2Ph	56.5	$10^{-4.80}$
(115)	(A) CH_2OH	37.3	$10^{-4.40}$
(116)	(B) CH_2OH	32.0	$10^{-4.40}$
(123)	(A) $CH_2C(O)OMe$	54.5	$10^{-4.55}$
(124)	(B) $CH_2C(O)OMe$	52.5	$10^{-4.60}$
(127)	(A) $CH_2C(O)NMe_2$	47.6	$10^{-4.70}$
(128)	(B) $CH_2C(O)NBu_2$	58.1	$10^{-5.15}$
Philips Ionophore		56.5	$10^{-5.00}$

Table 2.2 *Calibration of Electrodes Using the Dip-Type Method in Pure Lithium Chloride Solutions at 37°C;* †*Values averaged from three separate measurements.*

(4) The rather poor slope exhibited by ligand (127) is somewhat surprising in conjunction with other values. Though the presence of impurities might account for such a poor response, analysis of ligand (127) shows this to be no less pure than any other ligands in this study as gauged by ^{1}H NMR, ^{13}C NMR, IR and mass spectral data (≥ 98% purity). Furthermore, the fact that values listed for ligand (127) are averaged over three separate experiments with minimal deviation being apparent, tends to lend validity to the measured values.

(5) Of the electrodes measured, the diamide (128) seems to offer a significant improvement to the commercially available Philips (Li^+ 561) electrode, both in terms of measured slope and limit of detection. The dibenzyl derivative (109) seems comparable to the Philips lithium ionophore in terms of slope, yet shows a slightly lower limit of detection.

(6) In all cases the response times were fast - following the IUPAC definition which states "the response time is the time taken to reach a value 1 mV from the equilibrium value" - all response times were less than one minute, and typically of the order of 30 seconds.

2.6.2 Lithium Selectivity Measurements (Dip-Type Method)

The lithium selectivity of electrodes was measured by the fixed interference method. This method involved measurements of ΔE values for decade changes in lithium chloride concentration with a constant background of:

(a) 150 mM NaCl (upper concentration limit of $[Na^+]$ in whole blood)

(b) 4.3 mM KCl (upper concentration limit of $[K^+]$ in whole blood)

(c) 1 mM NaCl.

No ion selective electrode responds exclusively to the ion which it is designed to measure. The degree of selectivity of the electrode for the primary ion (Li^+) with respect to the interfering ion (B) is expressed by the selectivity coefficient, K^{Pot}_{LiB} defined by the Nickolsky equation:

$$E = E^o + \frac{61.54\ mV}{z(Li^+)F} \log \left([Li^+] + \sum_B K^{Pot}_{LiB}\ z_{Li}/z_B \right)$$

If the concentration of the primary ion $[Li^+]$ is varied with a constant concentration of interfering ion, a graph of the type shown in Figure 2.11 is seen.

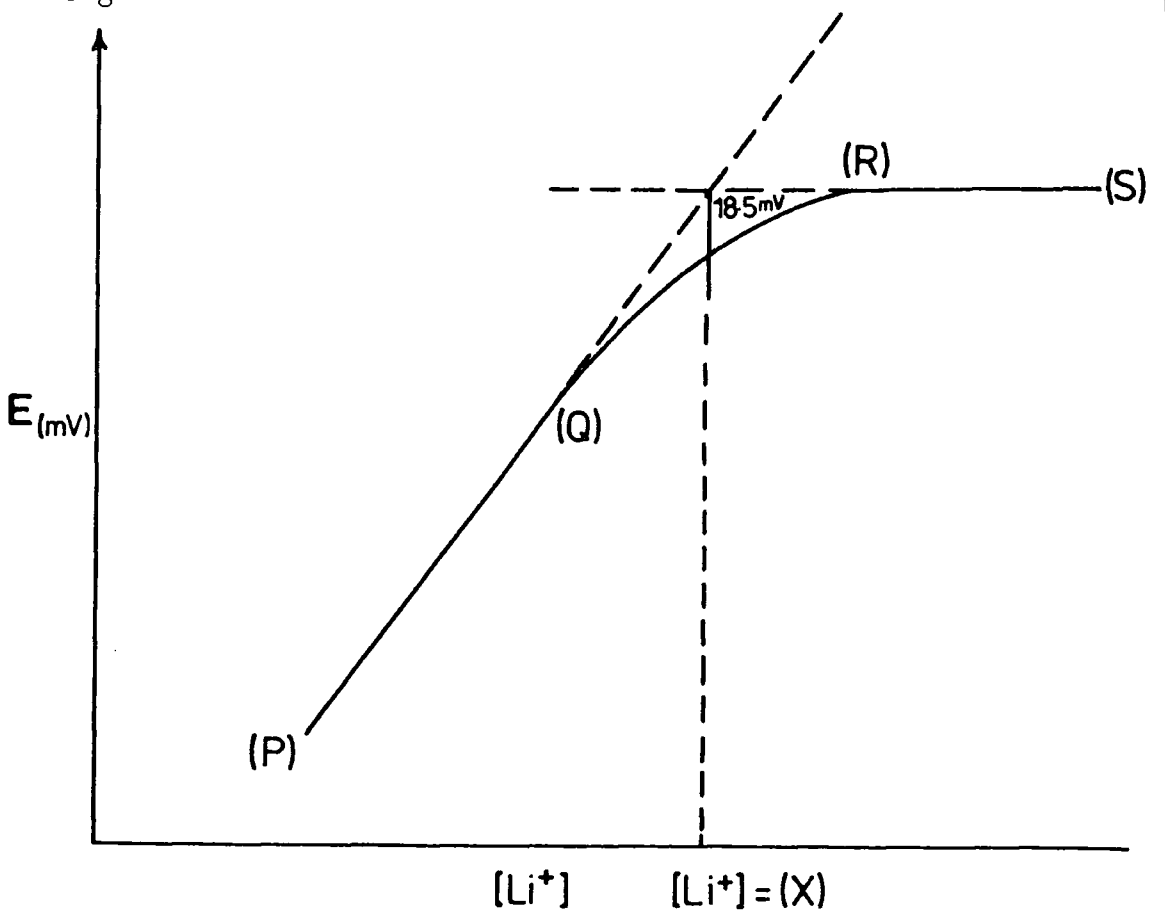

Figure 2.11 *Graph of Electrode Potential vs. Lithium Ion Concentration with a Fixed Background of Interferent Ion.*

In the region (P)-(Q) the electrode is responding to the primary ion (Li^+) in a Nernstian manner. In the region (Q)-(R), as the lithium concentration falls, the electrode potential is increasingly affected by the interferent ion (B), and in the region (R)-(S) the electrode is responding entirely to the interferent ion (B). Both ions contribute equally to the electrode response when:

$$[Li^+] = K^{Pot}_{LiB}\,[B]\; z_{Li}/z_B$$

If the lithium ion concentration at which this occurs is $[Li^+]^1$ then:

$$E = E^o + \frac{2.303\ RT}{z_{Li}F} \log \left([Li^+]^1 + K^{Pot}_{LiB}\ [B]\ z_{Li}/z_B \right)$$

$$= E^o + \frac{2.303\ RT}{F} \log \left(2[Li^+]^1 \right)$$

The difference between EMF in solutions of lithium chloride with and without interferent E can be expressed:

$$E = \frac{2.303\ RT}{F} \left(\log 2[Li^+]^1 - \log [Li^+]^1 \right)$$

$$= E^o + \frac{2.303\ RT}{F} \left(\log 2 \right)$$

$$= 18.5 \text{ mV (at } 37^oC).$$

Therefore, selectivity coefficients were measured in the following manner:

(1) Solutions of 1 mM sodium chloride, 150 mM sodium chloride, 4.3 mM potassium chloride and 1.26 mM calcium chloride were prepared. Solid lithium chloride was added to each solution so that it was present at a concentration of 1×10^{-1} M.

(2) The stock solutions of interferent ions and 1×10^{-1} M lithium chloride were used to prepare 1×10^{-2} M - 1×10^{-6} M lithium chloride solutions in the presence of interferent ions by serial dilution.

(3) Electrode potentials were measured at 37^oC and a curve was plotted of electrode potential against lithium ion concentration. Selectivity coefficients were measured from these graphs by methods previously outlined. The results of these measurements are listed in Table 2.3.

LIGAND	PURE LiCl SOLNS.		150 mM NaCl MEDIA		A	B	C
	SLOPE	DL	SLOPE	DL			
(108)	53.1	$10^{-4.80}$	35.2	$10^{-2.00}$	-1.73	-1.17	
(109)	56.5	$10^{-4.80}$	41.4	$10^{-2.15}$	-2.13	-1.24	
(115)	37.3	$10^{-4.40}$					
(116)	32.0	$10^{-4.40}$					
(123)	54.5	$10^{-4.55}$	38.5	$10^{-2.00}$	-1.93	-1.17	
(124)	52.5	$10^{-4.60}$	29.5	$10^{-2.05}$	-1.98	-1.23	
(127)	47.6	$10^{-4.70}$	29.0	$10^{-1.73}$	-1.68	-0.97	
(128)	58.1	$10^{-5.15}$	43.0	$10^{-2.50}$	-2.43	-1.67	<-2.43
Philips Ionophore	56.5	$10^{-5.00}$	40.0	$10^{-2.05}$	-1.93	-1.23	<-1.93

$$A = \log K^{Pot}_{LiK} \quad B = \log K^{Pot}_{LiNa} \quad C = \log K^{Pot}_{LiCa}$$

Table 2.3 *Lithium Selectivity and Limits of Detection Measured Using the Dipped System by the Fixed Interference Method (at 37°C); DL=Detection Limit; Units of slope= mV/decade [LiCl]; A=Fixed Background 4.3 mM KCl; B=Fixed Background 1.26 mM $CaCl_2$; C=Fixed Background 150 mM NaCl.*

There are several points to note from these results:

(1) The slopes (ΔE) per decade change in lithium chloride concentration are all substantially lower with a fixed background of 150 mM sodium chloride than in pure lithium chloride solutions. This suggests that even at lithium concentrations of 100 mM, interference from sodium is evident.

(2) The 150 mM sodium chloride background confers substantially lower limits of detection on all electrodes compared to those in pure lithium chloride solutions. The limits of detection define the ideal 'working range' of these electrodes. For all electrodes aside from the diamide (128), the detection limits were very similar, with response to the primary lithium ion for the concentration range 100 mM - 10 mM being sufficiently exclusive over the interferent sodium ion to allow accurate lithium ion

concentration measurement. The diamide (128) has a 'working range' substantially larger and lithium ion concentrations as low as 3 mM are able to be accurately measured. However, the clinical lithium concentration range of 0.5 mM - 1 mM is slightly lower, and electrodes used in this study are clearly inadequate for accurate clinical lithium ion measurement in whole blood with a background sodium ion concentration of 150 mM.

(3) The benzyl derivatives (108,109) and ester derivatives (123,124) display very similar selectivity coefficients for lithium over sodium, and for lithium over potassium. Furthermore, their values are very close to those of the Philips ionophore. The dibutylamide (128) shows by far the highest selectivity for this series of ligands, yet, though the selectivity for lithium over potassium is near to the selectivity required for measurement of lithium ion concentration in whole blood with less than 1% interference ($\log K^{Pot}_{LiK} = -3.0$), the selectivity for lithium over sodium ($\log K^{Pot}_{LiNa} = -1.67$) is substantially lower than the required value ($\log K^{Pot}_{LiNa} = -4.50$).

(4) Selectivity for lithium over calcium was measured for the dibutylamide (128) and Philips ionophore. It is impossible to derive exact selectivity coefficients in this case since deviations of 18.5 mV with calcium interference do not occur within the Nernstian range of these electrodes. It can, however, be inferred that for both ionophores, calcium interference can be neglected within the lithium concentration range (1×10^{-1} M - 1×10^{-6} M).

Figure 2.12 graphically displays ΔE changes for the ligands (108), (109), (123), (124), (127), (128) and Philips ionophore with a fixed background of 150 mM sodium chloride for the lithium ion concentration

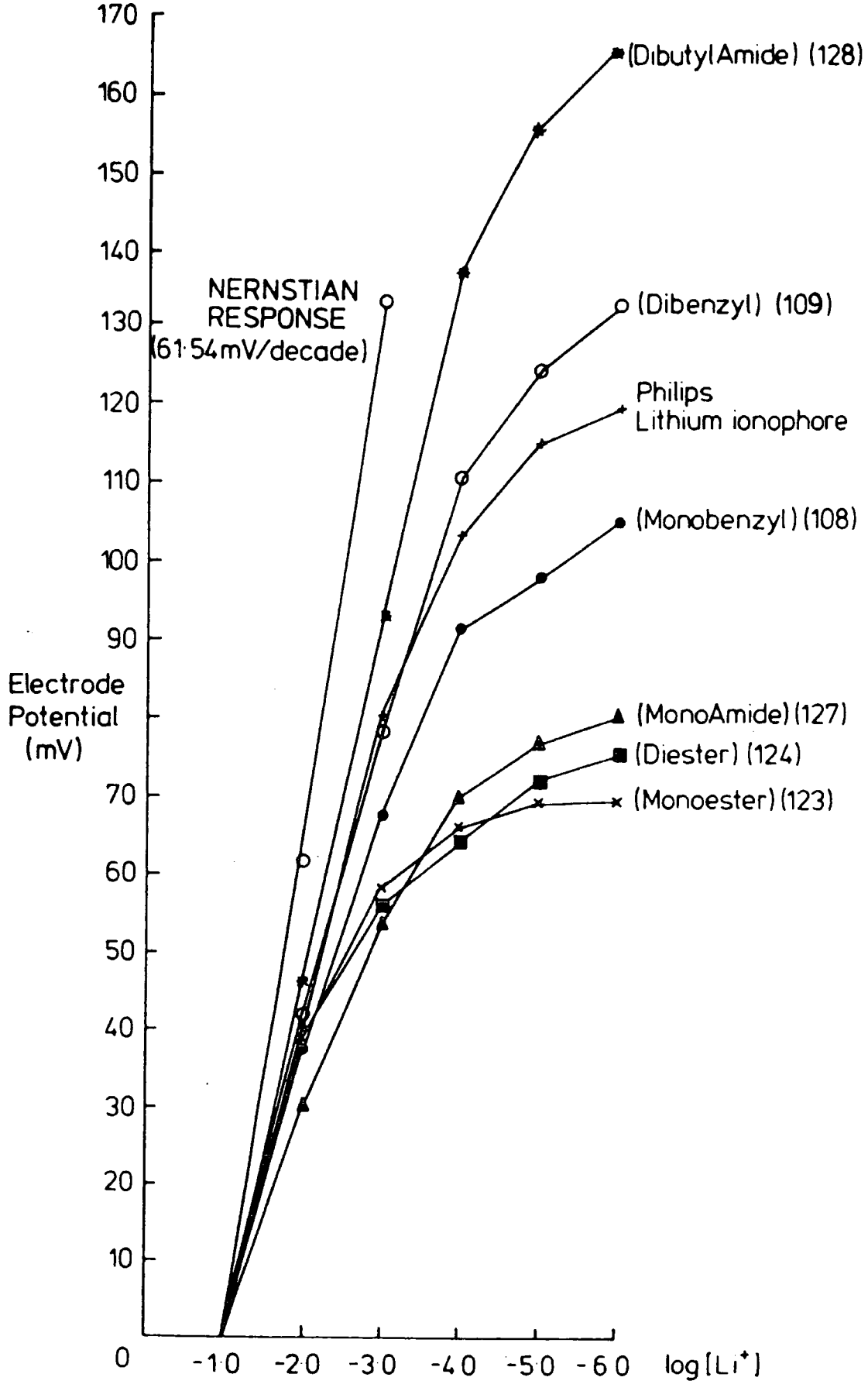

Figure 2.12 *Plot of ΔE for Ligands (108,109), (123,124), (127,128) and Philips Ionophore with a Fixed Background of 150 mM NaCl for the Lithium Ion Concentration Range $1x10^{-1}$ M - $1x10^{-6}$M.*

range 1×10^{-1} M - 1×10^{-6} M. There are several discernible trends:

(1) For all ionophores, appreciable sodium interference is seen when the lithium ion concentration falls below 1×10^{-4} M.

(2) For the ester derivatives (123,124), it is possible to join measured values with smooth curves over the entire lithium ion concentration range. It is difficult to justify a linear response for these ligands aside from concentrations of lithium chloride that are close to 100 mM. There is substantial interference below a lithium ion concentration of 10 mM, and the monoester, below a lithium ion concentration of 1×10^{-5} M, responds entirely to the interfering sodium ion. The monoamide derivative (127) displays a similar response to the two ester derivatives.

(3) The benzyl derivatives (108) and (109), and the Philips ionophore however, exhibit near perfect linearity for lithium ion concentrations between 100 mM and 1 mM. These results are a little surprising. Table 2.3 has shown that substantial deviation from near Nernstian slopes in pure lithium chloride solutions is seen with a fixed background of 150 mM sodium chloride even at a lithium ion concentration of 100 mM. Indeed, measured slopes with a fixed sodium chloride background imply deviations from slopes in pure lithium chloride solutions where the lithium ion concentration approaches the level (150 mM) of the interferent. Taking this into account, it is difficult to explain the fact that departure from linearity is only evident when the lithium ion concentration falls below 1 mM. This point is even more pertinent in the case of the dibutylamide (128). Here again, Table 2.3 has shown a substantial decrease in measured slope with a fixed background of sodium chloride (150 mM) from the near Nernstian slope in pure lithium chloride solutions at a lithium ion concentration of 100 mM. Yet,

the response for this electrode remains linear at lithium ion concentrations as low as 1 x 10^{-4} M. The linearity displayed by benzyl derivatives (108,109), the dibutylamide (128) and the Philips ionophore, thus seem at odds with the substantial decrease in measured slope when sodium chloride interferent is present.

Table 2.4 shows a list of electrode potential changes (ΔE) for benzyl derivatives (108,109), ester derivatives (123,124), amide derivatives (127,128) and the Philips ionophore over the lithium ion concentration range 1 x 10^{-1} M - 1 x 10^{-6} M.

LIGAND	ΔE /mV
(108)	105
(109)	132
(123)	69
(124)	75
(127)	80
(128)	165
Philips ionophore	119

Table 2.4 *Sensitivity of Electrodes for Lithium over the Concentration Range 1x10^{-1}-1x10^{-6} M at 37^{0}C with a Fixed Background of 150 mM sodium chloride.*

The values depicted in Table 2.4 provide an insight into the relative sensitivities of these electrodes for the lithium ion concentration 1 x 10^{-1} M - 1 x 10^{-6} M in a clinical sodium chloride background. If these values are combined with relative selectivity coefficients for lithium over sodium (log K^{Pot}_{LiNa}, see Table 2.3) then there are discernible trends:

(1) For benzyl (108,109) and ester derivatives (123,124), the difunctionalised ligands display greater selectivity coefficients for lithium over sodium and potassium, and larger ΔE values over the lithium ion concentration range 1 x 10^{-1}M - 1 x 10^{-6} M than

their monofunctionalised counterparts. The mono- and di-functionalised structures are represented in Figure 2.13.

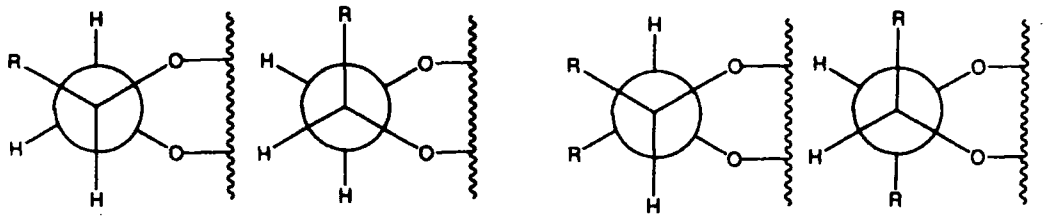

MONOFUNCTIONALISED DERIVATIVES

(108) R=CH_2OCH_2Ph
(123) R=$CH_2C(O)OMe$

DIFUNCTIONALISED DERIVATIVES

(109) R=CH_2OCH_2Ph
(124) R=$CH_2C(O)OMe$

Figure 2.13 *Newman Projections of the CHR-CHR Fragment for Monofunctionalised Ligands (108) and (123) and for Difunctionalised Ligands (109) and (124).*

In order to coordinate effectively to the metal cation the axial orientation (a,a) must be adopted. The conformation of the free ligand will thus, optimally, also be (a,a), necessitating minimal conformational change on complexation. Infrared data suggests that, in a methanol thin film, the vast majority of axial donors for mono-functionalised and difunctionalised ester (123,124) and amide (127,128) derivatives coordinate to the lithium cation and are therefore in the (a,a) orientation. Clearly, if free ligand (X) exists in the (e,e) conformation, whereas free ligand (Y) exists in the (a,a) conformation, free ligand (X) must undergo a far greater conformational change in order to coordinate the metal cation than the free ligand (Y). The resultant metal cation ligand (X) complex will therefore be destabilised relative to that of ligand (Y). In seeking to explain the enhanced lithium selectivity of difunctionalised ligands (124) and (109), one possible contributing factor might be that for monofunctionalised derivatives, the lowest energy conformer of the free ligand exhibits the (e,e) orientation, whereas for the difunctionalised derivatives steric effects, as a result of substituting an (R) group for a hydrogen atom,

dictate that the lowest energy conformation of the free ligand will tend more toward the (a,a) orientation. In order to clarify the relevance of this factor, it is necessary to know the orientation of axial groups for the benzyl (108,109) and ester (123,124) free ligands. Attempts to grow crystals of the free ligands have failed, and therefore nothing is known of the orientation of (R) groups in the free ligands in the solid state. Added to this, ^{1}H spectra proved to be too complex in the region of the CHR signals to gain information from the coupling constants J_{H-H} by ^{13}C NMR satellite resonances as to the relative proportion of (a,a) and (e,e) orientations of these free ligands in solution. Therefore, at present, the relevance of this factor to observed differences in lithium selectivity remains unclear.

Regardless of orientations of axial substituents for these ligands, there are two essential differences between the difunctionalised derivatives (109,124) and the monofunctionalised derivatives (108,123).

(a) The difunctionalised ligands are hexa-coordinate, whereas the monofunctionalised ligands are penta-coordinate.

(b) Functionalised groups lie, one above and one below the ring plane for difunctionalised derivatives, whereas for monofunctionalised derivatives the single axial substituent may lie either above or below the ring plane.

The sixth donor group may enhance lithium selectivity through a more effective coordination to the lithium ion than other larger alkali metal cations. If the monofunctionalised ligands are considered (Figure 2.14).

Figure 2.14

Sodium, whose ionic radius exceeds that of the 14-crown-4 cavity,would be expected to lie above the ring plane. Lithium, on the other hand, can potentially lie within the ring plane since its ionic radius is, if anything, slightly smaller than that of the 14-crown-4 cavity. If a sixth donor site is introduced then the structures depicted in Figure 2.15 can be envisaged.

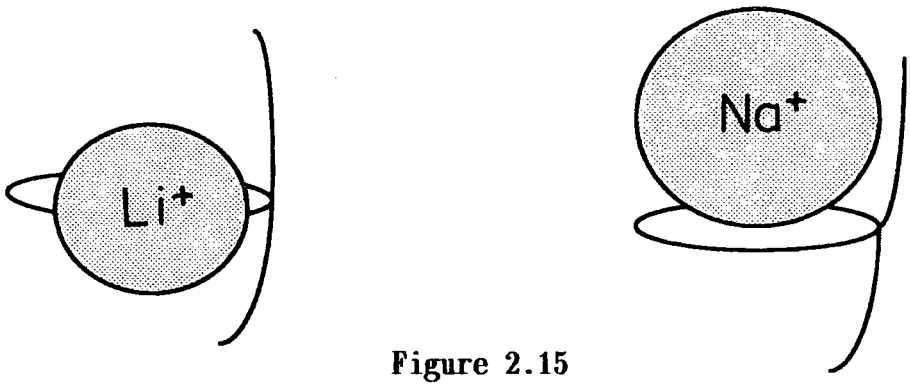

Figure 2.15

If the lithium ion is considered to lie in the plane of the 14-crown-4 cavity, then both donor groups can, through appropriate design, coordinate strongly at an equal distance from the lithium ion. In the case of the sodium complex however, its greater size means that it must lie above the ring plane and consequently the distance from the sixth coordination site is appreciably longer, and hence interaction between this donor site and the sodium ion will be weaker. Therefore the sixth donor site might be expected to enhance lithium selectivity.

Kimura and Kitizawa[106,125] have performed studies which suggest that the formation of 2:1 sandwich complexes with sodium and potassium ions (which exceed the 14-crown-4 cavity size) can occur in PVC membranes of identical composition to those of this study. It is reasoned that ionophores that can inhibit 2:1 sandwich formation will accordingly display enhanced lithium selectivities over those ionophores which are unable to form such 2:1 sandwich complexes. In seeking to explain the enhanced lithium selectivity of dibenzyl (108) and diester

(124) derivatives over their monofunctionalised counterparts, a contributing factor might be that the difunctionalised derivatives are more effective inhibitors of 2:1 complexation by larger cations than monofunctionalised derivatives. In order to clarify the importance of this effect, it is necessary to ascertain the extent to which 2:1 complexation may occur for these ligands. Fixed interference measurements using varying concentrations of ionophore in the PVC membrane can be used for this purpose. The logic behind this is that for a ligand which forms exclusive 1:1 complexes with alkali metal cations (Li^+, Na^+, K^+), variations in ionophore concentration within the membrane will have no effect on lithium selectivity. For ligands that are able to form 2:1 complexes with larger cations, a rise in ligand concentration within the membrane will lead to a concurrent fall in lithium selectivity. These studies are being undertaken at present and if results show that the monofunctionalised derivatives are able to entertain sodium and potassium ions with a 2:1 stoichiometry, whereas difunctionalised derivatives are less able to do so, then this would be deemed an important factor in governing the relative lithium selectivities of these ionophores.

(2) The benzyl derivative (108) exhibits a higher ΔE value over the lithium ion concentration range 1×10^{-1} M - 1×10^{-6} M than the ester (123) or amide (127) derivatives. Axial coordination to the lithium ion involves the formation of a five-membered chelate ring for the benzyl derivative (108) as opposed to six-membered chelate rings for ester (123) and amide (127) derivatives. Differences in observed lithium selectivities might reflect differing chelate ring sizes. It has been argued by Hancock[123], that the inherent lithium selectivity of the 14-crown-4 ring stems largely from the presence of two six-membered chelate

rings in the resulting complexes. For the small lithium ion, the hydrogens in these six-membered chelate rings are able to adopt the energetically favoured staggered orientation. However, the larger sodium ion forces the C_3 chain hydrogen atoms towards the energetically less favoured eclipsed position. It was further argued that introduction of more six-membered chelate rings into the metal cation complex would cause steric crowding for the small lithium ion and that this would outweigh the energetically favoured staggered hydrogen orientation. Sodium, however, being a larger cation, would experience less unfavourable energy through steric crowding and thus selectivity for lithium over sodium would fall relative to the unsubstituted 14-crown-4 ring. If the ligands (108), (123) and (127) are considered, they would seem to give credence to this argument. When the five-membered chelate ring formed by axial coordination by the benzyl derivative (108), is replaced by the six-membered chelate rings of ester (123) or amide (127) derivatives, a concurrent drop in lithium selectivity is seen.

The six-membered chelate rings formed by ester (123) and amide (127) derivatives are more flexible than the five-membered chelate ring formed by the benzyl derivative (108). Axial coordination by ester and amide ligands will thus be entropically less favourable. The axial coordination by these ligands might therefore be weak and indiscriminate for all alkali metal cations. Hence, though axial coordination might marginally increase the stability of lithium complexes relative to those of unsubstituted 14-crown-4, a concurrent enhancement in lithium selectivity would not be seen. The very similar lithium selectivity displayed by amide (127) and ester (123) derivatives in both FAB mass spectrometry and potentiometric studies, tends to suggest weak axial coordination by these ligands, since if the orientation of axial carbonyl donors were favourable for lithium complexation, the

substantial difference in σ-donating power of axial donors would be expected to result in a substantial difference in lithium selectivities. The less flexible axial substituent of the benzyl derivative (108) however, might appreciably increase the stability of the the lithium complex relative to that of the unsubstituted 14-crown-4 ligand. Furthermore, the larger size of sodium and potassium might preclude such a favourable axial interaction and thus lithium selectivity would also be enhanced relative to that of the unsubstituted 14-crown-4 ligand. In order to clarify observed differences, further ligands of the general structure shown in Figure 2.16 must be synthesised where stronger axial σ-donors are introduced that form five-membered chelate rings.

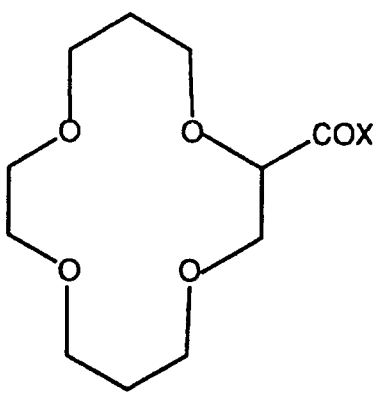

Figure 2.16 *X = OR, NR_2.*

If, as has been suggested, five-membered chelate rings formed by axial donors are more favourable for lithium complexation than six-membered chelate rings on steric and entropic grounds, then stronger axial σ-donors in the general structure shown (Figure 2.16) should lead to higher lithium selectivities than those displayed by the benzyl derivative (108).

(3) The dibutylamide ligand (128) displays a markedly higher lithium selectivity than any other ligand of this series. Based on previous

arguments, enhancement of lithium selectivity relative to the monoamide (127) can be explained by three possible differences:

(a) The dibutylamide (128) coordinates more strongly to lithium by virtue of the sixth donor site.

(b) The dibutylamide (128) inhibits 2:1 complexation by larger cations more efficiently.

(c) The dibutylamide (128) tends more to the (a,a) conformation as the free ligand.

However, previous arguments suggest that axial coordination is sterically and entropically less favoured for six-membered chelate rings relative to five-membered chelate rings. Based on these arguments, the dibutylamide (128) would be expected to exhibit a very similar lithium selectivity in comparison to ester derivatives (123,124) and the amide derivative (127). The obvious implication from the marked deviation from expected behaviour, is that the dibutyl group must in some way override steric and entropic factors. In order to clarify observed differences, two further ligands must be made (Figure 2.17).

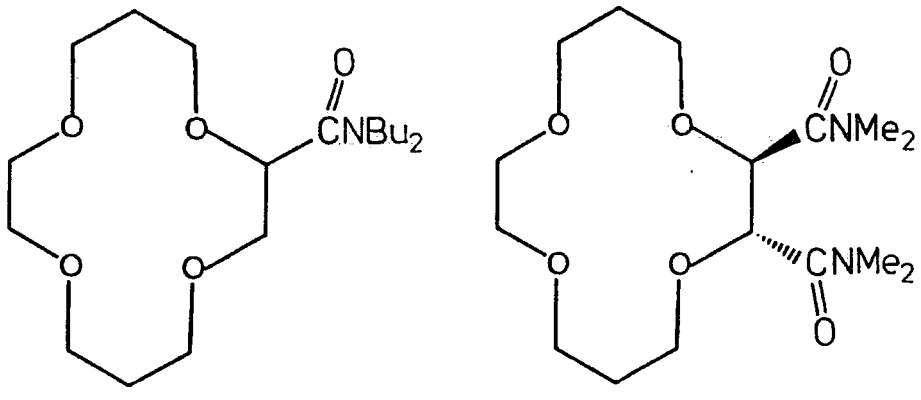

Figure 2.17 *Further Ligands to be Made.*

Potentiometric studies of these ligands would demonstrate whether or not the marked lithium selectivity of ligand (128) can be attributed to the nature of the butyl group.

Figures 2.18, 2.19 and 2.20 graphically display response of the dibutylamide (128), dibenzyl (109) and Philips electrodes to lithium ion concentrations (1×10^{-1} M - 1×10^{-6} M) in a fixed background of 1 mM sodium chloride, 150 mM sodium chloride, 4.3 mM potassium chloride and 1.26 mM calcium chloride. Most of the information from these figures has been discussed above. The only remaining point to note is the marked difference in response with a 1 mM sodium chloride background as compared to a 150 mM background. In a number of recent publications, highly selective lithium ionophores have been reported[106,125,130], unfortunately selectivities for lithium over sodium were measured in a 50 mM sodium chloride background. It is clear from Figures 2.18-2.20 that this lower sodium chloride background will almost certainly lead to a markedly different electrode response to that measured in a clinical (150 mM) sodium chloride background. In order to assess the potential utility of a lithium ionophore for measuring lithium ion concentration in whole blood, it is vital to measure lithium selectivity coefficients where interfering ions are at clinical levels.

2.6.3 Measurement of Electrode Response Using a Flow System - Calibration of Electrodes.

Electrodes based on the dibenzyl (109), diester (124), dibutylamide (128) derivatives and the Philips lithium ionophore were calibrated for the lithium ion concentration range (1×10^{-1} M - 1×10^{-6} M) using the system depicted in Figure 2.21. The ion selective electrodes were conditioned overnight at room temperature in 1×10^{-3} M lithium chloride solution. Thereafter, they were thoroughly rinsed and immersed in a constant volume cell containing 1×10^{-1} M lithium chloride as the initial solution. The diluent solution (deionised water) was introduced

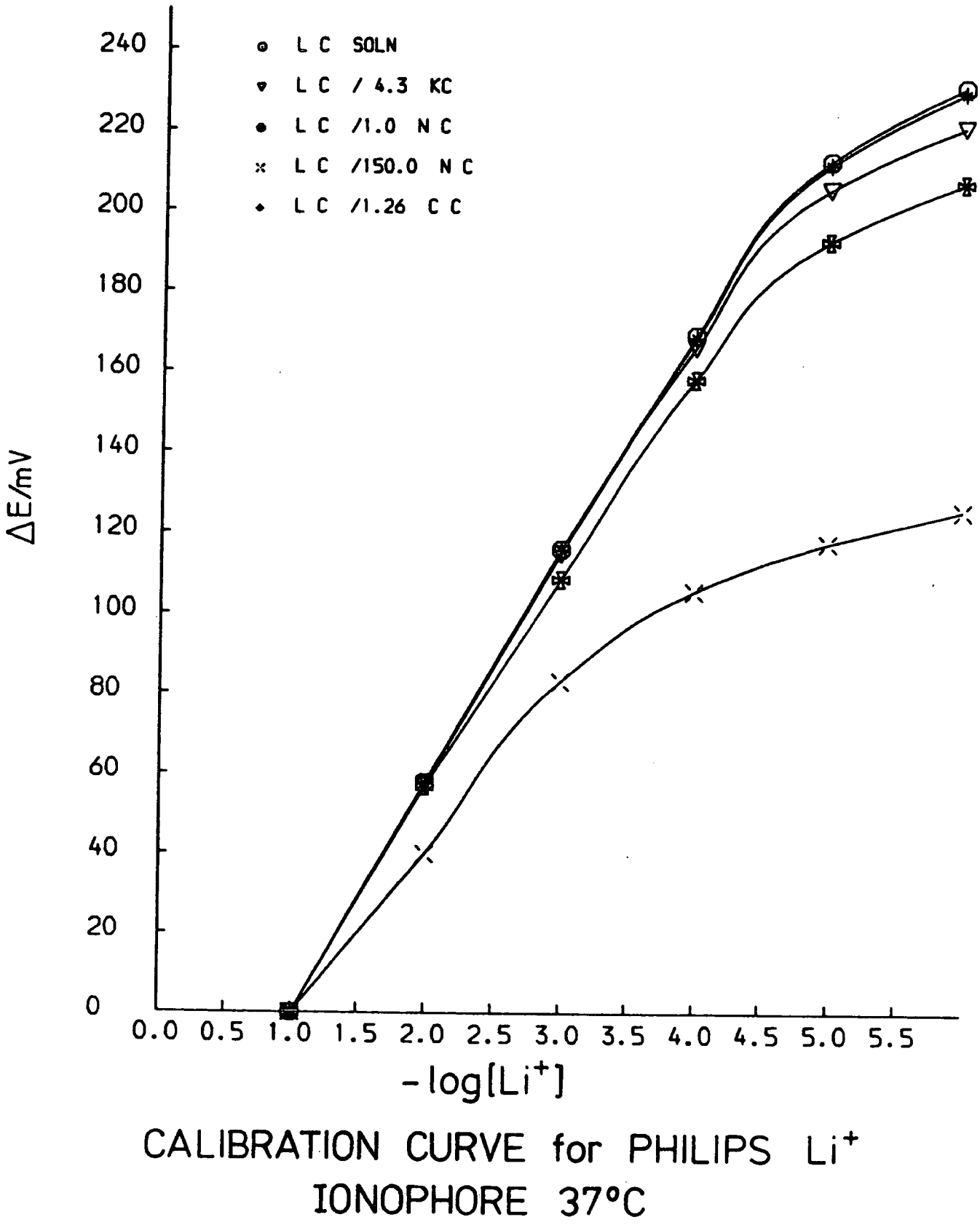

Figure 2.18 *Calibration Curve for Philips Lithium Ionophore at 37°C.*

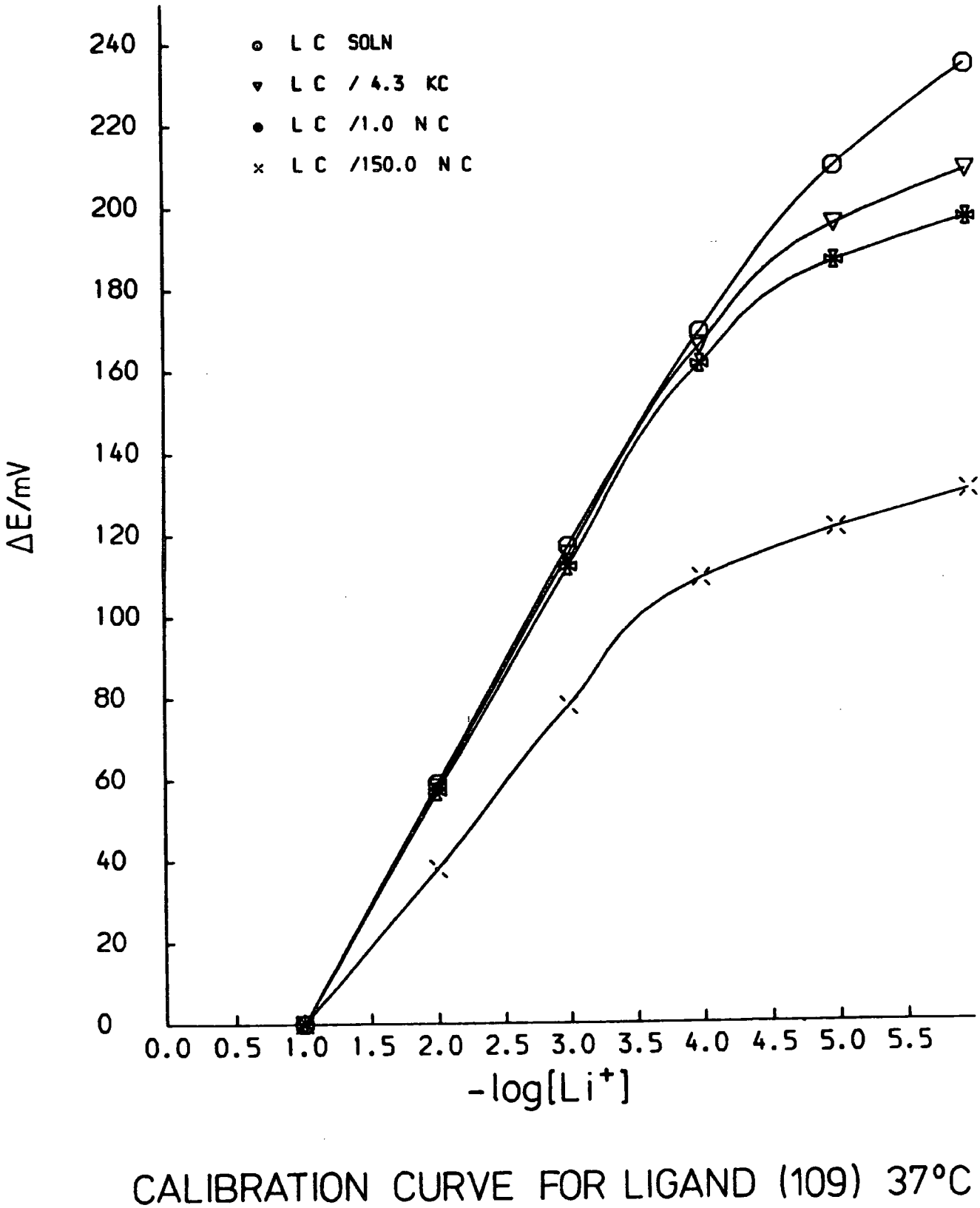

Figure 2.19 *Calibration Curve for Lithium Ionophore (109) at 37°C.*

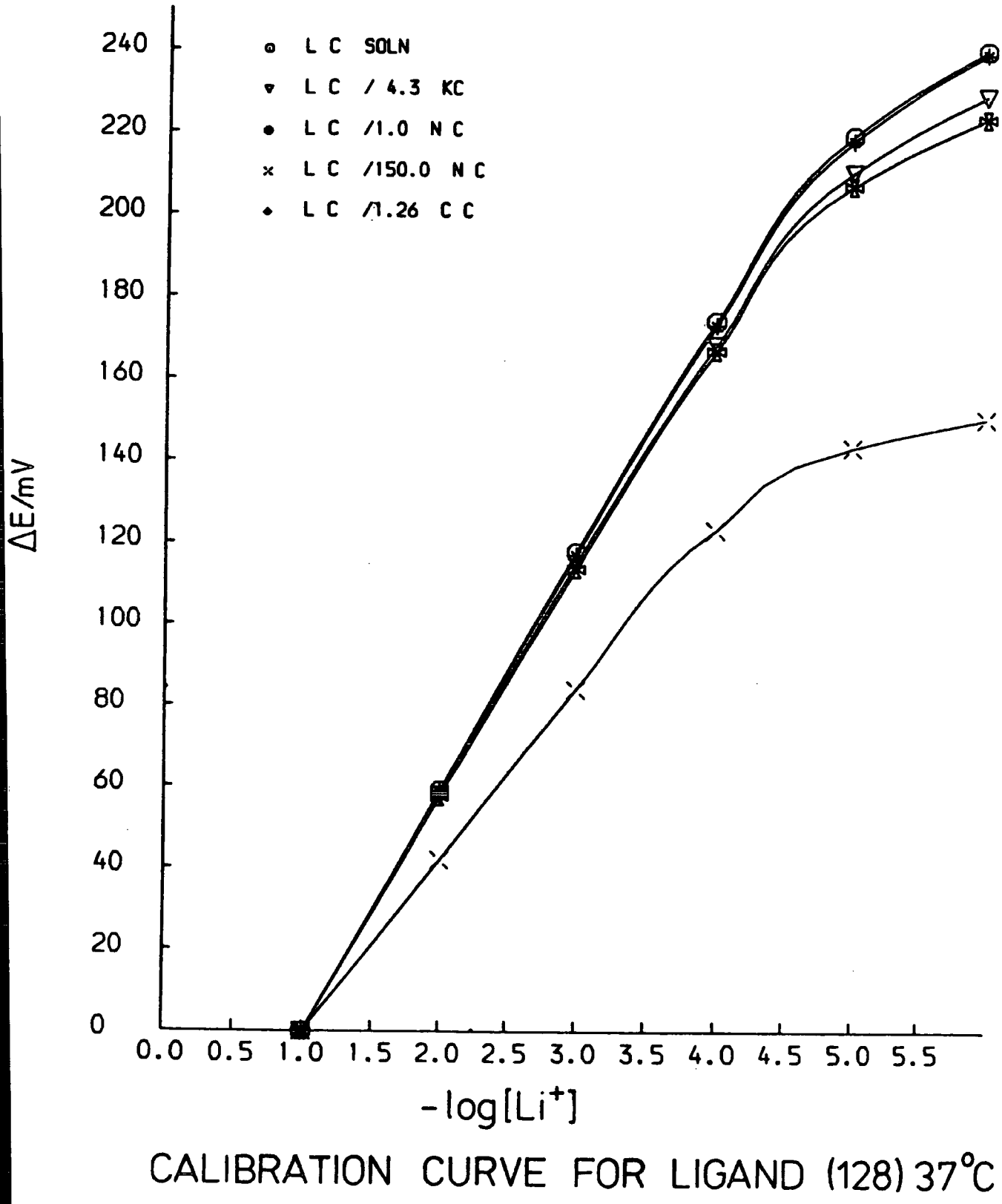

Figure 2.20 *Calibration Curve for Lithium Ionophore (128) at 37°C.*

into the constant volume cell (36.7 ml) at a rate of 6 ml/min by using a peristaltic pump.

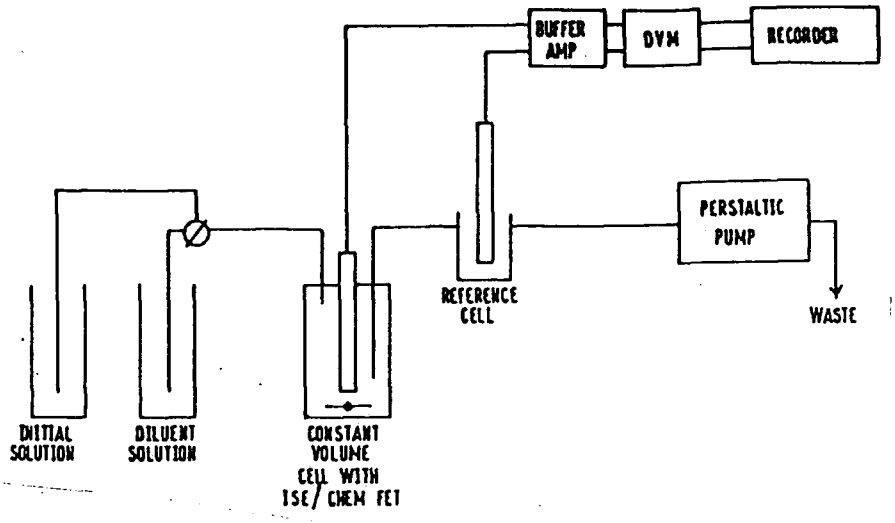

Figure 2.21 *Apparatus Used in the Flow System.*

All solutions were maintained at 37^{o}C throughout the process. Therefore, the initial lithium chloride solution (1 x 10^{-1} M) was diluted at a constant rate and the electrode response was measured directly on a Y/t recorder. This process can be described by the following equation[136]:

$$t = Vv \frac{Ln\ (C/C_o)}{-W}$$

where: t = Time Elapsed from the beginning of the dilution process
Vv = Constant Volume of the Cell (36.7 ml)
W = Flow Rate (6 ml/min)

The variation in potential was monitored on a Y/t recorder and the calibration graph may be obtained directly from this by rescaling the t-axis in log C units.

Trioctyl phosphine oxide (TOPO) has, in recent publications, been shown to enhance lithium selectivities for certain ligands in membranes of similar composition to this study. It is reasoned that the soft polarisable phosphonate donor will interact much more favourably with the small lithium ion of high surface charge than with larger alkali

metal cations that display lower charge density ratios, and hence, inherent lithium selectivity of the electrode might be enhanced. For this reason, fresh membranes were made up for the dibenzyl (109), diester (124) and dibutylamide (128) derivatives as before, and 1% TOPO was added. Electrodes using these membranes with added TOPO were calibrated at 37°C using the flow system previously described. Results from calibration experiments for ligands (109), (124) and (128) with and without TOPO, and the Philips ionophore over the lithium concentration range (1×10^{-1} M - 1×10^{-6} M) are depicted in Table 2.5.

LIGAND	WITHOUT TOPO		WITH TOPO	
	SLOPE	DL	SLOPE	DL
(109)	55	$<10^{-5.00}$	60	$10^{-4.20}$
(124)	61	$10^{-3.20}$	28	---
(128)	57	$<10^{-5.00}$	59	$10^{-4.70}$
Philips Ionophore	61	$10^{-4.50}$	--	---

Table 2.5 *Calibration of Electrodes in Pure Lithium Chloride Solution ($1x10^{-1}$-$1x10^{-6}$ M) Using Flow Method at 37°C; DL=Detection Limit; Units of slope=mV/decade [LiCl].*

There are several points to note:

(1) For derivatives without TOPO, all slopes are near Nernstian. Indeed, the Philips ionophore and diester derivative (124) display apparent perfect Nernstian behaviour.

(2) The diamide (128) and dibenzyl (109) derivatives, though exhibiting slightly lower slopes than the Philips ionophore, show appreciably greater limits of detection.

(3) The diester derivative (124), although exhibiting apparently perfect Nernstian behaviour for the lithium ion concentration range (1×10^{-1} M - 1×10^{-2} M), has a poor detection limit compared to other ligands in this study.

(4) Addition of 1% TOPO to membranes containing dibenzyl (109) and diamide (128) derivatives, serves to improve measured slopes. However, the detection limits are less good.

(5) The diester (124) derivative displays a drastically reduced slope with added TOPO and the detection limit is consequently very poor.

2.6.4 Measurements of Lithium Selectivity Using the Flow System

Measurements of lithium selectivity for ligands (109), (124) and (128) (with and without TOPO) and the Philips ionophore were made against a fixed background of 150 mM sodium chloride, 4.3 mM potassium chloride and 1.26 mM calcium chloride by using the flow system outlined previously.

In this case the electrodes were conditioned overnight in a 1 x 10^{-1} M lithium chloride solution containing 150 mM sodium chloride, 4.3 mM potassium chloride and 1.26 mM calcium chloride at 37°C. The diluent solution consisted of interferent ions in deionised water and the flow rate and cell volume were identical to those in the calibration experiments. Hence lithium selectivity coefficients were calculated directly from the curves plotted on the Y/t recorder. These results are depicted in Table 2.6.

LIGAND	WITHOUT TOPO		WITH TOPO	
	SLOPE	DL	SLOPE	DL
(109)	55	$10^{-2.90}$	47	$10^{-2.70}$
(124)	25	---	13	---
(128)	57	$10^{-3.40}$	59	$10^{-3.20}$
Philips Ionophore	47	$10^{-2.15}$	--	---

Table 2.6 *Lithium Selectivity Measurements Using the Flow System by the Fixed Interference Method at 37°C; LiCl Solutions with a Fixed Background of 150 mM NaCl, 4.3 mM KCl and 1.26 mM $CaCl_2$; DL=Detection Limit; Units of slope=mV/decade [LiCl].*

Electrode responses for these derivatives, with and without interferents, as measured in the flow system are depicted graphically in Figures 2.22-2.26.

Since previous results for these ligands have demonstrated that interference from both potassium and calcium ions do not define a detection limit within the lithium ion concentration used (1×10^{-1} M - 1×10^{-4} M), the interference which gives rise to measured detection limits can be assumed to be entirely due to sodium. With this in mind a table of lithium/sodium selectivity coefficients may be constructed (Table 2.7).

LIGAND	$\log K^{Pot}_{LiNa}$	
	WITHOUT TOPO	WITH TOPO
(109) Dibenzyl	-2.07	-1.88
(128) Diamide	-2.57	-2.37
Philips Ionophore	-1.32	---

Table 2.7 *Lithium/Sodium Selectivity Ratios Using the Flow System.*

There are several points to note from these results:

(1) In comparison to the dip-type method used in preliminary experiments, the diamide (128), dibenzyl (109) derivatives and Philips ionophore exhibit higher slopes in a fixed background of 150 mM sodium chloride using the flow system. In the flow system, the electrodes are in contact with the analyte throughout the lithium ion concentration range 1×10^{-1} M - 1×10^{-6} M. However, the dip-type method necessitates dipping the electrodes in separate lithium chloride solutions. Studies have shown[136] that the dip-type method generates lower slopes in the presence of interferents than in the flow system.

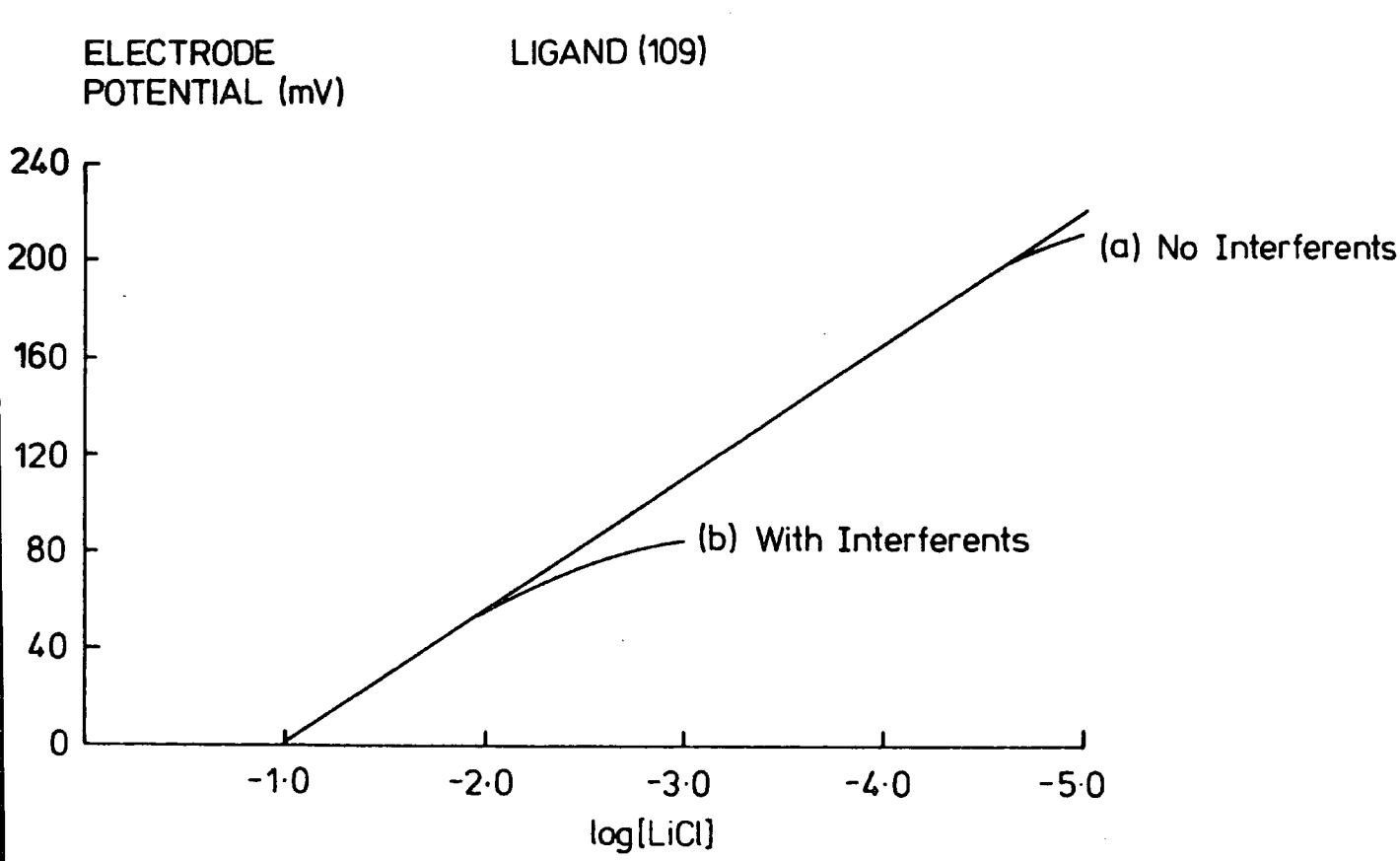

Figure 2.22 *Graph of Electrode Potential Against Lithium Chloride Concentration for Ligand (109) at 37°C; (a) in Pure LiCl Solutions and (b) With a Fixed Background of 150 mM NaCl, 4.3 mM KCl and 1.26 mM $CaCl_2$.*

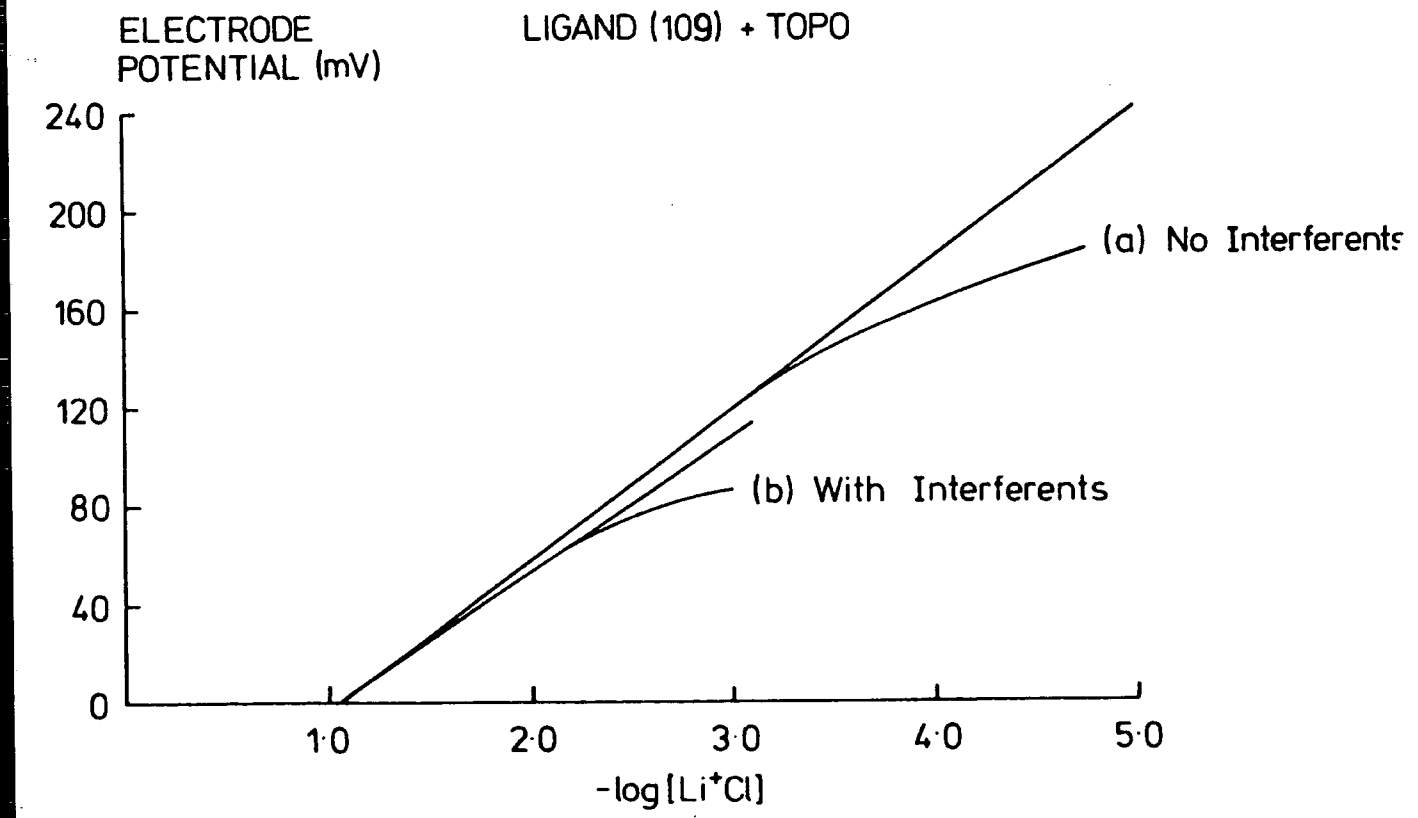

Figure 2.23 *Graph of Electrode Potential Against Lithium Chloride Concentration for Ligand (109) at 37°C; (a) in Pure LiCl Solutions with TOPO and (b) With a Fixed Background of 150 mM NaCl, 4.3 mM KCl and 1.26 mM $CaCl_2$ with TOPO.*

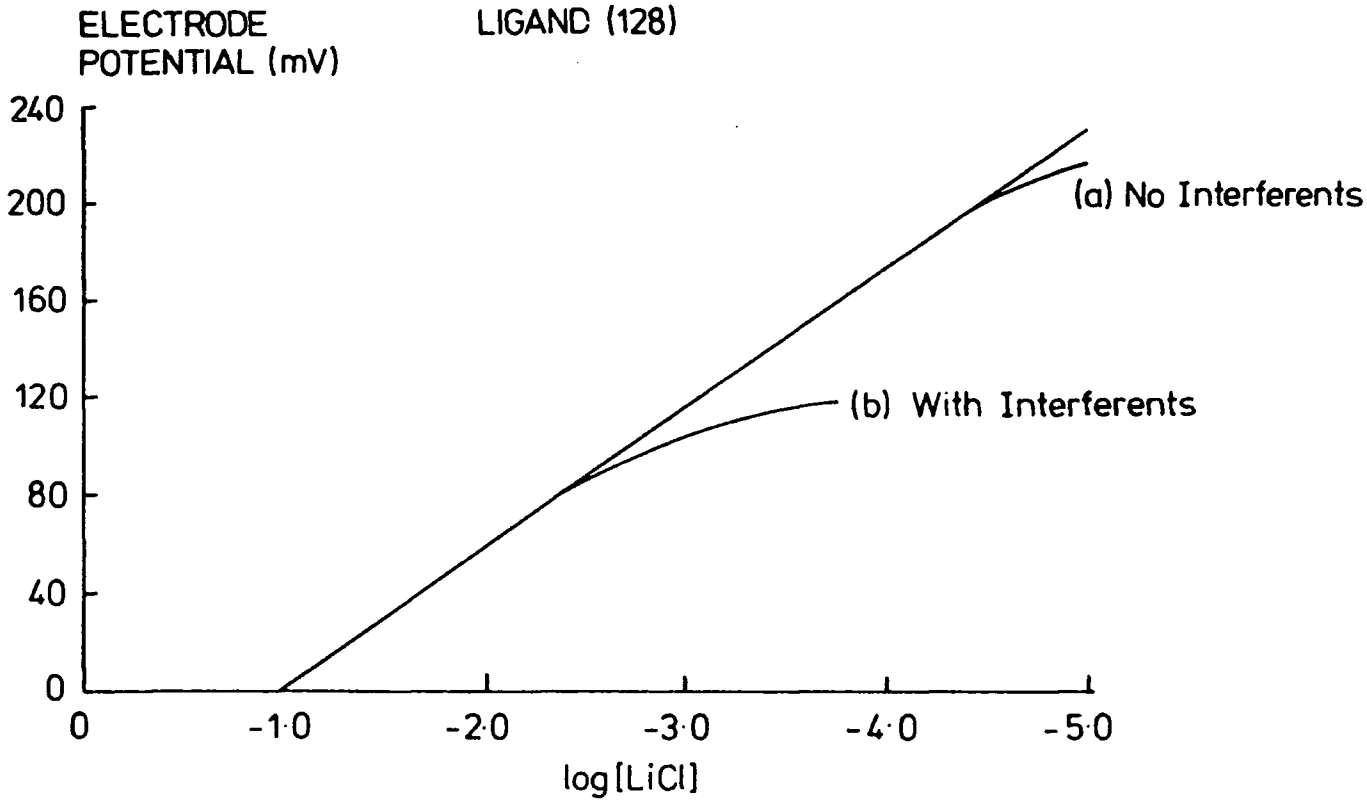

Figure 2.24 *Graph of Electrode Potential Against Lithium Chloride Concentration for Ligand (128) at 37°C; (a) in Pure LiCl Solutions and (b) With a Fixed Background of 150 mM NaCl, 4.3 mM KCl and 1.26 mM $CaCl_2$.*

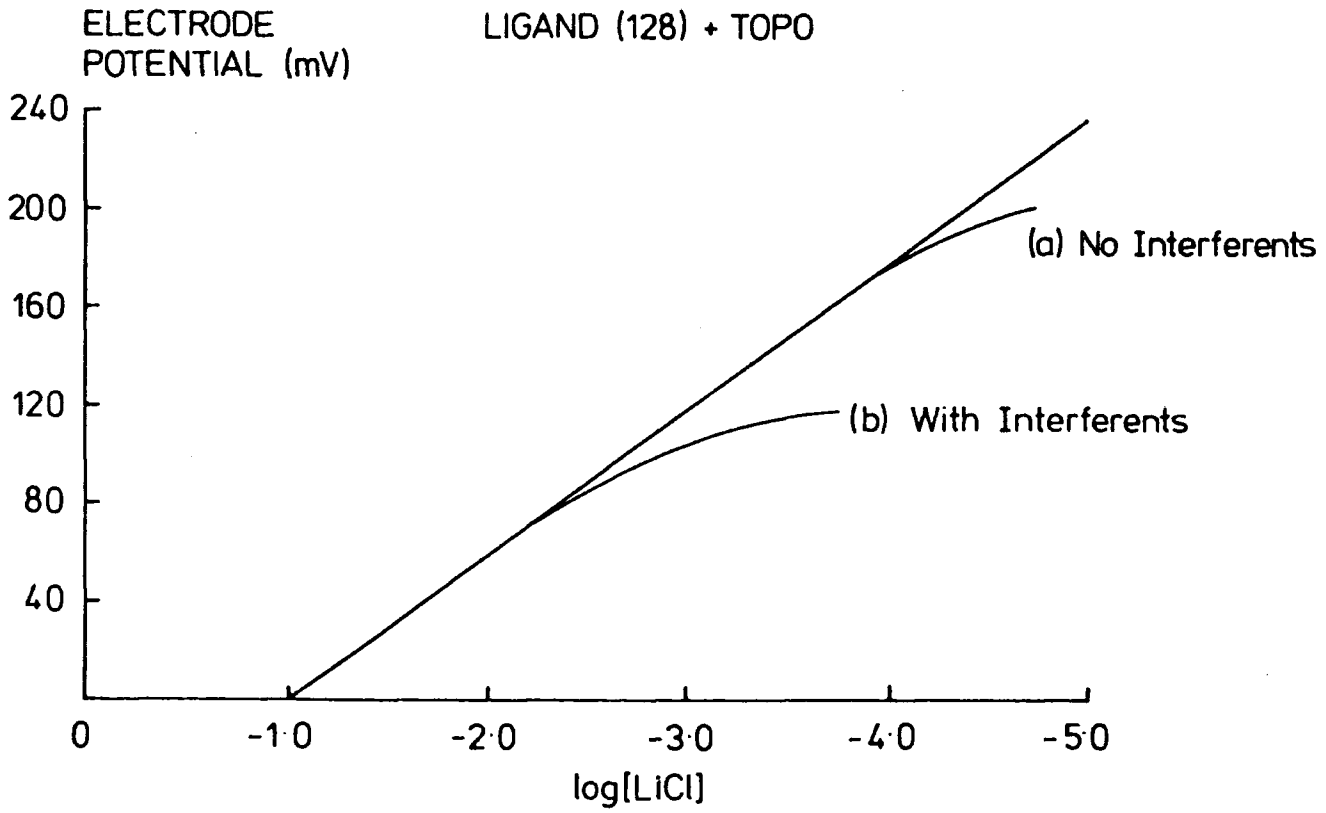

Figure 2.25 *Graph of Electrode Potential Against Lithium Chloride Concentration for Ligand (128) at 37°C; (a) in Pure LiCl Solutions with TOPO and (b) With a Fixed Background of 150 mM NaCl, 4.3 mM KCl and 1.26 mM $CaCl_2$ with TOPO.*

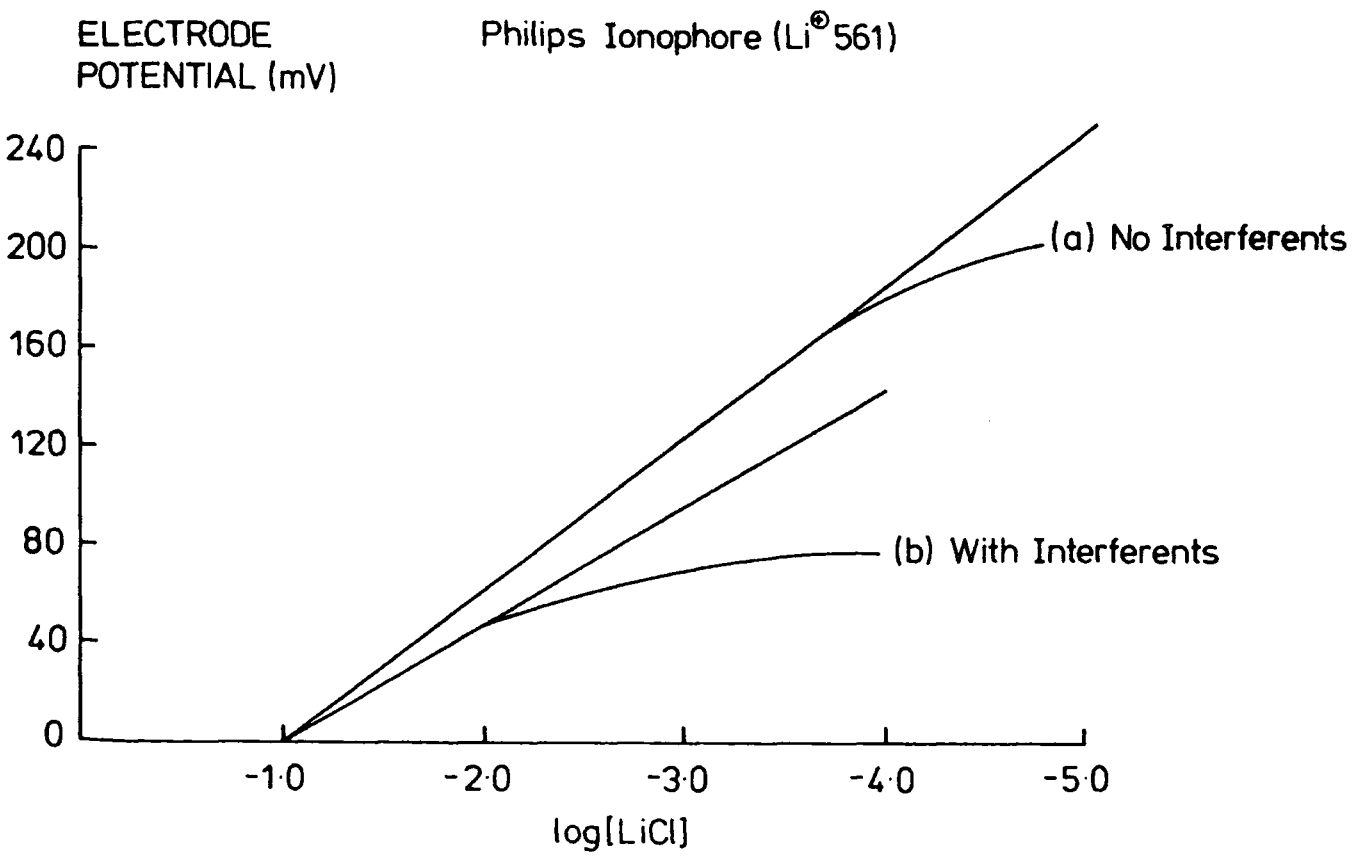

Figure 2.26 *Graph of Electrode Potential Against Lithium Chloride Concentration for Philips Ionophore (Li^+ 561) at 37°C; (a) in Pure LiCl Solutions and (b) With a Fixed Background of 150 mM NaCl, 4.3 mM KCl and 1.26 mM $CaCl_2$.*

It has been reasoned that this is due to relatively fast concentration changes occurring in the dip-type method as the electrodes are dipped into each different lithium chloride solution with the fixed background of interferents, as opposed to a slower constant dilution rate in the flow system. This has been further emphasised by the results of a series of calibration experiments carried out at different flow rates. It was found that the difference between the slopes obtained using the dip-type method and the flow system increased when the flow rate was increased and when the concentration of primary ion was lower than 10^{-5} M [136]. The flow system would seem an eminently preferable technique since it allows direct electrode potential measurements over the entire

lithium chloride concentration range (1×10^{-1} M - 1×10^{-6} M). In the dipped system, on the other hand, measurements were taken at increments of one decade change in the lithium ion concentration. Added to this, the measured selectivity coefficient for the Philips ionophore ($\log K^{Pot}_{LiNa} = -1.32$) by the flow system, compares very favourably with the selectivity coefficient ($\log K^{Pot}_{LiNa} = -1.30$) quoted by the manufacturers.

(2) For the dibenzyl (109) and diamide (128) derivatives, with no added TOPO, the slopes in a fixed background of interferents remain identical to those measured in pure lithium chloride solutions. For the Philips ionophore, and especially the diester derivative without added TOPO, measured slopes fall when interferents are present. As a consequence, the diamide (128) and dibenzyl (109) derivatives show appreciably higher limits of detection when interferents are present as compared to the Philips ionophore and diester derivative (124).

(3) Addition of 1% TOPO to the benzyl derivative confers a lower slope in the presence of interferents. This is at variance with the improved slope with added TOPO measured in pure lithium chloride solutions. The mechanism of action of TOPO within the membrane is still not clearly understood, and hence it is difficult to explain the observed differences in behaviour. The low slope exhibited by the benzyl derivative with added TOPO confers a lower limit of detection for this electrode in the presence of interferents.

(4) The addition of 1% TOPO to the diamide derivative confers a higher slope in the presence of interferents. The limit of detection is, however, lower than when no TOPO is present.

(5) The lithium/sodium selectivity coefficients indicate that both the diamide (128) and dibenzyl (109) derivatives, with or without TOPO, are substantially more lithium selective with respect to sodium, than the Philips lithium ionophore. The addition of TOPO confers lower selectivities on both diamide (128) and dibenzyl (109) derivatives.

The difunctionalised dibutylamide (128) emerges from this study as by far the most promising lithium ionophore. In both dip-type and flow systems, it exhibits the highest lithium selectivity and the highest detection limits, in both pure lithium chloride solution, and with interferents present. The lithium/sodium selectivity coefficient (log K^{Pot}_{LiNa} = -2.60), as measured in the flow system, marginally improves on that of ligand (10) (Figure 2.27), which displays a lithium/sodium selectivity of -2.50 as measured in a flow system[50], and was widely recognised to be the most selective ligand for lithium over sodium in a clinical sodium background before the present study.

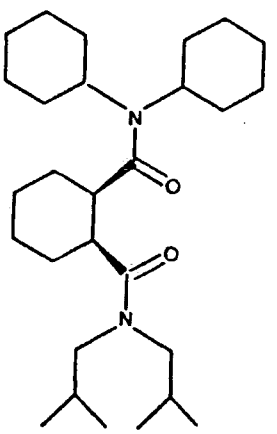

Figure 2.27 *Structure (10).*

The response times for the dibutylamide electrode are fast (< 60 seconds), the stability of the electrode in aqueous solutions seems excellent and response is near Nernstian in either pure lithium chloride solution or in the presence of interferent ions. Though the lithium/

sodium selectivity value is still lower than that required for ideal accurate lithium ion measurement in whole blood (log K^{Pot}_{LiNa} = -4.50), interference from potassium and calcium ions can be safely ignored within the clinical lithium ion concentration range (0.5 mM - 1.0 mM). Since the clinical sodium levels fluctuate over a narrow concentration range (135 mM - 150 mM), a practical application for this electrode, using adequate calibration solutions, seems possible.

CHAPTER THREE

AMIDE FUNCTIONALISED TRIAZA AND TETRAAZA MACROCYCLES AS IONOPHORES FOR LITHIUM AND CALCIUM IONS

3.1 DESIGN OF A LITHIUM SELECTIVE IONOPHORE

Ligands (129)-(132) (Figure 3.1) have been synthesised primarily as selective ionophores for lithium.

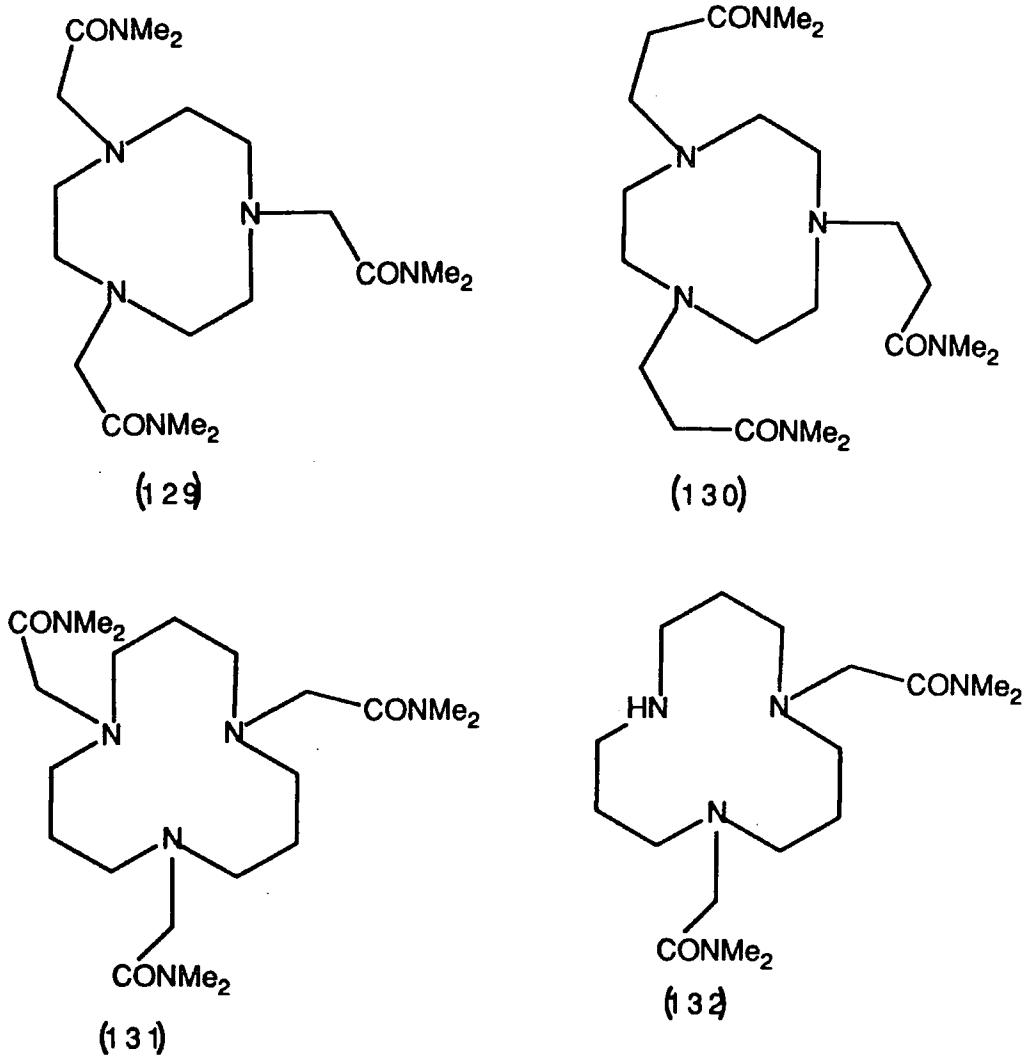

Figure 3.1

There are two features common to all ligands of this series:

(1) Amide Substituents.

These donor groups display two important features: (i) they have a large dipole moment which ensures a high electron density on the oxygen, and (ii) they are softer and more polarisable than ether oxygen donors. These features dictate that the most favourable interaction will occur

with cations of high charge density, as these cations not only form strong ion-dipole interactions, but are also able to polarise the relatively soft amide donors and enjoy ion-induced dipole interactions. Amide donors are therefore expected to co-ordinate most strongly to lithium, magnesium and calcium ions, whose charge density exceeds that of other alkali and alkaline earth metal cations.

(2) Amine Ring Donors.

The more polarisable, softer amine donors should interact more favourably and more selectively, with cations of high charge density, than ether oxygen donors. Therefore, the nature of donors, common to all ligands of this series, is expected to favour complexation of lithium, magnesium and calcium over other alkali and alkaline earth metal cations. The structural features of the ligands in this series are worthy of consideration.

3.1.1 Ligands (129) and (130)

The triazacyclononane ring in ligands (129) and (130) may adopt either a [333] or [234] conformation in both its free and complexed forms (Figure 3.2).

The [333] conformer is stabilised (by about 35 KJ mol^{-1}) relative to the [234] conformer in both free and complexed forms as deduced from molecular mechanics calculations[137]. It is therefore likely that ligands (129) and (130) will exhibit the [333] conformation in both free and uncomplexed forms, with alkali and alkaline earth metal cations. Assuming the [333] conformation is maintained during the complexation process, this doesn't imply that the triazacyclononane ring is wholly

preorganised for complexation; in that torsional angles may change during the complexation process.

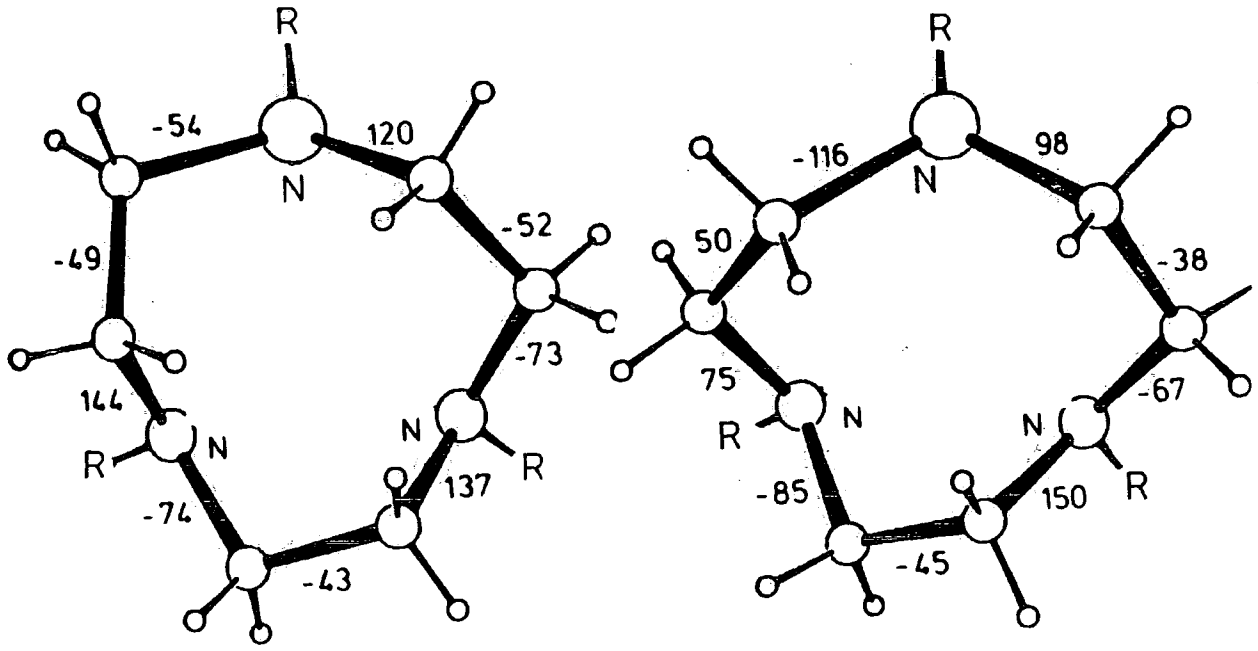

Figure 3.2 *Diagrammatic Representation of [234] and [333] Conformations of Trisubstituted Triazacyclononane Ligands; Anti (>±90⁰); Gauche (<±90⁰); R=CONMe₂ (129); R=CH₂CONMe₂ (130).*

However, as can be seen from the large energy difference between [333] and [234] conformations, a change in torsional angles in this small rigid ring, from the conformation in its uncomplexed form, is energetically expensive. Therefore it seems probable that steric strain in the ring will increase rapidly with increasing metal size, potentially allowing selective complexation of small cations such as lithium and magnesium over other larger alkali and alkaline earth metal cations.

Complexation of alkali and alkaline earth metal cations with ligands (129) and (130) will be facial, and co-ordination of the metal cation with all six donor sites will result in a distorted octahedral geometry (Figure 3.3).

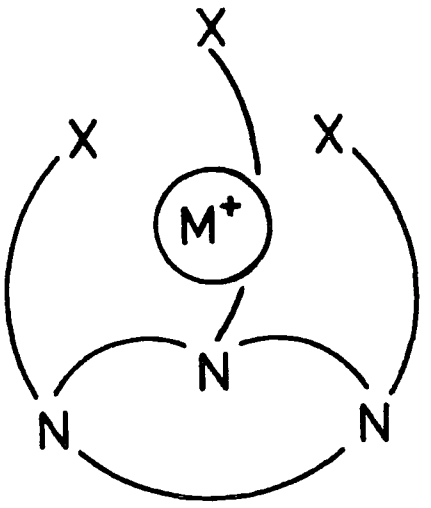

Figure 3.3 *Diagrammatic Representation of the Facial Co-ordination of Ligands (129) and (130) to Metal cations.*

Since the triazacyclononane ring is too small to accommodate any alkali and alkaline earth metal cations, the lone pairs of the amine ring donors are focused to a point above the centre of the ring and these donors co-ordinate from below the metal cation sphere. The three amide donors may then potentially orientate themselves so as to complete the distorted octahedral co-ordination from above the metal cation sphere. As the metal cation size increases, steric strain increases within the ring as the amine donors attempt to increase the distance between themselves. As a consequence of this, the CH_2N bonds of the three amide substituents are forced farther away from the centre of the ring, which introduces further steric strain within the ligand as amide substituents attempt to co-ordinate the metal cation. Furthermore, as the the size of the metal cation increases, so the amide substituents are less and less able to envelop the cation. Clearly then, ligands (129) and (130) will be expected to to exhibit a pronounced selectivity on the basis of metal cation size.

Ligands (129) and (130) are hexacoordinate and will therefore favour complexation of alkali metal and magnesium ions, whose optimal co-ordination number is six.

Ligands (129) and (130) differ in the length of side arm substituent. For ligand (129), co-ordination by amide substituents leads to the formation of five-membered chelate rings, whereas for ligand (130) six-membered chelate rings are formed. Studies by Hancock[123] suggest that for six-membered chelate rings, the carbon substituents can adopt the more favoured staggered arrangement with small metal cations, but as the size of the metal cation increases, the substituents are increasingly forced into the less favourable eclipsed orientation. In the case of the five-membered chelate rings, no such favourable staggered arrangement is possible, and the effect of an increase in metal ion size is less marked. Clearly ligand (130) may therefore provide a more pronounced size selectivity relative to ligand (129) in favour of small metal cations, by virtue of its three six-membered chelate rings. However, it must be remembered that the longer side-arms of ligand (130) may have three other effects:

(1) A more complete envelopment of larger cations may be possible, thereby increasing stability of resultant complexes relative to those of lithium and magnesium, as compared to ligand (129) complexes.

(2) The co-ordination to lithium and magnesium ions by all three amide donors may be sterically impossible, thereby decreasing stability of lithium and magnesium complexes relative to those of larger cations as compared to ligand (129) complexes.

(3) The longer, more flexible amide substituents may bind less strongly to all metal cations as compared to ligand (129) due to a less favourable complexation entropy.

All three effects would lead to a lower lithium and magnesium selectivity as compared with ligand (129).

3.1.2 Ligand (131)

The triazacyclododecane ring of ligand (131) can exist in a number of conformations as the free ligand. The most stable is the [444] conformation and it is likely that ligand (131) will exhibit this orientation in the free form (Figure 3.4).

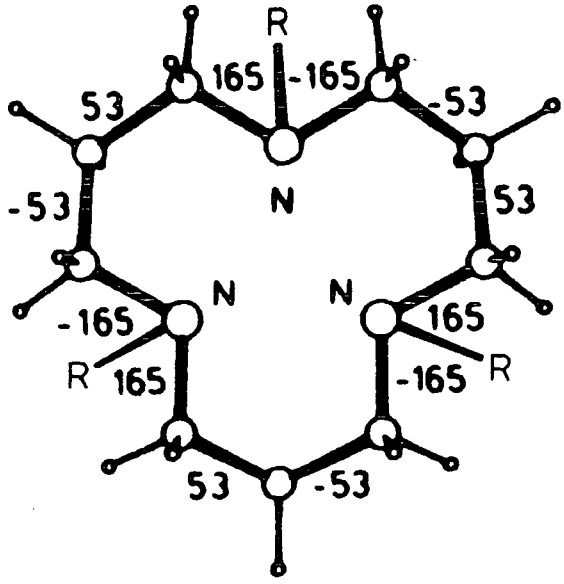

Figure 3.4 *Diagrammatic Representation of the [444] Conformation of Trisubstituted Triazacyclododecane Ring; Anti (>±90°); Gauche (<±90°); R=CH_2CONMe_2.*

In this conformation the nitrogen lone pairs are focused to a point at the centre of the ring approximately level with the ring plane. The ring is too small to accommodate even lithium and magnesium cations, and therefore, in order to complex any alkali or alkaline earth metal cation, the conformation of the free ligand must change in order to allow the nitrogen lone pairs to focus to a point above the centre of the ring plane. As the size of the metal cation increases, the amine ring donors will attempt to increase the distance between themselves

which will have three effects:

(1) Steric strain in the ring will increase, however, as the twelve-membered triazacyclododecane ring is more flexible than the nine-membered triazacyclononane rings of ligands (129) and (130), this effect will be less extreme for ligand (131).

(2) The nitrogen lone pairs will focus to a point further above the ring plane and the CH_2N bond of the amide substituents will be forced further away from the centre of the ring. For larger cations, additional steric strain may be caused as the angle through which the CH_2N bond must turn inward toward the ring centre, in order to allow co-ordination to the central metal cation, is increased.

(3) The hydrogen atoms in the six-membered chelate rings formed by co-ordination between metal cation and amine ring donors will be increasingly forced into the more unfavourable eclipsed orientation. In addition, as the size of the metal cation increases, the amide substituents are less able to envelop that metal cation.

It must be emphasised that, that though the design of ligand (131) would appear to potentially favour complexation of lithium and magnesium ions by virtue of the nature of donor groups, formation of six-membered chelate rings and the presence of six donor groups, the topology of he ligand may dictate that complexation of even these seemingly most favoured cations might be rendered unfavourable on steric grounds. If this were the case, then ligand (131) might co-ordinate weakly to alkali and alkaline earth metal cations and binding would, as a consequence, be indiscriminate. In designing ligand (131), however, it was hoped that the larger ring size as compared to ligands (129) and (130), might ensure a more complete wrapping of lithium and magnesium ions, and that

this, in addition to the six-membered chelate rings formed by co-ordination of the metal cation to amine ring donors, might lead to an increased selectivity for lithium and magnesium as compared with ligands (129) and (130).

3.1.3 Ligand (132)

Ligand (132) differs from ligands (129)-(131) in that it is penta-coordinate. Examination of the crystal structures of lithium complexes reveals that, in a high proportion of cases, lithium is penta-coordinate. This is at variance with larger alkali and alkaline earth metal cations, whose co-ordination number rarely falls below six. It was therefore hoped that decreasing the number of ligand donors from six in ligands (129)-(131), to five in ligand (132), might decrease the resultant stability of the lithium complex to less of an extent than complexes of larger alkali and alkaline earth metals, thereby enhancing lithium selectivity.

3.2 DESIGN OF A CALCIUM SELECTIVE IONOPHORE

Ligand (133) was synthesised primarily as a selective ionophore for calcium. The free ligand is likely to adopt the most stable [3333] conformation (Figure 3.5).

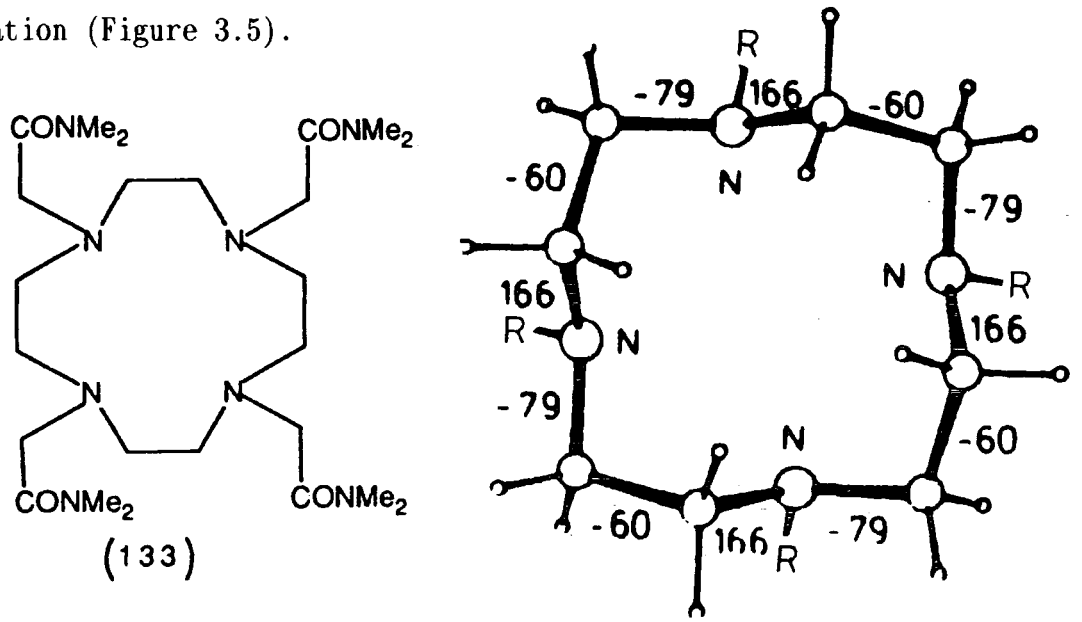

Figure 3.5 *Diagrammatic Representation of the [3333] Conformation of Ligand (133); Anti (>±90⁰); Gauche (<±90⁰); R=CONMe₂.*

Dale[138] has synthesised ligand (143) (Figure 3.6) and performed complexation studies with alkali and alkaline earth metal cations.

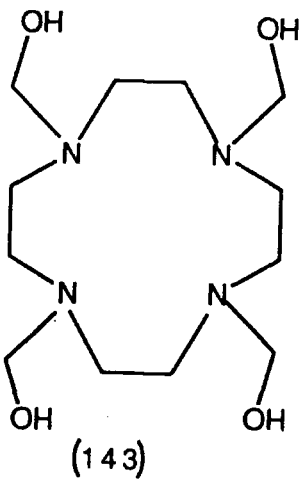

Figure 3.6

There are several points that emerge from these studies:

(1) During complexation of alkali metal cations, the [3333] conformation of the free ligand is maintained, and torsional angles vary only slightly as a consequence of complexation. Comparison of the torsional angles in complexes of lithium, sodium and potassium reveal that two changes in ligand structure occur as the size of the complexing cation increases: (a) the nitrogen lone pairs focus to a point increasingly above the centre of the ring as amine donors increased donor-acceptor distance by furthering the distance between themselves and, as a consequence, (b) the CH_2N bonds of ethanol substituents are directed further away from the centre of the ring. It must be stressed that torsional angle variation is only marginal with increasing cation size, and it is obvious that the tetraazacyclododecane ring can be considered to 'cap' the complexed metal cation and little size selectivity can be envisaged as regards the ring itself owing to the flexibility of the [3333] conformation.

(2) Ligand (143) was found to be sodium selective by ^{13}C NMR studies. Crystal structures reveal that in the solid state the sodium cation is hepta-coordinate, coordinating to all four amine donors and three side-arm oxygen donors, whereas the lithium cation is penta-coordinate, only coordinating to one side-arm donor (Figure 3.7). The small size of of the lithium cation precludes the coordination to more than one side-arm donor. As can be seen from the crystal structure, the coordinating oxygen donor lies vertically above the centre of the ring and further favourable coordination from above the ring plane is sterically impossible. The sodium cation is coordinated by three oxygen donors because coordination cannot occur vertically above the centre of the ring, rather it must be at

an angle of approximately 30^{o} from the vertical owing to the larger size of the sodium cation. This means that it is sterically possible for simultaneous coordination of three side-arm donors.

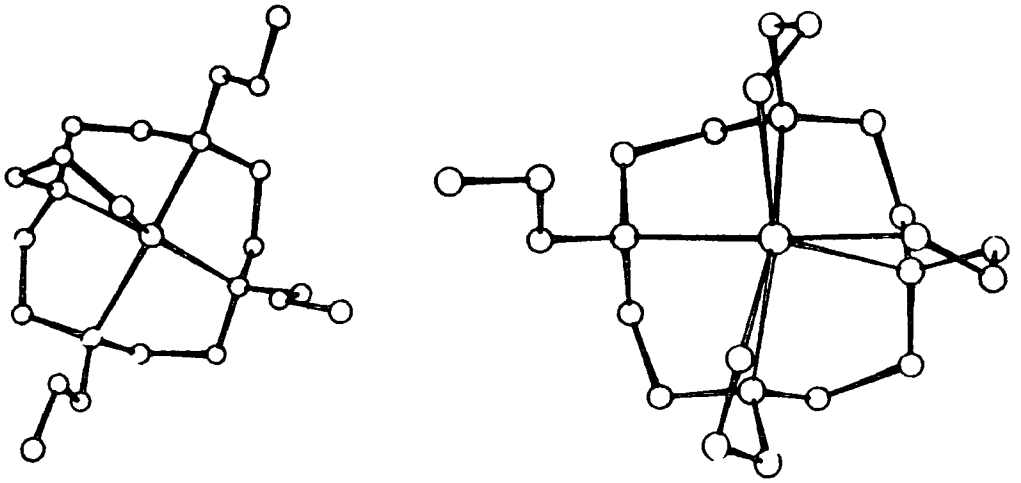

(A) (B)

Figure 3.7 *Crystal Structures of (a) LiSCN and (b) NaSCN with Ligand (143).*

The selectivity of ligand (143) for sodium over lithium can be rationalised by the relative coordination numbers displayed by these metals in their complexes. However, the potassium ion is octa-coordinate in the solid state, coordinating to all available oxygen donors. Clearly the relative weakness of the potassium complex must be due to either (a) a need for still higher coordination and/or (b) a poor matching of ligand topology to the large size of the potassium cation.

(3) Ligand (143) was found to complex more strongly to calcium than other alkali and alkaline earth metal cations. This can be rationalised in that: (a) calcium is of a very similar radius to sodium, (b) calcium displays a higher charge density than sodium and is able to enjoy a more favourable interaction with the relatively soft polarisable amine ring donors, and (c) the topology

of the ligand dictates that calcium will be selectively complexed over other alkaline earth metal cations on the basis of size.

The reasoning behind the design of ligand (133) as a calcium selective ionophore was therefore that: (i) the topology of ligand (133), being virtually identical to ligand (143), would selectively complex calcium and sodium on the basis of cation size, and (ii) the more effective σ-donor properties of the amide carbonyls might enhance the selectivity of calcium over alkali metal cations, in particular sodium.

3.3 SYNTHESIS OF LIGANDS (129)-(133)

3.3.1 Synthesis of Ligand (129)

Ligand (129) was synthesised from triazacyclononane (134) by reacting one equivalent of triazacyclononane (134) with three equivalents of N,N'-dimethylbromoacetamide (135) using powdered sodium carbonate as a base and refluxing the mixture in dry acetonitrile (Scheme 3.1). The product was purified by column chromatography using alumina to yield a clear viscous oil.

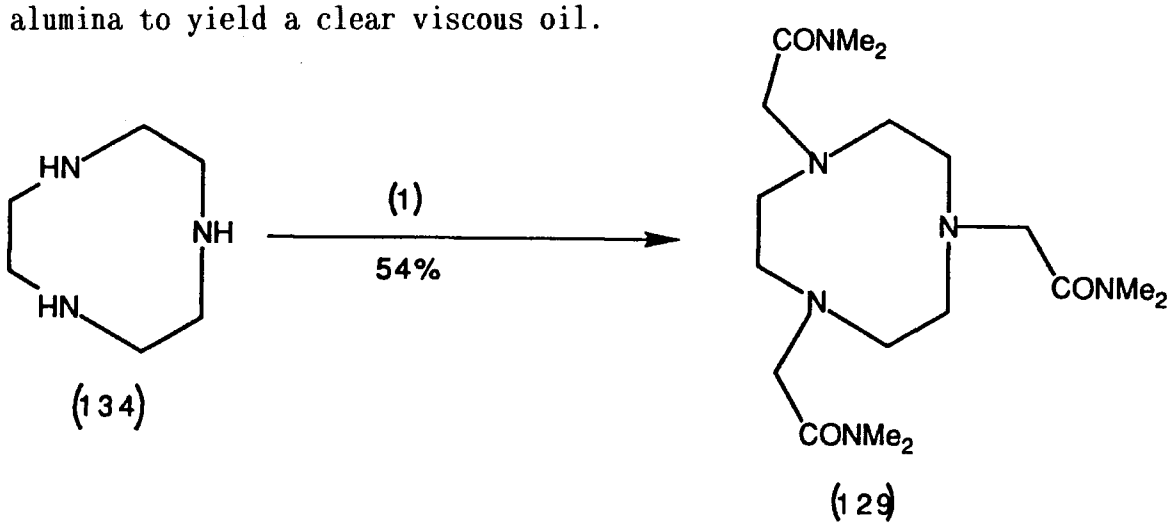

(134) (129)

Scheme 3.1 *(1) Na_2CO_3, $BrCH_2CONMe_2$ (135), MeCN, 83°, N_2.*

3.3.2 Synthesis of Ligand (130)

Ligand (130) was synthesised by reacting triazacyclononane (134) with six equivalents of N,N'-dimethylpropenamide in methanol, heating under reflux for 3 hours ensured a complete reaction (Scheme 3.2). The product was purified by column chromatography using alumina to yield a clear viscous oil.

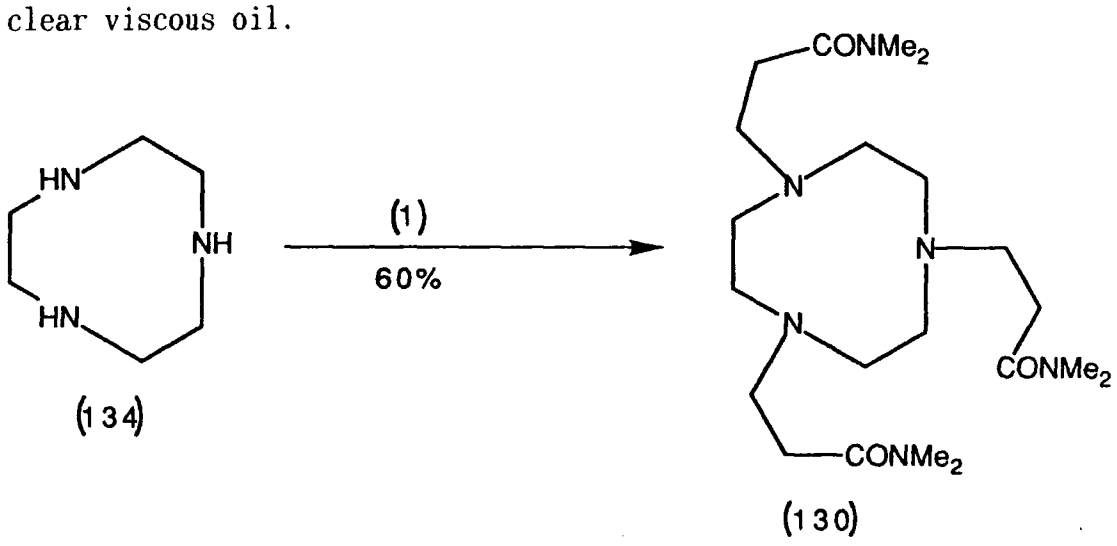

Scheme 3.2 *(1) $BrCH_2CONMe_2$, MeOH, Reflux, N_2.*

3.3.3 Synthesis of Ligand (131)

Ligand (131) was synthesised according to Scheme 3.3. In the first attempted synthesis of this ligand, an identical procedure to that of ligand (129) was followed. Though alkylation was successful, the ^{13}C spectra of the product indicated that an adduct had been formed and it was inferred that the acetonitrile solvent was complexing in some way to the triamide product. When the reaction was repeated using caesium carbonate as a base and dry ethanol as a solvent, the synthesis proved successful. Pure product was obtained by column chromatography using alumina to yield a clear viscous oil.

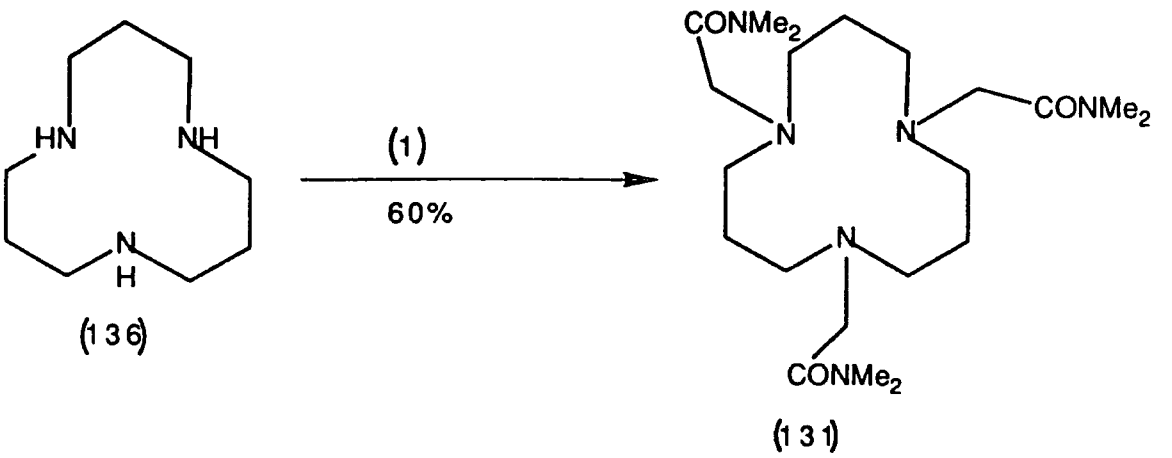

Scheme 3.3 *(1) $BrCH_2CONMe_2$ (135), Cs_2CO_3, EtOH, Reflux, N_2.*

3.3.4 Synthesis of Ligand (132)

Ligand (132) was synthesised according to Scheme 3.4.

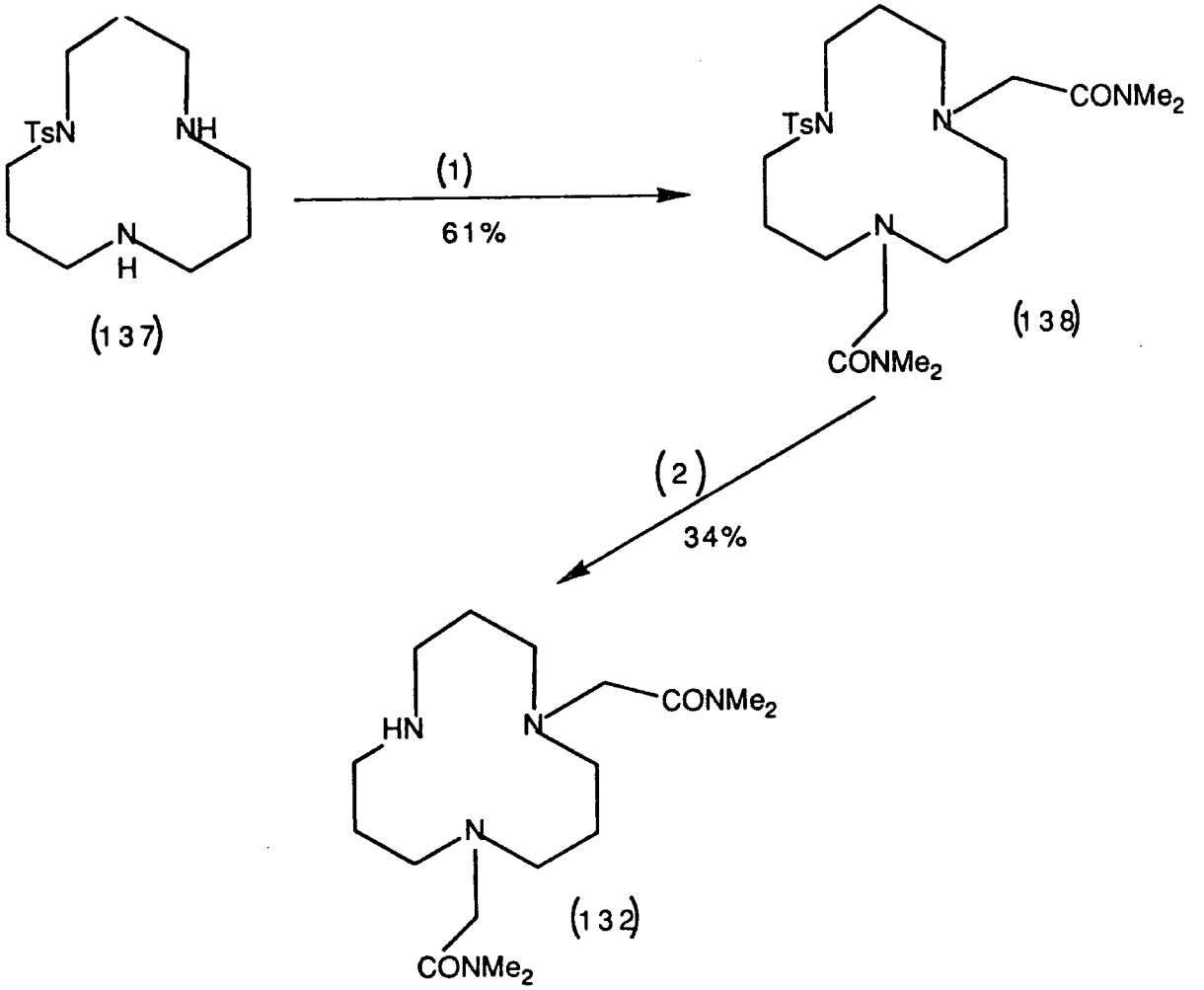

Scheme 3.4 *(1) $BrCH_2CONMe_2$ (135), Cs_2CO_3, CH_3CN, 83°, N_2; (2) HBr/acetic acid/phenol, 90°.*

The first step involved alkylating 1-p-toluenesulphonyl-1,5,9-triazacyclododecane (137) using N,N'-dimethylbromoacetamide (135) with caesium carbonate as above and refluxing in acetonitrile. The product (138) was purified by column chromatography using alumina to yield a clear viscous oil. The first attempted detosylation of (138) involved stirring ligand (138) (1 equivalent) in a 1:10 mixture of dry methanol/-tetrahydrofuran at -78^{o} under an atmosphere of dry nitrogen. Ammonia was condensed into the reaction vessel and lithium metal (40 equivalents) was added in small portions. The reaction mixture turned deep-blue and was stirred at -78^{o} until the blue colour had disappeared. The reaction was then warmed to room temperature and the product was isolated. This method, however, though successfully removing the p-toluenesulphonyl group, also reduced the amide substituents. The second attempted detosylation using HBr/acetic acid/phenol mixture proved successful. The product was purified by column chromatography to yield a clear viscous oil. This procedure however did not prove ideal, as firstly, the detosylation could not be forced to completion, which necessitated separation of product (132) from tosylated material (138) by column chromatography, and secondly, the overall yield of the process was rather disappointing.

3.3.5 Synthesis of Ligand (133)

The first step involved tosylation of 1,4,7,10-tetraazadecane (139) to yield the tetratosylate (140) as a white solid (Scheme 3.5). As the product was insoluble in both water and dichloromethane, purification was afforded by washing the crude product in both of these solvents, followed by filtration. The tetratosylate (140) was then reacted with ethane-1,2-di-p-toluenesulphonate (89) in dimethylformamide according to

the method of Kellogg[148] to yield the cyclic tetratosylate (141) as a white solid. The cyclic tetratosylate (141) was detosylated by using lithium metal as an electron source, ammonia as a solvent for electrons and methanol as a proton source[149], to yield 1,4,7,10-tetraazacyclododecane (142) as a white solid.

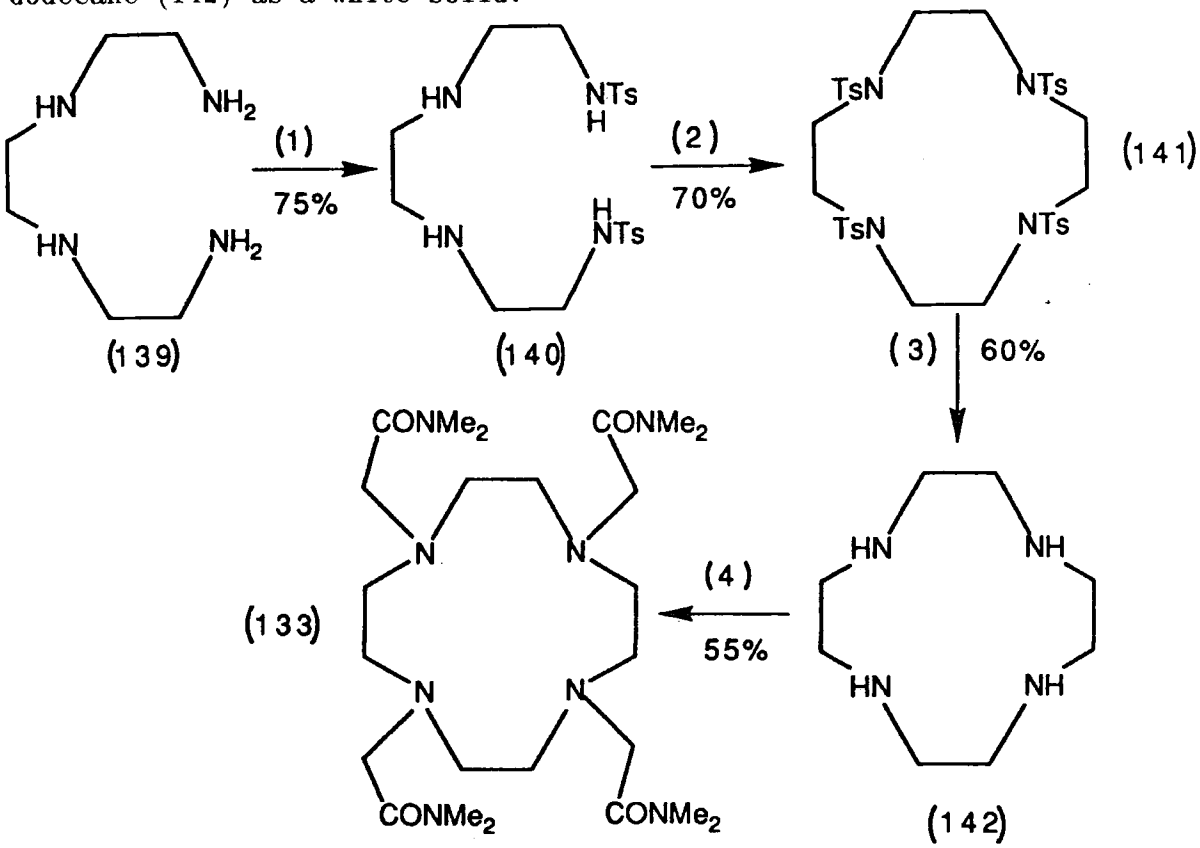

Scheme 3.5 *(1) TsCl, K_2CO_3, H_2O, 80^0; (2) Ethane-1,2-di-ptoluene sulphonate (89), Cs_2CO_3, DMF, N_2; (3) Li(s), $NH_3(l)$, -78^0, N_2; (4) $BrCH_2CONMe_2$ (135), EtOH, Cs_2CO_3, N_2, Reflux.*

Alkylation of (142) to yield ligand (133) was first attempted using sodium carbonate as a base with acetonitrile as the reaction solvent. However, though alkylation was successful, spectral data indicated that a mixture of free ligand (133) and the sodium complex of (133) had been formed. Attempts to separate free ligand from complexed ligand failed and so a second alkylation was attempted using caesium carbonate as a base with ethanol as the reaction solvent. This method proved successful and ligand (133) was purified by column chromatography using alumina to yield a pale yellow viscous oil.

3.4 FAST ATOM BOMBARDMENT EXPERIMENTS

FAB mass spectrometry has been used to determine the selectivity of ligands (129)-(133) for alkali metals (Li^+, Na^+, K^+, Cs^+) and alkaline earth metals (Mg^{2+}, Ca^{2+}, Sr^{2+}, Ba^{2+}) using a procedure adapted from that reported by Johnstone and Rose[44] and Meili and Seibl[135].

An aqueous solution of the chlorides of lithium, sodium, potassium and caesium was prepared with each cation being present at 1.25×10^{-2} M. Methanol solutions of ligands (129)-(133) were also prepared at a concentration of 1.25×10^{-2} M. Analytical solutions were prepared by mixing an equal volume of the cation solution with each of the ligand solutions together with an equal volume of glycerol. Thus, all components were present at equal concentrations as a 1:1:1 methanol:-water:glycerol solvent mixture which allowed metal cations to compete for a limited amount of ligand. The stainless steel tip of the FAB mass spectrometry probe was coated with a thin layer of the analytical solution and positive FAB mass spectrometry was performed (see Chapter 4 for details). The procedure for alkaline earth metal cations was identical to that described for alkali metal cations and concentrations of ligands (129)-(133) and alkaline earth metal cations were 1.25×10^{-2} M. Cation selectivity has been evaluated using the expression:

$$S = \log \left[\frac{I(L+M^1)}{I(L+M^2)} \right]$$

where: S = selectivity factor.
$I(L+M^1)$ = signal intensity of ligand and metal cation that is selectively bound
$I(L+M^2)$ = signal intensity of ligand and metal cation less selectively bound

The poorer the selectivity of ligand (L) for M^1 over M^2 the lower the value (S).

3.4.1 Ligand (129)

The selectivities are listed in Table 3.1 and depicted graphically in Figure 3.8.

	Li^+	Na^+	K^+	Cs^+	Mg^{2+}	Ca^{2+}	Sr^{2+}	Ba^{2+}
Selectivity S(1)	0	1.380	1.610	---	0	0.750	---	---
Selectivity S(2)	0	1.420	1.590	---	0	0.750	---	---
Average	0	1.400	1.600	---	0	0.750	---	---

Table 3.1 *Selectivities for Ligand (129) for Alkali And Alkaline Earth Metal Cations Measured by FAB MS.*

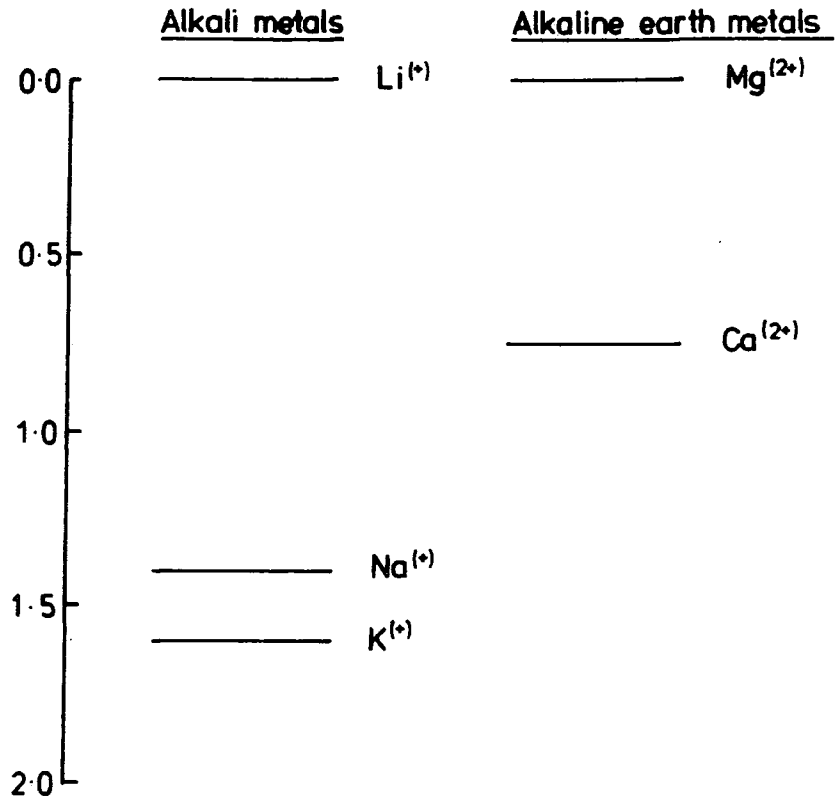

Figure 3.8 *Fast Atom Bombardment Selectivity values (S) for Ligand (129).*

Selectivity of Ligand (129) with Alkali Metal Cations.

Ligand (129) shows a distinct selectivity for lithium over other alkali metal cations. From these studies, it is impossible to know the relative coordination numbers exhibited by the alkali metal cations in

their complexes with ligand (129). However, as the unsubstituted triazacyclononane ring would be unlikely to generate complexes that were stable in this solvent system, and further, would not be expected to exhibit such marked selectivity patterns, side-arm coordination is almost certainly evident. If it is assumed that side-arm coordination is occurring for lithium, sodium and potassium ions, the selectivity of ligand (129) can be rationalised in that:

(1) Lithium, by virtue of its highest charge density, will coordinate most strongly to amide donors.

(2) Lithium, by virtue of its smallest size, will be more effectively enveloped by ligand (129) than larger sodium and potassium ions.

(3) The larger sodium and potassium cations introduce increased steric strain in the ligand relative to that experienced in the lithium complex as a consequence of: (a) amine donors attempting to increase donor-acceptor distances, and (b) CH_2N bonds being forced to an increased angle from that required to allow favourable coordination by amide donors.

(4) The need for still higher coordination by sodium and potassium ions.

The absence of a signal corresponding to coordination of ligand (129) by caesium probably results from the mismatch between the topology of ligand (129) and the large caesium ion, the low charge density of the caesium ion and perhaps the need for higher coordination by the caesium ion.

Selectivity of Ligand (129) with Alkaline Earth Metal Cations

Ligand (129) shows a distinct selectivity for magnesium over calcium and no evidence of coordination to either strontium or barium.

The selectivity pattern can be rationalised as follows:

(1) Magnesium has an identical ionic radius to lithium and ligand topology will thus best suit magnesium.

(2) The higher charge density of the magnesium ion will ensure a more favourable interaction than with the calcium ion.

(3) Calcium requires octa-coordination for optimal interaction, whereas magnesium requires hexa-coordination.

Use of FAB mass spectrometry to gauge the selectivity of ligand (129) for alkali metal cations in relation to alkaline earth metal cations is difficult owing to the existence of complexes of the form $(M_1^{2+}CL_1Ligand)^-$ with alkaline earth cations, which cannot be reliably compared with (M^+-Ligand) complexes formed with alkali metal cations. However, it is likely that ligand (129) would show the selectivity order $Mg^{2+} > Li^+ > Ca^{2+} > Na^+$.

3.4.2 Ligand (130)

Ligand (130) showed very little evidence of binding to alkali or alkaline earth metal cations, and can be thought of as a weak, indiscriminate complexing agent in this solvent system. Several inferences can be made from these results:

(1) The longer side-arm substituents of ligand (130) are unlikely to impede coordination of alkali or alkaline earth metal cations to the amine donors of the triazacyclononane ring, relative to the side-arm substituents of ligand (129). Therefore, the difference in behaviour of ligands (129) and (130) must stem from axial coordination for ligand (129) as opposed to very weak or absent axial coordination for ligand (130).

(2) The absence of axial coordination for ligand (130) must result from the fact that, though the longer substituents may reduce steric strain for complexation of lithium relative to larger cations, the increased flexibility of the six-membered chelates formed by axial coordination in complexes of ligand (130), must disfavour complexation of all cations on entropic grounds, and that this must be the overriding factor.

3.4.3 Ligands (131) and (132)

Both ligands (131) and (132) show very little evidence of binding to alkali or alkaline earth metal cations, and appear to act as weak, indiscriminate complexing agents in this solvent system. There are two factors which might explain these results:

(1) Complexation is rendered weak for small metal cations (Li^+, Mg^{2+}) because the presence of three six-membered chelate rings formed by coordination to amine ring donors induces unfavourable steric strain within the ligand. For larger cations (Na^+, K^+, Ca^{2+}), as the amine donors increase the distance between themselves so as to increase donor-acceptor distance, there will be two effects: (a) steric strain in the ring itself will increase as the hydrogen atoms in the C_3 chains are increasingly forced into the more unfavourable eclipsed orientation, and (b) increased strain as the CH_2N bonds are forced to turn through an increased angle in order to affect favourable coordination by axial amide donors.

(2) As the free ligands, ligands (131) and (132) will exist in the [444] conformation and will be monoprotonated in the aqueous solvent system employed in this study. The monoprotonated form of these ligands is stable owing to the fact that the hydrogen atom

may form planar hydrogen bonds of equal strength within the ring plane, to amine donors. In order to complex an incoming cation the ligand must first be deprotonated and secondly undergo a conformational change so as to focus the nitrogen lone pairs above the centre of the ring. The [333] conformation of the triazacyclononane ring of ligand (129) renders this ligand less basic because of the fact that the hydrogen atom in the monoprotonated form is bound above the ring plane which doesn't allow planar hydrogen bonding to occur. Added to this, once the ligand has been deprotonated, the conformational change in order to complex an incoming metal cation is minimal. Therefore, the marked difference in behaviour between ligands (131) and (132) in relation to ligand (129) doesn't necessarily imply a lower stability or selectivity for the former, but rather, might reflect a difference in complex formation rates for the monoprotonated ligands in this solvent system.

3.4.4 Ligand (133)

The selectivities are given in Table 3.2 and represented graphically in Figure 3.9.

	Li^+	Na^+	K^+	Cs^+	Mg^{2+}	Ca^{2+}	Sr^{2+}	Ba^{2+}
Selectivity S(1)	1.550	0	0.895	---	1.000	0	0.870	---
Selectivity S(2)	1.450	0	0.905	---	1.000	0	0.890	---
Average	1.500	0	0.900	---	1.000	0	0.880	---

Table 3.2 *Selectivities for Ligand (133) for Alkali And Alkaline Earth Metal Cations Measured by FAB MS.*

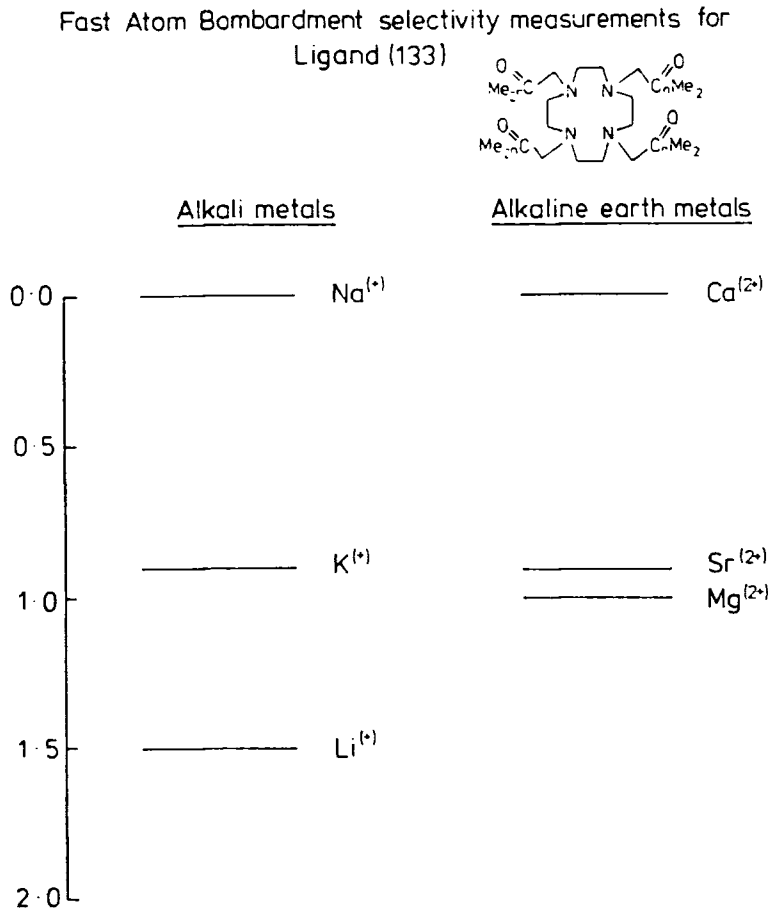

Figure 3.9 *Fast Atom Bombardment Selectivity values (S) for Ligand (133).*

Selectivities of Ligand (133) for Alkali Metal Cations.

Ligand (133) shows a distinct preference for sodium over other alkali metal cations, exhibiting a selectivity in the order $Na^+ > K^+ > Li^+$. The selectivity for sodium over lithium is probably a result of octa or hepta coordination for the sodium ion as opposed to penta coordination for the lithium ion. The selectivity for potassium over lithium is also likely to stem from differing coordination number in respective complexes. Finally the selectivity for sodium over potassium is likely to result from: (a) the fact that the topology of ligand (133) best matches the smaller sodium cation, and/or (b) the need for still higher coordination by the potassium ion, and/or (c) the higher charge density of sodium relative to potassium.

Selectivities of Ligand (133) for Alkaline Earth Metal Cations

Ligand (133) shows a distinct preference for calcium over other alkaline earth metal cations. This selectivity can be rationalised as for Group (I) metal cations if lithium is substituted by magnesium, sodium by calcium and potassium by strontium.

For reasons previously outlined, it is difficult to use the fast atom bombardment technique to reliably gauge relative selectivities of ligand (133) for alkali metal cations in relation to alkaline earth metal cations. However, it is likely that ligand (133) would exhibit the selectivity order $Ca^{2+} > Na^{+} > Sr^{2+} > K^{+} > Mg^{2+} > Li^{+}$.

3.5 NMR EXPERIMENTS

3.5.1 Ligand (129)

Ligand (129) was dissolved in a 2:1 d_4-methanol/$CDCl_3$ mixture and titrated with solid lithium chloride. Discrete lines for free and complexed ligand were seen, indicating the formation of a relatively strong lithium complex, in that exchange was slow on the NMR timescale. The signals corresponding to free ligand disappeared when one equivalent of lithium chloride had been added, indicating that a 1:1 complex was formed. The relative shifts ($\Delta\delta$) for carbons of ligand (129) are depicted in Table 3.3 and spectra are recorded in Figure 3.10. The major point to notice is that $\Delta\delta$ values shift for both carbon atoms in the ring and carbon atoms in the side-arm. Taking this into account as well as the $\Delta\delta \approx 1$ ppm for the carbonyl carbon atoms, data would suggest that: (i) 1:1 complexation involves co-operation between between amine donors and side-arm amide donors, and (ii) lithium is coordinated by all three amide donors in the 1:1 complex.

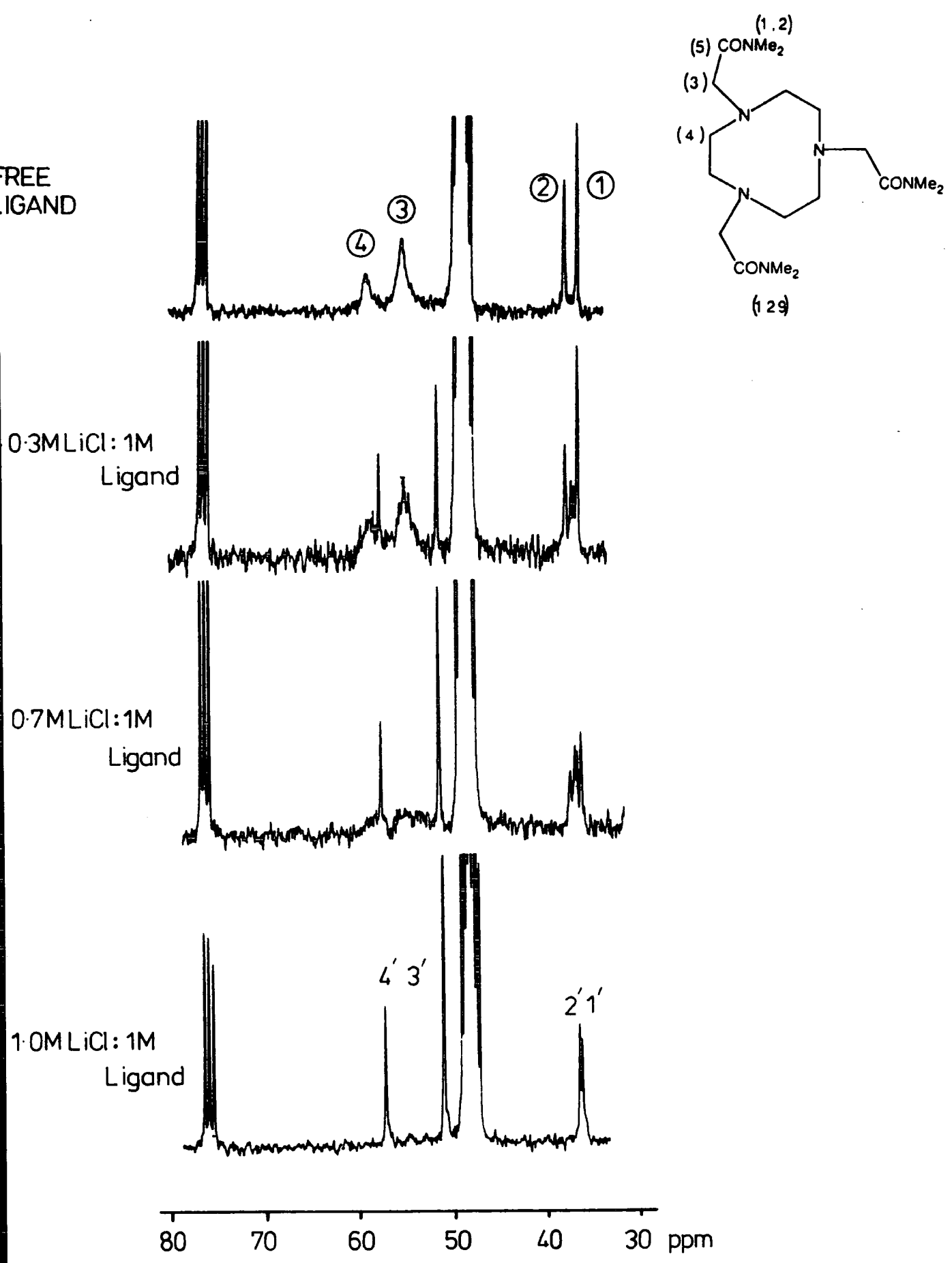

Figure 3.10 *^{13}C NMR Spectra Recorded in a 2:1 d^4-methanol/$CDCl_3$ Mixture for the Titration of Ligand (129) with Solid Lithium Chloride.*

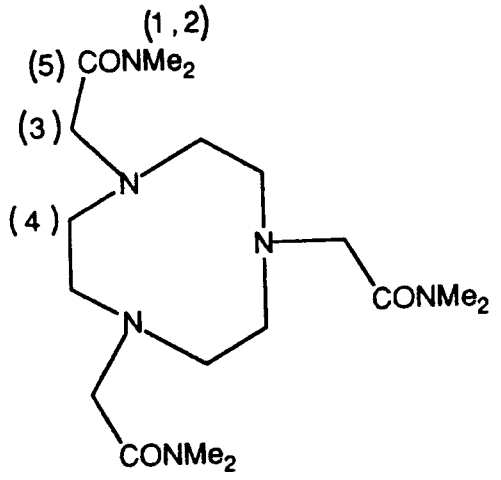

(129)

CARBON ATOM	Δδ /ppm
(1)	0.47
(2)	0.74
(3)	1.36
(4)	3.98
(5)	1.02

Table 3.3 *^{13}C NMR Shifts (Δδ) for Carbon Atoms of Ligand (129) With Lithium Chloride in 2:1 $CD_3OD/CDCl_3$.*

Rather surprising is the large Δδ (≈ 4 ppm) shift experienced by carbon atoms within the triazacyclononane ring. As discussed earlier in this chapter, the [333] conformation is stabilised considerably relative to the [234] conformation and was not expected to undergo a large conformational change during complexation. Rather, it was predicted to cap the complexed lithium cation with minimal concurrent variation in torsional angles. It must be remembered, that the Δδ shift on complexation will not just be a consequence of conformational change and that effects such as the degree to which the complexed metal cation 'deshields' the different carbon atoms must be considered.

3.5.2 Ligand (130)

Ligand (130) was dissolved in a 2:1 d_4-methanol/$CDCl_3$ mixture and titrated with solid lithium chloride. Averaged signals for free and complexed ligand were seen and Δδ values for carbons are listed in Table 3.4 and depicted graphically in Figure 3.11.

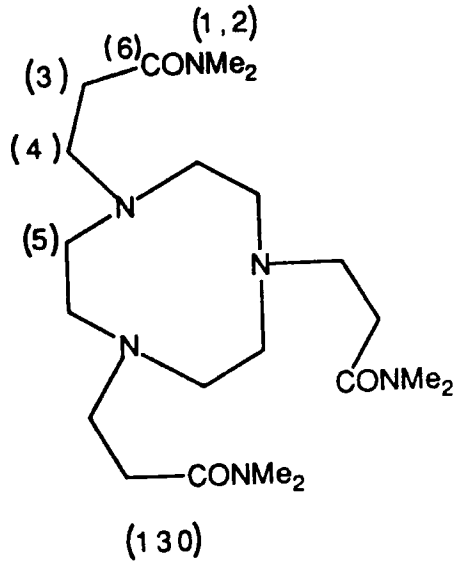

(130)

CARBON ATOM	$\Delta\delta$ /ppm
(1)	0.05
(2)	0.14
(3)	1.05
(4)	0.07
(5)	0.02
(6)	0.70

Table 3.4 *^{13}C NMR Shifts ($\Delta\delta$) for Ligand (130) With LiCl in 2:1 $CD_3OD/CDCl_3$ (298K).*

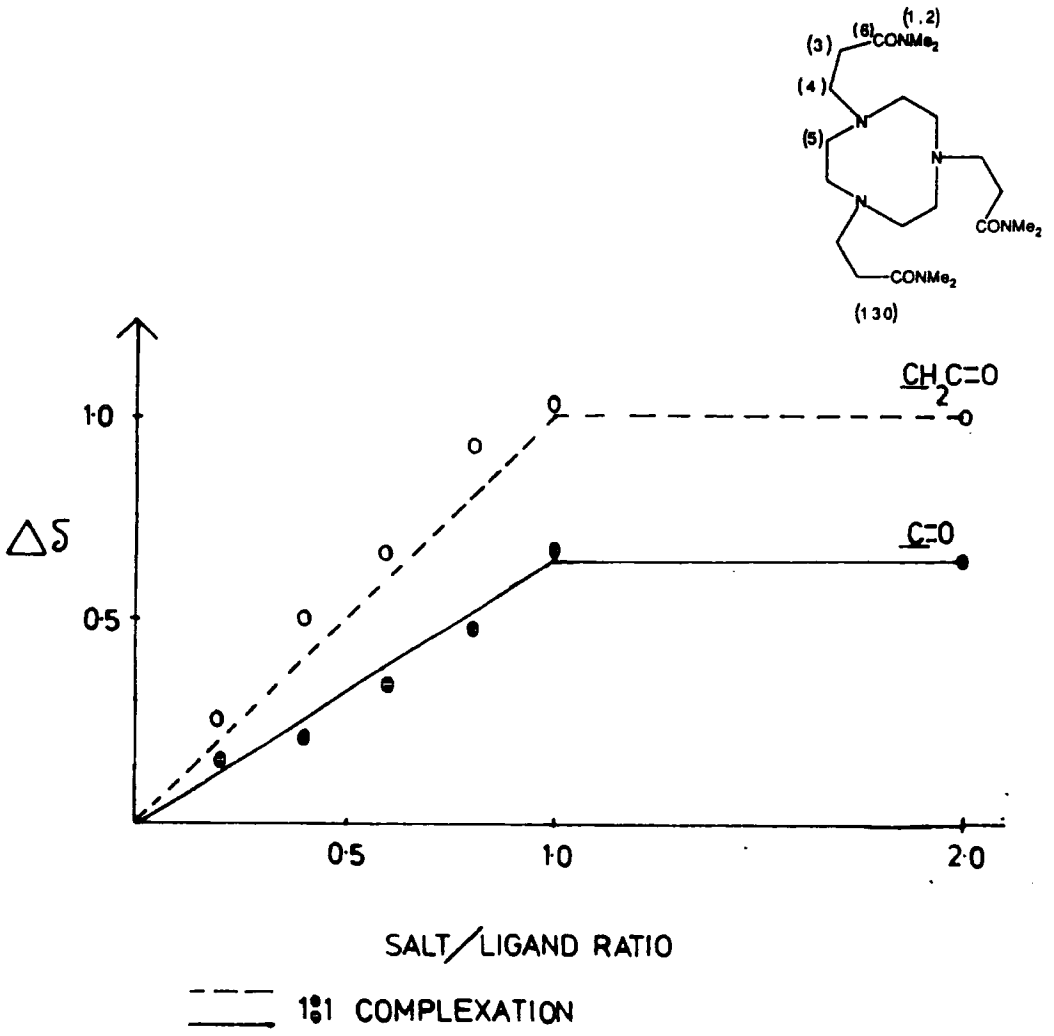

Figure 3.11 *Graph of $\Delta\delta$ Values for Carbon Atoms (3) and (6) of Ligand (130) During a Titration of Ligand (130) and a 2:1 d^4-Methanol/$CDCl_3$ Solvent Mixture Using Solid LiCl.*

There are several points to note:

(1) Ligand (130) forms a 1:1 complex with lithium as $\Delta\delta$ values quickly reach a limiting value when one equivalent of lithium chloride is added.

(2) Averaged signals exhibited by ligand (130) as opposed to discrete signals for ligand (129), indicate that in this solvent system, the 1:1 lithium complex of (129) appears to be more stable.

(3) The $\Delta\delta$ values depicted in Table 3.4 strongly suggest that only the carbonyl carbon (6) and adjacent carbon (3) experienced a conformational change during the complexation process. The carbon (5) of the triazacyclononane ring and the CH_2N side-arm carbons (4) show minimal $\Delta\delta$ values. These values seem to suggest a 1:1 lithium complex in which the lithium cation coordinates to side-arm amide donors with little or no interaction with the triazacyclononane ring itself.

3.5.3 Ligand (131)

Ligand (131) was dissolved in a 2:1 d_4-methanol/$CDCl_3$ mixture and titrated with lithium chloride. Discrete lines for free and complexed ligand were seen and signals corresponding to free ligand had almost disappeared when one equivalent of lithium chloride had been added, indicating that a 1:1 complex was formed. The $\Delta\delta$ values for carbons in ligand (131) are depicted in Table 3.5 and spectra are depicted in Figure 3.12. There are several points to note:

(1) Though free and bound signals were evident for ligand (131) the signals are exchange broadened at 25^{o}C. This indicates that the lithium complex of ligand (131) is stronger than that of ligand (130) yet weaker than than that of ligand (129) in the 2:1 d^4-

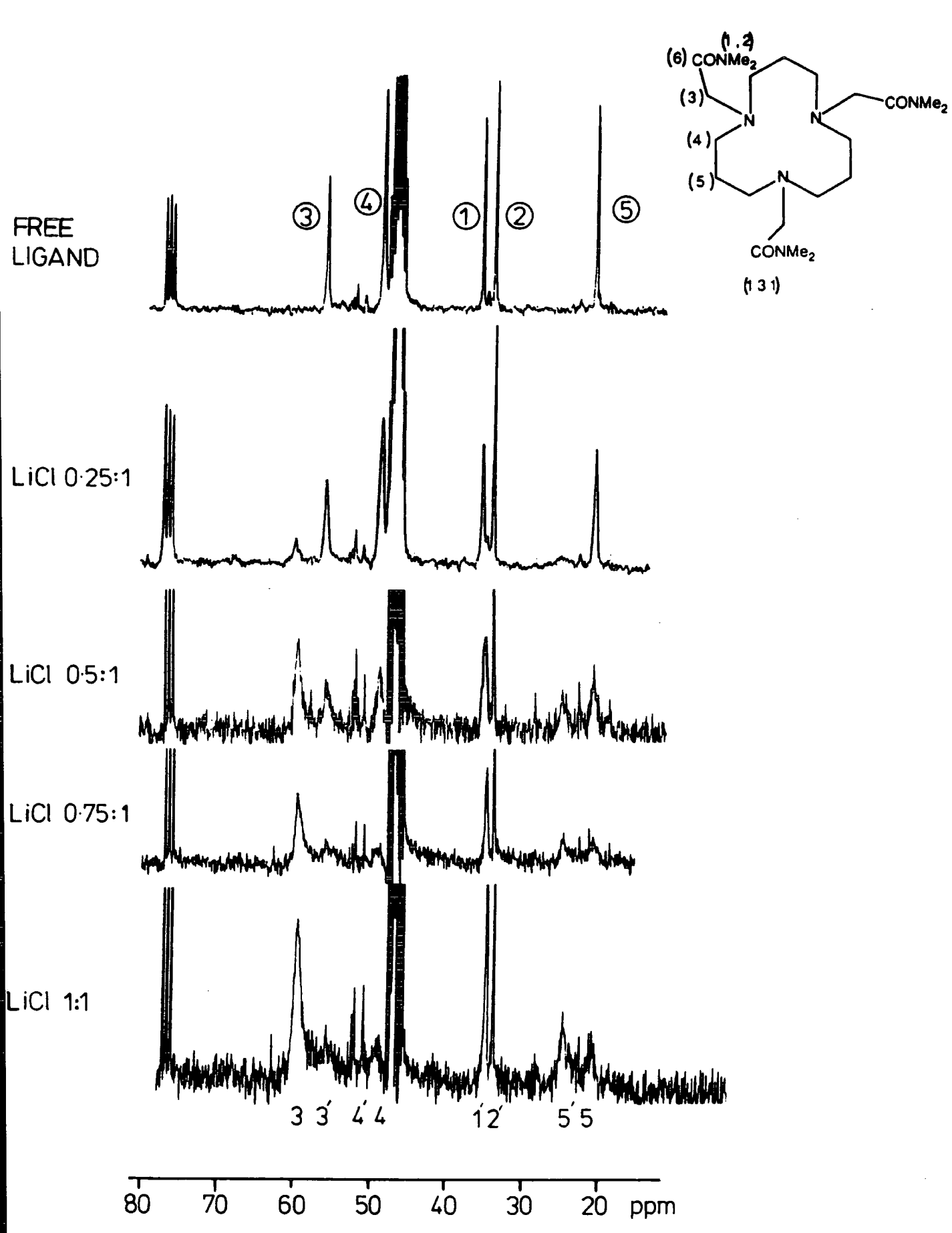

Figure 3.12 *^{13}C NMR Spectra Recorded in a 2:1 d^4-methanol/$CDCl_3$ Mixture for the Titration of Ligand (131) with Solid Lithium Chloride.*

methanol/$CDCl_3$ solvent system used in these studies.

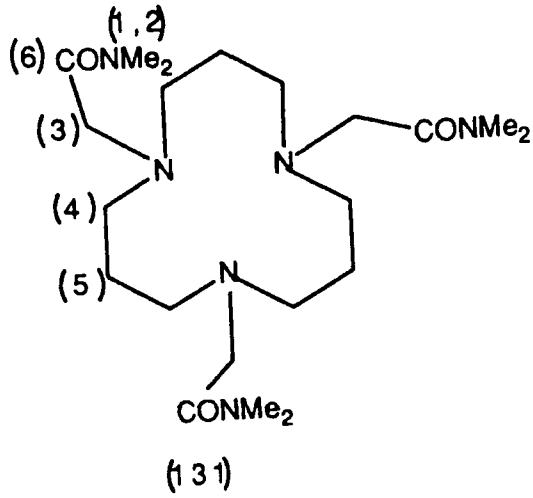

(131)

CARBON ATOM	$\Delta\delta$ /ppm
(1)	0.10
(2)	0.70
(3)	3.55
(4)	3.35
(5)	4.20
(6)	0.20

Table 3.5 *^{13}C NMR Shifts ($\Delta\delta$) for Ligand (131) With Lithium Chloride in 2:1 $CD_3OD/CDCl_3$ (298K).*

(2) Large $\Delta\delta$ values for ring carbons (4) and (5) and carbon atom (3) in the side-arm suggest that: (a) 1:1 complexation almost certainly involves coordination by both ring donors and and side-arm donors, and (b) in order to complex the lithium cation, large conformational changes probably occur in both ring and side-arm from the conformation of ligand (131) in its uncomplexed form.

3.5.4 Ligand (133)

Ligand (133) was dissolved in a 2:1 d_4-methanol/$CDCl_3$ mixture and titrated with calcium chloride. Discrete lines were seen for free and complexed ligand, indicating slow exchange on the NMR timescale and thus relatively strong complexation. When one equivalent of calcium chloride had been added the signals corresponding to free ligand disappeared, indicating that a 1:1 complex had been formed. $\Delta\delta$ values for carbons in ligand (133) are depicted in Table 3.6 and spectra are depicted in Figure 3.13.

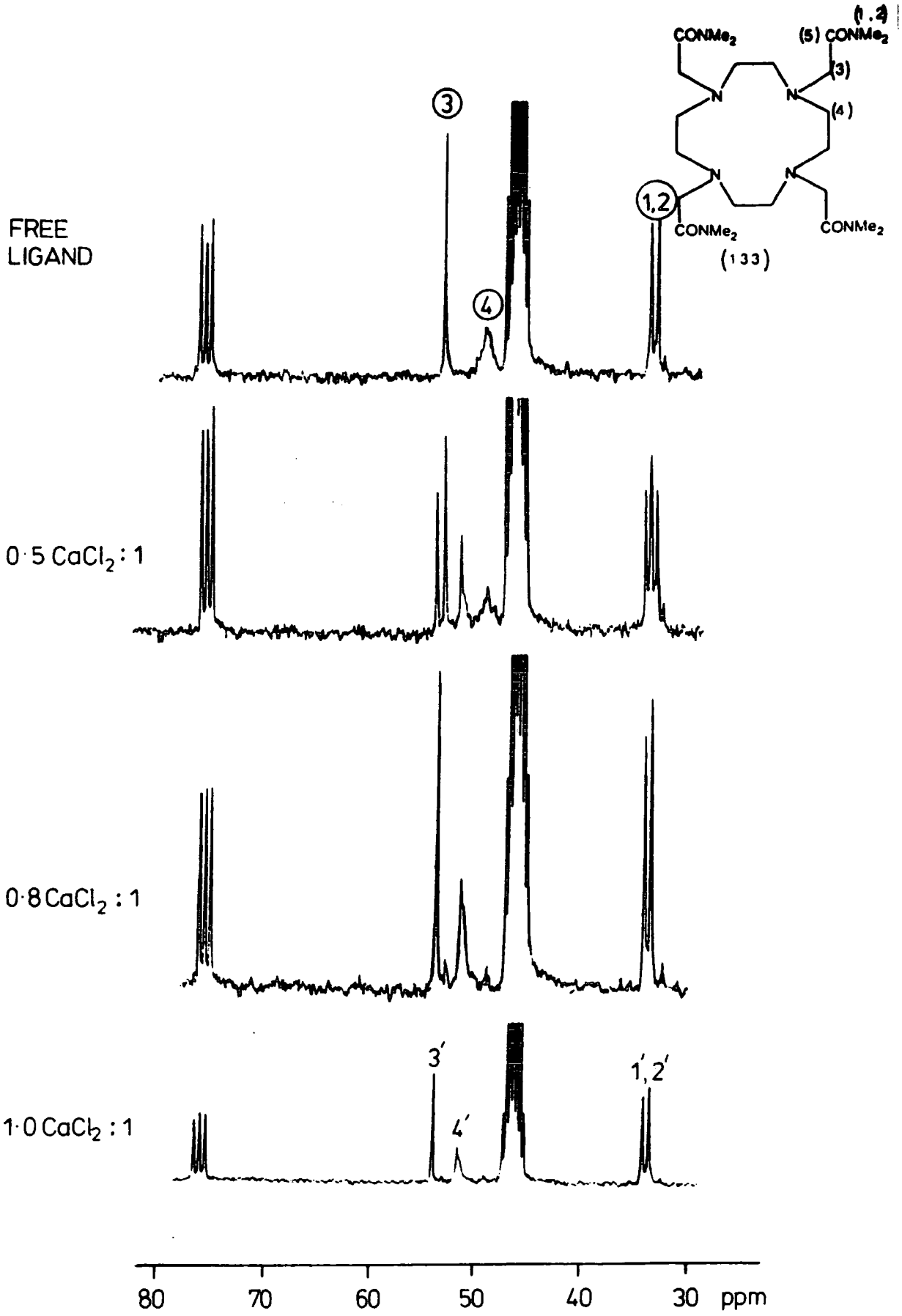

Figure 3.13 *^{13}C NMR Spectra Recorded in a d^4-methanol/$CDCl_3$ Solvent System for the Titration of Ligand (133) with Solid Calcium Chloride.*

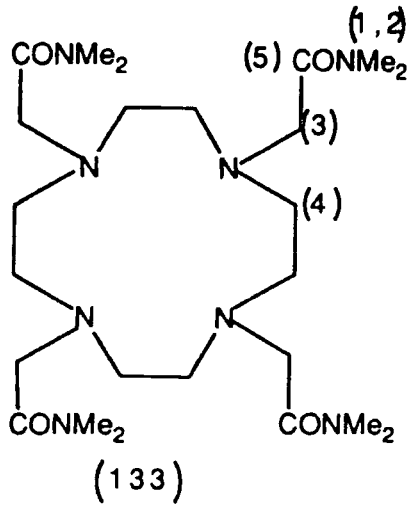

(133)

CARBON ATOM	Δδ /ppm
(1)	0.53
(2)	0.47
(3)	0.78
(4)	2.32
(5)	1.30

Table 3.6 *^{13}C NMR Shifts (Δδ) for Ligand (133) With Calcium Chloride in 2:1 $CD_3OD/CDCl_3$ (298K).*

There are several points to note:

(1) Δδ values for ring carbon (4) and side-arm carbons (3) and (5) indicate that 1:1 complexation with calcium probably involves a conformational change for both the ring and side-arm from that of the free ligand. This data suggests that complexation involves coordination to both amine ring donors and amide side-arm donors. Indeed, the existence of one discrete signal for the carbonyl carbon atom (5) in the calcium complex, added to the fact that when one equivalent of calcium chloride had been added the signal corresponding to the carbonyl carbon (5) in the free ligand completely disappeared, suggests that in forming a 1:1 complex with calcium, all four amide donors coordinate to the calcium ion.

(2) Overall Δδ values are modest, and would seem to indicate a greater conformational change in the ring than the side-arm of ligand (133) during 1:1 complexation with the calcium ion.

3.6 IR EXPERIMENTS

The complexation of ligands (129)-(131) with lithium and ligand (133) with calcium, was studied using IR spectroscopy. Each ligand was dissolved in methanol, and the appropriate solid thiocyanate salt was added to each solution such that the ratio of ligand to cation was 1:1. These solutions were left to stand for 2 days. IR spectra were recorded by taking a drop of methanol solution and allowing it to evaporate on a KBr plate to form a thin film. IR spectra of the free ligands were recorded by first dissolving the ligand in methanol and then taking a drop of the the methanol solution and allowing it to evaporate on a KBr plate to form a thin film. The results of these measurements are depicted in Table 3.7.

LIGAND	ν_{max} (C=O)	Δ(C=O)
(129)	1645	
(129) + LiSCN	1619	26 ± 2
(130)	1637	
(130) + LiSCN	1635	2 ± 2
(131)	1646	
(131) + LiSCN	1615	31 ± 2
(133)	1647	
(133) + $Ca(SCN)_2$	1618	29 ± 2

Table 3.7 *IR Data (cm^{-1}) for Free Ligands (129)-(131) and their Lithium Complexes, and for Ligand (133) and its Calcium Complex, Measured as a Thin Film in MeOH on a KBr Plate.*

There are several discernible trends:

(1) For ligands (129), (131) and (133) complexation resulted in a shift of the amide carbonyl stretch of approximately 30 cm^{-1}. Furthermore in each case, only one shifted amide carbonyl stretch was seen. This strongly suggests that the lithium cation is binding to all

three amide donors in ligands (129) and (131) and the calcium cation is binding to all four amide donors in ligand (133).

(2) In the case of ligand (130) no shift in the amide carbonyl was seen, which suggests that complexation of this ligand with lithium in methanol is weak and does not involve coordination to axial amide donors.

3.7 pH METRIC TITRATIONS

3.7.1 Determination of Acid Dissociation Constants

The acid dissociation constants for ligands (129) and (131)-(133) were determined by potentiometric titration.

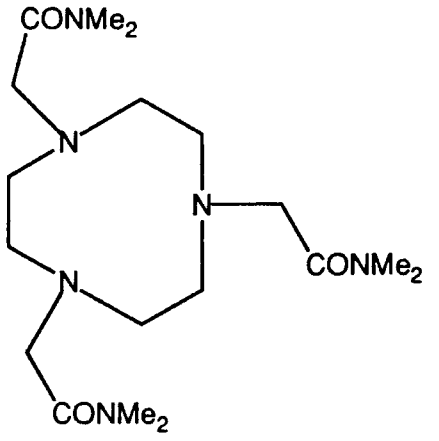

(129)

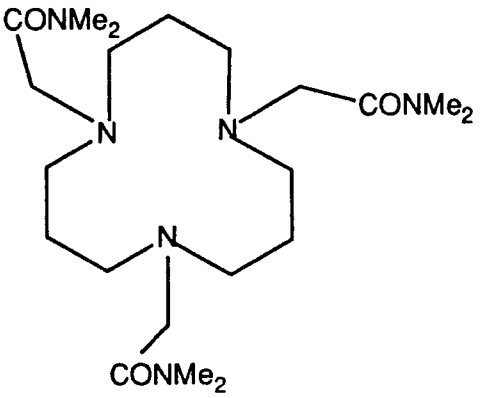

(131)

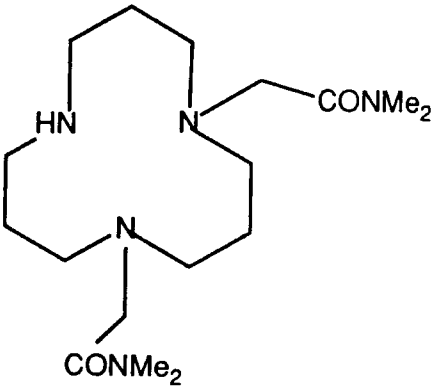

(132)

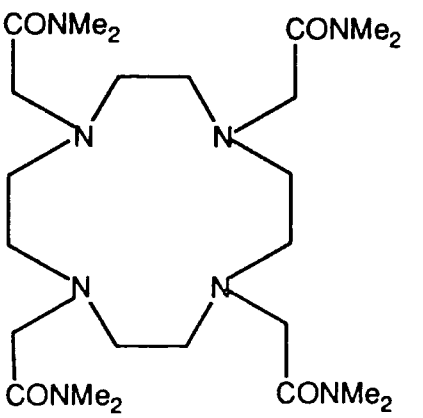

(133)

Stock ligand solutions were made up containing 0.001 mol dm^{-3} ligand, 0.00n mol dm^{-3} nitric acid (n = number of amine nitrogen atoms) and 0.1 mol dm^{-3} tetramethylammonium nitrate, to ensure a constant ionic strength in 25 ml MilliQ water. For each titration, 3 ml of ligand solution was placed in the titration cell. The titrant vessel was maintained at 25^{o} using a thermostat bath. The titrations were performed under nitrogen and controlled by the use of basic software on a BBC microprocessor through a Mettler DL20 automatic titrator. The apparatus used is represented in Figure 3.14.

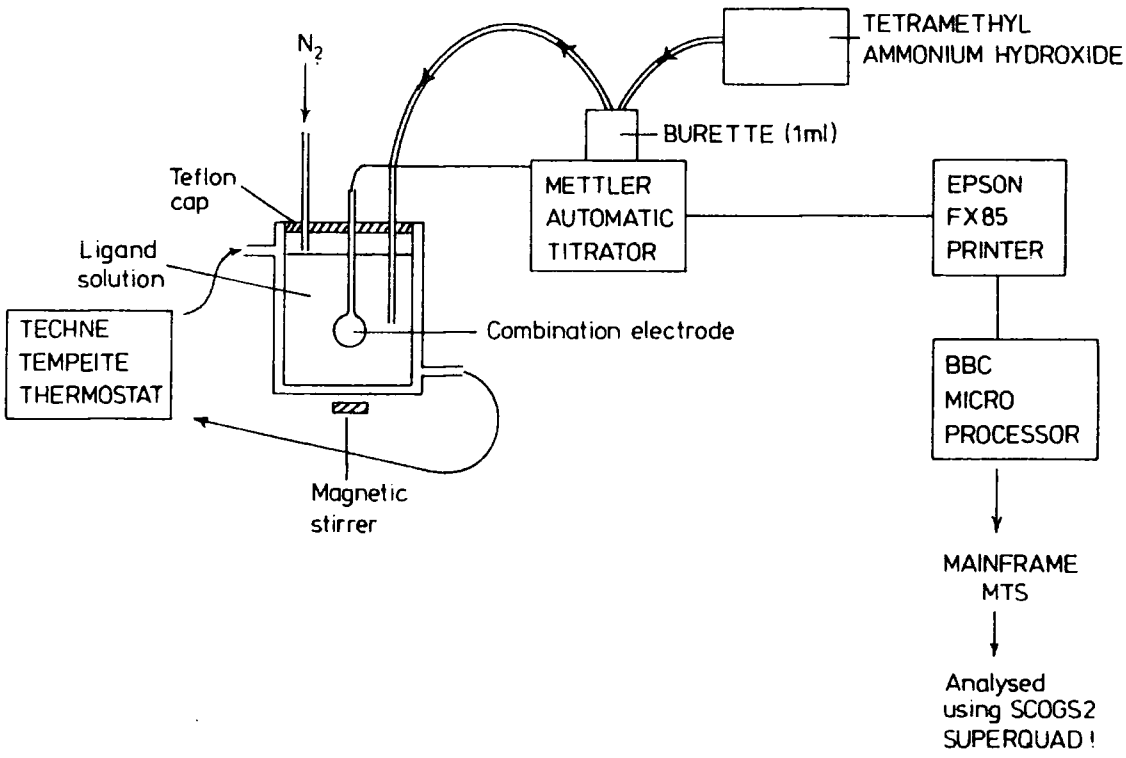

The data was stored on the BBC microprocessor and transferred to the MTS mainframe using Kermit and subsequently analysed by two non-linear least squares programs SCOGS2 and Superquad. Two titrations were performed for each ligand and the results are depicted in Table 3.8.

LIGAND	$PK_a\ LH_3^{3+}$	$PK_a\ LH_2^{2+}$	$PK_a\ LH^+$	ψ^2	σ
129	3.22	7.32	10.31	12.36	1.77
	3.30	7.45	10.36	4.00	1.29
131	----	7.19	11.13	6.96	2.91
	----	7.12	11.20	5.04	1.90
132	----	6.23	10.01	10.40	2.76
	----	6.05	10.31	5.16	2.68
133	----	10.25	11.37	14.68	1.65
	----	10.23	11.34	8.52	2.74

Table 3.8 *Acid Dissociation Constants for Ligands (129) and (131)-(133) as Measured by pH-Metric Titrations.*

The first point to note is that in all cases the deviations (σ) for these titrations lie below the upper limit of 3, and that ψ^2 (which gives an indication of how closely the results fit the Superquad model) is in all cases lower than the upper limit of 12.6 (for $\geq$ 95% accuracy). For all four ligands in this study, PK_a (LH^+) values are high indicating that they are highly basic. Comparative values of 1,4,7-triazacyclononane (134) and diethylenetriamine (144) acid dissociation constants are shown in Table 3.9[139].

LIGAND	$PK_a\ LH^+$	$PK_a\ LH_2^{2+}$	$PK_a\ LH_3^{3+}$
1,4,7-Triazacyclononane (134)	10.6	6.88	< 2.5
Diethylenetriamine (144)	9.7	8.98	4.25

Table 3.9 *Acid Dissociation Constants Measured by pH-Metric Titration in Water at 25° for 1,4,7-triazacyclononane (134) and diethylenetriamine (144).*

The basicity of the first amine nitrogen ($PK_a\ LH^+$) increases upon cyclisation, but the basicity of the second and especially the third nitrogens ($PK_a\ LH_2^{2+}$ and $PK_a\ LH_3^{3+}$ respectively) diminish. The non-bonded electron pairs of the amine nitrogens in 1,4,7-triazacyclononane (134)

are probably directed towards the centre of the ring because of the [333] conformation imposed by the cyclic structure. Thus the first proton uptake is facilitated by the increased electron density in the macrocycle cavity. The first proton is therefore more strongly bound in the macrocycle than in the open chain triamine. The increased electron density in the cycle and the close proximity of the amine nitrogens is thought to allow hydrogen bonding such that the structure depicted in Figure 3.15 may be envisaged, in which the proton is trapped by internal hydrogen bonding. At variance with this, in the acyclic diethylenetriamine, there is little co-operation between amine donors.

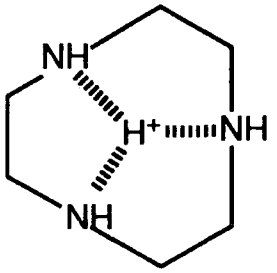

Figure 3.15 *Diagrammatic Representation of "Internal Hydrogen Bonding" in 1,4,7-Triazacyclononane-H⁺.*

The view of proton trapping by internal hydrogen bonding within the ring cavity has been bolstered by measurements of acid dissociation constants of N_2X donor macrocycles[140] and open chain N_2X analogues[139] where X = oxygen or sulphur (Table 3.10).

LIGAND	$PK_a\ LH^+$	$PK_a\ LH_2^{2+}$
9-ane N_3	10.6	6.88
9-ane N_2O	9.59	5.32
9-ane N_2S	9.67	3.98
$HN(CH_2CH_2NH_2)_2$	9.70	8.98
$O(CH_2CH_2NH_2)_2$	9.75	8.90
$S(CH_2CH_2NH_2)_2$	9.50	8.70

Table 3.10 *Acid Dissociation Constants for N_2X Macrocycles and their Acyclic Analogues (X = O or S); Measured by pH-Metric Titration in Water at 25°.*

When the central donor atom is changed from nitrogen to sulphur or oxygen, $PK_a\ LH^+$ values do not change much for open chain ligands. This tends to indicate that for these ligands there is little co-operative action between nitrogen donors during formation of either LH^+ or LH_2^{2+} species. In the cyclic systems however, when the central donor atom is changed from nitrogen to sulphur or oxygen, the $PK_a\ LH^+$ and $PK_a\ LH_2^{2+}$ values fall, which is precisely what would be expected if the donor atoms of the macrocyclic ring were involved in a co-operative stabilisation of the attached proton by internal hydrogen bonding (since the hydrogen bonding ability is N >> O > S).

There seems little doubt that for ligands (129) and (131)-(133) the LH^+ species are stabilised due to co-operative hydrogen bonding by amine ring donors resulting in high $PK_a\ LH^+$ values. The differences between $PK_a\ LH^+$ values for these ligands are a result of many factors. The strength of the hydrogen bonds in the LH^+ species will be determined to an extent by the ring size of the ligand which will dictate both the symmetry of co-operative hydrogen bonding by amine ring donors and the number of donors that are in close enough proximity to effect a reasonable interaction with the proton. Added to this, the conformation of the ring will determine the direction of the amine nitrogen lone pairs and therefore the planarity, and thus strength, of the co-operative hydrogen bond. Clearly, for maximum stability of the LH^+ species, the nitrogen lone pairs should be directed toward the centre of the ring, level with the ring plane delineated by the amine nitrogen donors and ideally the ring conformation should be such that all nitrogen donors can co-operate in a symmetrical intramolecular hydrogen bond. Finally, the conformation of the ring in the LH^+ species should be minimally destabilised relative to the lowest free energy conformation of the free ligand. Data would suggest that the C_3

symmetric [444] conformation of ligand (132) and C_4 symmetry [3333] conformation of ligand (133) are more pre-disposed to effectively trap the first proton than ligands ligands (129) and (131). the precise reasons for this are difficult to pinpoint.

The PK_a LH_2^{2+} values for triaza ligands (129), (131) and (132) closely parallel 1,4,7-triazacyclononane (6.88)[139] and 1,5,9-triazacyclododecane (7.57)[141] and are appreciably lower than those of diethylenetriamine (8.98)[137] and dipropylenetriamine (9.57)[139]. In the cyclic ligands (129), (131) and (132) the proton bound in the LH^+ species will have a high localised positive charge which will cause electrostatic repulsion to a second proton attempting to co-ordinate in close proximity. In the case of the acyclic ligands, the positive charge in the LH^+ species will have less of an electrostatic repulsion as the proximity of the amine donors is lower. Therefore the LH_2^{2+} species will be more basic in cyclic systems.

The PK_a LH_2^{2+} value for the tetraaza ligand (133) (10.25) is significantly higher. This parallels the values measured for 1,4,7,10-tetraazacyclododecane (PK_a LH^+ = 10.97; PK_a LH_2^{2+} = 9.87)[142]. The probable reason for this is that the second proton may add *trans* to the first proton thereby lessening the electrostatic repulsion relative to that experienced by triaza ligands (129), (131) and (132).

If the PK_a LH_3^{3+} values are examined with the view that the closer the amine donors are to one another, the higher the electrostatic repulsion and hence the higher the acidity of the LH_3^{3+} species, then the lowest acidity of the seemingly smallest ligand (129) (PK_a LH_3^{3+} = 3.26) would seem illogical. A tentative explanation might be that the conformations of LH_2^{2+} species for ligands (131), (132) and (133) are such that the third nitrogen lone pair is more effectively sterically shielded and/or more effectively electrostatically shielded by the

ligand by protonated amine nitrogens than for ligand (129).

3.7.2 Determination of Stability Constants

The metal binding constants for ligands (129) and (131) with lithium and sodium ions, and ligand (133) with lithium, sodium and calcium ions were determined by the potentiometric titration method. Stock ligand solutions were prepared as for the acid dissociation constants but in this case the appropriate metal chlorides were added such that the ratio of ligand to cation was 1:1. The titration procedure was identical to that previously described and two titrations were performed for each ligand cation combination.

The basis of this method is that protons are liberated during complex formation between metal cation and the protonated ligand:

$$M^+_{(aq)} + LH_2^{2+}{}_{(aq)} \rightleftharpoons ML^+ + 2H^+$$

$$M^+_{(aq)} + LH^+_{(aq)} \rightleftharpoons ML^+ + H^+$$

By determination of the hydrogen ion concentration the degree of complex formation or the position of equilibrium can be established. The complex forming agent, the weak acid (protonated base) is titrated potentiometrically with a standard solution of a strong base in the presence of an inert electrolyte of suitable concentration and a pH vs (a) curve is plotted (a = degree of neutralisation of the acid). Then a solution of a similar composition but also containing the metal ion is titrated similarly and the titration curve is again constructed. If complex formation occurs extensively in the pH range 3-10 (*ie.* if the complex is rather stable) and the ligand concentration is equal to the metal ion concentration then there will be an appreciable difference

between the two curves. If the protonation constants of the ligands are known, then by using values of the coordinates, from points on the curves, the stability constants may be calculated. If metal complexation is occurring,then this will have the effect of increasing the acidity of both LH^+ and LH_2^{2+} species due to a competition between proton(s) and the metal cation for the ligand. The calculated log K_{ML} values are depicted in Table 3.11.

LIGAND	CATION	log K_{ML}	ψ^2	σ
129	Li^+	3.910	18.18	1.85
		3.905	7.32	2.10
129	Na^+	4.230	5.79	1.76
		4.220	1.58	2.04
132	Li^+	4.230	15.05	2.05
		4.200	6.67	2.62
132	Na^+	4.020	12.40	1.60
		4.030	10.00	1.47
133	Li^+	5.230	2.81	2.07
		5.265	2.17	2.51
133	Na^+	5.810	16.21	1.92
		5.840	6.74	2.12
133	Ca^{2+}	6.780	11.85	1.15
		6.850	12.12	2.93

Table 3.11 *Log K(ML) Values Measured Potentiometrically by pH Titration at 25^0 in MilliQ Water.*

The complexation process can be represented:

$$M^+_{(aq)} + L_{(aq)} \rightleftharpoons ML^+_{(aq)}$$

where: $M^+(aq)$ = free metal cation
$L\ (aq)$ = free ligand
$ML^+(aq)$ = metal/ligand complex

The stability constant K_{ML} can be represented:

$$K_{ML} = \frac{[ML^+]}{[M^+][L]}$$

The fraction of the $M^+_{(aq)}$ as the free aquo ion (X_0) can be represented:

$$\alpha_0 = \frac{[M^+]}{Cm}$$

where: $[M^+]$ = concentration of free aquo metal ion
Cm = total concentration of metal ion.

The fraction of the $M^+_{(aq)}$ as the free aquo ion (X_0) can now be further represented:

$$\alpha_0 = \frac{[M^+]}{Cm} = \left[\frac{[M^+]}{[M^+]} + \frac{[ML^+]}{[M^+]} \right]^{-1} = (1 + K_S[L])^{-1}$$

Therefore it is possible to calculate α_0 for a range of ligand concentrations and thus calculate the % metal cation bound at each ligand concentration: % Metal Bound = $(1 - \alpha_0)*100$.

Figures 3.16, 3.17 and 3.18 represent the % metal bound for ligands (129), (132) and (133) respectively for a range of ligand concentrations as calculated from log K_{ML} data in Table 3.11.

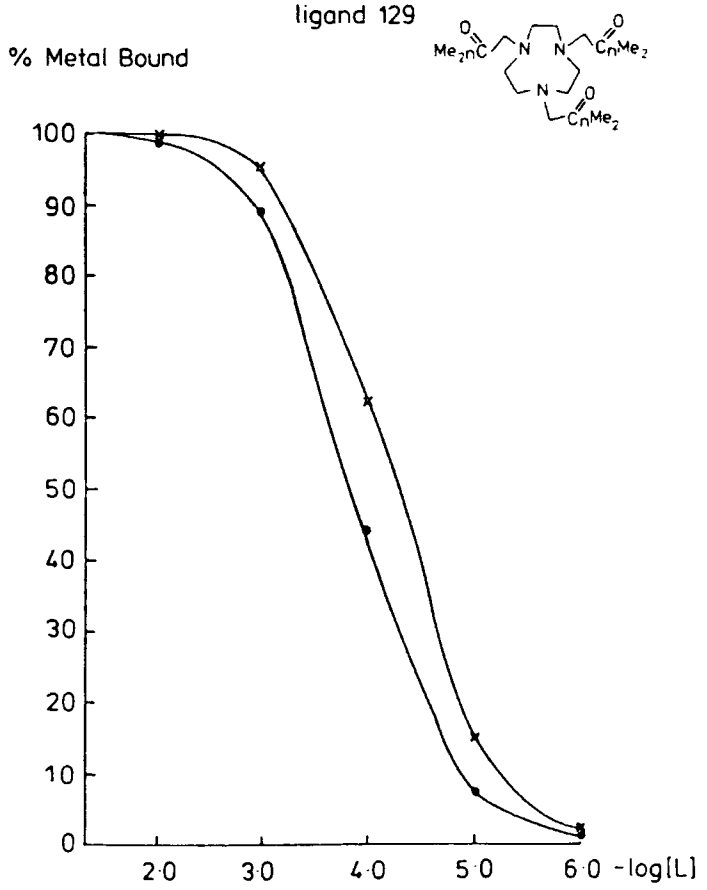

Figure 3.16 *Graph Showing Percentage of Lithium (o) and Sodium (x) Bound <u>vs</u> Concentration of Ligand (129) (L).*

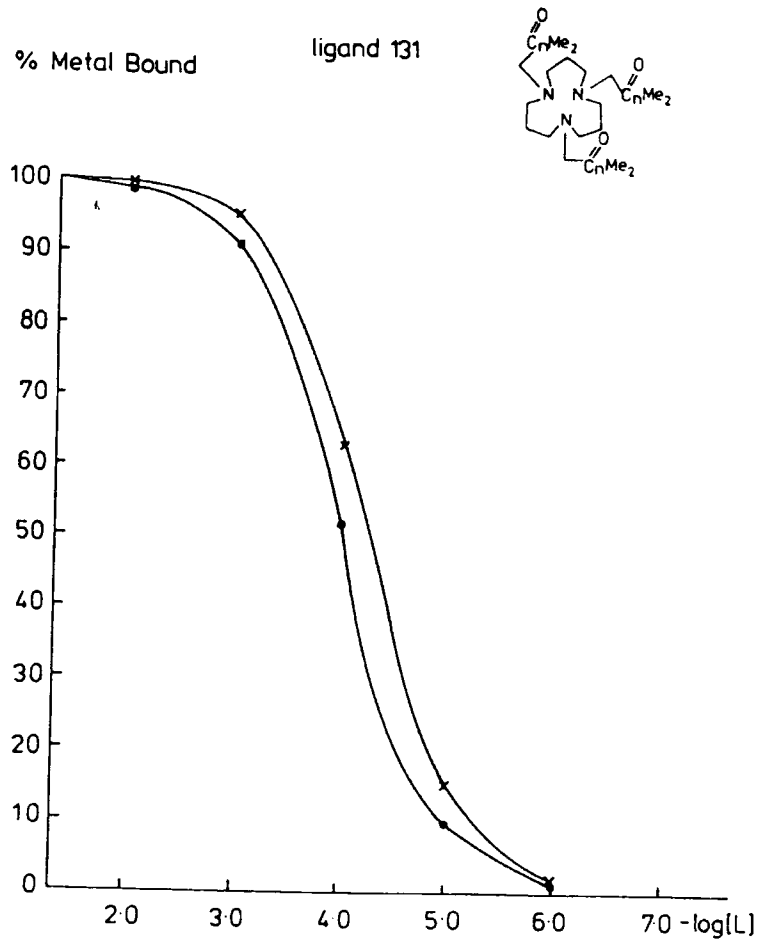

Figure 3.17 *Graph Showing Percentage of Lithium* (x) *and Sodium* (o) *Bound vs Concentration of Ligand (131).*

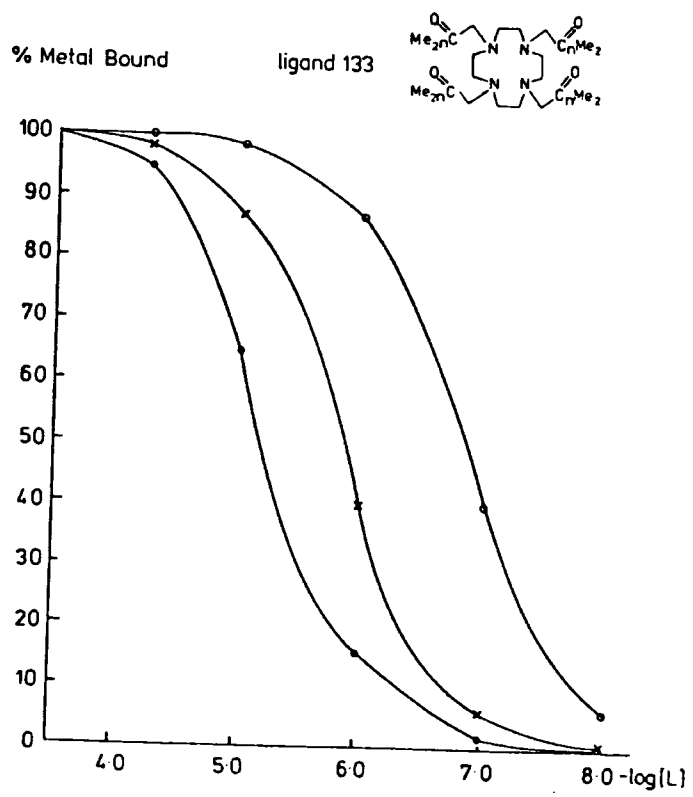

Figure 3.18 *Graph Showing Percentage of Lithium* (•), *Sodium* (x) *and Calcium* (o) *Bound vs Concentration of Ligand (133).*

3.7.2.1 Ligand (129)

As can be seen from Figure 3.16 and Table 3.11, separate potentiometric titrations for lithium and sodium indicated a preference of ligand (129) for sodium. This is at variance with FAB mass spectral data which suggested that ligand (129) is lithium selective. In comparing results obtained using these techniques it must be stressed that there are several differences.

(1) In the FAB mass spectral experiments alkali metal cations were competing for a deficiency of ligand (129) and competitive selectivity was being measured. In the pH-metric titration experiments a comparison is made of separately measured stability constants where in each case the ratio of ligand to metal cation is 1:1; in this case the measured values do not represent a true competitive selectivity.

(2) FAB mass spectral experiments were performed in a mixed solvent system of 1:1:1 water:glycerol:methanol, whereas pH-metric experiments were performed in MilliQ water.

(3) It is uncertain whether the FAB mass spectral data represents a competitive selectivity measurement at equilibrium since the effect of bombarding 3 μL of analytical solution with argon atoms accelerated by a potential difference of 8 eV is not fully understood. The pH-metric titration technique more accurately represents an equilibrium measurement since analytical solutions were allowed to stand for 48 hrs before being titrated, and further, during the titration, stable pH values were attained within 1-2 minutes of each titrant addition.

^{13}C NMR and IR data suggest that the lithium cation coordinates to all three amide axial donors and that formation of a 1:1 lithium complex

with ligand (129) also involves co-ordination to the amine ring donors. It is therefore likely that the relatively strong 1:1 lithium complex formed in water will involve co-ordination of the lithium cation to both amine and amide donors. The data from pH-metric studies suggests that formation of a 1:1 sodium complex by ligand (129) must also involve coordination of the sodium ion by both amine and amide donors. The selectivity of ligand (129) implies that either: (a) ligand (129) is sodium selective regardless of the solvent in which complexation takes place, or (b) ligand (129) is only sodium selective in a solvent of high dielectric constant and/or high donor number.

The measurement of stability constants in water will favour sodium strongly over lithium in terms of reaction enthalpy owing to the higher solvation energy of the lithium cation. However, the higher charge density ratio of the lithium cation will lead to a more favourable entropy of complexation than for the sodium ion. It it thus possible that if the unfavourable enthalpy outweighs the favourable entropy for the lithium cation in water, ligand (129) may merely be sodium selective in this solvent. In order to ascertain whether or not this is the case, further pH-metric studies need to be performed in solvents of lower dielectric constant. Clearly, calorimetric studies in a variety of solvents would clarify both the effect of solvent on selectivity of ligand (129) for these alkali metal cations, and lead to a more thorough understanding of the thermodynamics of the cation/ligand interaction.

3.7.2.2 Ligand (131)

As can be seen from Figure 3.17 and Table 3.11, separate pH-metric titrations for lithium and sodium indicated a preference of ligand (131) for lithium. Once again pH-metric data conflicts with FAB mass spectral

data. The FAB mass spectral data suggested that ligand (131) was indiscriminate and formed weak complexes with alkali metal cations. However, pH-metric studies point very definitely to formation of relatively strong complexes. In seeking to explain the difference, the relevance of the FAB mass spectral technique as a representation of an equilibrium situation must be questioned.

^{13}C NMR and IR studies both indicated interaction of the three amide and amine ring donors of ligand (131) in forming a 1:1 complex with the lithium cation. Further, the ^{13}C NMR data supports the formation of a relatively strong 1:1 lithium complex as measured by pH-metric titration.

Interestingly, ligand (131) is lithium selective whereas ligand (129) is sodium selective. The measured difference in selectivity must reflect a difference in the free energy of complexation of lithium and sodium ions by these ligands in the absence of solvent effects since results are obtained in and identical solvent system. The reversal in selectivity suggests two things:

(1) The six-membered chelate rings formed by coordination of amine ring donors to lithium and sodium cations in ligand (131) tend to favour small cations (lithium) over larger cations (sodium).

(2) The fact that both the size of ring and chelate ring has an effect on lithium vs sodium selectivity suggests that 1:1 complexation by these cations with ligands (129) and (131) involves co-ordination to amine ring donors.

Unfortunately, supplies of ligand (132) were not sufficient to measure lithium and sodium complexation constants using this technique. It would be interesting to ascertain whether the lower donor number (5) of ligand (132) might enhance the lithium selectivity exhibited by ligand (131).

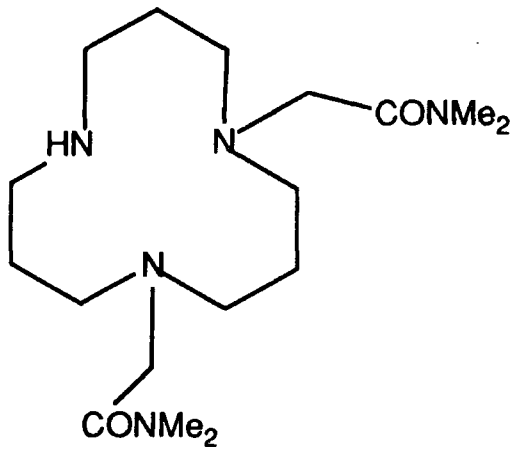

(132)

Ligand (132)

3.7.2.3 Ligand (133)

Potentiometric titration studies point to a selectivity order of $Ca^{2+} > Na^{+} > Li^{+}$ for ligand (133). The topological match of the tetra-azacyclododecane ring exhibited by this ligand for sodium and calcium ions has previously been noted[4]. It is likely that the selectivity of ligand (133) for calcium over sodium reflects the expected stronger interaction of amide axial donors with the small calcium ion which exhibits a higher charge density. The selectivity for sodium over lithium probably results from hepta- or octa-coordination of the sodium ion in solution as opposed to penta-coordination by the lithium ion and hence an enhanced enthalpy of complexation for sodium.

Comparison of the stability constants for complexation of ligand (133) with lithium and sodium ions in relation to those of ligand (143)[138], indicate that ligand (133) forms stronger complexes.

^{13}C NMR studies in methanol[4] showed fast exchange on the NMR timescale for complexation of lithium and sodium ions with ligand (143), implying that log $K_{ML} \leq 4$ in both cases. Even in water, the stability

constants for complexation of ligand (133) with lithium and sodium ions are higher.

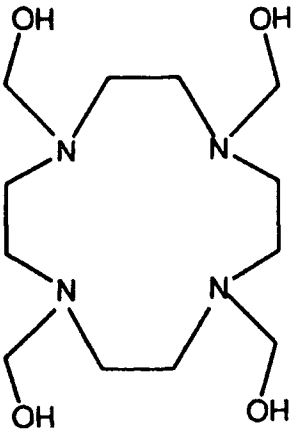

(143)

Ligand (143)

This comparison strongly suggests that amide donors are involved in complexation and that, as expected, a strong interaction with cations of high charge density ratios (Li^+, Ca^{2+}, Na^+) is taking place. Indeed, the relatively strong lithium and sodium complexes formed by ligands (129) and (131) in water serve to reiterate this point.

CHAPTER FOUR

EXPERIMENTAL SYNTHESIS

4.1 INTRODUCTION

For all compounds used in this work, temperatures are quoted in ^{o}C unless otherwise stated. Alumina refers to Merck Alumina (activity II to III) and silica refers to Fluka silica gel 60 (230-400 mesh).

Proton NMR spectra and ^{13}C spectra were recorded using a Bruker AC250 spectrometer operating at 250.134 MHz and 62.896 MHz respectively. Chemical shifts are given in ppm (relative to Me_4Si (TMS) at 0 ppm). Chemical shifts for protons showing an AB pattern have been calculated using the formula: $(1-3) = (2-4) = [(\Delta v)^2 + j^2]^{1/2}$. The peak positions 1-4 are numbered from left to right and are given in Hz from TMS. Δv is the chemical shift difference in Hz and J is the scalar coupling constant in Hz. It follows that the shift position of each proton is $\Delta v/2$ from the midpoint of the pattern.

Infrared spectra were recorded on a Perkin-Elmer 577 spectrometer either as a thin film or as a mull in Nujol as stated. Mass spectra were recorded on a VG 7070E mass spectrometer, operating in FAB, DCI, CI and EI modes as stated. Optical Rotations were measured with a Perkin-Elmer 141 Polarimeter and Combustion Analyses were performed by Mrs. M. Cox (University of Durham). Gas Chromatography was carried out with a Hewlett Packard HP 5890 using an SE 30 capillary column.

4.2 SYNTHESIS OF COMPOUNDS

(R,R)-(+)-N,N,N',N'-Tetramethyltartramide (80). A solution of (R,R)-(+)-diethyltartrate (82) (10.3g, 0.05 mmol) in dry methanol (100 ml) was stirred at -10^{o} in an ice salt slush bath under an atmosphere of nitrogen. Anhydrous dimethylamine was added dropwise to the stirred solution by condensation from a dry ice/acetone cold-finger. After the

addition was complete, the resultant solution was allowed to warm to room temperature and was stirred overnight under dry nitrogen. As the reaction proceeded, the solution darkened from a pale yellow straw colour to a deep orange, viscous mixture. The solvents were evaporated off *in vacuo* to yield crude product, which was purified by recrystallisation from a 1:1 mixture of ethanol/petroleum ether (40-60) to afford a white crystalline solid (7.15g, yield 60%). Mpt. 185-186 (lit. 187)[143]; $[\alpha]_D^{20}$ = +35° (C = 1.00, CH_2Cl_2) (lit. $[\alpha]_D$ = +42.7° (C = 3.00, C_2H_5OH); ^1H NMR ($CDCl_3$) δ: 2.90 (3H,s,CH_3N), 3.10 (3H,s,CH_3N), 4.20 (2H,s,OH), 4.66 (2H,s,CH); ^{13}C NMR ($CDCl_3$) δ: 35.9 (CH_3N), 36.9 (CH_3N), 69.5 (CHOH), 170.7 (C=O); IR ν_{max} cm^{-1} (Nujol): 3600-3100 (OH), 1632 (C=O); m/e (CI,isobutane): 205 $(M+1)^+$, 160 ($-NMe_2$), 132 ($-CONMe_2$), 72 ($CONMe_2$); % Analysis Calculated: C, 23.2; H, 3.3; N, 1.3; Found: C, 23.1; H, 3.2; N, 1.3%.

(R,R)-1,2-p-toluenesulphonyl-N,N,N',N'-Tetramethylsuccinamide (94).
(R,R)-(+)-tetramethyltartramide (80) (2g, 10 mmol) was stirred in dry dichloromethane (10 ml) with dry triethylamine (5.05g, 50 mmol) at a temperature of -10° in an ice salt/slush under an atmosphere of nitrogen. A solution of p-toluenesulphonyl chloride (4.20g, 0.022 mol) in dry dichloromethane (10 ml) was added dropwise, keeping the temperature at less than 0° throughout the addition. After the addition was complete the reaction mixture was allowed to warm to room temperature and stirred under nitrogen overnight. Distilled water (15 ml) was added, and the lower, organic layer was separated. This was washed with 6 M HCl (2 x 5 ml), distilled water (2 x 10 ml), dried over anhydrous $MgSO_4$ and concentrated *in vacuo* to yield crude product. The product was purified by recrystallisation from methanol to afford a white crystalline solid (1.8g, 35%). Mpt. 152-153; ^1H NMR ($CDCl_3$) δ:

2.35 (6H,s,CH_3 aromatic), 2.72 (6H,s,CH_3N), 3.00 (6H,s,CH_3N), 5.53 (2H,s,CHOTs), 7.23 (2H,d,J=8Hz,half of AA'XX' system,CH aromatic), 7.73 (2H,d,J=8Hz,half of AA'XX' system,CH aromatic); ^{13}C NMR ($CDCl_3$) δ: 21.5 (CH_3 aromatic), 35.8 (CH_3N), 37.5 (CH_3N), 73.5 (CHOTs), 127.8, 129.5, 132.7, 145.1 (CH aromatic), 164.1 (C=O); % Analysis Calculated: C, 51.6; H, 5.5; N, 5.4; Found: C, 51.9; H, 5.6; N, 5.3.

1-Benzyloxymethyl-2,2-dimethyl-propan-3-ol (100). A mixture of benzyl chloride (5.3g, 42.2 mmol), excess 2,2-dimethyl-propan-1,3-diol (10g, 96 mmol), sodium hydroxide (1.69g, 42.2 mmol) and a phase transfer catalyst, tetrapropylammonium bromide (50 mg) were refluxed in dry THF under an atmosphere of nitrogen for 24h. The mixture was allowed to cool and the THF was removed under reduced pressure. The residue was taken up in dichloromethane (30 ml) and any solid was filtered off. The filtrate was washed with distilled water (2 x 10 ml), brine (2 x 10 ml), dried over $MgSO_4$ and concentrated *in vacuo* to yield crude product. The product was purified by column chromatography using silica with dichloromethane as the eluent (R_f product = 0.5), to yield a clear oil (7.5g, yield 92%). ^1H NMR ($CDCl_3$) δ: 0.78 (6H,s,CH_3C), 3.13 (2H,s,CH_2O), 3.28 (2H,s,CH_2OH), 4.33 (2H,s,$PhCH_2$), 7.17 (5H,s,Ph); ^{13}C NMR ($CDCl_3$) δ: 21.2 (CH_3C), 35.8 (C), 69.4 (CH_2OH), 77.8 (CH_2Ph), 126.7, 127.7, 137.8 (CH,aromatic); IR ν_{max} cm^{-1} (Thin Film): 3600-3100 (OH), 3050, 3075 (CH, aromatic), 1595 (ring vibration), 1127 (CH_3), 1095 (C-O-C).

1-Benzyloxymethyl-2,2-dimethyl-3-p-toluenesulphonyl-propane (101). A solution 1-benzyloxy-2,2-dimethylpropan-3-ol (100) (2.5g, 12.8 mmol) in dry pyridine was stirred at -10^0 in an ice/salt slush bath under an atmosphere of nitrogen. p-Toluenesulphonyl chloride (2.9g, 15 mmol) was added in small portions whilst maintaining the temperature at -10^0. The

reaction vessel was sealed under nitrogen and left to stand at -20° for 48h. The mixture was then poured into iced water and the crude product was filtered off. This was dissolved in dichloromethane (20 ml), washed with 1 M HCl (4 x 10 ml), dried over $MgSO_4$ and concentrated *in vacuo* to yield crude product uncontaminated with pyridine. The product was purified by recrystallisation from hot methanol as it cooled to room temperature to afford a white crystalline solid (3.5g, yield 79%). ^1H NMR ($CDCl_3$) δ: 0.82 (6H,s,CH_3C), 2.28 (3H,s,CH_3 aromatic), 3.08 (2H,s, CH_2O), 3.78 (2H,s,CH_2OTs), 4.30 (2H,s,$OC\underline{H}_2Ph$), 7.17 (5H,s,CHPh), 7.20 (2H,d,J=8Hz,half of AA'XX' system,CH aromatic), 7.66 (2H,d,J=8Hz,half of AA'XX' system,CH aromatic).

1-Benzyloxymethyl-2,2-dimethyl-3-iodopropane (102). 1-Benzyloxymethyl-2,2-dimethyl-3-p-toluenesulphonyl-propane (101) (5.0g, 14.3 mmol) and sodium iodide (2.6g, 17.2 mmol) were stirred in dry dimethylformamide at 90° under nitrogen for 48h. The solution was allowed to cool and the solvent was removed under reduced pressure. The residue was taken up into dichloromethane (30 ml) and washed with sodium thiosulphate (2 x 10 ml, 5% solution), distilled water (2 x 10 ml) and dried over $MgSO_4$ and concentrated *in vacuo* to afford crude product. The product was purified by vacuum distillation to give a clear oil (2.15g, yield 49%). ^1H NMR ($CDCl_3$) δ: 0.95 (6H,s,CH_3C), 3.14 (4H,broad,s,CH_2I,CH_2O), 7.17 (5H,s, CH_2Ph); ^{13}C NMR ($CDCl_3$) δ: 23.6 (CH_3C), 20.1 (CH_2I), 34.3 (C), 72.3 (CH_2O), 76.3 ($Ph\underline{C}H_2O$), 126.5, 127.4, 137.6 (CH aromatic); m/e (Intensity %) (CI,isobutane): 305(100,M^++1), 177(35,M^+-I).

3,6-Dioxa-1,8-di-p-toluenesulphonyloctane (86). Triethylene glycol (85) (15g, 0.2 mol) was stirred in dry pyridine (30 ml) at -10° in an ice-salt slush bath under nitrogen. p-Toluenesulphonyl chloride (38.1g, 0.2

mol) was added in small portions whilst keeping the temperature of the reaction mixture at -10°. When the addition was complete the reaction vessel was sealed under nitrogen and left to stand at -20 °C for 48 hr. The reaction mixture was poured into iced water (100 ml) and the crude product was filtered as an off-white solid. Pure product was obtained by recrystallisation from a 1:1 mixture of methanol/petroleum ether (40-60) affording a white crystalline solid (42.1g, yield 86%). Mpt. 77-78° (lit.[144] 78°); % Analysis Calculated: C, 52.2; H, 6.1; Found: C, 52.1; H, 6.1.

Ethane-1,2-di-p-toluenesulphonate (89). Ethane-1,2-diol (91) (6.2g, 0.1 mol) was stirred in dry pyridine at -10° under nitrogen. p-toluene-sulphonyl chloride (38.1g, 0.2 mol) was added in small portions whilst maintaining the temperature at -10°. When the addition was complete, the reaction vessel was sealed under nitrogen and left to stand at -20° for 48 hr. The reaction mixture was then poured into iced water (100 ml) and the crude product was filtered off as a white solid. The crude product was dissolved in dichloromethane (30 ml) and washed with 1 M HCl (3 x 20 ml) to remove traces of pyridine. The dichloromethane was removed under reduced pressure and the product was purified by recrystallisation from methanol at room temperature to afford a white crystalline solid (31.2g, yield 84%). Mpt. 118-119°; ^{1}H NMR ($CDCl_3$) δ: 2.30 (6H,s,CH_3), 4.10 (4H,s,CH_2OTs), 7.30 (2H,d,J=8Hz,half of an AA'XX' system,CH aromatic), 7.74 (2H,d,J=8Hz,half of an AA'XX' system, CH aromatic); ^{13}C NMR ($CDCl_3$) δ: 21.6 (CH_3), 66.7 (CH_2OTs); 127.7, 129.9, 132.3, 145.2 (CH aromatic).

1,8-Dicyano-3,6-dioxaoctane (87) - Procedure A. 3,6-Dioxa-1,8-di-p-toluenesulphonyloctane (86) (5g, 0.011 mol) was stirred with dry

potassium cyanide (1.43g, 0.022 mol) in dry dimethylsulphoxide (20 ml) at room temperature, under an atmosphere of nitrogen, for five days. During the course of the reaction, the solution changed from colourless to a clear brown. The solution was then poured into distilled water (50 ml) and extracted with dichloromethane (4 x 20 ml). The organic layer was washed with distilled water (2 x 10 ml), dried over $MgSO_4$ and concentrated *in vacuo* to yield crude product. The product was purified by vacuum distillation (90^o, 0.1 mm Hg) to afford a clear oil (0.65g, yield 35%).

1,8-Dicyano-3,6-dioxaoctane (87) - Procedure B. To a stirred solution of 2% aqueous sodium hydroxide (40 ml) and ethane-1,2-diol (91) (24.8g, 0.2 mol) at 0^o was added acrylonitrile (90) (43g, 0.4 mol) dropwise whilst maintaining the temperature at 0^o. When the addition was complete, the reaction mixture was warmed to room temperature and stirred for 24 hr. The mixture was then allowed to stand for 10 minutes during which time two layers separated. The lower, aqueous layer was discarded. The upper, organic layer was dried over $MgSO_4$ and concentrated *in vacuo* to yield crude product. The product was purified by vacuum distillation ($90-95^o$, 0.1 mm Hg) to afford a clear oil (28.6g, yield 85%). ^1H NMR ($CDCl_3$) δ: 2.58 (4H,t,J=6Hz,CH_2CN), 3.58 (4H,t, J=6Hz,CH_2O), 3.53 (4H,s,CH_2O); ^{13}C NMR ($CDCl_3$) δ: 17.9 (CH_2CN), 64.9 (CH_2O), 69.5 (CH_2O), 117.7 (C≡N); IR ν_{max} cm^{-1} (Thin Film): 2225 (C≡N), 840, 1105 (C-O-C); m/e (Intensity%) (CI,isobutane): 169(15,M^++1), 98 (M^+-CH_2CH_2CN).

Diethyl-4,7-dioxadecan-1,10-dioate (92). Concentrated sulphuric acid (20g) was added with care to a solution of ethanol (100 ml) at 0^o. 1,8-Dicyano-3,6-dioxaoctane (87) (50.2g, 0.3 mol) was added and the mixture

was stirred under reflux for 24 hr. The mixture was allowed to cool and evaporated to dryness *in vacuo*. Distilled water (100 ml) was added to the residue and the mixture was extracted with dichloromethane (3 x 20 ml) and diethyl ether (3 x 20 ml). The pooled organic extracts were washed with brine (2 x 20 ml), dried over $MgSO_4$ and concentrated *in vacuo* to yield crude product. The product was purified by vacuum distillation (40^0, 0.1 mm Hg) to give a clear oil (65.5g, yield 84%). ^1H NMR ($CDCl_3$) δ: 1.25 (6H,t,J=7Hz,CH_3), 2.60 (4H,t,J=6.3Hz,CH_2CO), 3.75 (4H,t,J=6.4Hz,CH_2O), 3.61(4H,s,CH_2O), 4.15 (4H,q,J=7Hz,$C\underline{H}_2CH_3$); ^{13}C NMR ($CDCl_3$) δ: 13.9 (CH_3), 34.8 (CH_2CO), 60.2 (CH_3CH_2), 66.3 (CH_2O), 68.7 (CH_2O), 171.3 (C=O); IR ν_{max} cm^{-1} (Thin Film): 1110, 840 (C-O-C), 1735 (C=O); m/e (CI,isobutane): $(M+1)^+$ Found: 263.147740, $C_{12}H_{22}O_6$ requires 263.149463.

1,10-Dihydroxy-4,7-dioxadecane (84) - Procedure A. Sodium metal (1.104g, 0.048 mol, 2 equivalents) was stirred in excess propan-1,3-diol (89) (20 equivalents, 36.5g) at room temperature under nitrogen until all of the sodium had dissolved. The temperature was raised to 50^0 and ethane-1,2-di-p-toluenesulphonate (1 equivalent, 8.7g, 0.024 mol) was added. The reaction mixture was stirred at 50^0 under nitrogen for 24 hr. during which time the colourless solution turned pale brown. The mixture was allowed to cool and was filtered. The filtrate was concentrated *in vacuo* and dichloromethane (50 ml) was added to the residue, any undissolved solid was filtered off. The dichloromethane filtrate was dried over $MgSO_4$ and concentrated *in vacuo* to yield crude product mixed with excess propan-1,3-diol. The majority of the excess propan-1,3-diol was removed by vacuum distillation and the product was purified by column chromatography using silica, with dichloromethane as elutant, followed by a 2% methanol/dichloromethane solution (R_f product

in CH_2Cl_2/2% MeOH = 0.45). This yielded a colourless viscous oil (0.35g, yield 9%).

1,10-Dihydroxy-4,7-dioxadecane (84) - Procedure B. A suspension of lithium aluminium hydride (4 equivalents, 20g) was stirred at 0^0 under nitrogen in dry diethyl ether (50 ml). Diethyl-4,7-dioxa-1,10-dioate (38.8g, 0.148 mol, 1 equivalent) in dry diethyl ether (50 ml) was added at such a rate as to gently reflux the system. Once the addition was complete, the mixture was warmed to room temperature and stirred under nitrogen for 2 hr. The reaction was cooled to 0^0 and distilled water (20 ml) was added (CARE - any excess lithium aluminium hydride reacts highly exothermically with water). This was followed by the careful addition of 15% aqueous sodium hydroxide solution (40 ml) and distilled water (20 ml). Throughout the additions the mixture was stirred in ice and the ether level was topped up so as to ensure that the mixture was continuously stirred. The white precipitate was then filtered and washed with diethyl ether (6 x 100 ml). The solvents were evaporated off under reduced pressure to leave an oily residue. The residue was stirred in dichloromethane (100 ml) for 2 hr. and after this time any undissolved material was filtered off. The filtrate was dried over $MgSO_4$ and concentrated *in vacuo* to yield crude product. The product was purified by vacuum distillation (90^0, 0.05 mm Hg) as a clear oil (13.9g, yield 51%). ^1H NMR ($CDCl_3$) δ: 1.70 (4H,q,J=6Hz,CH_2OH), 3.52 (4H,t, J=6Hz,CH_2O), 3.49 (4H,s,CH_2O), 3.60 (4H,t,J=6Hz,CH_2OH); ^{13}C NMR ($CDCl_3$) δ: 31.8 ($CH_2CH_2CH_2$), 59.1 (CH_2OH), 68.3 (CH_2O), 69.5 (CH_2O); IR ν_{max} cm^{-1} (Thin Film): 3550-3100 (OH), 1105, 845 (C-O-C); m/e (CI,isobutane): $(M+1)^+$ Found: 179.117410, required for $C_8H_{18}O_4$: 179.120509.

1,10-Dichloro-4,7-dioxadecane (83). A stirred solution of 1,10-dihydroxy-4,7-dioxadecane (84) (9.2g, 52 mmol), dry pyridine (0.12 mol) in dry benzene (50 ml) was heated to reflux under an atmosphere of nitrogen. Thionyl chloride (14.3g, 0.12 mol) was added dropwise. When the addition was complete, the mixture was stirred under reflux under nitrogen for 24 hr. The mixture was allowed to cool and 3 M HCl (5 ml) was added dropwise to the stirred solution. The reaction mixture was allowed to stand and two layers separated. The lower, aqueous layer was discarded. The organic layer was washed with distilled water (2 x 20 ml), dried over $MgSO_4$ and concentrated *in vacuo* to yield crude product. The product was purified by vacuum distillation (89-93^{o}, 0.4 mm Hg) to yield a pale yellow liquid (6.9g, yield 62%). ^{1}H NMR ($CDCl_3$) δ: 1.94 (4H,txt,J=6.1Hz,$CH_2CH_2CH_2$), 3.55 (12H,m,CH_2O,CH_2Cl); ^{13}C NMR ($CDCl_3$) δ: 32.4 ($CH_2CH_2CH_2$), 41.6 (CH_2Cl), 67.3 (CH_2O), 69.9 (CH_2O); IR ν_{max} cm^{-1} (Thin Film): 1120 (C-O-C), 655 (C-Cl); m/e (CI, isobutane): M^{+} Found: 214.053765, required for $C_8H_{16}O_2Cl_2$: 214.052735.

1,10-Diiodo-4,7-dioxadecane (81). Sodium iodide (1.5g, 0.01 mol) was added to a solution of 1,10-dichloro-4,7-dioxadecane (83) (0.86g, 4 mmol) in analar acetone containing a catalytic amount of tetrapropylammonium bromide (15 mg). The mixture was stirred and refluxed for 72 hr. The reaction was cooled to room temperature, the solid removed by filtration and filtrate concentrated *in vacuo* to yield a light brown waxy residue. The residue was dissolved in ethyl acetate (15 ml), washed with aqueous 5% sodium thiosulphate solution (2 x 20 ml), distilled water (10 ml) and brine (10 ml). The ethyl acetate solution was dried over $MgSO_4$ and concentrated *in vacuo* to yield crude product. The product was purified by column chromatography using silica with dichloromethane as elutant to yield a pure product as a light yellow oil

[$R_f(CH_2Cl_2)$ = 0.75] (1.25g, yield 78%). ^{1}H NMR ($CDCl_3$) δ: 2.00 (4H,txt, J=6.1Hz,$CH_2CH_2CH_2$), 3.27 (4H,t,J=6.9Hz,CH_2I), 3.50 (4H,t,J=6.3Hz,CH_2O), 3.56 (4H,s,CH_2O); ^{13}C NMR ($CDCl_3$) δ: 3.8 (CH_2I), 33.4 ($CH_2CH_2CH_2$), 70.3 (CH_2O), 70.4 (CH_2O); m/e (Intensity%) (CI,isobutane): 399(70,M^++1).

(2R,3R)-N,N,N',N',-Tetramethyl-1,4,8,11-tetraoxa-cyclotetradecane-2,3-dicarboxamide (78). Lithium metal (0.2g, 28.6 mmol) was added to dry t-butanol (150 ml) which was being stirred and refluxed under nitrogen. When all of the lithium had dissolved, (R,R)-(+)-N,N,N',N'-tetramethyl-tartramide (80) (2.9g, 9.3 mmol) was added. To the homogeneous mixture were added, 1,10-dichloro-4,7-dioxadecane (83) (2g, 9.3 mmol) and lithium bromide (0.8g, 9.3 mmol) in distilled water (2 ml). This mixture was refluxed under nitrogen for two weeks. The reaction was allowed to cool to room temperature and was concentrated to a volume of 25 ml under reduced pressure. Distilled water (100 ml) was added, and the resultant mixture was extracted with dichloromethane (5 x 30 ml). The combined extracts were washed with distilled water (2 x 20 ml), dried over $MgSO_4$ and concentrated *in vacuo* to yield crude product. The product was purified by column chromatography using alumina with ethyl acetate as elutant [R_f(EtOAc) = 0.5] to yield a white crystalline product (60mg, yield 1.8%). ^{1}H NMR ($CDCl_3$) δ: 1.77 (4H,txt,J=5Hz,$CH_2CH_2CH_2$), 2.87 (6H,s,CH_3N), 3.10 (6H,s,CH_3N), 3.40 (12H,m,CH_2O), 4.87 (2H,s,CH); ^{13}C NMR ($CDCl_3$) δ: 30.7 ($CH_2CH_2CH_2$), 36.0 (CH_3N), 37.8 (CH_3N), 66.1, 66.8, 70.6 (CH_2O), 78.2 (CHO), 170.5 (C=O); IR ν_{max} cm^{-1} (Nujol): 1645 (C=O), 1110 (C-O-C); m/e (Intensity%) (FAB,glycerol): 347(100,M^++1), 274 (-$CONMe_2$), 72 ($CONMe_2$).

3-Benzyloxymethyl-propan-1,2-diol (104). 3-Benzyloxymethyl-propan-1,2-diol (104) was synthesised from commercially available 2,2-dimethyl-4-hydroxymethyl-1,3-dioxalane (110) according to the procedure by Howe and Malkin[134].

Trans-(4R,5R)-(-)-4,5-bis(ethoxycarbonyl)-2,2-dimethyl-1,3-dioxalane (112). (R,R)-(+)-Diethyl tartrate (82) (10.2g, 50 mmol), 2,2-dimethyoxy-propane (6.25g, 60 mmol) and p-toluenesulphonic acid (100 mg) were refluxed in dry toluene (100 ml) under nitrogen for 3 hr. The reaction mixture was allowed to cool and the solution was neutralised with potassium carbonate. Excess 2,2-dimethoxypropane and toluene were removed under reduced pressure. The residue was dissolved in dichloromethane (100 ml), washed with distilled water (2 x 30 ml), dried over $MgSO_4$ and concentrated *in vacuo* to yield crude product. Vacuum distillation (89-94^o, 0.1 mm Hg) (lit. 80-85^o, 0.1 mm Hg)[145] yielded desired product as a clear oil contaminated with 5% *trans*-esterification ethylmethylester product impurity (10.5g, yield 85%). $[\alpha]_D^{20}$ = -40.7^o (C = 1.00, CH_2Cl_2); ^{1}H NMR ($CDCl_3$) δ: 1.24 (6H,t,J=7.1Hz,CH_3CH_2), 1.42 (6H,s,CH_3C), 4.20 (4H,q,J=7.1Hz,CH_3CH_2), 4.72 (2H,s,CH); ^{13}C NMR ($CDCl_3$) δ: 13.9 (CH_3CH_2), 26.2 (CH_3C), 61.8 (CH_3CH_2), 76.9 (CH), 113.7 (C), 169.6 (C=O); IR ν_{max} cm^{-1} (Thin Film): 1745 (C=O), 1100 (C-O-C), 1374 (CH_3); m/e (CI,isobutane): $(M+1)^+$ Found: 247.118163, $C_{11}H_{18}O_6$ requires 247.119380. The mixture of desired product (112) and trans-esterification impurity was used in the next step without further purification.

Trans-(4S,5S)-(+)-4,5-bis(hydroxymethyl)-2,2-dimethyl-1,3-dioxalane (113). Trans-(4R,5R)-(-)-4,5-bis(ethoxycarbonyl)-2,2-dimethyl-1,3-dioxalane (112) (12.1g, 50 mmol) in anhydrous ethanol (50 ml) was added dropwise to a vigorously stirred mixture of sodium borohydride (5.7g,

0.15 mol) in anhydrous ethanol (200 ml) at room temperature under nitrogen. The rate of addition was so as to maintain a gentle reflux in the system. When the addition was complete, the mixture was refluxed under nitrogen for 3 hr. The reaction was allowed to cool and the ethanol was removed under reduced pressure. The residue was taken up into dichloromethane (50 ml) and any dissolved solid was filtered off. The filtrate was dried over $MgSO_4$ and concentrated *in vacuo* to yield crude product. The product was purified by vacuum distillation (140^o, 0.1 mm Hg) to yield a clear viscous oil (6.5g, yield 80%). ^1H NMR ($CDCl_3$) δ: 1.34 (6H,s,CH_3C), 3.65 (4H,s,CH_2OH), 3.87 (2H,s,CH); ^{13}C NMR ($CDCl_3$) δ: 26.5 (CH_3C), 61.9 (CH_3OH), 78.2 (CH), 108.9 (C); IR ν_{max} cm^{-1} (Thin Film): 3600-3100 (OH), 1373 (CH_3), 1070 (C-O-C); m/e (CI, isobutane): $(M+1)^+$ Found: 163.095057, $C_7H_{14}O_4$ requires 163.097034.

(4S,5S)-(-)-4,5-bis(benzyloxymethyl)-2,2-dimethyl-1,3-dioxalane (114). (4S,5S)-(+)-4,5-bis(hydroxymethyl)-2,2-dimethyl-1,3-dioxalane (113) (5g, 31 mmol), sodium hydroxide (2.95g, 74 mmol), benzyl chloride (9.0g, 74 mmol) and tetrapropylammonium bromide (100 mg) were refluxed in anhydrous tetrahydrofuran (200 ml) under nitrogen for 24 hr. The mixture was allowed to cool and was filtered. The filtrate was concentrated *in vacuo* and the residue was taken up into dichloromethane (50 ml). The dichloromethane layer was washed with distilled water (2 x 20 ml), dried over $MgSO_4$ and concentrated *in vacuo* to yield crude product. The product was purified by vacuum distillation (115^o, 0.1 mm Hg) (lit. 173-175^o, 0.2 mm Hg)[146] to yield a clear oil (7.1g, yield 60%). $[\alpha]_D^{20} = -8.5^o$ (C = 1.00, CH_2Cl_2) (lit. $[\alpha]_D^{20} = -7.5^o$, C = 2.6, $CHCl_3$)[146]; G.C. Analysis indicated that the product was $\geq$ 99.7% chemically homogeneous. ^1H NMR ($CDCl_3$) δ: 1.44 (6H,s,CH_3C), 3.61 (4H,d,J=3Hz,CH_2O), 4.00 (2H,m,J=3Hz,CH), 4.57 (4H,s,CH_2Ph), 7.32 (10H,s,

CH aromatic); ^{13}C NMR ($CDCl_3$) δ: 26.9 ($\underline{C}H_3C$), 70.5 (CH_2O), 73.4 ($PhCH_2O$), 77.4 (CH), 109.5 ($CH_3\underline{C}$), 127.8, 128.3, 137.9 (CH aromatic); IR ν_{max} cm^{-1} (Thin Film): 1600 (ring vibration), 1372 (CH_3), 1081 (C-O-C).

(2S,3S)-(-)-1,4-bis(benzyloxybutan)-2,3-diol (111). Trans-(4S,5S)-4,5-bis(benzyloxymethyl)-2,2-dimethyl-1,3-dioxalane (114) (15g, 44 mmol), was refluxed and stirred in a solution of analar acetone (35 ml) and 1 M HCl (100 ml) for 24 hr. The mixture was then allowed to cool and solvents were removed under reduced pressure. The residue was dissolved in dichloromethane (40 ml) which was dried over $MgSO_4$ and concentrated *in vacuo* to yield crude product. The product was purified by column chromatography using silica with ethyl acetate as elutant (R_f product = 0.75) to yield a white waxy solid (12g, yield 90%). Mpt. 50-52°. $[\alpha]_D^{20}$ = -7.5° (C = 1.00, CH_2Cl_2) (lit. $[\alpha]_D^{25}$ = -5.0°, C = 5.0, $CHCl_3$)[146]; G.C. Analysis indicated that the diol was ≥ 99.7% chemically homogeneous. ^1H NMR ($CDCl_3$) δ: 3.60 (4H,d,J=3.4Hz,CH_2O), 3.87 (2H,m,CH), 4.54 (4H,s, $PhC\underline{H}_2O$), 7.3 (10H,s,CH aromatic); ^{13}C NMR ($CDCl_3$) δ: 70.4 (CH_2O), 73.4 ($Ph\underline{C}H_2O$), 71.7 (CH), 127.6, 128.3, 137.6 (CH aromatic); % Analysis Calculated: C, 71.5; H, 7.3; Found: C, 71.2; H, 7.4.

2-Benzyloxymethyl-1,4,8,11-tetraoxacyclotetradecane (108). Lithium metal (0.39g, 55.8 mmol) was added to dry t-butanol (200 ml) which was stirring under reflux under an atmosphere of nitrogen. Once all of the lithium had dissolved, 3-benzoyloxymethylpropan-1,2-diol (104) (3.39g, 18.6 mmol) was added. To the cloudy heterogeneous mixture 1,10-dichloro-4,7-dioxadecane (83) (4g, 18.6 mmol) and lithium bromide (1.62g, 18.6 mmol) were added. The resulting mixture was stirred and refluxed under nitrogen for two weeks. The reaction was allowed to cool and the t-butanol was removed under reduced pressure. The residue was

taken up in distilled water (50 ml) and neutralised using 6 M HCl. The aqueous layer was extracted with dichloromethane (5 x 40 ml) which was washed with distilled water (2 x 20 ml), dried over $MgSO_4$ and concentrated *in vacuo* to give crude product. The product was purified by column chromatography using alumina with a 5:1 hexane/ethyl acetate mixture as elutant (R_f product = 0.5) to yield a colourless oil (2.5g, yield 42%). ^1H NMR ($CDCl_3$) δ: 1.73 (4H,txt,J=5Hz,$CH_2\underline{CH_2}CH_2$), 3.65 (17H,m,CH_2O,CHO), 4.47 (2H,s,$C\underline{H_2}Ph$), 7.27 (5H,s,CH aromatic); ^{13}C NMR ($CDCl_3$) δ: 30.3 ($CH_2CH_2CH_2$), 30.4 ($CH_2CH_2CH_2$), 65.7, 66.6, 67.5, 68.8, 70.0, 70.9, 72.5 (CH_2O), 73.2 (CH_2Ph), 77,7 (CH), 127.5, 128.2, 138.1 (CH aromatic); IR ν_{max} cm^{-1} (Thin Film): 1600 (Aromatic ring vibration), 1112 (C-O-C); m/e (Intensity%) (CI,isobutane): 325(100,M^++1).

Trans-(2S,3S)-(-)-2,3-bis(benzyloxymethyl)-1,4,8,11-tetraoxacyclotetradecane (108). An analogous procedure to that of (108) was followed using lithium (0.9g, 129 mmol), t-butanol (500 ml), (2S,3S)-(-)- 1,4-dibenzyloxybutan-2,3-diol (111) (13g, 43 mmol), 1,10-dichloro-4,7-dioxadecane (9.25g, 43 mmol) and lithium bromide (3.75g, 43 mmol). Purification by column chromatography on alumina eluting with a 3:1 hexane/ethyl acetate mixture (R_f product = 0.5) yielded a clear viscous oil (9.8g, yield 51%). $[\alpha]_D^{20}$ = -10.5° (C = 1.00, CH_2Cl_2); ^1H NMR ($CDCl_3$) δ: 1.77 (4H,txt,J=5Hz,$CH_2CH_2CH_2$), 3.65 (18H,m,CH_2O,CHO), 4.44 (4H,s,$C\underline{H_2}Ph$), 7.26 (10H,s,CH aromatic); ^{13}C NMR ($CDCl_3$) δ: 30.5 ($CH_2CH_2CH_2$), 66.0, 66.3, 68.9, 69.9 (CH_2O), 72.4 (CH_2Ph), 79.7 (CHO), 127.0, 127.7, 137.7 (CH aromatic); IR ν_{max} cm^{-1} (Thin Film): 1600 (Aromatic ring vibration), 1113 (C-O-C); m/e (Intensity%) (CI, isobutane): 445(100,M^++1), 355(50,M^+-$PhCH_2$), 337(80,M^+-$PhCH_2O$), 245(70, M^+-$PhCH_2$-$PhCH_2O$).

2-Hydroxymethyl-1,4,8,11-tetraoxacyclotetradecane (115). 2-Benzyloxymethyl-1,4,8,11-tetraoxacyclotetradecane (5g, 15.4 mmol), Pearlmans catalyst, $Pd(OH)_2$ (30% v/v H_2O) (500 mg) and a catalytic amount of p-toluenesulphonic acid in ethanol (50 ml), were shaken under a hydrogen pressure of three atmospheres for 24 hr. at room temperature. The catalyst was removed by filtration and the filtrate was evaporated *in vacuo* to give crude product. The product was purified by column chromatography using ethyl acetate as the elutant (R_f product = 0.3). This yielded a clear viscous oil (3.3g, yield 92%). ^1H NMR ($CDCl_3$) δ: 1.50-1.90 (4H,m,$CH_2CH_2CH_2$), 2.85 (1H,s,OH), 3.20-3.90 (17H,m,CH_2O, CH_2OH,CHO); ^{13}C NMR ($CDCl_3$) δ: 30.3, 30.4 ($CH_2CH_2CH_2$), 62.8 (CH_2OH), 66.1, 66.8, 66.9, 67.5, 69.5, 71.3, 72.5 (CH_2O), 78.7 (CHO); IR ν_{max} cm^{-1} (Thin Film): 3600-3100 (OH), 1120, 1090 (C-O-C); m/e (CI, isobutane): $(M+1)^+$ Found: 235.159100, $C_{11}H_{22}O_5$ requires 235.154540.

Trans-(2S,3S)-(-)-2,3-bis(hydroxymethyl)-1,4,8,11-tetraoxacyclotetradecane (116). The procedure was analogous to the synthesis of (115). Purification by column chromatography using alumina with ethyl acetate as elutant (R_f product = 0.3) yielded a clear viscous oil (1.85g, yield 90%). $[\alpha]_D^{20} = -11.5^o$ (C = 1.00, CH_2Cl_2); ^1H NMR ($CDCl_3$) δ: 1.60-1-82 (4H,m,$CH_2CH_2CH_2$), 2.88 (2H,s,OH), 3.41-3.85 (18H,m,CH_2O,CH_2OH,CHO); ^{13}C NMR ($CDCl_3$) δ: 29.8 ($CH_2CH_2CH_2$), 61.5 (CH_2OH), 66.1, 67.4, 70.0, 71.4 (CH_2O), 78.5 (CHO); IR ν_{max} cm^{-1} (Thin Film): 3600-3100 (OH), 1135, 1072 (C-O-C); m/e (CI,isobutane): $(M+1)^+$ Found: 265.146890, $C_{12}H_{25}O_6$ requires 265.154890.

2-p-Toluenesulphonatomethyl-1,4,8,11-tetraoxacyclotetradecane (119). A solution of 2-hydroxymethyl-1,4,8,11-tetraoxacyclotetradecane (115((5g, 21.3 mmol) was stirred in dry pyridine (10 ml) under nitrogen at -10^o.

p-Toluenesulphonyl chloride (4.4g, 23.5 mmol) was added in small portions, keeping the temperature of the reaction mixture at -10^{o} throughout the addition. When the addition was complete, the mixture was sealed under nitrogen and left to stand at -20^{o} for 48 hr. The reaction mixture was poured onto iced water (30 ml) and acidified with cold 6 M HCl. The acidic aqueous layer was extracted with dichloromethane (5 x 30 ml) and the extracts were dried over $MgSO_4$ and concentrated *in vacuo* to yield crude product. The product was purified by column chromatography using silica with dichloromethane as elutant (R_f product = 0.7), yielding a clear viscous oil (3.7g, yield 45%). ^1H NMR ($CDCl_3$) δ: 1.45-1.75 (4H,m,$CH_2CH_2CH_2$), 2.43 (3H,s,CH_3 aromatic), 3.25-3.60 (14H,m,CH_2O), 3.71 (1H,m,CHO), 3.95 (2H,d,J=5Hz,CH_2OTs), 7.28 (2H,d,J=8Hz,part of an AA'XX' system, CH aromatic), 7.71 (2H,d,J=8Hz, part of an AA'XX' system, CH aromatic); ^{13}C NMR ($CDCl_3$) δ: 21.6 (CH_3 aromatic), 30.2 ($CH_2CH_2CH_2$), 65.8, 66.4, 66.5, 67.3, 69.3, 69.7, 70.7 (CH_2O), 76.2 (CHO), 127.2, 129.7, 132.9, 144.7 (CH aromatic); IR ν_{max} cm^{-1} (Thin Film): 1125, 1095 (C-O-C), 1360, 1192, 1176 (SO_2); m/e (Intensity%) (CI,isobutane): 389(100,M^++1), 216(30,-OTs).

(2S,3S)-(-)-2,3-bis(p-toluenesulphonatomethyl)-1,4,8,11-tetraoxacyclotetradecane (120). The procedure was analogous to the synthesis of (119) using *trans*-(2S,3S)-(-)-2,3-bis(hydroxymethyl)-1,4,8,11-tetraoxacyclotetradecane (116) (4g, 15.2 mmol), dry pyridine (15 ml) and p-toluenesulphonyl chloride (3.2g, 16.7 mmol). Purification by column chromatography using silica with dichloromethane as elutant (R_f product = 0.85) yielded a white crystalline solid (4.2g, yield 48%). Mpt. 73-75^{o}. $[\alpha]_D^{20} = -15^{o}$ (C = 1.00, CH_2Cl_2). ^1H NMR ($CDCl_3$) δ: 1.40-1.65 (4H,m,$CH_2CH_2CH_2$), 2.36 (6H,s,CH_3 aromatic), 3.20-3.77 (14H,m,CH_2O,CHO), 4.05 (4H,2xd,CH_2OTs), 7.27 (2H,d,J=7.6Hz,part of an AA'XX' system, CH

aromatic), 7.68 (2H,d,J=7.6Hz,part of an AA'XX' system, CH aromatic); ^{13}C NMR ($CDCl_3$) δ: 21.6 (CH_3 aromatic), 30.5 ($CH_2CH_2CH_2$), 66.5, 66.6, 68.6, 70.3 (CH_2O), 77.2 (CHO), 127.9, 129.8, 132.6, 144.9 (CH aromatic); IR ν_{max} cm^{-1} (Nujol): 1120, 1083 (C-O-C), 1360, 1185, 1178 (SO_2); m/e (Intensity%) (CI,isobutane): 573(100,M^++1), 229(35,-2OTs); % Analysis Calculated: C, 54.5; H, 6.3; Found: C, 54.6; H, 6.3.

2-Cyanomethyl-1,4,8,11-tetraoxacyclotetradecane (121). 2-p-Toluenesulphonatomethyl-1,4,8,11-tetraoxacyclotetradecane (119) (3.5g, 9 mmol) was added to a suspension of potassium cyanide (0.98g, 15 mmol) in dry dimethylsulphoxide (50 ml) which was stirring at 90^o under nitrogen. The resultant mixture stirred at this temperature under nitrogen for 3 hr. The reaction was was allowed to cool and distilled water (40 ml) was added. This was extracted with dichloromethane (5 x 20 ml) and the combined extracts were washed with distilled water (2 x 15 ml), dried over $MgSO_4$ and concentrated *in vacuo* to yield crude product. The product was purified by column chromatography using alumina with a 1:4 ethyl acetate/hexane mixture as elutant (R_f product = 0.6), yielding a clear viscous oil (1.35g, yield 62%). ^1H NMR ($CDCl_3$) δ: 1.76 (4H,m, J=5Hz,$CH_2CH_2CH_2$), 2.52 (2H,d,J=7Hz,CH_2N), 3.30-4.05 (15H,m,CH_2O,CHO); ^{13}C NMR ($CDCl_3$) δ: 20.8 (CH_2CN), 30.1 ($CH_2CH_2CH_2$), 66.2, 66.4, 67.5, 69.5, 70.2, 70.8, 71.9 (CH_2O), 75.7 (CHO), 117.7 (C≡N); IR ν_{max} cm^{-1} (Thin Film): 2250 (C≡N), 1123 (C-O-C); m/e (Intensity%) (CI,isobutane): 244(100,M^++1); $(M+1)^+$ Found: 244.140720, $C_{12}H_{21}NO_4$ requires 244.154880.

Trans-(2S,3S)-(-)-2,3-bis(cyanomethyl)-1,4,8,11-tetraoxacyclotetradecane (122). The procedure was analogous to that of (121), using *trans*-(2S,3S)-(-)-2,3-bis(toluenesulphonatomethyl)-1,4,8,11-tetraoxacyclotetradecane (120) (5.15g, 9 mmol), potassium cyanide (0.95g, 14 mmol)

and dry dimethylsulphoxide (50 ml). The product was purified by column chromatography using alumina with a 1:5 ethyl acetate/hexane mixture as elutant (R_f product = 0.65) to yield a white crystalline solid (1.2g, yield 48%). MPt. 77-78°; $[\alpha]_D^{20}$ = -6.5° (C = 1.00, CH_2Cl_2); ^1H NMR ($CDCl_3$) δ: 1.75 (4H,txt,J=5.5Hz,$CH_2CH_2CH_2$), 2.55 (4H,m,CH_2N), 3.40-3.85 (14H,m,CH_2O,CHO); ^{13}C NMR ($CDCl_3$) δ: 18.7 (CH_2CN), 30.1 ($CH_2CH_2CH_2$), 66.9, 67.3, 69.5 (CH_2O), 75.7 (CHO), 117.1 (C≡N); IR ν_{max} cm^{-1} (Nujol): 2250 (C≡N), 1023 (C-O-C); m/e (Intensity%) (FAB,glycerol): 283(30,M^++1); % Analysis Calculated: C, 59.6; H, 7.9; N, 9.9; Found: C, 59.3; H, 7.9; N, 9.8.

2-Methoxycarbonylmethyl-1,4,8,11-tetraoxacyclotetradecane (123). 2-(Cyanomethyl)-1,4,8,11-tetraoxacyclotetradecane (500mg, 2.05 mmol) was stirred in dry methanol (30 ml) under nitrogen. The methanol was then saturated with gaseous HCl and the resulting mixture stirred and refluxed under nitrogen for 5 hrs. The reaction was allowed to cool and the methanol was evaporated off under reduced pressure. The residue was taken up into distilled water (15 ml) which was extracted with dichloromethane (3 x 20 ml). The resulting organic layer was washed with 10% aqueous potassium carbonate solution (2 x 15 ml), dried over $MgSO_4$ and concentrated *in vacuo* to yield crude product. The product was purified by column chromatography using alumina with a 1:5 mixture of ethyl acetate/hexane as the elutant (R_f product = 0.8) to yield a clear viscous oil (360mg, yield 63%). ^1H NMR ($CDCl_3$) δ: 1.68 (4H,m,J=5.7Hz, $CH_2CH_2CH_2$), 2.36 (2H,m,$C\underline{H}_2CO$), 3.50-3.95 (18H,m,CH_3O,CH_2O,CHO); ^{13}C NMR ($CDCl_3$) δ: 30.6, 30.8 ($CH_2CH_2CH_2$), 37.1 (CH_2CO), 51.7 (CH_3O), 65.8, 66.7, 67.0, 67.2, 70.0, 71.3, 74.1 (CH_2O), 76.5 (CH), 171.7 (C=O); IR ν_{max} cm^{-1} (Thin Film): 1742 (C=O), 1120 (C-O-C); m/e (Intensity%)

(CI,isobutane): 277(100,M^++1); $(M+1)^+$ Found: 277.160950, $C_{13}H_{24}O_6$ requires 277.165110.

Trans-(2S,3S)-(-)-2,3-bis(methoxycarbonylmethyl)-1,4,8,11-tetraoxacyclotetradecane (124). The procedure was analogous to that of (123), using *trans*-(2S,3S)-(-)-2,3-bis(cyanomethyl)-1,4,8,11-tetraoxacyclotetradecane (122) (630mg, 2.2 mmol). The product was purified by column chromatography using alumina with a 1:7 ethyl acetate/hexane mixture as elutant (R_f product = 0.75), yielding a clear viscous oil (320mg, yield 52%). $[\alpha]_D^{20}$ = -39.5° (C = 1.00, CH_2Cl_2); ^{1}H NMR ($CDCl_3$) δ: 1.74 (4H,m, $CH_2CH_2CH_2$), 2.48 (4H,m,CH_2CO), 3.43-4.00 (20H,m,CH_3O,CH_2O,CHO); ^{13}C NMR ($CDCl_3$) δ: 30.8 ($CH_2CH_2CH_2$), 35.9 (CH_2CO), 51.7 (CH_3O), 66.4, 66.6, 70.1 (CH_2O), 76.5 (CHO), 171.5 (C=O); IR ν_{max} cm^{-1} (Thin Film): 1742 (C=O), 1115 (C-O-C); m/e (Intensity%) (CI,isobutane): 349(100, MeOCO-CH_2CH-CHCH_2COOMe), 171(80).

2-Carboxymethyl-1,4,8,11-tetraoxacyclotetradecane (125). 2-Methoxycarbonylmethyl-1,4,8,11-tetraoxacyclotetradecane (300mg, 1.1 mmol) was refluxed in a 1:1 methanol/water mixture (10 ml) with tetramethylammonium hydroxide (1g) for 2 hrs. The mixture was allowed to cool and was evaporated to dryness under reduced pressure. The residue was taken up into 6 M HCl (5 ml) and extracted with diethyl ether (6 x 20 ml). The combined extracts were dried over $MgSO_4$ and concentrated *in vacuo* to yield crude product as an off-white solid (250mg, yield 86%). ^{1}H NMR ($CDCl_3$) δ: 1.72 (4H,m,$CH_2CH_2CH_2$), 2.51 (2H,m,CH_2CO), 3.45-3.92 (15H,m, CH_2O,CHO), 8.17 (1H,OH); ^{13}C NMR ($CDCl_3$) δ: 30.1 ($CH_2CH_2CH_2$), 37.0 (CH_2CO), 65.7, 66.6, 67.2, 69.5, 70.0, 71.0, 73.5 (CH_2O), 74.9 (CHO), 175.8 (C=O); IR ν_{max} cm^{-1} (Nujol): 3600-2500 (OH), 1750 (C=O), 1120 (C-O-C); m/e (Intensity%) (CI,isobutane): 263(100,M^++1), 245(80,-H_2O).

Trans-(2S,3S)-2,3-bis(carboxymethyl)-1,4,8,11-tetraoxacyclotetradecane (126). The procedure was analogous to that of (125), using *trans*-(2S,3S)-(-)-2,3-bis(methoxycarbonylmethyl)-1,4,8,11-tetraoxacyclotetradecane (124) (220mg, 0.63 mmol). This yielded an off-white solid (150mg, yield 75%). ^{1}H NMR (D_2O) δ: 1.83 (4H,m,$CH_2CH_2CH_2$), 2.61 (4H,m, CH_2CO), 3.69-4.00 (14H,m,CH_2O,CHO); ^{13}C NMR (D_2O) δ: 29.9 ($CH_2CH_2CH_2$), 35.6 (CH_2CO), 66.1, 67.0, 69.5 (CH_2O), 75.3 (CHO), 174.9 (C=O); IR ν_{max} cm^{-1} (Nujol): 3600-2500 (COOH), 1752 (C=O), 1120 (C-O-C).

2-N,N'-Dimethylcarbamoylmethyl-1,4,8,11-tetraoxacyclotetradecane (127). 2-(Carboxymethyl)-1,4,8,11-tetraoxacyclotetradecane (125) (400mg, 1.5 mmol) was stirred in dry dichloromethane (5 ml) under nitrogen. Phosphorus pentachloride (285mg, 1.35 mmol) was added in small portions over a period of 10 minutes. After the addition was complete, the mixture was stirred at room temperature under nitrogen for 12 hrs. The mixture was evaporated to dryness under reduced pressure to yield the acid chloride of (125). A ^{1}H NMR (60 MHz) spectrum was run to ensure that there was no unreacted acid (125) left. The acid chloride was stirred in dichloromethane at 0^0, and a solution of dimethylamine in water (2 ml, 30% v/v) was added dropwise. When the addition was complete, the reaction mixture was allowed to warm to room temperature and stirred at this temperature for 30 min. The mixture was allowed to stand for 10 minutes and the lower, organic layer was separated. This layer was washed with distilled water (2 x 5 ml), dried over $MgSO_4$ and concentrated *in vacuo* to yield crude product. The product was purified by column chromatography using silica with ethyl acetate as elutant (R_f product = 0.65) to yield a clear viscous oil (220mg, yield 50%). ^{1}H NMR ($CDCl_3$) δ: 1.75 (4H,m,$CH_2CH_2CH_2$), 2.52 (2H,m,CH_2CO), 2.95 (3H,s,CH_3N), 3.03 (3H,s,CH_3N), 3.45-3.95 (15H,m,CH_2O,CHO); ^{13}C NMR ($CDCl_3$) δ: 30.3,

30.4 ($CH_2CH_2CH_2$), 35.6, 37.5 (CH_3N), 35.8 (CH_2CO), 65.6, 66.6, 67.1, 69.1, 71.0, 73.6 (CH_2O), 75.6 (CHO), 170.8 (C=O); IR ν_{max} cm^{-1} (Thin Film): 1637 (C=O), 1120 (C-O-C); m/e (Intensity%) (CI,isobutane): 290(100,M^++1), 179(15,-$CH_2CHCH_2CONMe_2$), 85(23,CH_2CONMe_2); m/e (CI): $(M+1)^+$ Found: 290.220740, $C_{14}H_{27}NO_5$ requires 290.220190.

Trans-(2S,3S)-(-)-2,3-bis(N,N-dibutylcarbamoylmethyl-1,4,8,11-tetraoxacyclotetradecane (128). *Trans*-(2S,3S)-2,3-bis(carboxymethyl)-1,4,8,11-tetraoxacyclotetradecane (126) (150mg, 0.47 mmol) was stirred in dry dichloromethane (5 ml) under nitrogen. Phosphorus pentachloride (95mg, 0.45 mmol) was added in small portions over a period of five minutes. After the addition was complete, the mixture was stirred at room temperature under nitrogen for 12 hrs. The mixture was evaporated to dryness under reduced pressure to yield the acid chloride of (126). A ^1H NMR (60 MHz) spectrum was run to ensure that there was no unreacted acid (126) left. With efficient stirring, a solution of the acid chloride of (126) in dry dichloromethane (5 ml) was added dropwise to dibutylamine (0.25g, 1.9 mmol) and triethylamine (0.19g, 1.9 mmol) in dry dichloromethane (10 ml) chilled in an ice-salt bath. After stirring for a further 15 minutes, the mixture was evaporated to dryness, the residue partitioned between heptane and water, and the organic phase washed with dilute hydrochloric acid, water and then dried over $MgSO_4$. Removal of the solvent *in vacuo* afforded crude product. The product was purified by column chromatography using alumina with a 1:1 ethyl acetate/hexane mixture as elutant (R_f product = 0.6) to yield a clear oil (153mg, yield 60%). $[\alpha]_D^{20}$ = -33.7° (C = 1.00, CH_2Cl_2); ^1H NMR ($CDCl_3$) δ: 0.85 (12H,q,J=7Hz,CH_3), 1.30 (8H,m,CH_2CH_3), 1.45 (8H,m, $CH_2CH_2CH_3$), 2.31 (8H,m,CH_2CO), 3.12 (4H,m,CH_2N), 3.34 (4H,m,CH_2N), 3.50-3.65 (12H,m,CH_2O), 3.82 (2H,m,CHO); ^{13}C NMR ($CDCl_3$) δ: 13.8 (CH_3),

20.1 (CH_2CH_3), 29.7, 31.1 (NCH_2CH_2), 45.9, 47.9 (NCH_2), 35.3 (CH_2CO), 66.7, 67.6, 70.2 (CH_2O), 80.1 (CHO), 170.6 (C=O); IR ν_{max} cm^{-1} (Thin Film): 1638 (C=O), 1115 (C-O-C); m/e (Intensity%) (CI,isobutane): 543(55,M^++1), 231(100,M^+-2CONBu).

N,N'-Dimethylbromoacetamide (135). This compound was synthesised according to the method of Weaver and Whaley[147].

1,4,7-Tris-(N,N'-dimethylacetamido)-1,4,7-triazacyclononane (129). 1,4,7-Triazacyclononane (134) (250mg, 1.93 mmol) was stirred in dry acetonitrile (20 ml) under an atmosphere of nitrogen. Potassium carbonate (0.828g, 6 mmol) and N,N'-dimethylbromoacetamide (135) (1g, 6 mmol) were added, and the whole refluxed for 48 hrs. The mixture was then cooled to room temperature and the inorganic salts were filtered off and the filtrate was evaporated under reduced pressure. The waxy brown-red solid was taken up into the minimum amount of 1 M hydrochloric acid and extracted with dichloromethane (5 x 10ml). The acid aqueous layer was then basified to pH 14 using 1 M potassium hydroxide solution and extracted with dichloromethane (5 x 10 ml). The combined basic extracts were washed with distilled water (2 x 10 ml), dried over potassium carbonate and evaporated *in vacuo* to yield crude product - a red-brown viscous oil. The product was purified by column chromatography using alumina with a gradient from dichloromethane to 2% methanol/-dichloromethane as elutant (R_f product = 0.3 - 1% MeOH/CH_2Cl_2). This yielded a clear viscous oil (400mg, yield 54%). ^1H NMR ($CDCl_3$) δ: 2.88 (12H,s,CH_2N), 2.92 (9H,s,CH_3N), 3.05 (9H,s,CH_3N), 3.42 (6H,s,CH_2CO); ^{13}C NMR ($CDCl_3$) δ: 35.4 (CH_3N), 36.9 (CH_3N), 55.5 (CH_2N), 59.9 (CH_2CO), 171.0 (C=O); IR ν_{max} cm^{-1} (Thin Film): 1645 (C=O); m/e (Intensity%) (DCI,isobutane): 385(100,M^++1), 300(60,-CH_2CONMe_2).

1,4,7-Tris-(N,N'-dimethylpropanamido)-1,4,7-triazacyclononane (130).

1,4,7-Triazacyclononane (134) (180mg, 1.43 mmol) was stirred in anhydrous methanol (15 ml) under an atmosphere of nitrogen. Dimethylacrylamide (0.85g, 8.6 mmol) was added and the mixture was refluxed under nitrogen for 3 hrs. The mixture was cooled to room temperature and the solvent was evaporated under reduced pressure. The residue was taken up into the minimum amount of 1 M hydrochloric acid and extracted with dichloromethane (5 x 10ml). The acid aqueous layer was then basified to pH 14 using 1 M potassium hydroxide solution and extracted with dichloromethane (5 x 10 ml). The combined basic extracts were washed with distilled water (2 x 10 ml), dried over potassium carbonate and evaporated *in vacuo* to yield crude product. The product was purified by column chromatography using alumina with a gradient from dichloromethane to 2% methanol/dichloromethane as elutant (R_f product = 0.45 - CH_2Cl_2/2% MeOH). This yielded a clear viscous oil (325mg, yield 53%). ^{1}H NMR ($CDCl_3$) δ: 2.43 (6H,t,J=7.5Hz,CH_2CO), 2.70 (12H,s,CH_2N ring), 2.82 (6H,t,J=7.5Hz,CH_2N sidearm), 2.86 (9H,s,CH_3N), 2.97 (9H,s,CH_3N); ^{13}C NMR ($CDCl_3$) δ: 31.7 (CH_2CO), 35.3, 37.4 (CH_3N), 54.4 (CH_2N ring), 55.7 (CH_2CN sidearm), 172.1 (C=O); IR ν_{max} cm^{-1} (Thin Film): 1637 (C=O); m/e (Intensity%) (CI,isobutane): 427(100,M^++1), 328(40,M^+-$CH_2CH_2CONMe_2$), 228(20,$2CH_2CH_2CONMe_2$).

1,5,9-Tris-(N,N'-dimethylacetamido)-1,5,9-triazacyclododecane (131).

1,5,9-Triazacyclododecane (136) (250mg, 1.46 mmol) was stirred in dry ethanol (20 ml) under a nitrogen atmosphere. To this was added caesium carbonate (1.42g, 4.4 mmol) and N,N'-dimethylbromoacetamide (135) (0.73g, 4.4 mmol) and the mixture was refluxed under nitrogen for 24 hrs. The mixture was then allowed to cool, and the ethanol was separated off under reduced pressure. The off-white waxy residue was

taken up into dichloromethane and filtered. The filtrate was then evaporated down under reduced pressure. The residue was taken up into the minimum amount of 1 M hydrochloric acid and extracted with dichloromethane (5 x 10ml). The acid aqueous layer was then basified with 1 M potassium hydroxide and extracted with dichloromethane (5 x 10 ml). The basic extracts were washed with distilled water (2 x 10 ml), dried over $MgSO_4$ and concentrated *in vacuo* to yield crude product. The product was purified by passing down an alumina column using a gradient from dichloromethane to 2% methanol/dichloromethane as elutant (R_f product = 0.55 - CH_2Cl_2/2% MeOH) to yield a clear viscous oil (365mg, yield 60%). ^1H NMR ($CDCl_3$) δ: 1.63 (6H,q,J=5.9Hz,$CH_2CH_2CH_2$), 2.61 (12H,t,J=5.8Hz, CH_2N ring), 2.96 (9H,s,CH_3N), 3.10 (9H,s,CH_3N), 3.27 (6H,s,CH_2CO); ^{13}C NMR ($CDCl_3$) δ: 21.5 ($CH_2CH_2CH_2$), 35.2, 36.8 (CH_3N), 46.6 (CH_2N), 57.7 (CH_2CO), 170.5 (C=O); IR ν_{max} cm^{-1} (Thin Film): 1646 (C=O); m/e (Intensity%) (CI,isobutane): 427(100,M^++1), 342(30,M^+-CH_2CONMe_2).

1-p-Toluenesulphonyl-5,9,bis(N,N-dimethylacetamido)-1,5,9- triazacyclododecane (138). 1-p-Toluenesulphonyl-1,5,9-triazacyclododecane (137) (700mg, 2.15 mmol) was stirred in dry acetonitrile (25 ml) under an atmosphere of nitrogen. Caesium carbonate (2.1g, 6.5 mmol) and N,N'-dimethylbromoacetamide (135) (1.07g, 6.5 mmol) were added and the whole refluxed under nitrogen for 48 hr. Crude product was obtained by an identical procedure to that of (131). The product was purified by column chromatography using alumina with ethyl acetate as elutant (R_f product = 0.4). This yielded a clear viscous oil (0.65g, yield 61%). ^1H NMR ($CDCl_3$) δ: 1.47 (6H,m,$CH_2CH_2CH_2$), 2.33 (3H,s,CH_3 aromatic), 2.40 (4H,t,J=5Hz,CH_2N), 2.50 (4H,t,J=4.3Hz,CH_2N), 2.83 (6H,s,CH_3N), 2.94 (6H,s,CH_3N), 3.09 (4H,s,CH_2COO, 3.37 (4H,t,J=7Hz,CH_2NTs), 7.19 (2H,d,

J=8Hz, part of an AA'XX' system, aromatic CH), 7.60 (2H,d,J=8.1Hz, part of an AA'XX' system, aromatic CH); ^{13}C NMR ($CDCl_3$) δ: 21.4 ($CH_2CH_2CH_2$), 23.7 ($CH_2CH_2CH_2$,CH_3 aromatic), 35.4, 36.8 (NCH_3), 42.6, 48.7, 52.0 (CH_2N), 56.2 (CH_2CO), 126.9, 129.4, 137.8, 142.7 (Aromatic CH), 170.5 (C=O); IR ν_{max} cm^{-1} (Thin Film): 1645 (C=O), 1600 (ring vibration), 1335, 1165 (SO_2); m/e (Intensity%) (DCI,isobutane): 497(100,M^++1), 341(20,M^+-Ts).

1-Amino-5,9,bis(N,N-dimethylacetamido)-1,5,9-triazacyclododecane (132). 1-p-Toluenesulphonyl-5,9-bis(N,N'-dimethylacetamido)-1,5,9-triazacyclododecane (138) (600mg, 1.2 mmol) was heated at 80^o in an HBr acetic acid/phenol mixture (HBr/acetic acid 50 equivalents, 5 ml; phenol 0.34g, 3.6 mmol) for 3 days. The mixture was allowed to cool and the HBr/-acetic acid was azeotroped off under vacuum with toluene (3 x 20 ml) to leave a deep red waxy solid. The residue was taken up into the minimum quantity of 1 M hydrochloric acid (3 ml) and extracted with diethyl ether (3 x 10 ml) and dichloromethane (3 x 10ml). The acid aqueous layer was then basified to pH 14 with 1 M aqueous potassium hydroxide and extracted with dichloromethane (5 x 10 ml). The combined basic extracts were washed with distilled water (2 x 10 ml), dried over potassium carbonate and concentrated *in vacuo* to yield crude product. This consisted of a mixture of 70% detosylated product and 30% tosylated starting material as analysed by ^1H NMR. The desired detosylated product was isolated by first running off the the tosylated starting material with ethyl acetate on neutral alumina (R_f = 0.4) and then eluting off the detosylated material from the same column using a 10% methanol/dichloroform mixture. This yielded a clear viscous oil (140mg, yield 34%). ^1H NMR ($CDCl_3$) δ: 1.83 (6H,m,$CH_2CH_2CH_2$), 2.43 (4H,t, J=7.2Hz,CH_2NH), 2.56 (4H,m,CH_2N), 2.66 (4H,t,J=5.5Hz,CH_2N), 2.96 (6H,s,

CH_3N), 3.04 (6H,s,CH_3N), 3.11 (4H,s,CH_2CO); ^{13}C NMR ($CDCl_3$) δ: 21.5 ($CH_2CH_2CH_2$), 22.2 ($CH_2CH_2CH_2$), 34.7, 35.6 (CH_3N), 45.5 (CH_2NH), 46.7 (CH_2N), 51.3 (CH_2N), 55.1 (CH_2CO), 170.0 (C=O); IR ν_{max} cm^{-1} (Thin Film): 3400 (NH), 1635 (C=O); m/e (Intensity%) (CI,isobutane): 342(100,M^++1).

1,4,7,10-Tetra(p-toluenesulphonyl)-1,4,7,10-tetraazacyclododecane (140). 1,4,7,10-Tetraazadecane (139) (15g, 102.7 mmol) and potassium carbonate (70.89g, 5 equivalents) were dissolved in distilled water (600 ml). p-Toluenesulphonyl chloride (103.74g, 5 equivalents), was added in small portions over a period of 3 hrs to the solution at 80^o. After the addition was complete the mixture was stirred at 80^o for 16 hr. The mixture was allowed to cool and the product was filtered off as an off-white solid. The solid was washed with a 1:1 ethanol/water mixture (100 ml) which was evaporated off under reduced pressure. The last traces of water were removed by azeotroping with ethanol (3 x 50 ml). The solid was then slurried with dichloromethane (40 ml) so as to remove any unreacted p-toluenesulphonyl chloride. Filtration followed by pumping under high vacuum (0.01 mm Hg, 50^o, 5 hr) yielded product as a white solid (57.5g, yield 73%). ^1H NMR and ^{13}C NMR were consistent with their proposed formulations and the product was used without further purification[142].

1,4,7,10-Tetra(p-toluenesulphonyl)-1,4,7,10-tetraazacyclododecane (141). This compound was synthesised according to the method of Kellogg[148].

1,4,7,10-Tetraazacyclododecane (142). This compound was synthesised according to the method of Cox, Jankowski and Craig[149].

N,N'-Dimethyl-1,4,7,10-Tetraacetamido-1,4,7,10-tetraazacyclododecane (133). 1,4,7,10-Tetraazacyclododecane (142) (200mg, 1.2 mmol) was stirred in dry ethanol under a nitrogen atmosphere. To this was added caesium carbonate (1.05g, 3.6 mmol) and N,N'-dimethylbromoacetamide (135) (0.60g, 3.6 mmol) and the mixture was refluxed for 24 hr. Crude product was obtained by an identical procedure to that of ligand (131). the product was purified by column chromatography using alumina with a gradient from dichloromethane to 3% methanol/dichloromethane as elutant (R_f product = 0.25 2%MeOH/CH_2Cl_2). This yielded a clear viscous oil (340 mg, yield 55%). ^{1}H NMR ($CDCl_3$) δ: 2.47 (16H,broad,s,CH_2N), 2.91 (12H,s,CH_3N), 2.96 (12H,s,CH_3N), 3.28 (8H,broad,s,CH_2CO); ^{13}C NMR ($CDCl_3$) δ: 35.5, 36.2 (CH_3N), 51.5 (CH_2N), 55.1 (CH_2CO), 171.1 (C=O); IR ν_{max} cm^{-1} (Thin Film): 1645 (C=O), m/e (Intensity%) (CI,isobutane): 513(100,M^++1); 428(14,M^+-CH_2CONMe_2), 257(10,M^+-3CH_2CONMe_2).

4.3 NMR EXPERIMENTS

Titration curves were obtained 2:1 d^4-methanol/$CDCl_3$ solution (3 ml) of the ligands and the solid alkali salts [LiCl (BDH), $CaCl_2$ (Aldrich)]. After each addition of salt, the ^{13}C NMR chemical shift (relative to TMS) was measured at 298K using a Bruker AC250 instrument operating at 62.896 MHz for the carbon nucleus.

4.4 FAB MS EXPERIMENTS

The stainless steel tip of a FAB-probe was coated with a thin layer of the analytical solution (3 μL). Positive FAB MS was performed using a primary ion atom beam of Ar (8 KeV) on a VG 7070E mass spectrometer coupled to a VG II-250 data system. At an accelerating voltage of 6 KV,

the mass range m/e 20-20,000 was scanned at 3s per decade (scan cycle time 10s). Twenty successive spectra of each analytical solution were acquired and scans 5 to 15 inclusive were averaged to afford the final spectrum. Two runs were performed for each analytical solution and the values were averaged to obtain selectivity(s) values for each ligand.

4.5 POTENTIOMETRIC EXPERIMENTS

4.5.1 Membrane Preparation

The membranes were made up by dissolving 1.2% sensor, 65.6% plasticiser (ONPOE), 32.8% PVC (high molecular weight - Fluka) and 0.4% lipophilic anion (KTpClPB), with or without TOPO as required in 6 ml of spectroscopic grade THF which was poured into a 33 mm I.D. glass ring resting on a sheet of plate glass. A pad of filter papers was placed on top of the ring and these were kept in place by a heavy weight[150]. The assembly was left for 48 hours to allow slow solvent evaporation. A small disc was cut from the membrane and affixed to a Philips pye electrode body to form the ion selective electrode.

4.5.2 Dip-Type Method

Solutions were made up using anhydrous lithium chloride (BDH), sodium chloride (BDH), potassium chloride (BDH) and calcium chloride (BDH) 1 mol L^{-1} solutions. The solid alkali metal salts were further dried by storing in a desiccator over silica gel. All solutions were made up using deionised water (MilliQ).

The ion selective and reference electrodes were connected to a digital multimeter (Keithley 197 auto-ranging microvolt DMM) *via* a

buffer amplifier. The reference electrode was a porous plug saturated calomel electrode (RE1 petiacourt). The temperature of the system was maintained at 37^{o} using a Techne Tempette Junior TE-8J thermostat bath.

Electrode potentials were measured by dipping both ion selective and reference electrodes into the analyte solution and recording the limiting potential value. The electrodes were thoroughly rinsed using deionised water between each measurement.

4.5.3 Flow System

A constant volume cell was used for ion selective electrodes. It was made from a water jacketed glass tube with a B19 ground glass joint. Drilled glass stoppers with a wax seal were used for fitting the electrodes.

The ion selective and reference electrodes were connected to a digital multimeter (Keithley 197 auto-ranging microvolt DMM) *via* a buffer amplifier. A flat-bed Linseis YT-chart recorder provided with back-off facilities, was used for monitoring potential difference changes. A suitable capacitance was connected across the input of the chart recorder to smooth out residual noise. The reference electrode was a porous plug, saturated calomel electrode (RE1 petiacourt). The peristaltic pump used was an RS330-812. The temperature of the system was maintained at 37^{o} using a Techne Tempette Junior TE-8J thermostat bath.

Solutions were made up using anhydrous lithium chloride (BDH), sodium chloride (BDH), potassium chloride (BDH) and calcium chloride (BDH) 1 mol L^{-1} solutions. The solid alkali metal salts were further dried by storing in a desiccator over silica gel. All solutions were made up using deionised water (MilliQ).

4.6 pH METRIC TITRATION EXPERIMENTS

4.6.1 Apparatus and Instrumentation

The titration cell was a double walled glass vessel of approximately 5 ml capacity. The temperature of the system was maintained at 25^{o} using a Techne Tempette Junior TE-8J. The solutions in the titration cell were stirred using a magnetic stirrer. An automatic burette (Mettler DL20) of 1 ml capacity was used and the pH was measured using a Corning 001854 combination microelectrode. The titrations were controlled and data was stored using a BBC microprocessor. The burette functions (volume increments, total volume delivered and time interval allowed for equilibration between each reading) were controlled by the use of basic software stored on a disc. The data was transferred to the MTS mainframe using Kermit. This data was subsequently analysed by two non-linear least-squares programs SCOGS2 and Superquad[151].

4.6.2 Measurement of Acid Dissociation Constants

The combination microelectrode was calibrated by using two buffers: (i) 0.05 mol dm^{-3} KHPH - pH 4.008, 25^{o} and (ii) 0.025 mol dm^{-3} KH_2PO_4, 0.025 mol dm^{-3} Na_2HPO_4 - pH 6.865, 25^{o}. Stock ligand solutions were made up containing 0.001 mol dm^{-3} ligand, 0.00N mol dm^{-3} nitric acid (N = number of amine nitrogen atoms in the ligand) and 0.1 mol dm^{-3} tetramethylammonium nitrate to ensure constant ionic strength in 25 ml deionised water (MilliQ). The titrant ligand solution (3 ml) was placed in the titration vessel which was fitted with a Teflon cap with three apertures for the combination electrode, burette tube and nitrogen

bubbler. The titrant was tetramethylammonium hydroxide whose exact molarity (0.070 mol dm^{-3}) was determined by titrating against 0.1 mol dm^{-3} HCl. Three separate titrations were performed on each ligand and the results were analysed by methods previously outlined.

4.6.3 Measurement of Metal Complexation Constants

Titrant ligand solutions were made up containing 0.001 mol dm^{-3} ligand, 0.001 mol dm^{-3} cation, 0.00N mol dm^{-3} (N = number of amine nitrogen atoms in the ligand) and 0.1 mol dm^{-3} tetramethylammonium nitrate. The titrant once again was tetramethylammonium hydroxide (0.070 mol dm^{-3}) and as before titrations were performed under an atmosphere of nitrogen. Two separate titrations were made for each particular ligand/cation combination and data was analysed as before. The cations used were chloride salts, lithium chloride and sodium chloride solids (BDH) and 0.1 mol dm^{-3} calcium chloride solution (BDH).

REFERENCES

1. Moore, C. and Pressman, B.C., *Biochem. Biophys.Res.Commun.* V15, 562 (1964).

2. a) Duax, L. and Hauptman, H., *Acta Cryst.*, B28, 2912 (1972).

   b) Karle, I.L., *J.Am.Chem.Soc.*, 97, 4379 (1975).

   c) Smith, G.D., Duax, W.L., Langs, D.A., DeTittu, G.T., Edmonds, J.W., Rohrer, D.C. and Weeks, C.M., *J.Am.Chem.Soc.*, 97, 7242 (1975).

3. Pederson, C.J., *J.Am.Chem.Soc.*, 89, 7017 (1967).

4. Michaux, G. and Reisse, J., *J.Am.Chem.Soc.*, 104, 6895 (1982).

5. Izatt, R.M., Terry, R.E., Haymore, B.L., Hansen, L.D., Dalley, N.K., Avondet, A.G. and Christensen, J.J., *J.Am.Chem.Soc.*, 98, 7620 (1976).

6. Ho, T.L., *Chem.Rev.*, 75, 1 (1975).

7. Frensdorff, H.K., *J.Am.Chem.Soc.*, 93, 600 (1971).

8. Buschmann, H.J., *Inorg.Chim.Acta.*, 125, 31 (1986).

9. Lamb, J.D., Izatt, R.M., Swain, S.W. and Christensen, J.J., *J.Am. Chem.Soc.*, 102, 475 (1980).

10. Buschmann, H.J., *Chem.Ber.*, 118, 2746 (1985).

11. Buschmann, H.J., *J.Solution Chem.*, In Press.

12. Dzidic, J. and Kebarle, P., *J.Phys.Chem.*, 74, 1466 (1970).

13. Dejong, F. and Reinhardt, D., *Tetrahed.Lett.*, 3985 (1977).

14. Chock, P.B., *Proc.Natl.Acad.Sci.USA.*, 69, 1939 (1972).

15. Grell, E., Funck, T., Eggers, F. and Eienman, G., "*Membranes - a series of advances*", Volume 3, Dekker, New York (1975), pages 1 - 175.

16. Cox, B.G., Knop, D. and Schneider, H., *J.Am.Chem.Soc.*, 100, 4746 (1978).

17. Cram, D.J., *J.Am.Chem.Soc.*, 107, 3657 (1985).

18. Eyring, G., Leisegang, G.W., Farrow, M.M., Arce-Vazquez, F. and Purdie, N., *J.Am.Chem.Soc.*, 98, 6905 (1976); *J.Am.Chem.Soc.*, 99, 3240 (1977).

19. Lehn, J.M., *Pure Appl.Chem.*, 51, 979 (1979).

20. Kirch, M, and Lehn, J.M., *Angew.Chem. Int.Ed.Engl.*, 14, 555 (1975).

21. a) Lehn, J.M., *Pure Appl.Chem.*, 52, 2741 (1980).

b) McBryde, D.W., Izatt, R.M., Lamb, J.D. and Christensen, J.J., "*Inclusion Compounds*", page 571.

c) Behr, J.P., Kirch, M. and Lehn, J.M., *J.Am.Chem.Soc.*, 107, 241 (1985).

22. Christensen, J.J., Izatt, R.M., Hawden, L.D. and Partridge, J.A. *J.Am.Chem.Soc.*, 70, 2003 (1966).

23. Izatt, R.M., Nelson, D.P., Rytting, J.H., Haymore, B.L. and Christensen, J.J., *J.Am.Chem.Soc.*, 93, 1619 (1971).

24. Buschmann, H.J., *ThermoChim.Acta.*, 102, 179 (1986).

25. Buschmann, H.J., *Inorg.Chim.Acta.*, 102, 95 (1985).

26. Matsuru, N., Umemoto, K., Takeda, Y. and Susaki, A., *Bull.Soc.Chem. Japan*, 49, 1246 (1976).

27. Takeda, Y., Yano, H., Ishibashi, M. and Izozumi, *Bull.Soc.Chem. Japan*, 53, 72 (1980).

28. Takeda, Y. and Yano, H., *Bull.Soc.Chem. Japan*, 53, 1720 (1980).

29. Takeda, Y., *Bull.Soc.Chem. Japan*, 56, 866 (1983).

30. Ikeda, I., Yamamura, S., Nakatsuji, Y. and Okahara, M., *J.Org. Chem.*, 47, 147 (1982).

31. Aalmo, K.M. and Krane, J., *Acta Chem.Scand.*, A36, 227 (1982).

32. Parsons, D.G., Truter, M.R. and Wingfield, J.M., *Inorg.Chim.Acta*, L157, 45 (1980).

33. Lehn, J.M., Leconte, J.P., Martell, A.E. and Motekaitis, R.J., *Inorg.Chem.*, 22, 609 (1983).

34. Lehn, J.M., Simon, J., *Helv.Chim.Acta*, 60, 141 (1977).

35. Chang, C.A. and Ochaya, V.O., *Inorg.Chem.*, 275, 355 (1986).

36. Lehn, J.M. and Sauvage, J.P., *J.Am.Chem.Soc.*, 97, 6700 (1975).

37. Amble, E. and Dale, J., *Acta Chem.Scand.*, B33, 698 (1979).

38. Calverly, M. and Dale, J., *Acta Chem.Scand.*, B36, 241 (1982).

39. Lenkinski, R.E., Elgavish, G.A. and Reuben, J., *J.Magn.Res.*, 32, 367 (1978).

40. Reuben, J., *J.Am.Chem.Soc.*, 95, 3534 (1973).

41. Miller, J.M., *Advances in Inorg.Chem.Radiochem.*, 281 (1984).

42. Williams, D.H., Findeis, A.F., Naylor, S. and Gibson, B.W., *J.Am.Chem.Soc.*, 109, 1980 (1987).

43. Barber, M., Bordoli, R.S., Sedgewick, R.D. and Tyler, A.N., *J.C.S. Chem Commun.*, 325 (1981).

44. Johnstone, R.A.W. and Rose M.E., *J.C.S. Chem Commun.*, 1268 (1983).

45. Pederson, C.J., in "*Synthetic Multidentate Macrocyclic Compounds*" Ed. R.M. Izatt and J.J. Christensen, Academic Press, New York (1978), page 1.

46. Pederson, C.J., *J.Am.Chem.Soc.*, 89, 2495 (1967).

47. Anker, P., Jenny, H.B., Wuthier, V., Asper, R., Ammann, D. and Simon, W., *Clin.Chem.*, 29, 1508 (1983).

48. Ammann, D., Morf, W., Anker, P., Meier, P.C., Pretsch, E. and Simon, W., *Ion Selective Electrode Res.*, 5, 3 (1983).

49. Lanter, F., Erre, D. and Simon, W., *Anal.Lett.*, 7, 9 (1974).

50. Metzger, E., Ammann, D., Schefer, U., Pretsch, E. and Simon, W., *Chimia*, 639 (1984).

51. Fabrizzi, L., Paoletti, P. and Lever, A.B.P., *Inorg.Chem.*, 15, 1502 (1976).

52. Lamb, J.D., "*Synthetic Multidentate Ligands: Stability, Selectivity and Transport of their Cation Complexes*", Ph.D Dissertaton, Brigham Young University, Provo, Utah (1978).

53. Hinz, F.P. and Margerum, D.W., *Inorg.Chem.*, 13, 2941 (1974).

54. Dei, A. and Gori, A., *Inorg.Chem.*, 14, 157 (1975).

55. Paoletti, P., Fabrizzi, L. and Barbucci, R., *Inorg.Chem.*, 12, 1961 (1973).

56. "*Coordination Chemistry of Macrocyclic Compounds*", Ed. G. Melson, Plenum Press, New York (1979), page 166.

57. "*Stereochemistry of Organometallic and Inorganic Compounds*", Volume 2, Ed. I. Bernal and H.J. Buschman, (1987), Chapter 2, page 103.

58. Dunitz, J.D., Dobler, M., Seiler, P. and Phizackerly, R.P., *Acta Cryst.*, B30, 2773 (1974).

59. Dunitz, J.D. and Seiler, P., *Acta Cryst.*, B30, 2741 (1974).

60. Dobler, M. and Phizackerly, R.P., *Acta Cryst.*, B30, 2746 (1974).

61. Dobler, M. and Phizackerly, R.P., *Acta Cryst.*, B30, 2748 (1974).

62. Dalley, N.K., in "*Synthetic Multidentate Macrocyclic Compounds*", Ed. R.M. Izatt and J.J. Christensen, Academic Press, New York (1978), page 207.

63. Shannon, R.D. and Prewitt, C.J., *Acta Cryst.*, B25, 925 (1969).

64. Shannon, R.D. and Prewitt, C.J., *Acta Cryst.*, B26, 1046 (1970).

65. Gokel, G.W., Goli, D.M., Minganti, C. and Echegoyen, L., *J.Am.Chem.Soc.*, 105, 6786 (1983).

66. Bush, M.A. and Truter, M.R., *J.C.S. Perkin Trans.(II).*, 345 (1972).

67. Lamb, J.D., Izatt, R.M., Christensen, J.J. and Eatough, D.J., in "*Coordination Chemistry of Macrocyclic Compounds*", Ed. G. Melson, Plenum Press, New York (1979), page 537.

68. Kimura, K., Tamura, H., Tsuchida, T. and Shomo, T., *Chem.Lett.*, 611 (1979).

69. Kimura, K., Tsuchida, T. Mueda, T. and Shomo, T., *Talanta*, 27, 801 (1980).

70. Kimura, K., Ikeda, I., Katayama, T., Okahera, M. and Shomo, T., *Tetrahedron.Lett.*, 3615 (1981).

71. Tamura, H., Kimura, K., and Shomo, T., *Anal.Chem.*, 58, 1225 (1982).

72. Kimura, K., Ishikawa, A., Tamura, H. and Shomo, T., *J.C.S. Perkin Trans.(II).*, 447 (1984).

73. Shinkai, S., Ogawa, T., Kusano, Y. and Manabe, O., *Chem.Lett.*, 283 (1980).

74. Shinkai, S., Ogawa, T., Nakaji, T. and Manabe, O., *J.C.S. Chem Commun.*, 375 (1980).

75. Anzai, J.I., Sasaki, H., Veno, A. and Osa T., *J.C.S. Chem Commun.*, 1045 (1983).

76. Shinkai, S., Nakaji, T., Ogawa, T., Shigematsu, K. and Manabe, O., *J.Am.Chem.Soc.*, 103, 111 (1980).

77. Kimura, K., Sakamoto, H., Koseki, Y. and Shomo, T., *Chem.Lett.*, 1241 (1985).

78. Gokel, G.W., Dishong, D.M. and Diamond, C.J., *J.C.S. Chem Commun.*, 1053 (1980).

79. Dishong, D.M., Diamond, C.J. and Gokel, G.W., *Tetrahedron Lett.*, 1663 (1981).

80. Lehn, J.M., Behr, T.P., Girodean, J.M. and Sauvage, J.P., *Helv.Chim.Acta*, 2096 (1980).

81. Lambert, J.P., *Acc.Chem.Res.*, 4, 87 (1971).

82. Behr, J.P., Lehn, J.M., Thierry, J.C. and Moras, D., *J.Am.Chem. Soc.*, 103, 701 (1981).

83. Gokel, G.W., Kaifer, A., DupontDurst, H., Echegoyen, L., Dishong, D.M. and Shultz, *J.Org.Chem.*, 47, 3195 (1982).

84. Echegoyen, L., Gokel, G.W., Kimm, S., Eyring, E.M. and Petrucci, S., *J.Phys.Chem.*, 91, 3854 (1987).

85. Gatto, V.J. and Gokel, G.W., *J.Am.Chem.Soc.*, 106, 8240 (1984).

86. Gokel, G.W., Arnold, K.A., Echegoyen, L., Fronczek, F.R., Gundour, R.D., Gatto, V.J. and White, B.D., *J.Am.Chem.Soc.*, 109, 3716 (1987).

87. Gokel, G.W., Arnold, K.A., Echegoyen, L., Fronczek, F.R., Gundour, R.D., Gatto, V.J. and White, B.D., *J.Organic Chem.*, 53, 5652 (1988).

88. Gandour, R.D., Fronczek, F.R., Gatto, V.J., Minganti, C., Schultz, R.A., White, B.D., Arnold, K.A., Muzzochi, D., Muller, S.R. and Gokel, G.W., *J.Am.Chem.Soc.*, 108, 4078 (1986).

89. Dietrich, B., Lehn, J.M. and Sauvage, J.P., *Tetrahedron Lett.*, 2885 (1969).

90. Dietrich, B., Lehn, J.M. and Sauvage, J.P., *Tetrahedron Lett.*, 2889 (1969).

91. Dietrich, B., Lehn, J.M., Sauvage, J.P. and Blauzat, V., *Tetrahedron*, 29, 1629 (1973).

92. Dietrich, B., Lehn, J.M. and Sauvage, J.P., *Tetrahedron*, 29, 1647 (1973).

93. Sauvage, J.P. and Lehn, J.M., *J.Am.Chem.Soc.*, 97, 942 (1975).

94. Reviewed by N.K. Dalley in "*Synthetic Multidentate Macrocyclic Compounds*", Ed. R.M. Izatt and J.J. Christensen, Academic Press, New York (1978), page 209.

95. Kauffmann, E., Lehn, J.M. and Sauvage, J.P., *Helv.Chim.Acta*, 59, 1099 (1976).

96. "*Stereochemistry of Organometallic and Inorganic Compounds*", Volume 2, Ed. I. Bernal and H.J. Buschman, (1987), page 153.

97. Cram, D.J., Kaneda, T., Helgeson, R.C., Brown, S.B., Knobler, C.B., Maverick, E. and Trueblood, K.N., *J.Am.Chem.Soc.*, 107, 3645 (1985).

98. Cram, D.J. and Trueblood, K.N., *Topics Curr.Res.*, 98, 43 (1981).

99. Artz, S.P. and Cram, D.J., *J.Am.Chem.Soc.*, 106, 2160 (1984).

100. Lein, G.M. and Cram, D.J., *J.Am.Chem.Soc.*, 107, 448 (1985).

101. Cram, D.J., Peng Ho, S., Knobler, C.B., Maverick, E. and Trueblood, K.N., *J.Am.Chem.Soc.*, 108, 2989 (1986).

102. Shanzer, A., Samuel, D. and Korenstein, R., *J.Am.Chem.Soc.*, 105, 3815 (1983).

103. Kimura, K., Kitizawa, S. and Shomo, T., *Chem.Lett.*, 639 (1984).

104. Hiratani, H., Taguchi, K. and Iio, K., *Bull.Soc.Chem.Japan*, 57, 1976 (1984).

105.Canessa, M., Adragna, N., Soloman, H.S., Connolly, T.M. and Tosteson, *New Engl.J.Medic.*, 302, 52 (1978).

106.Kitizawa, S., Kimura, K. and Shomo, T., *J.Am.Chem.Soc.*, 106, 6978 (1984).

107."*Lithium Research and Therapy*", Ed. F.N. Johnson, Academic Press, London (1975).

108.Simon, W., Ammann, D., Oeheme, M. and Morf, W.E., *Annals New York Acad.Sci.*, 307, 52 (1978).

109.Schwochau, K., *Topics Curr.Res.*, 124, 93 (1984).

110.Goldschmidt, V.M., *Skrifter Norske Videnskaps Akad. Oslo Mat. Naturv, KL2* (1926).

111.Morf, W.E. and Simon, W., *Helv.Chim.Acta*, 54, 794 (1971).

112.Pearson, R.G. and Mawby, R.J., "*Halogen Chemistry*", Volume 3, Ed. V. Gaufmann, Academic Press, London-New York (1967).

113.Salzmann, J.J. and Jergensen, C.K., *Helv.Chim.Acta*, 51, 1276 (1968).

114.Moras, R.D. and Weiss, R., *Acta Cryst.*, B24, 400 (1973).

115.Lincoln, S.F., Horn, E., Hambley, T.W., Snow, M.R., Bereton, I.M. and Spotswood, T.M., *J.Chem.Soc.Dalton Trans.*, 1075 (1986).

116.Bradshaw, J.D., Maas, G.E., Lamb, J.D., Izatt, R.M. and Christensen, J.J., *J.Am.Chem.Soc.*, 99, 2365 (1977).

117.Bradshaw, J.D., Maas, G.E., Lamb, J.D., Izatt, R.M. and Christensen, J.J., *J.Am.Chem.Soc.*, 102, 467 (1980).

118.Donnay, G. and Gryder, S.W., *J.Chem.Educt.*, 42, 223 (1965).

119.Dalley, N.K. in "*Synthetic Multidentate Macrocyclic Compounds*", Ed. R.M. Izatt and J.J. Christensen, Academic Press, New York (1978)

120.Bartsch, R.A., Christian, G.D., Xie, R.Y., Wen, X. and Attiyat, A.S., *Anal.Chem.*, 60, 2561 (1988).

121.Bartsch, R.A., Czech, B.P., Son, B. and Babb, D.A., *J.Organic Chem.*, 40, 4805 (1984).

122.Bartsch, R.A., Czech, B.P., Kan, S.I., Stewart, L.E., Walkowalk, W., Charewiz, W.A., Heo, G.S. and Son, B. *J.Am.Chem.Soc.*, 107, 4997 (1985).

123.Hancock, R.D., *Pure and Applied Chem.*, 58, 1445 (1986).

124.Jyo, A., Seto, H. and Ishibashi, N., *Nippon Kagaku Kaishi*, 1423 (1980).

125.Kimura, K., Yano, H., Kitizawa, S. and Shoro, T., *J.C.S. Perkin Trans.(II).*, 1945 (1986).

126.Shohan, G., Christiansen, D.W., Bartsch, R.A., Heo, G.S., Olsher, W. and Lipscomb, N., *J.Am.Chem.Soc.*, 106, 1280 (1984).

127.Shohan, G., Lipscomb, N. and Olsher, W., *J.C.S. Chem Commun.*, 208 (1983).

128.Groth, P., *Acta Chem.Scand.*, A35, 463 (1981).

129.Groth, P., *Acta Chem.Scand.*, A35, 460 (1981).

130.Kimura, K., Sutomumura, T. and Shomo, T., "*Current Topics in Macrocyclic Chemistry in Japan*", Ed. K. Kimura (1987), page 18.

131.Bartsh, R.A., Woo Yung, I., Lee, H.K., Dip, N. and Pugia, M.G., *Anal.Chem.*, 58, 2723 (1986).

132.Shohan, G., Lipscomb, N. and Olsher, W., *J.Am.Chem.Soc.*, 105, 1247 (1983).

133.Myazaki, T.M., Yumagida, S., Itoh, A. and Okahara, M., *Bull.Chem. Soc.Japan.*, 55, 2005 (1982).

134.Howe, R.J. and Malkin, T., *J.Chem.Soc.*, 2663 (1951).

135.Merli, J. and Serbl, J., *Int.J.Mass Spec. and Ion Phys.*, 46, 367 (1983).

136.Horrai, G., Toth, K. and Pungor, E., *Analytica Chimica Acta*, 82, 45 (1976).

137.Dobson, S.M., PhD Thesis (1986), University of Witwaterstand.

138.Dale, J., Buoen, S., Groth, P. and Krane, J., *J.C.S. Chem Commun.*, 1172 (1982).

139.Smith, R.R. and Martell, A.E., "Critical Stability Constants", Volume 2 (Amines), Plenum, New York.

140.Hart, S.M., Boeyens, J.C.A., Michael, J.P. and Hancock, R.D., *J.C.S. Dalton Trans.*, 160 (1983).

141.Zompa, L.J., *Inorg.Chem.*, 17, 2531 (1978).

142.Kengger, A.P., Hertli, L. and Kaden, T.A., *Helv.Chim.Acta*, 61, 2296 (1978).

143.Seebach, D., Dörr, H., Bastani, B. and Shrig, V., *Angew.Chem. Int.Ed.Engl.*, 8, 392 (1969).

144.Dale, J. and Kristiansen, P.O., *Acta Chemica Scand.*, 26, 1471 (1972).

145.Carmack, M. and Kelley, C.J., *J.Org.Chem.*, 33, 2171 (1968).

146.Ando, N., Yamamoto, Y., Oda, J. and Inoye, Y., *Synthesis*, 688 (1978).

147.Weaver, W.E. and Whaley, W.M., *J.Am.Chem.Soc.*, 69, 515 (1947).

148.Kellogg, R.M., *J.Organometallic Chem.*, 49, 110 (1984).

149.Cox, J.P.L., Craig, A.S. and Jankowski, K., private communication.

150.Craggs, A., Moody, G.J. and Thomas, J.D.R., *J.Chem.Educt.*, 51, 541 (1974).

151.Gans, P., Sabatini, A. and Vacca, A., *J.C.S. Dalton Trans.*, 1195 (1985).

APPENDICES

COLLOQUIA, CONFERENCES AND PUBLICATIONS

APPENDIX I

RESEARCH COLLOQUIA, SEMINARS, LECTURES AND CONFERENCES ORGANISED BY THE DEPARTMENT OF CHEMISTRY DURING THE PERIOD: 1985-1986

* BARNARD, Dr. C.J.F. (Johnson Matthey Group) "Platinum Anti-Cancer Drug Development"	20th February 1986
BROWN, Dr. J.M. (University of Oxford) "Chelate Control in Homogeneous Catalysis"	12th March 1986
* CLARK, Dr. B.A.J. (Kodak Ltd.) "Chemistry & Principles of Colour Photography"	28th November 1985
CLARK, Dr. J.H. (University of York) "Novel Fluoride Ion Reagents"	29th January 1986
* DAVIES, Dr. S.G. (University of Oxford) "Chirality Control and Molecular Recognition"	14th November 1985
DEWING, Dr. J. (U.M.I.S.T.) "Zeolites - Small Holes, Big Opportunities"	24th October 1985
ERTL, Prof. G. (University of Munich) "Heterogeneous Catalysis"	7th November 1985
GRIGG, Prof. R. (Queen"s University, Belfast) "Thermal Generation of 1,3-Dipoles"	13th February 1986
HARRIS, Prof. R.K. (University of Durham) "The Magic of Solid State NMR"	27th February 1986
HATHWAY, Dr. D. (University of Durham) "Herbicide Selectivity"	5th March 1986
* IDDON, Dr. B. (University of Salford) "The Magic of Chemistry"	6th March 1986
JACK, Prof. K.H. (University of Newcastle) "Chemistry of Si-Al-O-N Engineering Ceramics"	21st November 1985
LANGRIDGE-SMITH, Dr.P.R.R. (Edinburgh University) "Naked Metal Clusters - Synthesis, Characterisation and Chemistry"	14th May 1986
LEWIS, Prof. Sir Jack (University of Cambridge) "Some more Recent Aspects in the Cluster Chemistry of Ruthenium and Osmium Carbonyls"	23rd January 1986
* LUDMAN, Dr. C.J. (University of Durham) "Some Thermochemical Aspects of Explosions"	17th October 1985
MACBRIDE, Dr. J.A.H. (Sunderland Polytechnic) "A Heterocyclic Tour on a Distorted Tricycle - Biphenylene"	20th November 1985

O'DONNELL, Prof. M.J. (Indiana-Purdue University) 5th November 1985
"New Methodology for the Synthesis of Amino Acids"

PARMAR, Dr. V.S. (University of Delhi) 13th September 1985
"Enzyme Assisted ERC Synthesis"

* PHILLIPS, Dr. N.J. (Loughborough Univ.Technology) 30th January 1986
"Laser Holography"

* PROCTOR, Prof. G. (University of Salford) 19th February 1986
"Approaches to the Synthesis of some Natural Products"

SCHMUTZLER, Prof. R. (University of Braunschweig) 9th June 1986
"Mixed Valence Diphosphorus Compounds"

* SCHRODER, Dr. M. (University of Edinburgh) 5th March 1986
"Studies on Macrocyclic Complexes"

SHEPPARD, Prof. N. (University of East Anglia) 15th January 1986
"Vibrational and Spectroscopic Determinations of the Structures of Molecules Chemisorbed on Metal Surfaces"

TEE, Prof. O.S. (Concordia University, Montreal) 12th February 1986
"Bromination of Phenols"

TILL, Miss C. (University of Durham) 26th February 1986
"ESCA and Optical Emission Studies of the Plasma Polymerisation of Perfluoroaromatics"

* TIMMS, Dr. P. (University of Bristol) 31st October 1985
"Some Chemistry of Fireworks"

WADDINGTON, Prof. D.J. (University of York) 28th November 1985
"Resources for the Chemistry Teacher"

WHITTLETON, Dr. S.N. (University of Durham) 30th October 1985
"An Investigation of a Reaction Window"

WILDE, Prof. R.E. (Texas Technical University) 23rd June 1986
"Molecule Dynamic Processes from Vibrational Bandshapes"

YARWOOD, Dr. J. (University of Durham) 12th February 1986
"The Structure of Water in Liquid Crystals"

DURING THE PERIOD: 1986-1987

* ALLEN, Prof. Sir G. (Unilever Research) 13th November 1986
"Biotechnology and the Future of the Chemical Industry"

BARTSCH, Dr. B. (University of Sussex) 6th May 1987
"Low Co-ordinated Phosphorus Compounds"

	BLACKBURN, Dr. M. (University of Sheffield) "Phosphonates as Analogues of Biological Phosphate Esters"	27th May 1987
*	BORDWELL, Prof. F.G.(Northeastern University,USA) "Carbon Anions, Radicals, Radical Anions and Radical Cations"	9th March 1987
	CANNING, Dr. N.D.S. (University of Durham) "Surface Adsorption Studies of Relevance to Heterogeneous Ammonia Synthesis"	26th November 1986
	CANNON, Dr. R.D. (University of East Anglia) "Electron Transfer in Polynuclear Complexes"	11th March 1987
	CLEGG, Dr. W. (University of Newcastle-upon-Tyne) "Carboxylate Complexes of Zinc; Charting a Structural Jungle"	28th January 1987
	DÖPP, Prof. D. (University of Duisburg) "Cyclo-additions and Cyclo-reversions Involving Captodative Alkenes"	5th November 1986
	DORFMÜLLER, Prof. T. (University of Bielefeld) "Rotational Dynamics in Liquids and Polymers"	8th December 1986
*	GOODGER, Dr. E.M. (Cranfield Inst.Technology) "Alternative Fuels for Transport"	12th March 1987
*	GREENWOOD, Prof. N.N. (University of Leeds) "Glorious Gaffes in Chemistry"	16th October 1986
	HARMER, Dr. M. (I.C.I. Chemicals & Polymer Group) "The Role of Organometallics in Advanced Materials"	7th May 1987
*	HUBBERSTEY, Dr. P. (University of Nottingham) "Demonstration Lecture on Various Aspects of Alkali Metal Chemistry"	5th February 1987
	HUDSON, Prof. R.F. (University of Kent) "Aspects of Organophosphorus Chemistry"	17th March 1987
	HUDSON, Prof. R.F. (University of Kent) "Homolytic Rearrangements of Free Radical Stability"	18th March 1987
*	JARMAN, Dr. M. (Institute of Cancer Research) "The Design of Anti Cancer Drugs"	19th February 1987
	KRESPAN, Dr. C. (E.I. Dupont de Nemours) "Nickel(0) and Iron(0) as Reagents in Organofluorine Chemistry"	26th June 1987
*	KROTO, Prof. H.W. (University of Sussex) "Chemistry in Stars, between Stars and in the Laboratory"	23rd October 1986

* LEY, Prof. S.V. (Imperial College) — 5th March 1987
"Fact and Fantasy in Organic Synthesis"

MILLER, Dr. J. (Dupont Central Research, USA) — 3rd December 1986
"Molecular Ferromagnets; Chemistry and Physical Properties"

* MILNE/CHRISTIE, Dr.A./Mr.S.(International Paints) — 20th November 1986
"Chemical Serendipity: A Real Life Case Study"

NEWMAN, Dr. R. (University of Oxford) — 4th March 1987
"Change and Decay: A Carbon-13 CP/MAS NMR Study of humification and Coalification Processes"

* OTTEWILL, Prof. R.H. (University of Bristol) — 22nd January 1987
"Colloid Science a Challenging Subject"

PASYNKIEWICZ, Prof. S. (Technical Univ.,Warsaw) — 11th May 1987
"Thermal Decomposition of Methyl Copper and its Reactions with Trialkylaluminium"

ROBERTS, Prof. S.M. (University of Exeter) — 24th June 1987
"Synthesis of Novel Antiviral Agents"

* RODGERS, Dr. P.J. (I.C.I. Billingham) — 12th February 1987
"Industrial Polymers from Bacteria"

* SCROWSTON, Dr. R.M. (University of Hull) — 6th November 1986
"From Myth and Magic to Modern Medicine"

SHEPHERD, Dr. T. (University of Durham) — 11th February 1987
"Pteridine Natural Products; Synthesis and Use in Chemotherapy"

THOMSON, Prof. A. (University of East Anglia) — 4th February 1987
"Metalloproteins and Magneto-optics"

* WILLIAMS, Prof. R.L. (Metropolitan Police Forensic Science) — 27th November 1987
"Science and Crime"

WONG, Prof.E.H. (University of New Hampshire,USA) — 29th October 1986
"Coordination Chemistry of P-O-P Ligands"

WONG, Prof.E.H. (University of New Hampshire,USA) — 17th February 1987
"Symmetrical Shapes from Molecules to Art and Nature"

DURING THE PERIOD: 1987-1988

BIRCHALL, Prof. D. (I.C.I. Advanced Materials) — 25th April 1988
"Environment Chemistry of Aluminium"

* BORER, Dr. K. (University of Durham Industrial Research Laboratories) — 18th February 1988
"The Brighton Bomb - (A Forensic Science View)"

BOSSONS, L. (Durham Chemistry Teachers' Centre) 16th March 1988
"GCSE Practical Assessment"

BUTLER, Dr. A.R. (University of St.Andrews) 5th November 1987
"Chinese Alchemy"

CAIRNS-SMITH, Dr. A. (Glasgow University) 28th January 1988
"Clay Minerals and the Origin of Life"

* DAVIDSON, Dr. J. (Herriot-Watt University) November 1987
"Metal Promoted Oligomerisation Reactions of Alkynes"

GRAHAM, Prof. W.A.G. (University of Alberta, Canada) 3rd March 1988
"Rhodium and Iridium Complexes in the Activation of Carbon-Hydrogen Bonds"

GRAY, Prof. G.W. (University of Hull) 22nd October 1987
"Liquid Crystals and their Applications"

HARTSHORN, Prof. M.P. (University of Canterbury, New Zealand) 7th April 1988
"Aspects of Ipso-Nitration"

HOWARD, Dr. J. (I.C.I. Wilton) 3rd December 1987
"Chemistry of Non-Equilibrium Processes"

JONES, Dr. M.E. (Durham Chemistry Teachers' Centre) 29th June 1988
"GCSE Chemistry Post-mortem"

JONES, Dr. M.E. (Durham Chemistry Teachers' Centre) 6th July 1988
"GCE Chemistry A-Level Post-mortem"

KOCH, Prof. H.F. (Ithaca College, U.S.A.) 7th March 1988
"Does the E2 Mechanism Occur in Solution"

LACEY, Mr. (Durham Chemistry Teacher's Centre) 9th February 1988
"Double Award Science"

LUDMAN, Dr. C.J. (Durham University) 10th December 1987
"Explosives"

McDONALD, Dr. W.A. (I.C.I. Wilton) 11th May 1988
"Liquid Crystal Polymers"

MAJORAL, Prof. J.-P. (Université Paul Sabatier) 8th June 1988
"Stabilisation by Complexation of Short-Lived Phosphorus Species"

MAPLETOFT, Mrs. M. (Durham Chemistry Teachers' Centre) 4th November 1987
"Salters' Chemistry"

NIETO DE CASTRO, Prof. C.A. (University of Lisbon and Imperial College) 18th April 1988

"Transport Properties of Non-Polar Fluids"

OLAH, Prof. G.A. (University of Southern California) — 29th June 1988
"New Aspects of Hydrocarbon Chemistry"

* PALMER, Dr. F. (University of Nottingham) — 21st January 1988
"Luminescence (Demonstration Lecture)"

PINES, Prof. A. (University of California, Berkeley, U.S.A.) — 28th April 1988
"Some Magnetic Moments"

RICHARDSON, Dr. R. (University of Bristol) — 27th April 1988
"X-Ray Diffraction from Spread Monolayers"

ROBERTS, Mrs. E. (SATRO Officer for Sunderland) — 13th April 1988
Talk - Durham Chemistry Teachers' Centre
"Links between Industry and Schools"

* ROBINSON, Dr. J.A. (University of Southampton) — 27th April 1988
"Aspects of Antibiotic Biosynthesis"

* ROSE, van Mrs. S. (Geological Museum) — 29th October 1987
"Chemistry of Volcanoes"

SAMMES, Prof. P.G. (Smith, Kline and French) — 19th December 1987
"Chemical Aspects of Drug Development"

* SEEBACH, Prof. D. (E.T.H. Zurich) — 12th November 1987
"From Synthetic Methods to Mechanistic Insight"

SODEAU, Dr. J. (University of East Anglia) — 11th May 1988
Durham Chemistry Teachers's Centre: "Spray Cans, Smog and Society"

SWART, Mr. R.M. (I.C.I.) — 16th December 1987
"The Interaction of Chemicals with Lipid Bilayers"

TURNER, Prof. J.J. (University of Nottingham) — 11th February 1988
"Catching Organometallic Intermediates"

UNDERHILL, Prof. A. (University of Bangor) — 25th February 1988
"Molecular Electronics"

* WILLIAMS, Dr. D.H. (University of Cambridge) — 26th November 1987
"Molecular Recognition"

WINTER, Dr. M.J. (University of Sheffield) — 15th October 1987
"Pyrotechnics (Demonstration Lecture)"

* - Indicates Colloquia attended by the author.

FIRST YEAR INDUCTION COURSE

OCTOBER 1985

This course consists of a series of one hour lectures in the services available in the department.

1. Departmental Organisation.
2. Safety Matters.
3. Electrical appliances and infrared spectroscopy.
4. Chromatography and Microanalysis.
5. Atomic absoption and inorganic analysis.
6. Library facilities.
7. Mass spectroscopy.
8. Nuclear Magnetic Resonance.
9. Glass blowing techniques.

RESEARCH CONFERENCES ATTENDED

1. GRADUATE SYMPOSIUM, Durham University, 16th April, 1986
2. GRADUATE SYMPOSIUM, Durham University, 19th April, 1988
3. INTERNATIONAL MACROCYCLIC CONFERENCE, Hamburg, Germany, September 4th - September 9th, 1988. A poster was presented by the author entitled "*Binding Studies with Amide Functionalised Macrocyclic Ligands*".

APPENDIX II

PUBLICATIONS

1. "*Comparative Study of Mono- and Disubstituted 14-Crown-4 Derivatives as Lithium Ionophores*", Ritu Kataky, Patrick E. Nicholson, David Parker. Accepted for publication, J. Chem. Soc. Perkin (II).

2. "*Synthesis and Binding Properties of Amide Functionalised Polyaza Macrocycles*", Ritu Kataky, Patrick E. Nicholson, David Parker. Submitted for publication, J. Chem. Soc. Perkin (I).

3. "*Synthesis of C and N Functionalised Derivatives of 1,5,9-Triazacyclododecane*", Ian M. Helps, K. Jankowski, Patrick E. Nicholson, David Parker, J. Chem. Soc. Perkin (I) 1989. In Press.

4. "*Synthesis and Binding Properties of Lithium Selective [14]-O_4 Macrocycles and their Use in a Lithium Selective Electrode*", Ritu Kataky, Patrick E. Nicholson, David Parker. Accepted for publication, Tetrahedron Letters.

UNIV. DUNELM